Electronic Supplementary Material (ESI) for Organic Chemistry Frontiers.

Supplementary Information

From a 1,2-Azaborinine to Large *BN*-PAHs via Electrophilic Cyclization: Synthesis, Characterization and Promising Optical Properties

Yannik Appiarius,[a] Tim Stauch,[b] Enno Lork,[c] Pascal Rusch,[d] Nadja C. Bigall[d] and Anne Staubitz[a]*

a. University of Bremen, Institute for Analytical and Organic Chemistry, Leobener Straße 7, D-28359 Bremen, Germany, MAPEX Center for Materials and Processes, Bibliothekstraße 1, D-28359 Bremen, Germany, E-mail: staubitz@uni-bremen.de

b. University of Bremen, Institute for Physical and Theoretical Chemistry, Leobener Straße 7, D-28359 Bremen, Germany Bremen Center for Computational Materials Science, Am Fallturm 1, D-28359 Bremen, Germany MAPEX Center for Materials and Processes, Bibliothekstraße 1, D-28359 Bremen, Germany

c. University of Bremen, Institute of Inorganic Chemistry and Crystallography, Leobener Straße 7, D-28359 Bremen, Germany

d. Leibniz University Hannover, Institute for Physical Chemistry and Electrochemistry, Callinstraße 3a, D-30167 Hannover, Germany Cluster of Excellence PhoenixD (Photonics, Optics, and Engineering - Innovation Across Disciplines), Hannover, Germany

Abstract: We present a convergent synthetic route towards boron-nitrogen containing polycyclic aromatic hydrocarbons (*BN*-PAHs) that allowed us to synthesize six derivatives. Starting from the conjunction of a 1,2-azaborinine nucleophile and various aryl electrophiles, the key step was the extension of the aromatic system via an electrophilic ring closure of the respective alkyne precursors. Our route allows to circumvent the use of substituted PAH precursors, which are often unavailable. Instead, it builds up the *BN*-PAHs solely from easily accessible monocycles. All derivatives were emissive in solution and solid state with quantum yields up to Φ_{lum} = 0.40 and small Stokes shifts. The emission wavelengths in solid state were notably dependent on the connectivity of the rings. Due to excimer formation in one derivative, its emission was significantly redshifted with a comparatively slow secondary photoluminescence (PL) decay.

Table of Contents

Abbreviations

abs.	Absolute
aq.	Aqueous
ATR	Attenuated total reflectance
BPin	Boronic acid pinacol ester
br	Broad signal (IR)
calcd.	Calculated
cod	Cyclooctadiene
COSY	Correlation spectroscopy (NMR)
CV	Cyclic voltammetry
d	Doublet (NMR)
DCM	Dichloromethane
DFT	Density functional theory
DIPA	Di*iso*propylamine
DMAP	4-Dimethylaminopyridine
dtbpy	4,4'-Di-*tert*-butylbipyridine
EI	Electron ionization
λ_{em}	Emission wavelength
eq.	Equivalent
λ_{ex}	Excitation wavelength
GC-MS	Gas chromatography / mass spectrometry
HMBC	Heteronuclear multiple-bond correlation spectroscopy (NMR)
HONTO	Highest occupied natural transition orbital
HR-MS	High resolution mass spectrometry
HSQC	Heteronuclear single-quantum correlation spectroscopy (NMR)
IR	Infrared spectroscopy
$[Ir(OMe)(1,5\text{-cod})]_2$	(1,5-Cyclooctadiene)(methoxy)iridium(I) dimer
J	Coupling constant (NMR)
LDA	Lithium *N,N*-di*iso*propylamide
LUNTO	Lowest unoccupied natural transition orbital
m	Multiplet (NMR), medium intensity (IR)
m_c	Multiplet centered (NMR)
m.p.	Melting point
λ_{max}	Wavelength at intensity maximum
MCP-PMT	Micro channel plate photomultiplier
Mes	Mesityl group
MTBE	Methyl-*tert*-butyl ether
mw	Microwave irradiation
*n*BuLi	*n*-Butyllithium
NBS	*N*-Bromosuccinimide
NICS	Nucleus-independent chemical shift
NMR	Nuclear magnetic resonance spectroscopy
NTO	Natural transition orbital
PAH	Polycyclic aromatic hydrocarbon
$[Pd(dppf)Cl_2]$	[1,1'-Bis(diphenylphosphino)ferrocene] dichloropalladium(II)
$[Pd(PPh_3)_4]$	Tetrakis(triphenylphosphine)palladium(0)
$[Pd(PPh_3)_2Cl_2]$	Bis(triphenylphosphine)palladium(II) dichloride
PTFE	Polytetrafluoroethylene

ppm	Parts per million
R_f	Retardation factor
s	Strong intensity (IR), singlet (NMR)
sat.	Saturated
sol.	Solution
t	Triplet (NMR)
TBAF	Tetra-*n*-butylammonium fluoride
TCSPC	Time-correlated single photon counting
THF	Tetrahydrofuran
TLC	Thin layer chromatography
TMS	Tetramethylsilane
t_R	Retention time
UFF	Universal force field
w	Weak intensity (IR)

1. General Methods and Materials

Unless stated otherwise, all syntheses were carried out under standard Schlenk conditions under an atmosphere of nitrogen or argon. If necessary, reactions were carried out in a nitrogen flushed glovebox from Inert Innovative Technology Inc. or reagents were prepared and stored there. All glassware was heated under a vacuum below 0.1 mbar and flushed with inert gas at least three times prior to use. Syringes were flushed with inert gas at least three times before use. NMR tubes were dried in an oven at 110 °C for at least 2 h before use.

1.1. NMR Spectroscopy

^{1}H NMR, ^{13}C{^{1}H} NMR, ^{7}Li NMR, ^{11}B{^{1}H} NMR and ^{29}Si{^{1}H} NMR spectra were recorded at 300 K. The respective spectrometers and the measuring frequencies are given in the left table below. The chemical shifts (δ) are given in ppm, relative to the residual solvent signals as denoted in the right table below (^{1}H and ^{13}C NMR).

Nucleus	Spectrometer frequency
^{1}H	500 MHz (Bruker DRX 500)
	601 MHz (Bruker AVANCE NEO)
^{13}C{^{1}H}	126 MHz (Bruker DRX 500)
	151 MHz (Bruker AVANCE NEO)
^{7}Li	194 MHz (Bruker DRX 500)
^{29}Si{^{1}H}	99 MHz (Bruker DRX 500)
	119 MHz (Bruker AVANCE NEO)

Solvent	Reference signal / ppm
$CDCl_3$	7.26 (^{1}H)
	77.16 (^{13}C)
C_6D_6	7.16 (^{1}H)
	128.06 (^{13}C)
DCM-d_2	5.32 (^{1}H)
	54.00 (^{13}C)
DMSO-d_6	2.50 (^{1}H)
	39.52 (^{13}C)
THF-d_8	3.58 (^{1}H)
	67.57 (^{13}C)

The signals were identified by using two dimensional methods such as ^{1}H - ^{1}H COSY, ^{1}H - ^{13}C{^{1}H} HSQC and ^{1}H - ^{13}C HMBC experiments when possible. The positions of hydrogen and carbon atoms are labelled with letters to simplify their assignment.

1.2. IR Spectroscopy

IR spectra were recorded with a Thermo Scientific Nicolet FT-IR Spectrometer System spectrometer with an ATR unit, equipped with a diamond window. The resolution was 4 cm^{-1}. The absorption bands are reported in cm^{-1}.

1.3. UV/vis Spectroscopy

UV/vis spectra were recorded with a resolution of 0.1 nm on a Shimadzu UV-2700 spectrometer with double monochromator.

1.4. Fluorescence Measurements

Emission measurements were performed using an Edinburgh Instruments FLS 1000 photoluminescence spectrometer. Absolute quantum yields were measured using an Edinburgh integrating sphere. The error of the used measurement setup was estimated by repeated measurements of a reference sample (Rhodamin 6G in EtOH) over the course of 2 weeks to be around an absolute ±0.05. TCSPC measurements were performed using a fast response MCP-PMT detector on the FLS 1000 and a 376 nm Edinburgh EPL Laser as excitation source with 10 – 20 MHz repetition rate and 80 ps pulse width. If excitation at 376 nm was not possible due to low or non-existent absorption at this energy, TCSPC measurements were performed using

a Horiba FluoroHub coupled with a Horiba Fluoromax-4 spectrometer. A NanoLED by Horiba was used as excitation source with 254 nm wavelength with 5 MHz repetition rate and a pulse width of 1.2 ns. All measurements were performed at 23 °C in Quartz Cuvettes with 10 mm path length by Hellma Analytics.

1.5. Melting Points

Melting points were determined with a Büchi Melting Point M-560 apparatus with a heating rate of 5 °C/min. All melting points are uncorrected.

1.6. Mass Spectrometry

GC-MS analyses were performed using an Agilent Technologies 7890 B chromatograph with an Agilent Technologies 5977A mass selective detector and an Agilent Technologies dimethylpolysiloxane column (19091S-931E, nominal length 30 m, 0.25 mm diameter, 0.25 µm grain size). High resolution EI mass spectra were recorded on a double focusing mass spectrometer ThemoQuest MAT 95 XL from Finnigan MAT (EI, 70 eV, R ~ 10 000). APCI mass spectra were recorded on an Advion Expression CMS via ASAP probe or direct inlet. High resolution ESI mass spectra were recorded on a Bruker Impact II. All signals were reported with the quotient from mass to charge (*m/z*).

1.7. Microwave Syntheses

All microwave experiments were performed in a Biotage Initiator+ microwave synthesizer with continuous irradiation power up to 300 W. The reactions were performed in 2 – 5 mL or 20 mL microwave vials, sealed with an aluminum / Teflon crimp top with a maximal exposure temperature of 250 °C and a maximum internal pressure of 20 bar. The temperature was measured with an external IR sensor during microwave heating.

1.8. Chromatography

TLC was performed using silica gel on alumina plates (Macherey-Nagel, ALUGRAM® Xtra SIL G/UV_{254}); the individual spots were visualized under a Lamag UV lamp (wavelengths: 254 nm / 365 nm). Manual chromatographic purifications were performed with the aid of silica gel provided by Macherey-Nagel (0.063 – 0.040 mm) and Merck (0.040 – 0.015 mm). Automated purifications were performed utilizing an Interchim Puriflash® 430 system. The cartridges were used depending on the amount of substance (15 g – 120 g; supplied from Interchim GmbH; grain size: 15 – 50 µm).

1.9. Single Crystals

Single crystals were grown from the respective solvents as denoted in the section Single Crystal Data. In all cases, a suitable crystal was selected and measured on a Bruker D8 Venture CMOS diffractometer. The crystal was kept at 100.00 K during data collection. Using Olex2[1], the structure was solved with the XT[2] structure solution program using Intrinsic Phasing and refined with the XL[3] refinement package using Least Squares minimization. The Deposition Numbers as denoted in the section Single Crystal Data contain the supplementary crystallographic data for this paper. These data are provided free of charge by the joint Cambridge Crystallographic Data Centre and Fachinformationszentrum Karlsruhe Access Structures service www.ccdc.cam.ac.uk/structures.

1.10. Chemicals

Unless stated otherwise, chemicals were used without further purification. In case the purity is not denoted in the table, it was not stated by the supplier.

Chemical	Supplier	Purity	Purification / Notes
Allyl amine	Acros	98%	
Allyl bromide	Acros/ Alfa Aesar	99%	Dist. from $CaCl_2$ [A] [B] [D] [E]
Ammonium chloride	Applichem	99.5%+	
Benzylidene-bis(tricyclohexyl-phosphine)dichlororuthenium(IV)	Alfa Aesar	96%	[C]
(1,1'-Bis(diphenylphosphino)-ferrocene)dichloropalladium(II)	abcr	99.9%	[B]
Bis(pinacolato)diboron	abcr	98%	
Bis(triphenylphosphine) palladium(II) dichloride	chempur	99%	[B]
Boron trifluoride diethyl etherate	Acros	Acroseal	48% sol. in diethyl ether
Boron trichloride	Acros	Acroseal	1.0 M sol. in heptane
1-Bromo-2-iodobenzene	Fluorochem		
1-Bromo-2-iodopyridine	BLDpharm		
2-Bromomesitylene	Aldrich	98%	[A] [B]
N-Bromosuccinimide	Alfa Aesar	99%	
tert-Butyldimethylsilyl chloride	TCI / Carbolution	98% / 99%	
n-Butyllithium	Acros	Acroseal	2.5 M sol. in hexanes
Calcium hydride	Acros	ca. 93%	
Celite® 535	Roth		
Chloral hydrate	J&K Scientific	99%	
Copper(I) iodide	Alfa Aesar	99.998%	[B]
(1,5-Cyclooctadiene)-(methoxy)iridium(I) dimer	Sigma-Aldrich	> 98%	[C]
2,5-Dibromoaniline	Fluorochem		
1,3-Dibromobenzene	Alfa Aesar	97%+	
1,4-Dibromobenzene	Alfa Aesar	98%	
Di*iso*propylamine	Sigma Aldrich	99.5%	dist. from CaH_2 [A] [B] [E]
4-(Dimethylamino)pyridine	Sigma Aldrich	97%	
4,4'-Di-*tert*-butyl-2,2'-bipyridyl	Sigma-Aldrich	98%	
Hydroxylamine hydrochloride	Acros	97%	
Iodine	abcr	99%	
3-Iodothiophene	Ark Pharm	97%+	
Isopentyl nitrite	Alfa Aesar	97%	Stabilized with 0.2% Na_2CO_3
Magnesium turnings	Fischer Scientific		
DL-Menthol	Alfa Aesar	98%+	

Chemical	Supplier	Purity	Purification / Notes
Palladium on activated charcoal	Sigma-Aldrich		10% w/w Pd [B]
1,10-Phenanthroline	Sigma-Aldrich	99%	
Periodic acid	Alfa Aesar	99%	
Platinum(II) chloride	chempur	99.9%	[B]
Potassium hydroxide	Sigma-Aldrich	85%+	
Potassium iodide	abcr	99%	
Potassium phosphate	Sigma-Aldrich	98%+	
Sodium chloride	Roth	99.5%+	
Sodium hydrogen carbonate	VWR	100%	
Sodium hydroxide	VWR	99%+	
Sodium sulfate	Merck	99%+	
Sodium thiosulfate pentahydrate	VWR	99.8%+	
Tetra-*n*-butylammonium fluoride	Aldrich	Sure/Seal	1.0 M sol. in THF
Tetrakis(triphenylphosphine) palladium(0)	TCI	97%	[C]
Triethylamine	Acros	99%	anhydrous [A] [B]
Trimethylsilylacetylene	abcr / fluorochem	98%	[A] [B]
Triphenylphosphine	Alfa Aesar	99%+	

1.11. Solvents

Unless stated otherwise, solvents were used without further purification. If a dried solvent was required, the additional purification / desiccation steps as denoted in the last column of the subsequent table were performed. Moreover, the usage of a dried solvent is mentioned in the regarding experimental procedure.

Solvent	Supplier	Purity / Purification	Additional Purifications / Desiccation
Acetic acid	VWR	99.9%	
Benzene-d_6	Deutero	>99.5%	[A] [B] [D] [E]
Chloroform-d_1	Deutero	99.8%	[D]
Cyclohexane	VWR	99.5%	
Cyclohexene	Sigma-Aldrich	99%	[A]
1,2-Dichloroethane	Carlo Erba,	99.8%	Dist. over CaH_2 [E]
Dichloromethane	VWR	100%	[B] [G]
Diethyl ether	VWR	technical grade, distilled by rotary evaporation	Pre-dried over $CaCl_2$, dist. over Na [A] [B] [D] [E]
DMSO-d_6	Eurisotop	99.8% D	
Ethyl acetate	VWR	99.9%	
n-Heptane	VWR	99.8%	
Hydrochloric acid	Merck,	37% aq. solution	
Methanol	VWR	100%	
MTBE	Acros	Acroseal, 99%	[A] [B]

Solvent	Supplier	Purity / Purification	Additional Purifications / Desiccation
n-Pentane	VWR	95%, distilled by rotary evaporation	[B] [D] [G]
Sulfuric acid	VWR	95%	
THF	VWR	100%	[A] [B] [D] [G]
THF-d_8	Eurisotop	99.5%+	[B] [D]
Toluene	VWR	HPLC grade	[G]
Water		Deionized	[A]

Purification methods:

[A] Degassed by at least 3 freeze-pump-thaw cycles or bubbling argon (30 min+)

[B] Stored under inert conditions in a glovebox and/ or in a J. Young's tube

[C] Stored in a freezer in a glovebox (–30 °C)

[D] Stored over molecular sieves (3 or 4 Å)

[E] Distilled under inert conditions

[F] Held under vacuum for at least 12 h prior to use

[G] Purified via an Inert PS-MD-6 solvent purification system (SPS)

[H] Heated to 200 °C under high vacuum for at least 12 h prior to use.

2. Experimental Procedures

2.1. Triallylborane (27)[4]

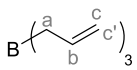

Boron trifluoride diethyl etherate (12.5 mL, 100 mmol) and dry diethyl ether (90 mL) were added to dry magnesium turnings (9.75 g, 401 mmol) at 20 °C. The reaction was started by adding allyl bromide (1.00 mL, 11.5 mmol) to the mixture immediately. Then, the remaining amount of allyl bromide (25.2 mL, 288 mmol), dissolved in dry diethyl ether (40 mL), was added to the reaction mixture over the course of 70 min, using a syringe pump. The reaction mixture was allowed to reflux and after it was cooled to 21 °C, stirring was continued for 17 h. The ethereal layer was transferred into a second flask under inert conditions, using a PTFE cannula. Under inert conditions, the remaining magnesium salts were washed with dry diethyl ether (2 × 30 mL) and the organic layer was transferred to the second flask as well. The diethyl ether was removed, using a slight vacuum (50 °C, 900 mbar → 150 mbar). The boron trifluoride etherate residue was slowly removed by Kugelrohr distillation (50 °C, 200 mbar → 20 mbar). The product was obtained as a colorless liquid via Kugelrohr distillation (50 °C, 13 mbar) to yield 6.21 g, 47%, (Lit.[4]: 66%). It was stored under inert conditions.

^{1}H NMR (500 MHz, C_6D_6): δ = 5.81 (ddd, ^3J = 21.2, 10.5 Hz, 3H, b), 4.95 (br s, 6H, c, c'), 2.03 (br s, 6H, a) ppm.

^{13}C{^{1}H} NMR (126 MHz, C_6D_6): δ = 135.2 (b), 114.9 (c), 34.6 (a) ppm.

^{11}B{^{1}H} NMR (160 MHz, C_6D_6): δ = 81.0 ppm.

Due to air- and moisture sensitivity of this compound, mass spectrometric data and IR spectra could not be collected.

The analytical data are consistent with the literature.[4]

2.2. *N*-Allyl-1-(*tert*-butyl)-1,1-dimethylsilanamine (28)[5]

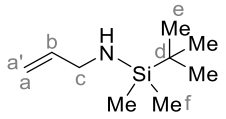

Triethylamine (7.90 g, 78.0 mmol) and DMAP (358 mg, 2.80 mmol, 4 mol%) were dissolved in dry diethyl ether (20 mL). The solution was added to a solution of allylamine (4.00 g, 70.2 mmol) in dry diethyl ether (20 mL) at 0 °C. Then, *tert*-butyldimethylsilyl chloride (12.8 g, 84.2 mmol) was diluted in dry diethyl ether (15 mL) and added to the mixture over the course of 20 min at 0 °C, using a syringe pump. The mixture was allowed to warm to 20 °C and stirring was continued for 15 h. Most of the colorless precipitation was removed by filtration over Celite, using a frit and additional *n*-pentane (100 mL). The solvent was removed in vacuo. The raw product was filtered twice by a PTFE filter (pore size: 0.45 µm) at 0 °C and purified by distillation (53 – 55 °C, 15 mbar). A colorless oil was obtained (9.74 g, 81%, Lit.[5]: 76%).

^{1}H NMR (500 MHz, C_6D_6): δ = 5.83 (ddt, ^3J = 17.0, 10.1, 5.0 Hz, 1H, b), 5.13 (dtd, ^3J = 17.0 Hz, ^2J = 1.8 Hz, ^4J = 1.8 Hz, 1H, a), 4.97 (dtd, ^3J = 10.1 Hz, ^2J = 1.8 Hz, ^4J = 1.8 Hz, 1H, a'), 3.26 (dddd, ^3J = 8.0, 5.0 Hz, ^4J = 1.8 Hz, 2H, c), 0.91 (s, 9H, e), -0.00 (s, 6H, f) ppm.

^{13}C{^{1}H} NMR (126 MHz, C_6D_6): δ = 141.3 (b), 112.7 (a), 45.4 (c), 26.6 (e), 18.6 (d), -4.9 (f) ppm.

^{29}Si{^{1}H} NMR (99 MHz, C_6D_6): δ = 8.6 ppm.

IR (ATR): $\tilde{\nu}$ [cm^{-1}] = 3412 (w), 3080 (w), 3007 (w), 2952 (m), 2927 (m), 2855 (m), 1641 (m), 1471 (m), 1417 (w), 1398 (m), 1251 (s), 1101 (s), 827 (s), 774 (s).

HR-MS (EI, 70 eV): *m/z* calcd. for $C_9H_{21}NSi$ 171.14378 $[M]^+$, found 171.14397 $[M]^+$.

The analytical data are consistent with the literature.[5]

2.3. *N*-Allyl-*N*-(allylchloroboryl)-1-(*tert*-butyl)-1,1-dimethylsilanamine (29)[6]

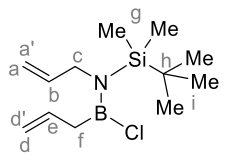

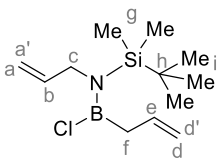

Triallylborane (**27**, 2.68 g, 20.0 mmol) was dissolved in dry dichloromethane (100 mL) and cooled to -78 °C. Boron trichloride (40.0 mL, 40.0 mmol, 1.0 M in heptane) was added over the course of 20 min via a syringe pump and the mixture was stirred for 4 h 15 min. A solution of *N*-allyl-1-(*tert*-butyl)-1,1-dimethylsilanamine (**28**, 10.3 g, 60.0 mmol) in dry dichloromethane (10 mL) was added over the course of 20 min via a syringe pump, while the temperature was maintained at -78 °C. Then, triethylamine (6.07 g, 60.0 mmol) was added over the course of 10 min at the same temperature and the mixture was allowed to warm to 19 °C. After 17 h of stirring, the mixture was filtered via a glass frit (size: 3) in a glovebox, using additional dry dichloromethane (20 mL). The solvent was removed in vacuo. To the crude product, calcium hydride (100 mg, 2.38 mmol) was added. Kugelrohr distillation (85 °C → 95 °C, 0.06 – 0.13 mbar) gave the product as a colorless, slightly milky oil (8.29 g, 54%, Lit.[6]: 84%), which was stored under inert conditions. A 1.0 : 0.9 mixture of rotamers (20 °C) was obtained.

^{1}H NMR* ** (500 MHz, C_6D_6): δ = 6.26 – 5.97 (m, 2H, b^1, b^2), 5.71 (br, 1H, e^1), 5.53 (br, 1H, e^2), 5.21 – 4.82 (m, 8H, a^1, $a^{1'}$, a^2, $a^{2'}$, d^1, $d^{1'}$, d^2, $d^{2'}$), 3.82 (br, 2H, c^1), 3.49 (br, 2H, c^2), 2.11, (br, 2H, f^1) 2.02 (br, 2H, f^2), 0.93 (br, 9H, i^1), 0.78 (br, 9H, i^2), 0.25 (br, 6H, g^1), 0.10 (br, 6H, g^2) ppm.

^{13}C{^{1}H} NMR ***** (126 MHz, C_6D_6): δ = 138.1 (e^1, e^2), 135.9 (b^1), 135.6 (b^2), 115.1-114.4 (a^1, a^2, d^1, d^2)****, 51.1 (c^1), 49.9 (c^2), 27.4 (i^1), 26.8 (i^2), -1.6 (g^1), -1.8 (g^2) ppm.

^{11}B{^{1}H} NMR (160MHz, C_6D_6): δ = 43.4 ppm.

^{29}Si{^{1}H} NMR (99 MHz, C_6D_6): δ = 13.6 ppm.

Due to air- and moisture sensitivity of this compound, mass spectrometric data and IR spectra could not be collected.

The analytical data are consistent with the literature.[6]

* Integrals are denoted separately for each rotamer.

** x^1 and x^2 represent the obtained rotamers. An assignment of signals to the respective rotamers was not performed.

*** The signal of carbon f was not detected because of the low quadrupole moment of the ^{11}B nucleus. Carbon h was not detectable because of its quaternary nature and resulting low signal intensity.

**** No assignment could be performed because of overlapping signals in the ^{13}C{^{1}H} NMR spectrum.

2.4. 1-(*tert*-Butyldimethylsilyl)-2-chloro-3,6-dihydro-1,2-azaborinine (30)[7]

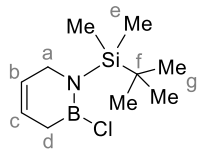

In a glovebox, *N*-allyl-*N*-(allylchloroboryl)-1-(*tert*-butyl)-1,1-dimethylsilanamine (**29**, 5.62 g, 21.8 mmol) was dissolved in dry dichloromethane (100 mL) at 20 °C. The Grubbs' catalyst 1st generation (181 mg, 0.22 mmol, 1.0 mol%) was dissolved in dry dichloromethane (10.0 mL) and added to the solution at 20 °C. The mixture was stirred for 15 h. The solvent was removed in vacuo in a glovebox and the product was obtained by inert Kugelrohr distillation (60 – 65 °C, 0.09 – 0.11 mbar). A colorless oil was obtained (4.32 g, 86%, Lit.[7]: 82%), which was stored under inert conditions.

^{1}H NMR (500 MHz, C_6D_6): δ = 5.64 (dtt, ^3J = 9.9, 5.1 Hz, ^4J = 1.9 Hz, 1H, b/c)*, 5.34 (dtt, ^3J = 9.9, 3.3 Hz, ^4J = 1.9 Hz, 1H, b/c)*, 3.43 (m_c, 2H, a), 1.75 (m_c, 2H, d), 0.93 (s, 9H, g), 0.23 (s, 6H, e) ppm.

^{13}C{^{1}H} NMR** (126 MHz, C_6D_6): δ = 125.1 (b), 125.1 (c), 48.4 (a), 27.3 (g), 20.2 (f), -1.8 (e) ppm.

^{11}B{^{1}H} NMR (160MHz, C_6D_6): δ = 42.6 ppm.

^{29}Si{^{1}H} NMR (99 MHz, C_6D_6): δ = 18.0 ppm.

Due to air- and moisture sensitivity of this compound, mass spectrometric data and IR spectra could not be collected.

The analytical data are consistent with the literature.[7]

* No assignment could be performed because of overlapping signals in the $^{13}C\{^1H\}$ NMR spectrum.

** The signal of carbon d was not detected because of the low quadrupole moment of the ^{11}B nucleus.

2.5. Mesityllithium (31)

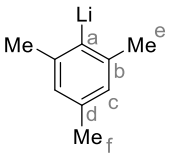

2-Bromomesitylene (9.95 g, 50.0 mmol) was dissolved in dry diethyl ether (80 mL) and cooled to -78 °C. *n*BuLi (19.0 mL, 47.5 mmol, 2.5 M in hexanes) was added over the course of 20 min and the mixture was stirred for 2 h 10 min. The cooling bath was removed and stirring was continued for 15 h. In a glovebox, the mixture was filtered via a glass frit (size: 3) and the solid was washed with dry *n*-pentane (2 × 20 mL). The product was dried in a high vacuum (< 0.01 mbar, 10 h) and obtained as a colorless powder (3.18 g, 51%, purity: 92%), which was stored under inert conditions. The purity was determined as follows:[8] In a glovebox, menthol (297 mg, 1.90 mmol) and 1,10-phenanthroline (4.00 mg, 22.2 µmol) were dissolved in dry THF (15.0 mL). A solution of **31** (361 mg, 2.86 mmol) in THF (20.0 mL) was added. From the required amount of solution, the purity was calculated. Consumption: 14.5 mL, 2.07 mmol.

^{1}H NMR (500 MHz, THF-d_8): δ = 6.47 (s, 2H, c), 2.40 (s, 6H, e), 2.09 (s, 3H, f) ppm.

$^{13}C\{^1H\}$ NMR (126 MHz, THF-d_8): δ = 180.8 (a), 149.8 (b), 132.1 (d), 123.5 (c), 29.1 (e), 21.8 (f) ppm.

^{7}Li NMR (99 MHz, THF-d_8): δ = 2.0 ppm.

Due to air- and moisture sensitivity of this compound, mass spectrometric data and IR spectra could not be collected.

2.6. 1-(*tert*-Butyldimethylsilyl)-2-mesityl-3,6-dihydro-1,2-azaborinine (32)

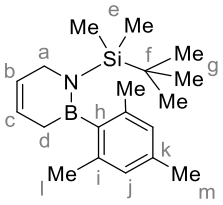

In a glovebox, 1-(*tert*-butyldimethylsilyl)-2-chloro-3,6-dihydro-1,2-azaborinine (**30**, 1.61 g, 7.00 mmol) was dissolved in dry THF (50 mL). Outside the box under inert conditions, the reaction mixture was cooled to -78 °C. A solution of mesityllithium (**31**, 883 mg, 7.00 mmol, purity: 92%) in dry THF (30 mL) was added at -78 °C over the course of 10 min and the solution was allowed to warm to 20 °C. The mixture was quenched with water (20 mL) and extracted with *n*-pentane (3 × 25 mL). The organic layers were combined and washed with brine (3 × 25 mL). The solvent was removed in vacuo, yielding the product as a colorless oil (1.85 g, 84%).

^{1}H NMR (500 MHz, DCM-d_2): δ = 6.70 (s, 2H, j), 5.98 (dtt, ^3J = 9.9, 4.0 Hz, ^4J = 1.8 Hz, 1H, b), 5.85 (dtt, ^3J = 9.9, 3.3 Hz, ^4J = 1.9 Hz, 1H, c), 3.73 (m_c, 2H, a), 2.22 (s, 3H, m), 2.14 (s, 6H, l), 1.59 (m_c, 2H, d), 0.93 (s, 9H, g), -0.21 (s, 6H, e).

$^{13}C\{^1H\}$ NMR* (126 MHz, DCM-d_2): δ = 137.6 (i), 136.4 (k), 128.1 (b), 127.3 (j), 126.5 (c), 45.5 (a), 28.4 (g), 22.4 (l), 21.4 (m), 19.8 (f), -3.7 (e) ppm.

$^{11}B\{^1H\}$ NMR (160MHz, C_6D_6): δ = 49.6 ppm.

$^{29}Si\{^1H\}$ NMR (99 MHz, C_6D_6): δ = 14.9 ppm.

IR (ATR): $\tilde{\nu}$ [cm^{-1}] = 3026 (w), 2959 (m), 2928 (m), 2856 (m), 1610 (w), 1462 (m), 1394 (m), 1308 (s), 1254 (s), 1053 (m), 832 (s), 776 (s).

HR-MS (EI, 70 eV): *m/z* calc. for $C_{19}H_{32}{}^{11}BNSi$ 313.23916 $[M]^+$, found 313.23949 $[M]^+$.

R_f (cyclohexane) = 0.50.

* The signals of carbons d and h were not detected because of the low quadrupole moment of the ^{11}B nucleus.

2.7. 1-(*tert*-Butyldimethylsilyl)-2-mesityl-1,2-azaborinine (33)

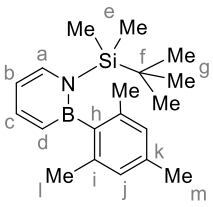

In a glovebox, a pressure flask was charged with 1-(*tert*-butyldimethylsilyl)-2-mesityl-3,6-dihydro-1,2-azaborinine (**32**, 939 mg, 3.00 mmol), Pd/C (319 mg, 0.30 mmol, 10% w/w Pd) and cyclohexene (12 mL). The mixture was heated at 100 °C for 16 h. The crude product was filtered via a PTFE filter (pore size: 0.45 µm) and the solvent was removed in vacuo. Via column chromatography (silica, eluent: cyclohexane, R_f = 0.33), the product could be obtained as a colorless solid (380 mg, 41%).

^{1}H NMR (500 MHz, $CDCl_3$): δ = 7.56 (ddd, ^3J = 10.9, 6.6 Hz, ^4J = 1.1 Hz, 1H, c), 7.44 (d, ^3J = 6.8 Hz, 1H, a), 6.79 (s, 2H, j), 6.63 (dd, ^3J = 10.9 Hz, ^4J = 1.5 Hz, 1H, d), 6.38 (ddd, ^3J = 6.8, 6.6 Hz, ^4J = 1.5 Hz, 1H, b), 2.29 (s, 3H, m), 2.09 (s, 6H, l), 0.91 (s, 9H, g), 0.00 (s, 6H, e) ppm.

^{13}C{^{1}H} NMR* (126 MHz, $CDCl_3$): δ = 142.7 (c), 139.0 (i), 138.4 (a), 136.5 (k), 127.0 (j), 111.6 (b), 27.6 (g), 23.6 (l), 21.3 (m), 19.4 (f), -3.2 (e) ppm.

^{11}B{^{1}H} NMR (160MHz, $CDCl_3$): δ = 40.0 ppm.

^{29}Si{^{1}H} NMR (99 MHz, $CDCl_3$): δ = 21.2 ppm.

IR (ATR): $\tilde{\nu}$ [cm^{-1}] = 3065 (w), 3023 (w), 2991 (w), 2948 (w), 2926 (m), 2854 (m), 1607 (s), 1503 (s), 1388 (s), 1269 (s), 837 (s), 809 (s), 714 (s).

HR-MS (EI, 70 eV): *m/z* calcd. for $C_{19}H_{30}{}^{10}BNSi$ 310.22714 $[M]^+$, found 310.22661 $[M]^+$; calcd. for $C_{19}H_{30}{}^{11}BNSi$ 311.22351 $[M]^+$, found 311.22350 $[M]^+$.

M.p.: 56 °C.

* The signals of carbons d and h were not detected because of the low quadrupole moment of the ^{11}B nucleus.

2.8. 1-Hydro-2-mesityl-1,2-azaborinine (34)[9]

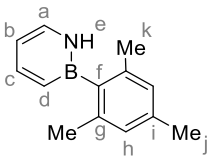

1-(*tert*-Butyldimethylsilyl)-2-mesityl-1,2-azaborinine (**33**, 311 mg, 1.00 mmol) was dissolved in THF (5 mL) at 20 °C. A solution of TBAF (1.20 mL, 1.20 mmol, 1.0 M in THF) was added to the solution over the course of 2 min and stirring was continued for 40 min. Because TLC indicated the completion of the reaction, water (5 mL) was added and the mixture was extracted with cyclohexane (3 × 10 mL). The combined organic layers were washed with an aq. solution of sodium hydrogen carbonate (2 M, 2 × 20 mL), dried over sodium sulfate, filtered, and the solvent was removed in vacuo. The crude product was purified by column chromatography (silica, eluents: 5% diethyl ether in cyclohexane, R_f = 0.43) to obtain a colorless, crystalline solid (179 mg, 91%, Lit.[9]: 74%).

^{1}H NMR (500 MHz, $CDCl_3$): δ = 7.89 (br s, 1H, e), 7.74 (ddd, ^3J = 11.1, 6.5 Hz, ^4J = 1.2 Hz, 1H, c), 7.41 (dd, ^3J = 6.5 Hz, 1H, a), 6.93 – 6.87 (m, 3H, d, h), 6.40 (dddd, ^3J = 6.5 Hz, ^4J = 1.5 Hz, 1H, b), 2.33 (s, 3H, j), 2.19 (s, 6H, k) ppm.

^{13}C{^{1}H} NMR* (126 MHz, $CDCl_3$): δ = 143.9 (c), 140.4 (g), 137.4 (i), 133.9 (a), 127.3 (h), 110.6 (b), 23.2 (k), 21.3 (j) ppm.

^{11}B{^{1}H} NMR (160MHz, $CDCl_3$): δ = 36.1 ppm.

IR (ATR): $\tilde{\nu}$ [cm^{-1}] = 3372 (m), 3086 (w), 3025 (w), 2956 (w), 2914 (w), 1652 (w), 1597 (m), 1540 (s), 1448 (s), 1339 (m), 1150 (m), 971 (m), 870 (m), 852 (s), 766 (s), 712 (s).

HR-MS (EI, 70 eV): *m/z* calcd. for $C_{13}H_{16}{}^{11}BN$ 197.13703 $[M]^+$, found 197.13732 $[M]^+$.

M.p.: 53 °C.

The analytical data are consistent with the literature.[9]

* The signals of carbons d and f were not detected because of the low quadrupole moment of the ^{11}B nucleus.

2.9. 1-Hydro-2-mesityl-6-(4,4,5,5-tetramethyl-1,3,2-dioxaborolan-2-yl)-1,2-azaborinine (1)[9]

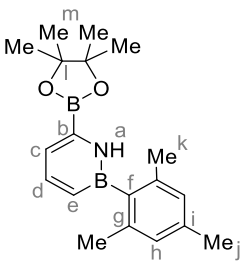

In a glovebox, $[Ir(OMe)(cod)]_2$ (17.9 mg, 27.0 µmol, 1.5 mol%), dtbpy (14.5 mg, 54.0 µmol, 3 mol%), bis(pinacolato)diboron (503 mg, 1.98 mmol) and MTBE (3 mL) were mixed. The mixture was added to a stirred solution of 1-hydro-2-mesityl-1,2-azaborinine (**34**, 355 mg, 1.80 mmol) in MTBE (2.5 mL) and stirring was continued for 5 h 30 min at 22 °C. The solvent was removed in vacuo and the dark brown, crude product was purified by column chromatography (silica, eluents: 5% diethyl ether in *n*-pentane, R_f = 0.33) to yield a yellow solid (448 mg, 77%, Lit.[9]: 95%).

^{1}H NMR (500 MHz, $CDCl_3$): δ = 8.40 (br s, 1H, a), 7.72 (dd, ^3J = 11.1, 6.5 Hz, 1H, d), 7.06 (ddd, ^3J = 11.1 Hz, ^4J = 1.7, 1.3 Hz, 1H, e), 6.97 (ddd, ^3J = 6.5 Hz, ^4J = 1.7, 1.3 Hz, 1H, c), 6.89 (s, 2H, h), 2.32 (s, 3H, j), 2.17 (s, 6H, k), 1.33 (s, 12H, m) ppm.

^{13}C{^{1}H} NMR* (126 MHz, $CDCl_3$): δ = 142.6 (d), 140.4 (g), 137.3 (i), 127.2 (h), 119.8 (c), 84.8 (l), 25.0 (m), 23.3 (k), 21.3 (j) ppm.

^{11}B{^{1}H} NMR (160MHz, $CDCl_3$): δ = 35.9 (azaborinine), 29.5 (BPin) ppm.

IR (ATR): $\tilde{\nu}$ [cm^{-1}] = 3394 (m), 3020 (w), 2972 (m), 2921 (m), 2854 (w), 1705 (w), 1609 (m), 1543 (m), 1446 (w), 1413 (m), 1370 (s), 1325 (s), 1142 (s), 960 (m), 847 (s).

HR-MS (EI, 70 eV): *m/z* calcd. for $C_{19}H_{27}{}^{10}B_2NO_2$ 321.22950 $[M]^+$, found 321.23008 $[M]^+$, calcd. for $C_{19}H_{27}{}^{10}B^{11}BNO_2$ 322.22587 $[M]^+$, found 322.22616 $[M]^+$.

M.p.: 141 °C.

The analytical data are consistent with the literature.[9]

* The signals of carbons e and f were not detected because of the low quadrupole moment of the ^{11}B nucleus.

2.10. 1,1'-Dihydro-2,2'-dimesityl-6,6'-bis(1,2-azaborinine) (20)

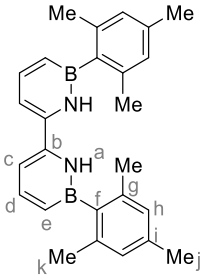

This compound arose as a side-product in almost every Suzuki cross-coupling approach with 1-hydro-2-mesityl-6-(4,4,5,5-tetramethyl-1,3,2-dioxaborolan-2-yl)-1,2-azaborinine (**1**). It was isolated from the reaction towards 1-hydro-2-mesityl-6-(3-((trimethylsilyl)ethynyl)thiophen-2-yl)-1,2-azaborinine (**15**), where the desired product and a bithiophene by-product were distilled by Kugelrohr distillation (0.05 mbar, up to 180 °C), whereby **20** remained in the flask.

^{1}H NMR (601 MHz, $CDCl_3$): δ = 8.14 (br s, 2H, a), 7.79 (dd, ^3J = 11.1, 6.9 Hz, 2H, d), 6.96 (d, ^3J = 11.1 Hz, 2H, e), 6.92 (s, 4H, h), 6.62 (ddd, ^3J = 6.9 Hz, ^4J = 2.2, 1.0 Hz, 2H, c), 2.33 (s, 6H, j), 2.22 (s, 12H, k) ppm.

^{13}C{^{1}H} NMR* (151 MHz, $CDCl_3$): δ = 144.0 (d), 141.5 (b), 140.4 (g), 137.8 (i), 132.5 (e), 127.4 (h), 107.8 (c), 23.4 (k), 21.3 (j) ppm.

^{11}B{^{1}H} NMR (192 MHz, $CDCl_3$): δ = 37.2 ppm.

HR-MS (EI, 70 eV, R ~ 10 000): *m/z* calcd. for $C_{26}H_{30}{}^{11}B_2N_2$ 392.25986 $[M]^+$, found 392.26023 $[M]^+$.

* The signal of carbon f was not detected because of the low quadrupole moment of the ^{11}B nucleus.

2.11. 1-Bromo-2-(2-(trimethylsilyl)ethynyl)benzene (8)[10]

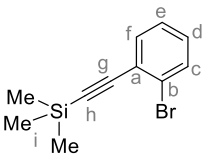

Copper(I) iodide (118 mg, 0.62 mmol) and $[Pd(PPh_3)_4]$ (116 mg, 0.10 mmol) were added to a Schlenk flask. In a second Schlenk flask, 1-bromo-2-iodobenzene (**2**, 5.00 g, 17.7 mmol, 1.00 eq.) was dissolved in triethylamine (25 mL) and THF (25 mL). The solution was degassed with bubbling argon through it for 10 min. Subsequently, it was added to the catalyst mixture. It was stirred for 10 min at 18 °C. Trimethylsilylacetylene (3.95 g, 40.2 mmol, 2.26 eq.) was added and the reaction mixture was

stirred at 18 °C for 3 d. It was filtered and rinsed with THF; subsequently the solvents were removed in vacuo. The residue was subjected to column chromatography (silica, eluent: *n*-heptane, R_f = 0.49), giving a pale, yellow oil (3.91 g, 87%, Lit.[10]: 94%).

^{1}H NMR (601 MHz, $CDCl_3$): δ = 7.57 (d, ^3J = 7.7 Hz, 1H, c), 7.49 (d, ^3J = 7.7 Hz, 1H, f), 7.24 (dd, ^3J = 7.7 Hz, 1H, e), 7.15 (dd, ^3J = 7.7 Hz, 1H, d), 0.28 (s, 9H, i) ppm.

^{13}C{^{1}H} NMR (151 MHz, $CDCl_3$): δ = 133.7 (f), 132.5 (c), 129.7 (d), 127.0 (e), 125.9 (b), 125.4 (a), 103.2 (g), 99.8 (h), -0.0 (i) ppm.

^{29}Si{^{1}H} NMR (119 MHz, $CDCl_3$): δ = -17.0 ppm.

IR (ATR): $\tilde{\nu}$ [cm^{-1}] = 3067 (w), 2959 (m), 2898 (w), 2162 (m), 1465 (s), 1434 (m), 1259 (m), 1249 (s), 1049 (s), 1027 (s), 861 (s), 838 (s), 750 (s), 669 (s).

HR-MS (EI, 70 eV, R ~ 10 000): *m/z* calcd. for $C_{11}H_{13}{}^{79}BrSi$ 251.99644 $[M]^+$, found 251.99657 $[M]^+$.

The analytical data are consistent with the literature.[10]

2.12. 1-Hydro-2-mesityl-6-(2-((trimethylsilyl)ethynyl)phenyl)-1,2-azaborinine (14)

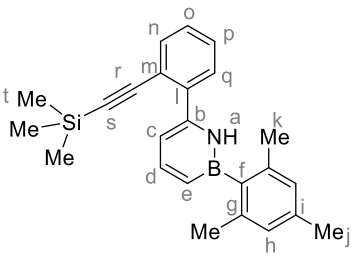

A 20 mL microwave vial was charged with 1-bromo-2-(2-(trimethylsilyl)-ethynyl)benzene (**8**, 127 mg, 0.50 mmol) and 2-mesityl-6-(4,4,5,5-tetramethyl-1,3,2-dioxaborolan-2-yl)-1,2-azaborinine (**1**, 161 mg, 0.50 mmol). In a glovebox, $[Pd(dppf)Cl_2]$ (11.0 mg, 15.0 µmol, 3 mol%), potassium phosphate (318 mg, 1.50 mmol, 3.00 eq.) and MTBE (8.4 mL) were added. Outside the box, degassed water (3.6 mL) was added. The reaction was heated at 80 °C for 6 h in a microwave reactor. The mixture was extracted with diethyl ether (5 × 2 mL). The combined organic phases were concentrated in vacuo and the crude residue was purified by column chromatography (silica, eluents: 1% diethyl ether in *n*-pentane, R_f = 0.23) to yield a yellow solid (154 mg, 82%).

^{1}H NMR (601 MHz, $CDCl_3$): δ = 8.58 (br s, 1H, a), 7.85 (dd, ^3J = 11.1, 6.9 Hz, 1H, d), 7.63 (dd, ^3J = 7.7 Hz, ^4J = 1.3 Hz, 1H, n), 7.54 (dd, ^3J = 7.7 Hz, ^4J = 1.3 Hz, 1H, q), 7.42 (ddd, ^3J = 7.7 Hz, ^4J = 1.3 Hz, 1H, p), 7.35 (ddd, ^3J = 7.7 Hz, ^4J = 1.3 Hz, 1H, o), 6.95 (ddd, ^3J = 11.1 Hz, ^4J = 1.5 Hz, 1H, e), 6.92 (s, 2H, h), 6.78 (ddd, ^3J = 6.9 Hz, ^4J = 1.5 Hz, 1H, c), 2.35 (s, 3H, j), 2.29 (s, 6H, k), 0.14 (s, 9H, t) ppm.

^{13}C{^{1}H} NMR (151 MHz, $CDCl_3$): δ = 143.9 (d), 143.8 (b), 140.3 (g), 139.9 (l), 138.3 (f), 137.2 (i), 134.7 (n), 130.7 (e), 129.1 (p), 128.7 (q), 128.3 (o), 127.3 (h), 120.7 (m), 111.3 (c), 103.5 (r), 99.9 (s), 23.5 (k), 21.3 (j), -0.3 (t) ppm.

^{11}B{^{1}H} NMR (192 MHz, $CDCl_3$): δ = 36.3 ppm.

^{29}Si{^{1}H} NMR (119 MHz, $CDCl_3$): δ = -17.2 ppm.

IR (ATR): $\tilde{\nu}$ [cm^{-1}] = 3377 (w), 3020 (w), 2958 (m), 2915 (w), 2855 (w), 2151 (m), 1608 (m), 1541 (s), 1477 (m), 1449 (s), 1444 (s), 1373 (m), 1261 (m), 1249 (s), 991 (m), 859 (s), 841 (s), 779 (m), 755 (s), 742 (s), 656 (m).

HR-MS (ESI positive): *m/z* calcd. for $C_{24}H_{29}{}^{11}BNSi$ 370.21615 $[M+H]^+$, found 370.21602 $[M+H]^+$.

M.p.: 90-92 °C.

2.13. 4-Hydro-3-mesityl-4,3-azaboraphenanthrene (*BN*-PAH1)

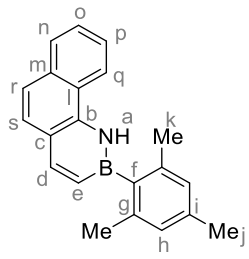

1-Hydro-2-mesityl-6-(2-((trimethylsilyl)ethynyl)phenyl)-1,2-azaborinine (**14**, 111 mg, 300 µmol) was dissolved in methanol (10 mL). Potassium hydroxide (16.8 mg, 300 µmol) was added and the mixture was stirred for 3 h at 25 °C, when the complete deprotection of the alkyne was confirmed by TLC analysis (eluents: 2% diethyl ether in *n*-pentane, R_f = 0.41, reactant: R_f = 0.48). The reaction mixture was extracted with diethyl ether (4 × 30 mL). The combined organic layers were dried over sodium sulfate, filtered and the solvent was removed in vacuo. The crude, deprotected alkyne was placed in a pressure tube. In a glovebox, platinum(II) chloride (23.9 mg, 90.0 µmol, 30 mol%) and toluene (15 mL) were added. The mixture was heated at 100 °C for 4 h. After cooling, it was filtered via a PTFE filter (pore size: 0.45 µm), using additional cyclohexane (5 mL). The solvents were removed in vacuo and the crude product was purified by filtration over silica (eluents: 1% diethyl ether in *n*-pentane, R_f = 0.47). A pale-yellow solid was obtained (65.2 mg, 73%).

^{1}H NMR (500 MHz, $CDCl_3$): δ = 8.89 (br s, 1H, a), 8.25 (d, ^3J = 11.3 Hz, 1H, d), 8.21 (d, ^3J = 7.8 Hz, 1H, q), 7.95 (d, ^3J = 7.2 Hz, 1H, n), 7.73 (d, ^3J = 8.6 Hz, 1H, s), 7.61 (d, ^3J = 8.6 Hz, 1H, r), 7.63 –7.56 (m, 2H, o, p), 7.11 (dd, ^3J = 11.3 Hz, ^4J = 1.8 Hz, 1H, e), 6.96 (s, 2H, h), 2.37 (s, 3H, j), 2.25 (s, 6H, k) ppm.

^{13}C{^{1}H} NMR* (126 MHz, $CDCl_3$): δ = 145.7 (d), 140.4 (g), 137.7 (i), 136.1 (b), 133.5 (m), 129.0 (n), 127.6 (s), 127.3 (h), 126.6 (o), 126.1 (p), 124.0 (l), 121.3 (r), 121.2 (c), 119.7 (q), 23.2 (k), 21.2 (j) ppm.

^{11}B{^{1}H} NMR (192 MHz, $CDCl_3$): δ = 37.3 ppm.

UV/Vis ($CHCl_3$): λ_{max} (ε) = 275 nm (50931 $mol^{-1}\,dm^3\,cm^{-1}$).

Fluorescence ($CHCl_3$): λ_{ex} = 338 nm, λ_{em} = 379 nm.

Fluorescence (solid): λ_{ex} = 338 nm, λ_{em} = 388 nm.

IR (ATR): $\tilde{\nu}$ [cm^{-1}] = 3397 (w), 3020 (w), 2914 (w), 2854 (w), 1626 (w), 1608 (m), 1589 (s), 1558 (s), 1503 (s), 1442 (s), 1428 (s), 1391 (m), 1264 (m), 1221 (m), 1141 (m), 976 (m), 833 (s), 793 (m), 703 (s).

HR-MS (ESI positive mode): *m/z* calcd. for $C_{21}H_{21}{}^{11}BN$ 298.17654 $[M+H]^+$, found 298.17632 $[M+H]^+$

M.p.: 136 °C.

* The signals of carbons e and f were not detected because of the low quadrupole moment of the ^{11}B nucleus.

2.14. 2-Bromo-3-iodothiophene (35)[11]

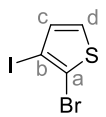

This reaction was not performed under inert conditions.

3-Iodothiophene (**3**, 2.10 g, 10.0 mmol) was dissolved in glacial acetic acid (30 mL). NBS (1.78 g, 10.0 mmol) was added to the stirred solution in one portion. The mixture was heated to 120 ˚C for 3 h 20 min, when the reaction was judged to be complete by means of TLC. The mixture was allowed to cool to 20 °C and subsequently neutralized by adding aq. solutions of sodium thiosulfate (1 M, 50 mL) and sodium hydroxide (5 M, 80 mL). It was extracted with ethyl acetate (3 × 40 mL), the organic phases were combined and washed with brine (3 × 50 mL). Drying over sodium sulfate, filtration, and removal of the solvent in vacuo gave a brown oil. The product was obtained after Kugelrohr distillation (95 – 105 °C, 5 mbar) as a slightly yellow oil (1.57 g, 54%, Lit.[11]: 76%).

^{1}H NMR (500 MHz, $CDCl_3$): δ = 7.23 (d, ^3J = 5.7 Hz, 1H, d), 6.96 (d, ^3J = 5.7 Hz, 1H, c) ppm.

^{13}C{^{1}H} NMR (126 MHz, $CDCl_3$): δ = 135.4 (c), 128.8 (d), 116.9 (a), 85.9 (b) ppm.

IR (ATR): $\tilde{\nu}$ [cm^{-1}] = 3102 (m), 3081 (m), 2921 (w), 1738 (w), 1567 (w), 1486 (m), 1389 (m), 1330 (m), 1152 (m), 1135 (m), 981 (s), 849 (m), 693 (s).

HR-MS (EI, 70 eV, R ~ 10 000): *m/z* calcd. for $C_4H_2{}^{79}BrIS$ 287.80998 $[M]^+$, found 287.81031 $[M]^+$.

R_f (cyclohexane): 0.76.

The analytical data are consistent with the literature.[11]

2.15. 2-Bromo-3-(2-(trimethylsilyl)ethynyl)thiophene (9)

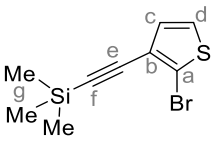

In a glovebox, 2-bromo-3-iodothiophene (**35**, 867 mg, 3.00 mmol), copper(I) iodide (40.0 mg, 240 µmol, 8 mol%) and $[Pd(PPh_3)_2Cl_2]$ (70.0 mg, 100 µmol, 3.30 mol%) were added to a mixture of DIPA and THF (20 mL, respectively). To the stirred mixture, trimethylsilylacetylene (309 mg, 3.00 mmol) was added immediately and stirring was continued for 2 h 10 min at 20 °C. When no reactant remained as detected by TLC, the colorless precipitate that had formed was removed by filtration and the solvent was removed in vacuo. Cyclohexane (150 mL) was added to the crude product and it was filtered over Celite. The solvent was removed in vacuo and the residue was purified by column chromatography (silica, eluent: cyclohexane, R_f = 0.47) to obtain the product as a slightly yellow oil (303 mg, 39%).

^{1}H NMR (500 MHz, $CDCl_3$): δ = 7.15 (d, ^3J = 5.7 Hz, 1H, d), 6.95 (d, ^3J = 5.7 Hz, 1H, c), 0.26 (s, 9H, g) ppm.

^{13}C{^{1}H} NMR (126 MHz, $CDCl_3$): δ = 130.1 (c), 125.7 (d), 124.7 (a), 118.0 (b), 99.0 (f), 98.2 (e), 0.1 (g) ppm.

^{29}Si{^{1}H} NMR (99 MHz, $CDCl_3$): δ = -17.0 ppm.

IR (ATR): $\tilde{\nu}$ [cm^{-1}] = 3109 (w), 2958 (m), 2898 (w), 2189 (w), 2153 (m), 1518 (w), 1405 (m), 1348 (m), 1249 (s), 1221 (m), 1004 (m), 964 (s), 838 (s), 826 (s), 713 (s).

HR-MS (EI, 70 eV, R ~ 10 000): *m/z* calcd. for $C_9H_{11}{}^{79}BrSSi$ 257.95286 $[M]^+$, found 257.95260 $[M]^+$.

2.16. 1-Hydro-2-mesityl-6-(3-((trimethylsilyl)ethynyl)thiophen-2-yl)-1,2-azaborinine (15)

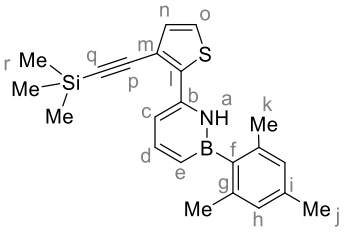

A 2 - 5 mL microwave vial was charged with 2-bromo-3-(2-(trimethylsilyl)ethynyl)-thiophene (**9**, 23.6 mg, 91.0 µmol, 1.30 eq.) and 2-mesityl-6-(4,4,5,5-tetramethyl-1,3,2-dioxaborolan-2-yl)-1,2-azaborinine (**1**, 22.6 mg, 70.0 µmol, 1.00 eq.). In a glovebox, $[Pd(dppf)Cl_2]$ (1.5 mg, 2.1 µmol, 3 mol%), potassium phosphate (44.6 mg, 210 mmol, 3.00 eq.) and MTBE (1.4 mL) were added. Outside the box, degassed water (0.6 mL) was added. The reaction was heated at 80 °C for 6 h in a microwave reactor. After cooling, the mixture was extracted with diethyl ether (3 × 2 mL). The combined organic phases were concentrated in vacuo and the crude residue was purified by column chromatography (silica, eluent: cyclohexane, R_f = 0.36) to furnish an orange solid (89.0 mg, 53%, purity 90%*). A clean sample for analytics was obtained as follows: The crude product was subjected to Kugelrohr distillation (0.05 mbar, up to 180 °C), whereby the bithiophene by-product was distilled and the product remained in the flask.

^{1}H NMR (500 MHz, $CDCl_3$): δ = 9.72 (br s, 1H, a), 7.72 (dd, ^3J = 11.1, 7.0 Hz, 1H, d), 7.16 (d, ^3J = 5.3 Hz, 1H, o), 7.07 (d, ^3J = 5.3 Hz, 1H, n), 6.87 (ddd, ^3J = 11.1 Hz, ^4J = 1.8, 1.0 Hz, 1H, e), 6.84 (s, 2H, h), 6.82 (ddd, ^3J = 7.0 Hz, ^4J = 1.0 Hz, 1H, c), 2.28 (s, 3H, j), 2.22 (s, 6H, k), -0.04 (s, 9H, r) ppm.

^{13}C{^{1}H} NMR** (126 MHz, $CDCl_3$): δ = 143.9 (d), 142.4 (l), 140.1 (g), 138.4 (b), 137.2 (i), 132.6 (n), 131.9 (e), 127.3 (h), 124.1 (o), 117.6 (m), 109.4 (c), 101.5 (q), 99.4 (p), 23.3 (k), 21.3 (j), -0.8 (r) ppm.

^{11}B{^{1}H} NMR (160MHz, $CDCl_3$): δ = 36.5 ppm.

^{29}Si{^{1}H} NMR (99 MHz, $CDCl_3$): δ = -16.7 ppm.

IR (ATR): $\tilde{\nu}$ [cm^{-1}] = 3349 (m), 3022 (w), 2956 (m), 2915 (m), 2854 (w), 2362 (w), 2142 (m), 1608 (m), 1598 (m), 1540 (s), 1455 (s), 1249 (s), 970 (s), 835 (s), 760 (s), 703 (s), 653 (s).

HR-MS (EI, 70 eV, R ~ 10 000): *m/z* calcd. for $C_{22}H_{26}{}^{11}BNSSi$ 375.16428 $[M]^+$, found 375.16516 $[M]^+$.

M.p.: 65 °C.

* Determined by integrating and comparing the signals of product and side product in the ^{1}H NMR spectrum.

** The signal of carbon f was not detected because of the low quadrupole moment of the ^{11}B nucleus.

2.17. 9-Hydro-8-mesityl-9,8-azaboranaphtho[1,2-*b*]thiophene (*BN*-PAH2)

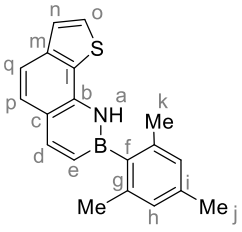

1-Hydro-2-mesityl-6-(3-((trimethylsilyl)ethynyl)thiophen-2-yl)-1,2-azaborinine (**15**, 37.5 mg, 100 µmol) was dissolved in methanol (5 mL). Potassium hydroxide (5.6 mg, 100 µmol) was added and the mixture was stirred for 3 h at 25 °C, when the complete deprotection of the alkyne was confirmed by TLC analysis (eluents: 2% diethyl ether in *n*-pentane, R_f = 0.49, reactant: R_f = 0.73). It was extracted with diethyl ether (4 × 30 mL). The combined organic layers were dried over sodium sulfate, filtered, and solvent was removed in vacuo. The crude, deprotected alkyne was placed in a pressure tube. In a glovebox, platinum(II) chloride (8.0 mg, 30.0 µmol, 30 mol%) and toluene (5 mL) were added. The mixture was heated at 100 °C for 4 h. After cooling, it was filtered via a PTFE filter (pore size: 0.45 µm), using additional cyclohexane (5 mL). The solvents were removed in vacuo and the crude product was purified by filtration over silica (eluents: 1% → 5% diethyl ether in *n*-pentane, R_f (1% diethyl ether in *n*-pentane) = 0.36). A pale-yellow, very viscous oil was obtained (25.2 mg, 83%).

^{1}H NMR (500 MHz, $CDCl_3$): δ = 8.23 (d, ^3J = 11.4 Hz, 1H, d), 8.03 (br s, 1H, a), 7.68 – 7.63 (m, 2H, p, q), 7.53 (d, ^3J = 5.3 Hz, 1H, o), 7.47 (d, ^3J = 5.3 Hz, 1H, n), 7.02 (dd, ^3J = 11.4 Hz, ^4J = 1.8 Hz, 1H, e), 6.97 (s, 2H, h), 2.37 (s, 3H, j), 2.26 (s, 6H, k) ppm.

^{13}C{^{1}H} NMR* (126 MHz, $CDCl_3$): δ = 145.7 (d), 140.4 (g), 140.2 (l/m)**, 138.0 (i), 135.8 (b), 129.1 (l/m)**, 127.5 (h), 126.8 (p), 125.9 (o), 125.6 (n), 121.2 (c), 117.1 (q), 23.2 (k), 21.3 (j) ppm.

^{11}B{^{1}H} NMR (160MHz, $CDCl_3$): δ = 37.4 ppm.

UV/Vis ($CHCl_3$): λ_{max} (ε) = 258 nm (40303 mol^{-1} dm^3 cm^{-1}).

Fluorescence ($CHCl_3$): λ_{ex} = 337 nm, λ_{em} = 372 nm.

Fluorescence (solid): λ_{ex} = 340 nm, λ_{em} = 378 nm.

IR (ATR): $\tilde{\nu}$ [cm^{-1}] = 3373 (w), 3021 (w), 2915 (m), 2853 (w), 2359 (w), 1608 (s), 1587 (s), 1541 (s), 1439 (s), 1354 (m), 1272 (s), 1265 (m), 1142 (m), 972 (s), 849 (s), 830 (s), 794 (s), 766 (s), 700 (s), 656 (s).

HR-MS (EI, 70 eV, R ~ 10 000): *m/z* calcd. for $C_{19}H_{18}{}^{11}BNS$ 303.12475 $[M]^+$, found 303.12505 $[M]^+$.

M.p.: 112 °C.

* The signals of carbons e and f were not detected because of the low quadrupole moment of the ^{11}B nucleus.

** No assignment could be performed because of equal correlations in the 2D NMR spectra.

2.18. 2-Bromo-3-(2-(trimethylsilyl)ethynyl)pyridine (10)

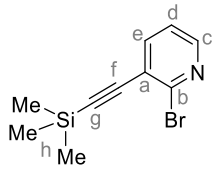

In a glovebox, 2-bromo-3-iodopyridine (**4**, 1.13 g, 4.00 mmol, 1.00 eq.), $[Pd(PPh_3)_2Cl_2]$ (140 mg, 0.20 mmol, 5 mol%) and copper(I) iodide (38.1 mg, 0.20 mmol, 5 mol%) were suspended in triethylamine and THF (25.0 mL, respectively). Trimethylsilylacetylene (432 mg, 4.40 mmol, 1.10 eq.) was added dropwise. Outside the box, the mixture was heated to 60 °C for 3 h. After cooling, a sat. aq. solution of ammonium chloride (50 mL) and water (50 mL) were added. It was extracted with DCM (3 × 40 mL) and the

combined organic phases were washed with water (3 × 40 mL). After drying over sodium sulfate, the volatiles were removed. Column chromatography (silica, eluents: 5% diethyl ether in *n*-pentane, R_f = 0.20) yielded the product as a pale-yellow oil (789 mg, 77%).

^{1}H NMR (601 MHz, $CDCl_3$): δ = 8.28 (dd, ^3J = 4.8 Hz, ^4J = 2.0 Hz, 1H, c), 7.73 (dd, ^3J = 7.7 Hz, ^4J = 2.0 Hz, 1H, e), 7.21 (dd, ^3J = 7.7, 4.8 Hz, 1H, d), 0.28 (s, 9H, h) ppm.

^{13}C{^{1}H} NMR (151 MHz, $CDCl_3$): δ = 148.7 (e), 144.8 (a), 141.3 (c), 123.6 (b), 122.1 (d), 103.3 (g), 100.9 (f), -0.2 (h) ppm.

^{29}Si{^{1}H} NMR (119 MHz, $CDCl_3$): δ = -16.3 ppm.

IR (ATR): $\tilde{\nu}$ [cm^{-1}] = 3040 (w), 2959 (m), 2899 (w), 2164 (m), 1570 (m), 1548 (m), 1442 (m), 1385 (s), 1249 (s), 1119 (m), 1052 (s), 857 (s), 839 (s), 825 (s), 799 (s), 759 (s), 684 (s).

HR-MS (EI, 70 eV, R ~ 10 000): *m/z* calcd. for $C_{10}H_{12}{}^{79}BrNSi$ 252.99169 $[M]^+$, found 252.99142 $[M]^+$.

2.19. 1-Hydro-2-mesityl-6-(3-((trimethylsilyl)ethynyl)pyridin-2-yl)-1,2-azaborinine (16)

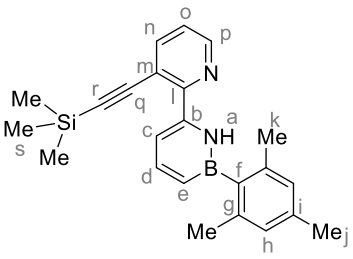

A 20 mL microwave vial was charged with 2-bromo-3-(2-(trimethylsilyl)-ethynyl)pyridine (**10**, 127 mg, 0.50 mmol) and 2-mesityl-6-(4,4,5,5-tetramethyl-1,3,2-dioxaborolan-2-yl)-1,2-azaborinine (**1**, 161 mg, 0.50 mmol). In a glovebox, $[Pd(dppf)Cl_2]$ (11.0 mg, 0.015 mmol, 3 mol%), potassium phosphate (318 mg, 1.50 mmol, 3.00 eq.) and MTBE (8.4 mL) were added. Outside the box, degassed water (3.6 mL) was added. The reaction was heated at 80 °C for 6 h in a microwave reactor. The mixture was extracted with diethyl ether (5 × 2 mL). The combined organic phases were concentrated in vacuo and the crude residue was purified by column chromatography (silica, eluents: 3% diethyl ether in *n*-pentane, R_f = 0.37) to yield a pale yellow, very viscous oil (134 mg, 71%).

^{1}H NMR (601 MHz, $CDCl_3$): δ = 10.08 (br s, 1H, a), 8.54 (dd, ^3J = 4.6 Hz, ^4J = 1.7 Hz, 1H, p), 8.22 (ddd, ^3J = 7.1 Hz, ^4J = 2.0, 1.0 Hz, 1H, c), 7.90 (dd, ^3J = 7.8 Hz, ^4J = 1.7 Hz, 1H, n), 7.85 (dd, ^3J = 10.9, 7.1 Hz, 1H, d), 7.20 (dd, ^3J = 7.8, 4.6 Hz, 1H, o), 7.05 (ddd, ^3J = 10.9 Hz, ^4J = 2.0, 1.0 Hz, 1H, e), 6.93 (s, 2H, h), 2.35 (s, 3H, j), 2.26 (s, 6H, k), 0.35 (s, 9H, s).

^{13}C{^{1}H} NMR (151 MHz, $CDCl_3$): δ = 152.1 (l), 148.0 (p), 143.2 (d), 143.2 (n), 140.5 (g), 140.4 (b), 138.7 (f), 137.2 (i), 133.9 (e), 127.3 (h), 121.9 (o), 116.5 (m), 112.1 (c), 104.1 (r), 103.0 (q), 23.4 (k), 21.3 (j), -0.3 (s) ppm.

^{11}B{^{1}H} NMR (192 MHz, $CDCl_3$): δ = 36.1 ppm.

^{29}Si{^{1}H} NMR (119 MHz, $CDCl_3$): δ = -16.6 ppm.

IR (ATR): $\tilde{\nu}$ [cm^{-1}] = 3331 (w), 2958 (m), 2919 (w), 2359 (w), 2342 (w), 2157 (w), 1609 (m), 1538 (s), 1448 (m), 1417 (m), 1250 (m), 867 (s), 842 (s), 803 (s), 757 (s), 668 (m).

HR-MS (ESI positive): *m/z* calcd. for $C_{23}H_{28}{}^{11}BN_2Si$ 371.21138 $[M+H]^+$, found 371.21122 $[M+H]^+$.

2.20. 10-Hydro-9-mesityl-10,9-azaborabenzo*[h]*quinoline (*BN*-PAH3)

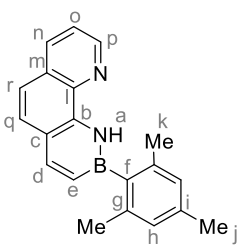

1-Hydro-2-mesityl-6-(3-((trimethylsilyl)ethynyl)pyridin-2-yl)-1,2-azaborinine (**16**, 44.8 mg, 121 µmol) was dissolved in methanol (5.0 mL). Potassium hydroxide (6.8 mg, 121 µmol) was added and the mixture was stirred for 3 h at 25 °C, when the complete deprotection of the alkyne was confirmed by TLC analysis (eluents: 3% diethyl ether in *n*-pentane, R_f = 0.33, reactant: R_f = 0.37). It was extracted with diethyl ether (4 × 30 mL). The combined organic layers were dried over sodium sulfate, filtered, and the solvent was removed in vacuo. The crude, deprotected alkyne was placed in a pressure tube. In a glovebox, platinum(II) chloride (9.7 mg, 36.3 µmol, 30 mol%) and toluene (5.0 mL)

were added. The mixture was heated at 100 °C for 4 h. After cooling, it was filtered via a PTFE filter (pore size: 0.45 µm), using additional cyclohexane (5 mL). The solvents were removed in vacuo and the crude product was purified by filtration over silica (eluents: 3% diethyl ether in *n*-pentane, R_f = 0.37) to give a pale yellow, very viscous oil (17.7 mg, 49%), that crystallized after one week at 25 °C.

^{1}H NMR (601 MHz, $CDCl_3$): δ = 10.45 (br s, 1H, a), 8.89 (dd, ^3J = 4.2 Hz, ^4J = 1.7 Hz, 1H, p), 8.28 (d, ^3J = 11.3 Hz, 1H, d), 8.23 (dd, ^3J = 8.2 Hz, ^4J = 1.7 Hz, 1H, n), 7.81 (d, ^3J = 8.6 Hz, 1H, q), 7.55 (d, ^3J = 8.6 Hz, 1H, r), 7.51 (dd, ^3J = 8.2, 4.2 Hz, 1H, o), 7.26 (dd, ^3J = 11.3 Hz, ^4J = 2.1 Hz, 1H, e), 6.97 (s, 2H, h), 2.39 (s, 3H, j), 2.29 (s, 6H, k) ppm.

^{13}C{^{1}H} NMR (151 MHz, $CDCl_3$): δ = 148.4 (p), 144.4 (d), 140.4 (g), 139.8 (l), 138.1 (f), 137.5 (i), 137.3 (b), 136.0 (n), 133.4 (e), 128.2 (q), 127.6 (m), 127.4 (h), 122.9 (c), 122.0 (o), 119.2 (r), 23.3 (k), 21.4 (j) ppm.

^{11}B{^{1}H} NMR (192 MHz, $CDCl_3$): δ = 36.8 ppm.

UV/Vis ($CHCl_3$): λ_{max} (ε) = 283 nm (42583 $mol^{-1}\,dm^3\,cm^{-1}$).

Fluorescence ($CHCl_3$): λ_{ex} = 347 nm, λ_{em} = 389 nm.

Fluorescence (solid): λ_{ex} = 340 nm, λ_{em} = 380 nm.

IR (ATR): $\tilde{\nu}$ [cm^{-1}] = 3350 (m), 3017 (w), 2952 (w), 2917 (m), 2853 (m), 1608 (m), 1603 (m), 1583 (s), 1552 (s), 1429 (s), 1393 (s), 1378 (m), 1092 (m), 1005 (m), 837 (s), 826 (s), 810 (s), 711 (s), 669 (m).

HR-MS (ESI positive): *m/z* calcd. for $C_{20}H_{20}{}^{11}BN_2$ 299.17177 $[M+H]^+$, found 299.17161 $[M+H]^+$

M.p.: 102 °C.

2.21. 1,5-Dibromo-2,4-diiodobenzene (36)[12]

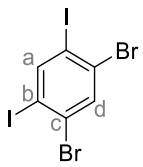

This reaction was not performed under inert conditions.

Under vigorous stirring, periodic acid (0.57 g, 2.50 mmol, 0.50 eq.) was dissolved in concentrated sulfuric acid (20 mL) at 25 °C. Potassium iodide (1.25 g, 7.50 mmol, 1.50 eq.) was added in small portions over the course of 15 min and the mixture was cooled to 0 °C. 1,3-Dibromobenzene (**5**, 1.18 g, 5.00 mmol, 1.00 eq.) was added in one portion and stirring was continued for 4 h at the same temperature. The reaction mixture was poured into ice water and filtered via a glass frit. The crude solid was recrystallized from hot methanol in four crops to yield a colorless solid (1.59 g, 65%, Lit.[12]: 68%).

^{1}H NMR (500 MHz, $CDCl_3$): δ = 8.28 (s, 1H, a), 7.83 (s, 1H, d) ppm.

^{13}C{^{1}H} NMR (126 MHz, $CDCl_3$): δ = 149.6 (a), 135.5 (d), 130.6 (c), 100.5 (b) ppm.

IR (ATR): $\tilde{\nu}$ [cm^{-1}] = 3058 (m), 1737 (w), 1431 (m), 1408 (s), 1353 (w), 1290 (w), 1278 (s), 1106 (s), 1094 (m), 1001 (s), 875 (s), 865 (m).

HR-MS: (EI, 70 eV, R ~ 10 000): *m/z* calcd. for $C_6H_2{}^{79}Br_2I_2$ 485.66072 $[M]^+$, found 485.66037 $[M]^+$.

M.p.: 166-168 °C (Lit.[12]: 166-167 °C).

The analytical data are consistent with the literature.[12]

2.22. 1,5-Dibromo-2,4-bis(2-(trimethylsilyl)ethynyl)benzene (11)[13]

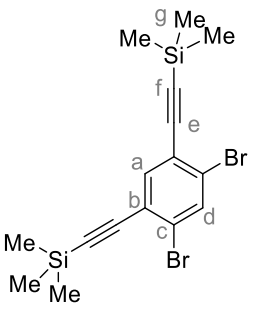

In a glovebox, 1,5-dibromo-2,4-diiodobenzene (**36**, 439 mg, 0.90 mmol, 1.00 eq.), $[Pd(PPh_3)_2Cl_2]$ (31.6 mg, 0.045 mmol, 5 mol%) and copper(I) iodide (8.57 mg, 0.045 mmol, 5 mol%) were suspended in triethylamine (30 mL). Trimethylsilylacetylene (177 mg, 1.80 mmol, 2.00 eq.) was added and the mixture was stirred at 25 °C for 22 h. After removing the solids by filtration, the volatiles were evaporated in vacuo and the residue was purified by column chromatography (silica, eluent: *n*-pentane, R_f = 0.46). A colorless, very viscous oil (287 mg, 75%, Lit.[13]: 96 %) was obtained.

^{1}H NMR (500 MHz, $CDCl_3$): δ = 7.80 (s, 1H, d), 7.59 (s, 1H, a), 0.26 (s, 18H, g) ppm.

^{13}C{^{1}H} NMR (126 MHz, $CDCl_3$): δ = 137.6 (a), 135.7 (d), 125.8 (c), 124.7 (b), 101.6 (f), 101.4 (e), -0.2 (g) ppm.

^{29}Si{^{1}H} NMR (99 MHz, $CDCl_3$): δ = -16.5 ppm.

IR (ATR): $\tilde{\nu}$ [cm^{-1}] = 2958 (m), 2898 (w), 2158 (m), 1450 (s), 1409 (w), 1339 (m), 1249 (s), 1174 (s), 1058 (s), 976 (m), 892 (m), 836 (s), 694 (s), 655 (m).

HR-MS: (EI, 70 eV, R ~ 10 000): *m/z* calcd. for $C_{16}H_{20}{}^{79}Br_2Si_2$ 425.94648 $[M]^+$, found 425.94673 $[M]^+$.

The analytical data are consistent with the literature.[13]

2.23. 6,6'-(4,6-bis((Trimethylsilyl)ethynyl)-1,3-phenylene)bis(1-hydro-2-mesityl-1,2-azaborinine) (17)

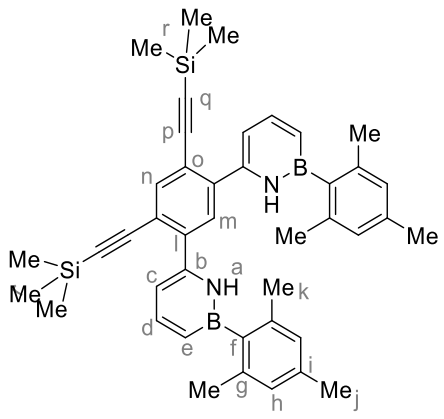

A 2-5 mL microwave vial was charged with 1,5-Dibromo-2,4-bis(2-(trimethylsilyl)ethynyl)benzene (**11**, 21.4 mg, 50.0 µmol, 1.00 eq.) and 2-mesityl-6-(4,4,5,5-tetramethyl-1,3,2-dioxa-borolan-2-yl)-1,2-azaborinine (**1**, 38.9 mg, 120 µmol, 2.40 eq.). In a glovebox, $[Pd(dppf)Cl_2]$ (1.10 mg, 1.50 µmol, 3 mol%), potassium phosphate (31.8 mg, 150 µmol, 3.00 eq.) and MTBE (2.1 mL) were added. Outside the box, degassed water (0.9 mL) was added. The reaction was heated at 80 °C for 6 h in a microwave reactor. The mixture was extracted with diethyl ether (3 × 2 mL). The combined organic phases were concentrated in vacuo and the crude residue was purified by column chromatography (silica, eluents: 1% diethyl ether in *n*-pentane, R_f = 0.33) to yield a colorless solid (29.6 mg, 89%).

^{1}H NMR (601 MHz, $CDCl_3$): δ = 8.57 (br s, 2H, a), 7.80 (dd, ^3J = 11.0, 6.8 Hz, 2H, d), 7.65 (s, 1H, m), 6.94 (ddd, ^3J = 11.0 Hz, ^4J = 1.9, 1.1 Hz, 2H, e), 6.87 (s, 4H, h), 6.78 (ddd, ^3J = 6.8 Hz, ^4J = 1.9, 1.1 Hz, 2H, c), 2.30 (s, 6H, j), 2.23 (s, 12H, k), 0.10 (s, 18H, r) ppm.

^{13}C{^{1}H} NMR (126 MHz, $CDCl_3$): δ = 143.8 (d), 142.6 (b), 140.8 (n), 140.3 (g), 139.7 (l), 138.0 (f), 137.4 (i), 131.7 (e), 129.2 (m), 127.4 (h), 120.5 (o), 111.7 (c), 102.1 (q), 102.0 (p), 23.5 (k), 21.3 (j), -0.4 (r) ppm.

^{11}B{^{1}H} NMR (192 MHz, $CDCl_3$): δ = 36.9 ppm.

^{29}Si NMR (119 MHz, $CDCl_3$): δ = -16.8 ppm.

IR (ATR): $\tilde{\nu}$ [cm^{-1}] = 3381 (w), 3022 (w), 2959 (m), 2917 (w), 2856 (w), 2360 (w), 2342 (w), 2147 (w), 1609 (m), 1542 (s), 1450 (m), 1409 (w), 1250 (m), 974 (m), 845 (s), 775 (m), 724 (m), 653 (w).

HR-MS: (EI, 70 eV, R ~ 10 000): *m/z* calcd. for $C_{42}H_{50}{}^{11}B_2N_2Si_2$ 660.37079 $[M]^+$, found 660.37052 $[M]^+$.

M.p.: 221 °C.

2.24. 1,13-Dihydro-2,12-dimesityl-1,13-diaza-2,12-diboradibenz[*a,j*]anthracene (*BN*-PAH4)

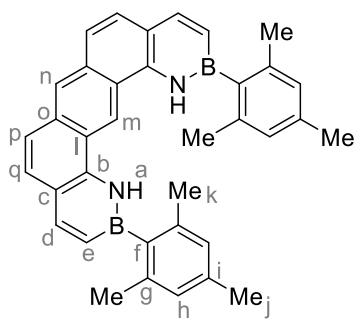

6,6'-(4,6-bis((Trimethylsilyl)ethynyl)-1,3-phenylene)bis(1-hydro-2-mesityl-1,2-azaborinine) (**17**, 242 mg, 0.37 mmol) was dissolved in methanol (20 mL). Potassium hydroxide (41.1 mg, 0.74 mmol) was added and the mixture was stirred for 3 h at 25 °C, when the complete deprotection of the alkyne was confirmed by TLC analysis (eluents: 1% diethyl ether in *n*-pentane, R_f = 0.11, reactant: R_f = 0.27). It was extracted with diethyl ether (4 × 30 mL). The combined organic layers were dried over sodium sulfate, filtered, and the solvent was removed in vacuo. The crude, deprotected alkyne was placed in a pressure tube. In a glovebox, platinum(II) chloride (29.2 mg, 0.11 mmol, 30 mol%) and toluene (15 mL) were added. The mixture was heated at 100 °C for 4 h. After cooling, it was filtered via a PTFE filter (pore size: 0.45 µm), using additional cyclohexane (5 mL). The solvents were removed in vacuo and the crude product was purified by column chromatography (silica, eluents: 1% diethyl ether in *n*-pentane, R_f = 0.30). The product was allowed to precipitate from impure fractions. Clean fractions from column chromatography and the clean precipitation were combined and yielded a yellow solid (76.3 mg, 40%).

^{1}H NMR (500 MHz, $CDCl_3$): δ = 9.17 (br s, 2H, a), 9.03 (s, 1H, m), 8.55 (s, 1H, n), 8.28 (d, ^3J = 11.2 Hz, 2H, d), 7.79 (d, ^3J = 8.7 Hz, 2H, p), 7.76 (d, ^3J = 8.7 Hz, 2H, q), 7.15 (dd, ^3J = 11.2 Hz, ^4J = 1.6 Hz, 2H, e), 6.93 (s, 4H, h), 2.33 (s, 6H, j), 2.22 (s, 12H, k) ppm.
^{13}C{^{1}H} NMR* (151 MHz, $CDCl_3$): δ = 146.2 (d), 140.3 (g), 137.9 (i), 136.5 (b), 132.0 (e/o),** 131.9 (e/o),** 128.7 (n), 128.5 (q), 127.5 (h), 123.4 (l), 121.6 (p), 120.9 (c), 111.5 (m), 23.4 (k), 21.4 (j) ppm.
^{11}B{^{1}H} NMR (160 MHz, $CDCl_3$): δ = 36.1 ppm.
UV/Vis ($CHCl_3$): λ_{max} (ε) = 317 nm (58811 $mol^{-1}\,dm^3\,cm^{-1}$).
Fluorescence ($CHCl_3$): λ_{ex} = 405.5 nm, λ_{em} = 451 nm.
Fluorescence (solid): λ_{ex} = 317 nm, λ_{em} = 574 nm.
IR (ATR): $\tilde{\nu}$ [cm^{-1}] = 3412 (w), 3011 (w), 2959 (w), 2913 (m), 2853 (w), 1608 (m), 1583 (s), 1550 (s), 1519 (m), 1440 (s), 1375 (s), 1265 (m), 1143 (w), 978 (m), 845 (s), 822 (m), 764 (s), 732 (s), 699 (s), 669 (m).
HR-MS: (EI, 70 eV): *m/z* calcd. for $C_{36}H_{34}{}^{11}B_2N_2$ 516.29146 $[M]^+$, found 516.29167 $[M]^+$.
M.p.: 305 °C (decomposes).

* The signal of carbon f was not detected because of the low quadrupole moment of the ^{11}B nucleus.

** No assignment could be performed because of overlapping signals in the ^{13}C{^{1}H} NMR spectrum.

2.25. 1,4-Dibromo-2,5-diiodobenzene (37)[14]

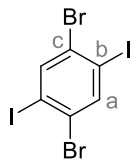

This reaction was not performed under inert conditions.

1,4-Dibromobenzene (**6**, 1.18 g, 5.00 mmol, 1.00 eq.) and iodine (5.08 g, 20.0 mmol, 4.00 eq.) were dissolved in concentrated sulfuric acid (25 mL). The reaction mixture was heated for 6 h at 135 °C. After cooling, it was allowed to stir for 16 h at 20 °C. The mixture was poured onto ice water and an aq. solution of sodium thiosulfate was added until it decolorized. It was extracted with dichloromethane (3 × 100 mL). The combined organic layers were dried over sodium sulfate. After filtration, the crude product was recrystallized from methanol (ca. 200 mL) to give off-white crystals (2.21 g, 91%, Lit.[14]: 85%).

^{1}H NMR (500 MHz, $CDCl_3$): δ = 8.05 (s, 2H, a) ppm.
^{13}C{^{1}H} NMR (126 MHz, $CDCl_3$): δ = 142.5 (a), 129.4 (c), 101.5 (b) ppm.

IR (ATR): $\tilde{\nu}$ [cm^{-1}] = 3063 (w), 1737 (w), 1733 (w), 1431 (m), 1408 (m), 1289 (w), 1279 (s), 1105 (s), 1000 (s), 875 (s), 806 (w), 745 (w), 658 (w).

HR-MS: (EI, 70 eV, R ~ 10 000): *m/z* calcd. for $C_6H_2{}^{79}Br_2I_2$ 485.66072 $[M]^+$, found 485.66075 $[M]^+$.

M.p.: 163-165 °C (Lit.[14]: 159-164°C).

The analytical data are consistent with the literature.[14]

2.26. 1,4-Dibromo-2,5-bis(2-(trimethylsilyl)ethynyl)benzene (12)

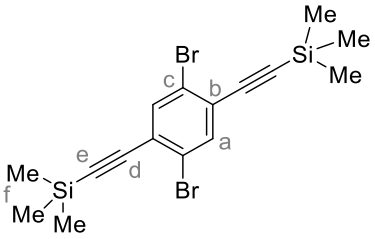

In a glovebox, 1,4-dibromo-2,5-diiodobenzene (**37**, 244 mg, 0.50 mmol, 1.00 eq.), $[Pd(PPh_3)_2Cl_2]$ (17.6 mg, 0.025 mmol, 5 mol%) and copper(I) iodide (4.8 mg, 0.025 mmol, 5 mol%) were suspended in triethylamine (10 mL) and THF (2 mL). Trimethylsilylacetylene (98.2 mg, 1.00 mmol, 2.00 eq.) was added and the mixture was stirred at 25 °C for 19 h. After removing the solids by filtration, the volatiles were evaporated in vacuo and the residue was purified by filtration over silica (eluent: *n*-pentane, R_f = 0.90). Pale yellow crystals (121 mg, 57%) were obtained.

^{1}H NMR (500 MHz, $CDCl_3$): δ = 7.67 (s, 2H, a), 0.27 (s, 18H, f) ppm.

^{13}C{^{1}H} NMR (126 MHz, $CDCl_3$): δ = 136.6 (a), 126.6 (c), 123.9 (b), 103.2 (e), 101.5 (d), -0.2 (f) ppm.

^{29}Si{^{1}H} NMR (99 MHz, $CDCl_3$): δ = -16.4 ppm.

IR (ATR): $\tilde{\nu}$ [cm^{-1}] = 2958 (w), 2926 (w), 2900 (w), 2854 (w), 2159 (w), 1460 (m), 1411 (w), 1339 (m), 1264 (m), 1249 (m), 1063 (m), 842 (s), 759 (s), 737 (s), 702 (s), 660 (m).

HR-MS (EI, 70 eV, R ~ 10 000): *m/z* calcd. for $C_{16}H_{20}{}^{79}Br_2Si_2$ 425.94648 $[M]^+$, found 425.94643 $[M]^+$.

M.p.: 116 °C, Lit.[15]: 118 °C.

The analytical data are consistent with the literature.

2.27. 6,6'-(2,5-bis((Trimethylsilyl)ethynyl)-1,4-phenylene)bis(1-hydro-2-mesityl-1,2-azaborinine) (18)

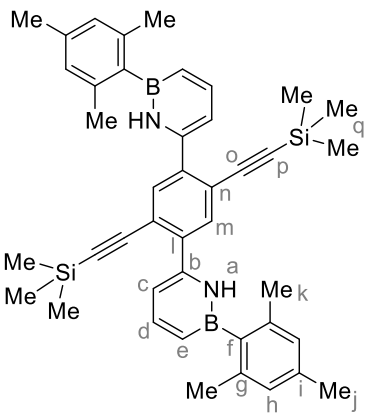

A 2-5 mL microwave vial was charged with 1,4-dibromo-2,5-bis(trimethylsilylethynyl)benzene (**12**, 85.7 mg, 200 µmol, 1.00 eq.) and 2-mesityl-6-(4,4,5,5-tetramethyl-1,3,2-dioxaborolan-2-yl)-1,2-azaborinine (**1**, 155 mg, 480 µmol, 2.40 eq.). In a glovebox, $[Pd(dppf)Cl_2]$ (4.4 mg, 6.00 µmol, 3 mol%), potassium phosphate (127 mg, 600 µmol, 3.00 eq.) and MTBE (8.4 mL) were added. Outside the box, degassed water (3.6 mL) was added. The reaction was heated at 80 °C for 6 h in a microwave reactor. Then, the mixture was extracted with diethyl ether (5 × 2 mL). The combined organic phases were concentrated in vacuo and the crude residue was purified by column chromatography (silica, eluents: 1% diethyl ether in *n*-pentane, R_f = 0.29). The obtained, still slightly contaminated orange solid was recrystallized from methanol to yield a yellow solid (51.9 mg, 39%).

^{1}H NMR (500 MHz, $CDCl_3$): δ = 8.51 (br s, 2H, a), 7.80 (dd, ^3J = 11.2, 6.9 Hz, 2H, d), 7.71 (s, 2H, m), 6.94 (d, ^3J = 11.2 Hz, 2H, e), 6.88 (s, 4H, h), 6.81 (ddd, ^3J = 6.9 Hz, ^4J = 2.0, 1.1 Hz, 2H, c), 2.30 (s, 6H, j), 2.23 (s, 12H, k), 0.09 (s, 18H, r) ppm.

^{13}C{^{1}H} NMR* (126 MHz, $CDCl_3$): δ = 143.8 (d), 142.1 (b), 140.3 (g), 139.1 (l), 137.4 (i), 135.0 (m), 127.4 (h), 121.1 (n), 111.7 (c), 102.7 (p), 102.5 (o), 23.5 (k), 21.3 (j), -0.4 (q) ppm.

^{11}B{^{1}H} NMR (160MHz, $CDCl_3$): δ = 36.4 ppm.

^{29}Si NMR (99 MHz, $CDCl_3$): δ = -16.7 ppm.

IR (ATR): $\tilde{\nu}$ [cm^{-1}] = 3387 (w), 3022 (w), 2956 (w), 2917 (w), 2360 (w), 2157 (w), 1609 (m), 1542 (s), 1449 (m), 1414 (m), 1264 (s), 1249 (s), 1153 (w), 1000 (m), 859 (s), 842 (s), 776 (s), 730 (s), 721 (s).

HR-MS (EI, 70 eV, R ~ 10 000): *m/z* calcd. for $C_{42}H_{50}{}^{11}B_2N_2Si_2$ 660.37079 $[M]^+$, found 660.37005 $[M]^+$.

M.p.: 219 °C.

* The signals of carbons e and f were not detected because of the low quadrupole moment of the ^{11}B nucleus.

2.28. 1,8-Dihydro-2,9-dimesityl-1,8-diaza-2,9-diboradibenz[*a,h*]anthracene (*BN*-PAH5)

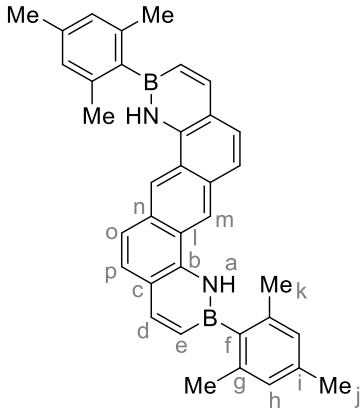

6,6'-(2,5-bis((Trimethylsilyl)ethynyl)-1,4-phenylene)bis(1-hydro-2-mesityl-1,2-azaborinine) (**18**, 49.6 mg, 75.0 µmol) was dissolved in methanol (5 mL) and diethyl ether (3 mL). Potassium hydroxide (8.4 mg, 150 µmol) was added and the mixture was stirred for 3 h at 25 °C, when the complete deprotection of the alkyne was confirmed by TLC analysis (eluents: 1% diethyl ether in *n*-pentane, R_f = 0.03, reactant: R_f = 0.29). Water (30 mL) and diethyl ether (30 mL) were added. After the separation of the phases, the organic layer was washed with water (5 × 20 mL) and dried over sodium sulfate. After filtration, the solvent was removed in vacuo. The crude, deprotected alkyne was placed in a pressure tube. In a glovebox, platinum(II) chloride (6.0 mg, 22.5 µmol, 30 mol%) and toluene (10 mL) were added. The mixture was heated at 100 °C for 4 h. After cooling, it was filtered via a PTFE filter (pore size: 0.45 µm), using additional cyclohexane (5 mL). The solvents were removed in vacuo and the crude product was purified by column chromatography (silica, eluents: 2% diethyl ether in *n*-pentane, R_f = 0.30) to yield a yellow solid (19.8 mg, 51%).

^{1}H NMR (601 MHz, $CDCl_3$): δ = 9.14 (br s, 2H, a), 8.79 (s, 2H, m), 8.29 (d, ^3J = 11.3 Hz, 2H, d), 7.79 (d, ^3J = 8.8 Hz, 2H, o), 7.75 (d, ^3J = 8.8 Hz, 2H, p), 7.21 (dd, ^3J = 11.3, ^4J = 1.5 Hz, 2H, e), 7.01 (s, 4H, h), 2.41 (s, 6H, j), 2.31 (s, 12H, k) ppm.

^{13}C{^{1}H} NMR* (126 MHz, $CDCl_3$): δ = 145.9 (d), 140.6 (g), 138.0 (i), 136.2 (b), 132.0 (e), 131.4 (n), 128.1 (p), 127.5 (h), 123.8 (l), 121.9 (o), 120.8 (c), 119.9 (m), 23.4 (k), 21.4 (j) ppm.

^{11}B{^{1}H} NMR (160 MHz, $CDCl_3$): δ = 36.9 ppm.

UV/Vis ($CHCl_3$): λ_{max} (ε) = 316 nm (122343 $mol^{-1}\,dm^3\,cm^{-1}$).

Fluorescence ($CHCl_3$): λ_{ex} = 399.5 nm, λ_{em} = 427 nm.

Fluorescence (solid): λ_{ex} = 316 nm, λ_{em} = 487 nm.

IR (ATR): $\tilde{\nu}$ [cm^{-1}] = 3412 (w), 3391 (w), 2954 (w), 2917 (m), 2853 (w), 1610 (m), 1578 (s), 1539 (w), 1524 (m), 1422 (m), 1370 (m), 1143 (m), 1017 (m), 863 (s), 847 (m), 790 (m), 711 (s).

HR-MS (EI, 70 eV, R ~ 10 000): *m/z* calcd. for $C_{36}H_{34}{}^{11}B_2N_2$ 516.29146 $[M]^+$, found 516.29128 $[M]^+$.

M.p.: 355 °C (decomposes).

* The signal of carbon f was not detected because of the low quadrupole moment of the ^{11}B nucleus.

2.29. (2,5-Dibromophenyl)-2-(hydroxyimino)acetamide (38)[16]

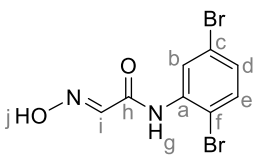

This reaction was not performed under inert conditions.

2,5-Dibromoaniline (**7**, 8.23 g, 32.8 mmol, 1.0 eq.), chloral hydrate (6.50 g, 39.3 mmol, 1.2 eq.), hydroxylamine hydrochloride (3.42 g, 49.1 mmol, 1.5 eq.) and sodium sulfate (39.6 g, 279 mmol) were dissolved in water (200 mL) and abs. ethanol (200 mL). The mixture was stirred at 80 °C for 23 h. Approx. 150 mL of the solvent were removed in vacuo. A precipitate formed, which was washed with a mixture of ethyl

acetate and cyclohexane (1:10, ca. 300 mL) and the product was dried in vacuo. A colorless solid was obtained (9.23 g, 87%, Lit.[16]: 72%).

^{1}H NMR (601 MHz, DMSO-d_6): δ = 12.54 (s, 1H, j), 9.49 (s, 1H, g), 8.15 (d, ^4J = 2.4 Hz, 1H, b), 7.67 (s, 1H, i), 7.65 (d, ^3J = 8.5 Hz, 1H, e), 7.35 (dd, ^3J = 8.5, ^4J = 2.4 Hz, 1H, d) ppm.

^{13}C{^{1}H} NMR (151 MHz, DMSO-d_6): δ = 160.5 (h), 143.2 (i), 136.8 (a), 134.2 (e), 129.2 (d), 126.6 (b), 120.6 (c), 115.1 (f) ppm.

IR (ATR): $\tilde{\nu}$ [cm^{-1}] = 3339 (w), 3149 (w), 3042 (w), 3002 (w), 2866 (w), 1660 (s), 1613 (m), 1583 (s), 1529 (m), 1403 (s), 1241 (m), 1032 (s), 1022 (s), 791 (s), 771 (m), 681 (m).

HR-MS (EI, 70 eV, R ~ 10 000): *m/z* calcd. for $C_8H_6{}^{79}Br_2N_2O_2$ 319.87905 $[M]^+$, found 319.87927 $[M]^+$.

M.p.: 190 °C.

The analytical data are consistent with the literature.[16]

2.30. 4,7-Dibromoindolin-2,3-dione (39)[16]

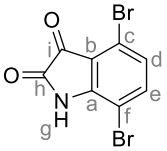

This reaction was not performed under inert conditions.

Concentrated sulfuric acid (30 mL) was heated to 50 °C. (2,5-Dibromophenyl)-2-(hydroxyimino)-acetamide (**38**, 2.67 g, 8.30 mmol) was added in small portions. The mixture was heated to 100 °C for 30 min, before it was poured onto ice water (200 mL). The resulting precipitation was washed with water (200 mL) and dried in vacuo to give an orange solid (2.37 g, 94%, Lit.[16]: 68%).

^{1}H NMR (601 MHz, DMSO-d_6): δ = 11.42 (s, 1H, g), 7.67 (d, ^3J = 8.6 Hz, 1H, e), 7.18 (d, ^3J = 8.6 Hz, 1H, d) ppm.

^{13}C{^{1}H} NMR (151 MHz, DMSO-d_6): δ = 181.1 (i), 159.0 (h), 151.1 (a), 140.6 (e), 127.9 (d), 118.5 (b/c/f)*, 118.4 (b/c/f)*, 103.4 (b/c/f)* ppm.

IR (ATR): $\tilde{\nu}$ [cm^{-1}] = 3153 (w), 3089 (w), 1743 (s), 1596 (s), 1567 (s), 1458 (s), 1385 (m), 1300 (s), 1256 (s), 1216 (m), 1189 (m), 1144 (s), 1110 (m), 902 (s), 820 (s), 702 (s).

HR-MS (EI, 70 eV, R ~ 10 000): *m/z* calcd. for $C_8H_3{}^{79}Br_2NO_2$ 302.85250 $[M]^+$, found 302.85229 $[M]^+$.

M.p.: 277 °C (decomposes).

The analytical data are consistent with the literature.[16]

* No assignment could be performed because of equal correlations in the 2D NMR spectra.

2.31. 2-Amino-3,6-dibromobenzoic acid (40)[16]

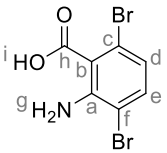

This reaction was not performed under inert conditions.

4,7-Dibromoindolin-2,3-dione (**39**, 4.47 g, 14.7 mmol) was dissolved in aq. sodium hydroxide (5% w/w, 100 mL) and heated to 50 °C. Aq. hydrogen peroxide (30% w/w, 100 mL) was added via a dropping funnel over the course of 30 min and heating was continued for 30 min at the same temperature. Diluted hydrochloric acid (2 M) was added until pH 4. The resulting precipitation was filtered and dried in vacuo to give a beige solid (3.12 g, 72%, Lit.[16] 65%).

^{1}H NMR (601 MHz, DMSO-d_6): δ = 13.71 (br s, 1H, i), 7.37 (d, ^3J = 8.4 Hz, 1H, e), 6.78 (d, ^3J = 8.4 Hz, 1H, d), 5.55 (br s, 2H, g) ppm.

^{13}C{^{1}H} NMR (151 MHz, DMSO-d_6): δ = 167.3 (h), 144.2 (a), 134.4 (e), 121.1 (d), 120.9 (b/c/f)*, 119.0 (b/c/f)*, 107.9 (b/c/f)* ppm.

IR (ATR): $\tilde{\nu}$ [cm^{-1}] = 3470 (w), 3456 (w), 3344 (m), 2981 (w), 1651 (s), 1586 (s), 1552 (s), 1524 (s), 1459 (w), 1435 (s), 1301 (s), 1248 (s), 1098 (m), 1058 (s), 883 (s), 834 (s), 809 (s), 794 (s), 712 (s).

HR-MS (EI, 70 eV, R ~ 10 000): *m/z* calcd. for $C_7H_5{}^{79}Br_2NO_2$ 292.86815 $[M]^+$, found 292.86761 $[M]^+$.

M.p.: 150 °C (decomposes).

The analytical data are consistent with the literature.[16]

* No assignment could be performed because of equal correlations in the 2D NMR spectra.

2.32. 1,4-Dibromo-2,3-diiodobenzene (41)[16]

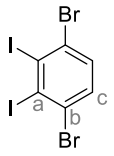

A solution of 2-amino-3,6-dibromobenzoic acid (**40**, 1.52 g, 5.00 mmol, 1.0 eq.) in THF (10.0 mL) was added dropwise over the course of 5 min to a refluxing mixture of iodine (1.90 g, 7.50 mmol, 1.5 eq.) and isopentyl nitrite (879 mg, 7.50 mmol, 1.5 eq.) in dry and degassed 1,2-dichloroethane (120 mL). Stirring was continued at this temperature for 1 h. A sat. aq. solution of sodium thiosulfate (20 mL) was added. The mixture was washed with water (2 × 30 mL). The organic layer was dried over sodium sulfate, filtered, and the solvents were removed in vacuo. By-products were removed by subjecting the crude product to column chromatography (silica, eluent: cyclohexane) and subsequent Kugelrohr distillation (100 °C, 0.07 mbar). Remaining sulfur was removed by heating the crude product with triphenylphosphine (800 mg, 3.05 mmol) in chloroform at 80 °C for 30 min. Filtration over silica (eluent: DCM) and evaporation of the solvent in vacuo gave the product as a colorless solid (534 mg, 22%, Lit.[16]: 65%).

^{1}H NMR (601 MHz, $CDCl_3$): δ = 7.50 (s, 2H, c) ppm.

^{13}C{^{1}H} NMR: (151 MHz, $CDCl_3$): δ = 132.9 (c), 127.9 (b), 117.5 (a) ppm.

IR (ATR): $\tilde{\nu}$ [cm^{-1}] = 3088 (w), 2924 (w), 2852 (w), 1532 (m), 1390 (s), 1309 (s), 1145 (s), 1001 (m), 802 (s), 747 (m), 686 (m).

HR-MS: (EI, 70 eV, R ~ 10 000): *m/z* calcd. for $C_6H_2{}^{79}Br_2I_2$ 485.66072 $[M]^+$, found 485.66055 $[M]^+$.

M.p.: 120 °C.

The analytical data are consistent with the literature.[16]

2.33. 1,4-Dibromo-2,3-bis(2-(trimethylsilyl)ethynyl)benzene (13)

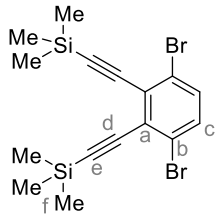

In a glovebox, 1,4-dibromo-2,3-diiodobenzene (**41**, 136 mg, 279 µmol, 1.00 eq.), $Pd(PPh_3)_2Cl_2$ (9.8 mg, 14.0 µmol, 5 mol%) and copper(I) iodide (2.7 mg, 14.0 µmol, 5 mol%) were suspended in triethylamine (5 mL) and THF (5 mL). Trimethylsilylacetylene (54.8 mg, 558 µmol, 2.00 eq.) was added and the mixture was stirred at 80 °C for 3 d. The mixture was filtered and the solvents were removed in vacuo. The residue was subjected to column chromatography (eluent: cyclohexane, R_f = 0.34) to yield a yellow oil (50.5 mg, 42%).

^{1}H NMR (601 MHz, $CDCl_3$): δ = 7.35 (s, 2H, c), 0.29 (s, 18H, f) ppm.

^{13}C{^{1}H} NMR (151 MHz, $CDCl_3$): δ = 132.7 (c), 129.3 (a), 124.7 (b), 105.7 (e), 101.3 (d), 0.0 (f) ppm.

^{29}Si{^{1}H} NMR (99 MHz, $CDCl_3$): δ = -16.5 ppm.

IR (ATR): $\tilde{\nu}$ [cm^{-1}] = 2958 (m), 2924 (w), 2899 (w), 2362 (w), 2161 (m), 1429 (s), 1387 (s), 1248 (s), 1210 (w), 1138 (s), 882 (s), 837 (s), 806 (s), 758 (s), 741 (s), 687 (s).

HR-MS (EI, 70 eV, R ~ 10 000): *m/z* calcd. for $C_{16}H_{20}{}^{79}Br_2Si_2$ 425.94648 $[M]^+$, found 425.94632 $[M]^+$.

2.34. 6,6'-(2,3-bis((Trimethylsilyl)ethynyl)-1,4-phenylene)bis(1-hydro-2-mesityl-1,2-azaborinine) (19)

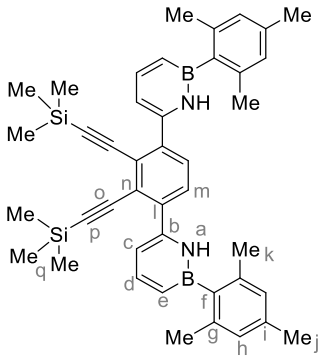

A 20 mL microwave vial was charged with 1,4-dibromo-2,3-bis(2-(trimethylsilyl)-ethynyl)benzene (**13**, 42.8 mg, 100 µmol, 1.00 eq.) and 2-mesityl-6-(4,4,5,5-tetramethyl-1,3,2-dioxaborolan-2-yl)-1,2-azaborinine (**1**, 77.5 mg, 240 µmol, 2.40 eq.). In a glovebox, [Pd(dppf)Cl_2] (2.2 mg, 3.00 µmol, 3 mol%), potassium phosphate (63.7 mg, 300 µmol, 3.00 eq.) and MTBE (7.2 mL) were added. Outside the box, degassed water (3.0 mL) was added. The reaction was heated at 80 °C for 6 h in a microwave reactor. The mixture was extracted with diethyl ether (5 × 2 mL). The combined organic phases were concentrated in vacuo and the crude residue was purified by column chromatography (silica, eluents: 2% diethyl ether in *n*-pentane, R_f = 0.34) to yield a light brown solid (48.0 mg, 73%).

^{1}H NMR (601 MHz, $CDCl_3$): δ = 8.29 (br s, 2H, a), 7.79 (dd, ^3J = 11.1, 6.9 Hz, 2H, d), 7.45 (s, 2H, m), 6.93 (dd, ^3J = 11.1 Hz, ^4J = 1.3 Hz, 2H, e), 6.87 (s, 4H, h), 6.72 (ddd, ^3J = 6.9 Hz, ^4J = 2.2, 1.3 Hz, 2H, c), 2.30 (s, 6H, j), 2.23 (s, 12H, k), 0.11 (s, 18H, q) ppm.

^{13}C{^{1}H} NMR* (151 MHz, $CDCl_3$): δ = 143.7 (d), 142.9 (b), 141.2 (l), 140.3 (g), 137.4 (i), 131.3 (e), 128.8 (m), 127.4 (h), 125.1 (n), 112.0 (c), 105.4 (p), 101.5 (o), 23.5 (k), 21.3 (j), -0.2 (q) ppm.

^{11}B{^{1}H} NMR (160MHz, $CDCl_3$): δ = 36.7 ppm.

^{29}Si NMR (99 MHz, $CDCl_3$): δ = -16.9 ppm.

IR (ATR): $\tilde{\nu}$ [cm^{-1}] = 3392 (w), 3021 (w), 2958 (m), 2920 (w), 2855 (w), 2360 (m), 2342 (m), 2154 (w), 1609 (m), 1541 (s), 1449 (s), 1249 (m), 906 (m), 844 (s), 761 (m), 668 (w).

HR-MS (EI, 70 eV, R ~ 10 000): *m/z* calcd. for $C_{42}H_{50}{}^{11}B_2N_2Si_2$ 660.37079 $[M]^+$, found 660.37031 $[M]^+$.

M.p.: 151 °C.

* The signal of carbon f was not detected because of the low quadrupole moment of the ^{11}B nucleus.

2.35. 1,12-Dihydro-2,11-dimesityl-1,12-diaza-2,11-diborapicene (*BN*-PAH6)

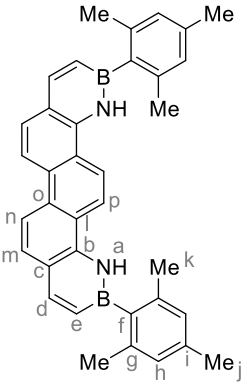

6,6'-(2,3-bis((Trimethylsilyl)ethynyl)-1,4-phenylene)bis(2-mesityl-1,2-azaborinine) (**19**, 43.8 mg, 66.3 µmol) was dissolved in methanol (15.0 mL) and diethyl ether (5.0 mL). Potassium hydroxide (7.4 mg, 133 µmol, 2.00 eq.) was added and the mixture was stirred for 3 h at 25 °C, when the complete deprotection of the alkyne was confirmed by TLC analysis (eluents: 2% diethyl ether in *n*-pentane, R_f = 0.24, reactant: R_f = 0.34). Water (20 mL) and diethyl ether (20 mL) were added. After separation of the phases, the organic layer was washed with water (5 × 20 mL) and dried over sodium sulfate. After filtration, the solvent was removed in vacuo. The crude, deprotected alkyne was placed in a pressure tube. In a glovebox, platinum(II) chloride (5.3 mg, 19.9 µmol, 30 mol%) and toluene (10 mL) were added. The mixture was heated at 100 °C for 4 h. After cooling, it was filtered via a PTFE filter (pore size: 0.45 µm), using additional cyclohexane (5 mL). The solvents were removed in vacuo and the crude product was purified by column chromatography (silica, eluents: 2% diethyl ether in *n*-pentane, R_f = 0.25) to yield a pale yellow solid (5.4 mg, 16%).

^{1}H NMR (601 MHz, $CDCl_3$): δ = 8.94 (br s, 2H, a), 8.61 (d, ^3J = 8.8 Hz, 2H, n), 8.33 (d, ^3J = 11.3 Hz, 2H, d), 8.32 (s, 2H, p), 7.99 (d, ^3J = 8.8 Hz, 2H, m), 7.18 (dd, ^3J = 11.3 Hz, ^4J = 1.6 Hz, 2H, e), 6.98 (s, 4H, h), 2.38 (s, 6H, j), 2.28 (s, 12H, k) ppm.

^{13}C{^{1}H} NMR* (126 MHz, $CDCl_3$): δ = 145.6 (d), 140.5 (g), 138.0 (i), 136.6 (b), 131.7 (e), 130.8 (o), 128.8 (m), 127.5 (h), 122.4 (c), 121.6 (l), 118.4 (p), 116.7 (n), 23.3 (k), 21.4 (j) ppm.

$^{11}B\{^{1}H\}$ NMR (160 MHz, $CDCl_3$): δ = 38.1 ppm.

UV/Vis ($CHCl_3$): λ_{max} (ε) = 341 nm (51736 mol^{-1} dm^3 cm^{-1}).

Fluorescence ($CHCl_3$): λ_{ex} = 340 nm, λ_{em} = 412 nm.

Fluorescence (solid): λ_{ex} = 341 nm, λ_{em} = 417 nm.

IR (ATR): $\tilde{\nu}$ [cm^{-1}] = 3406 (w), 3022 (w), 2920 (m), 2853 (m), 1608 (s), 1598 (s), 1572 (s), 1562 (s), 1441 (s), 1350 (m), 1019 (m), 852 (m), 835 (s), 749 (s), 730 (m), 660 (w).

HR-MS (EI, 70 eV, R ~ 10 000): *m/z* calcd. for $C_{36}H_{34}{}^{11}B_2N_2$ 516.29146 $[M]^+$, found 516.29080 $[M]^+$.

M.p.: 100 – 115 °C (melting range).

* The signal of carbon f was not detected because of the low quadrupole moment of the ^{11}B nucleus.

3. UV-Vis Absorption, Emission and Excitation Spectra

For all optical measurements in solution, stock solutions of the respective compounds were prepared by dissolving an appropriate amount in chloroform (spectral grade, not degassed) and diluting it to obtain different concentrations.

For the determination of the molar extinction coefficients, 1-3 mg of each compound were weighed using a precision balance. A dilution series was prepared to obtain solutions of five different concentrations, which were measured. A linear fitting according to Lambert-Beer law was applied to the resulting absorption curves.

For the determination of the emissions, each compound was not excited at its global absorption maximum but at one of the most bathochromically shifted, local maxima.

Luminescence lifetime curves were fitted with suitable exponential decay functions, depending on whether lifetimes were determined for the regarding compounds in solution (single exponential fit, Equation 1) or in bulk (double exponential fit, Equation 2).

$$A + B1 * e(-\frac{t}{\tau})$$

Equation 1 Single exponential fitting.

$$A + B1 * e\left(-\frac{t}{\tau_1}\right) + B2 * e(-\frac{t}{\tau_2})$$

Equation 2 Double exponential fitting.

When lifetimes were measured on an Edinburgh Instruments FLS 1000 photoluminescence spectrometer, the fittings were performed with the software Fluoracle®. If lifetimes were measured on a Horiba Fluoromax-4 spectrometer, the fittings were generated with Origin.

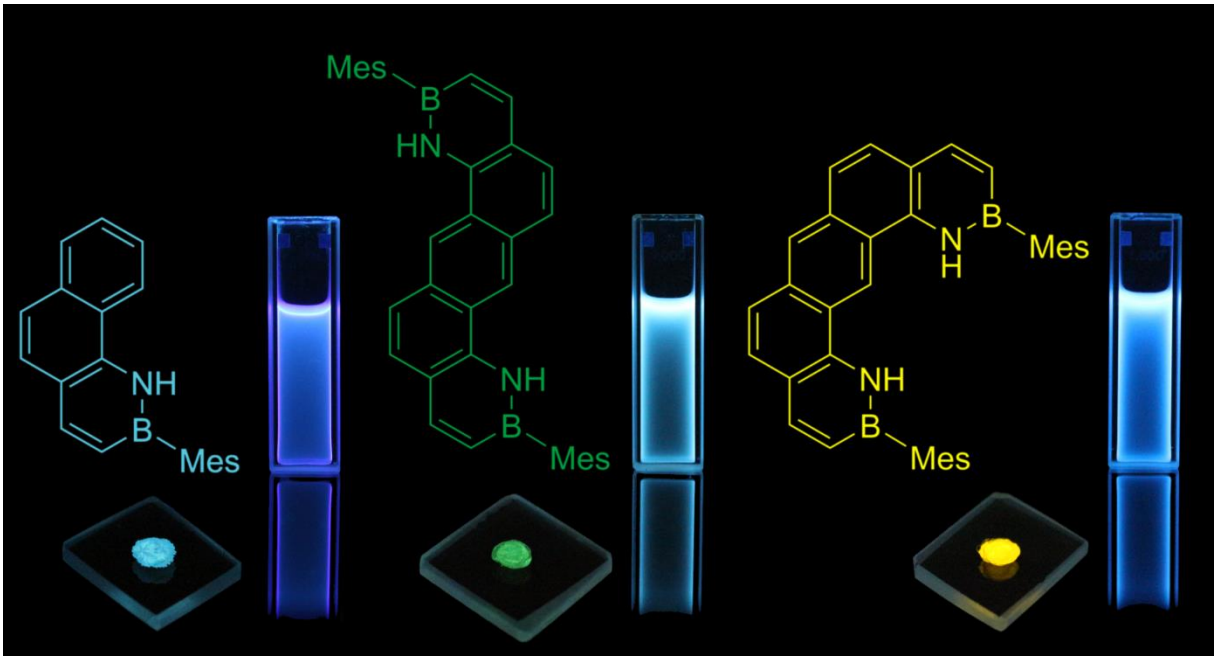

Fig. 1 Photographs of dissolved samples of ***BN*-PAH1**, ***BN*-PAH5** and ***BN*-PAH4** in glass cuvettes (solvent: chloroform) and in solid state on glass slides at irradiation with λ = 365 nm. The thin solid spots were generated by dropcasting from highly concentrated DCM solutions.

3.1. 4-Hydro-3-mesityl-4,3-azaboraphenanthrene (*BN*-PAH1)

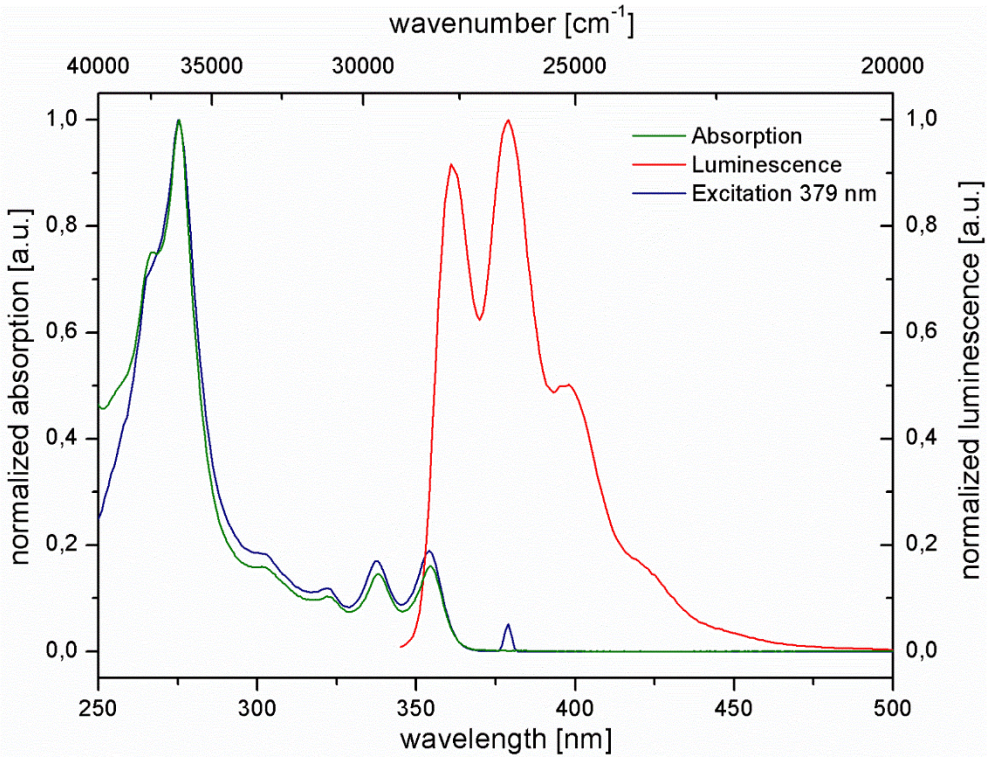

Fig. 2 Normalized absorption (green), luminescence (red) and excitation (blue, emission monochromator set to λ = 379 nm) spectra of ***BN*-PAH1** in chloroform solution. The concentration was 1×10^{-5} mol L^{-1}.

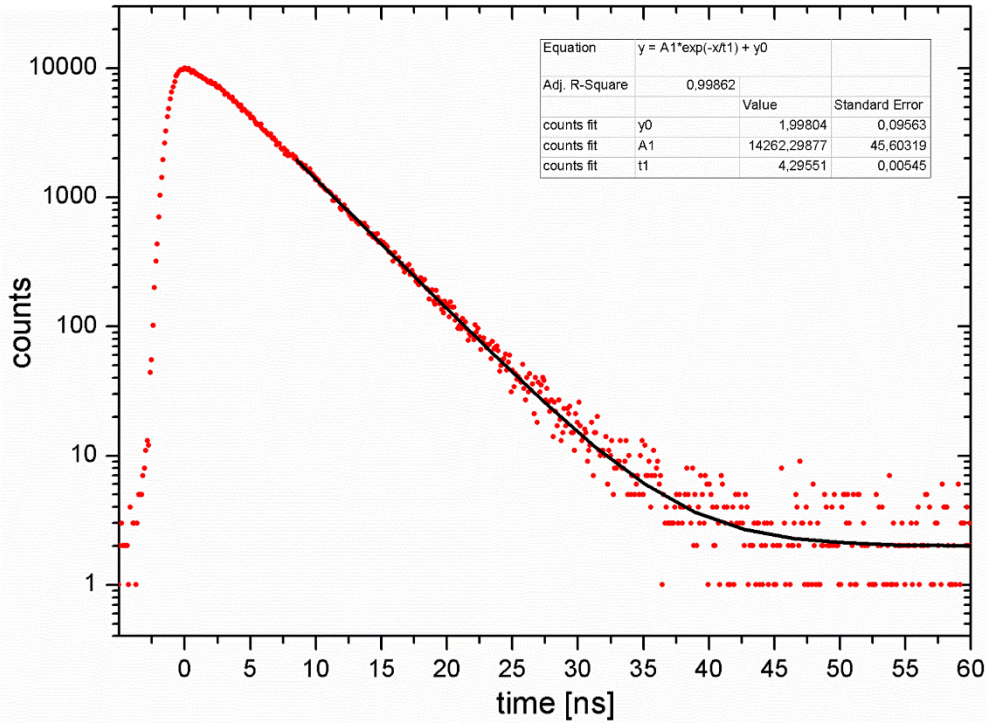

Fig. 3 Luminescence decay curve of ***BN*-PAH1** at an excitation wavelength of λ = 255 nm, measured in chloroform. An exponential fitting gives τ = 4.30 ns.

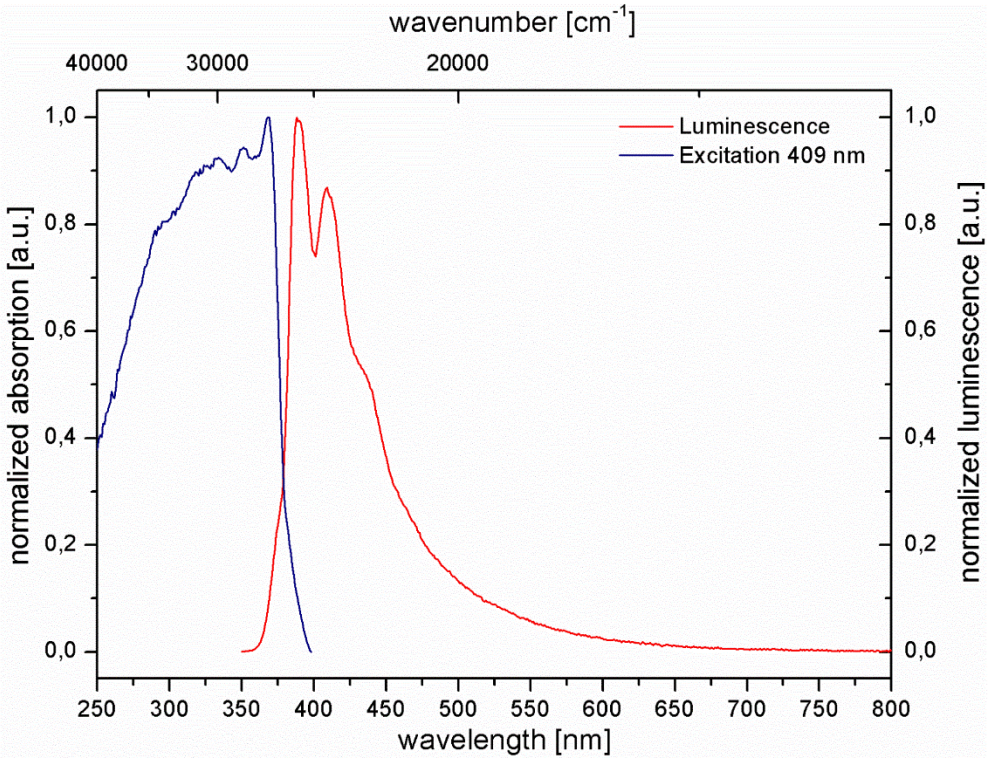

Fig. 4 Luminescence (red) and excitation (blue, emission monochromator set to λ = 409 nm) spectra of ***BN*-PAH1** in solid state. The excitation spectrum is cut from 400 nm to 800 nm because of an intense signal deriving from irradiation in the excitation wavelength.

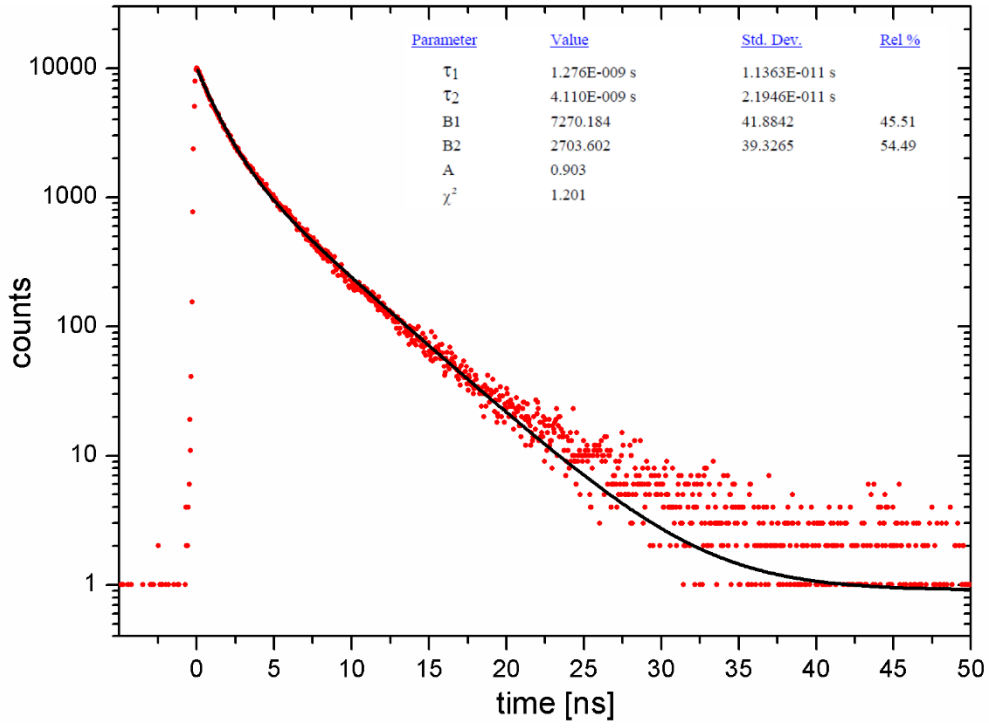

Fig. 5 Luminescence decay curve of ***BN*-PAH1** at an excitation wavelength of λ = 409 nm, measured in chloroform. An exponential fitting gives τ_1 = 1.28 ns and τ_2 = 4.11 ns.

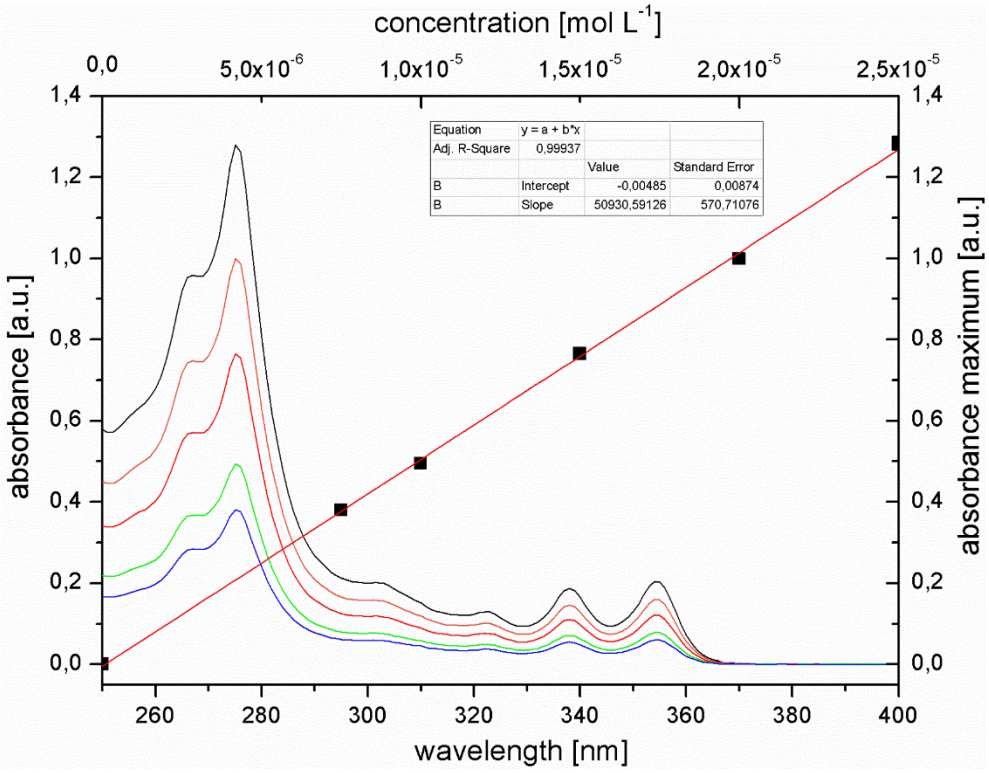

Fig. 6 Absorption spectra of ***BN*-PAH1** in different concentrations (7.5×10^{-6} to 2.5×10^{-5} mol L^{-1}) in chloroform and linear fitting according to Lambert-Beer law.

3.2. 9-Hydro-8-mesityl-9,8-azaboranaphtho[1,2-*b*]thiophene (*BN*-PAH2)

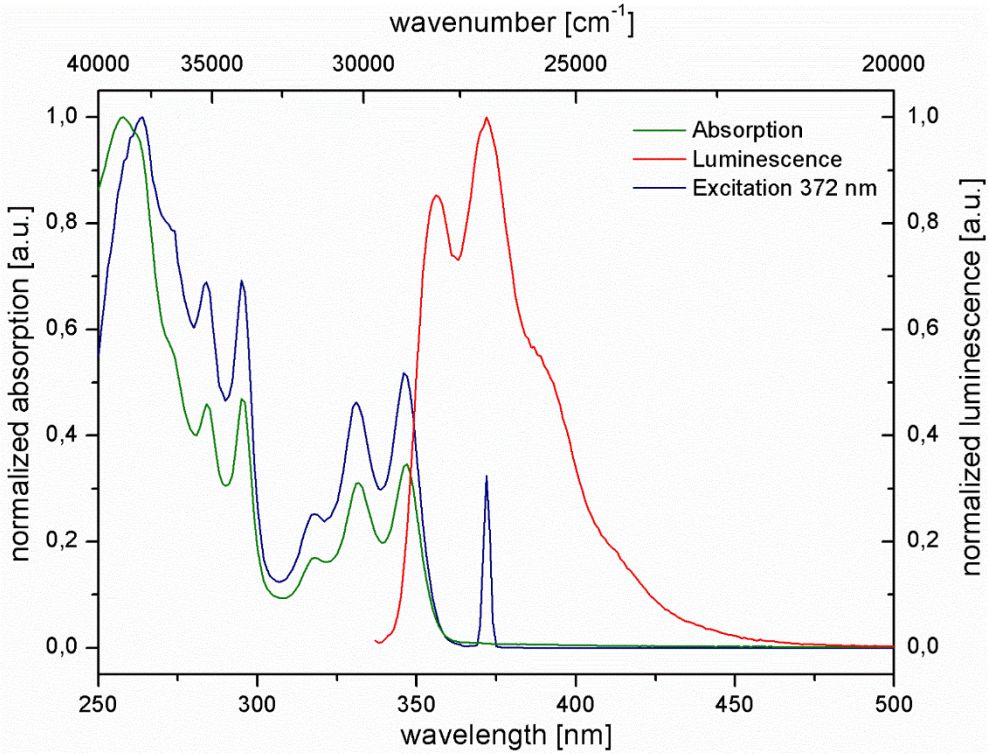

Fig. 7 Normalized absorption (green), luminescence (red) and excitation (blue, emission monochromator set to λ = 372 nm) spectra of ***BN*-PAH2** in chloroform solution. The concentration was 2×10^{-5} mol L^{-1}.

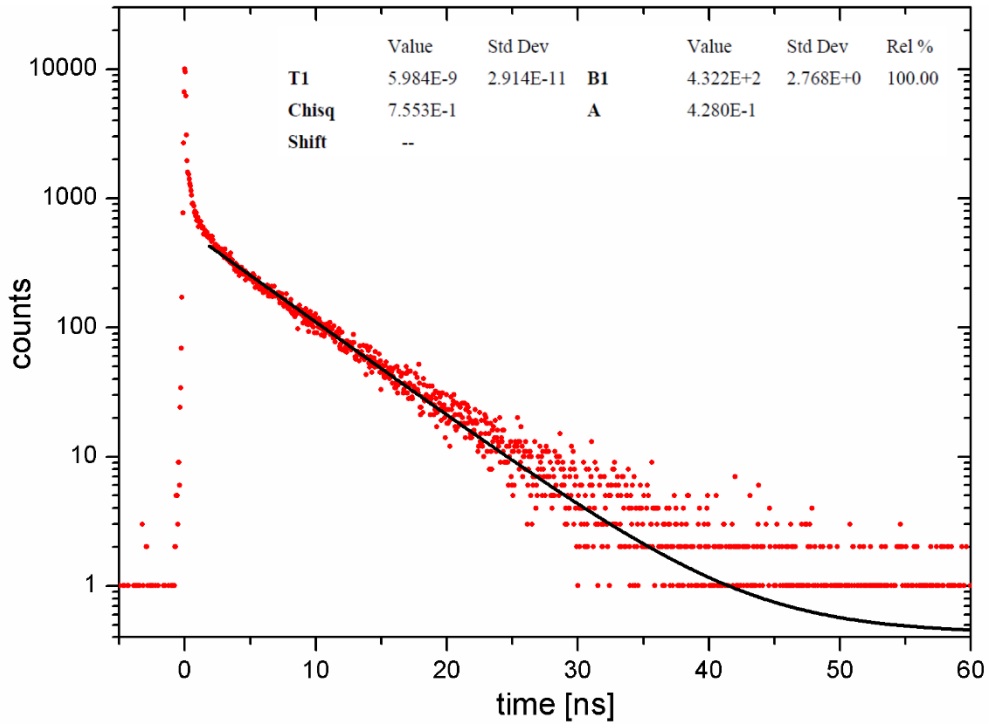

Fig. 8 Luminescence decay curve of ***BN*-PAH2** at an excitation wavelength of λ = 390 nm, measured in chloroform. An exponential fitting gives τ = 5.98 ns.

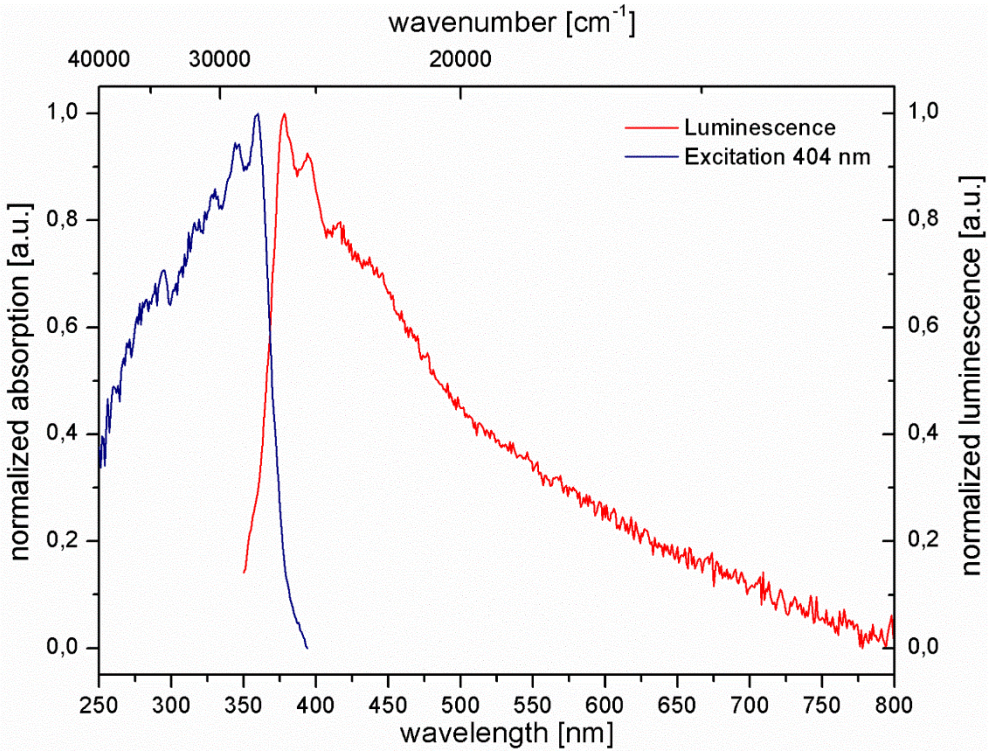

Fig. 9 Luminescence (red) and excitation (blue, emission monochromator set to λ = 404 nm) spectra of ***BN*-PAH2** in solid state. The excitation spectrum is cut from 395 nm to 800 nm because of an intense signal deriving from irradiation in the excitation wavelength.

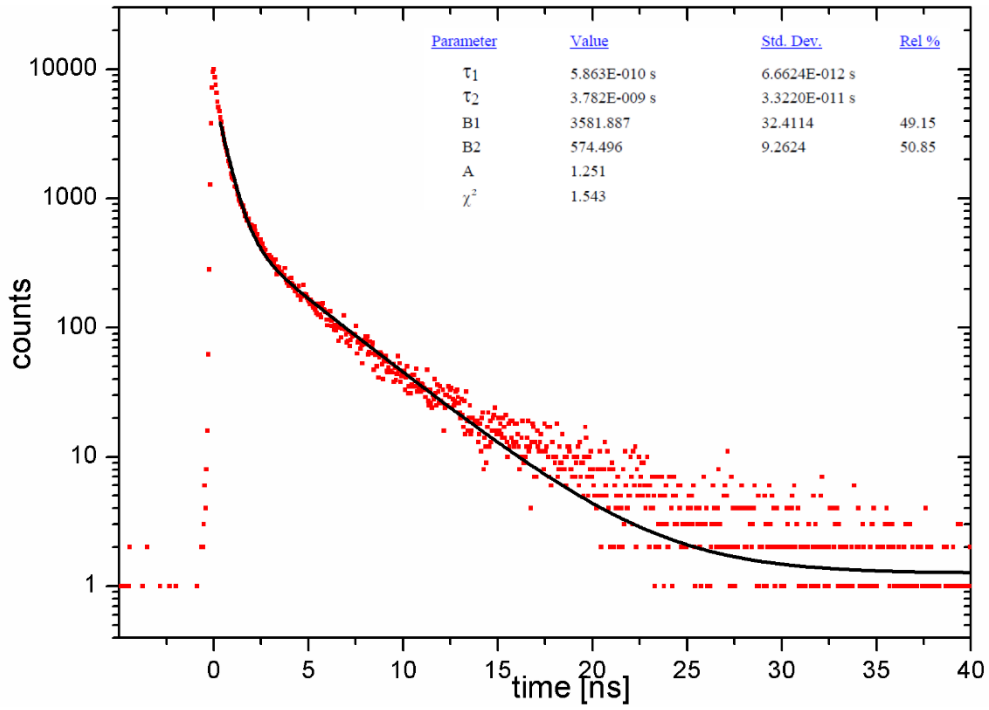

Fig. 10 Luminescence decay curve of ***BN*-PAH2** at an excitation wavelength of λ = 404 nm, measured in chloroform. An exponential fitting gives τ_1 = 0.59 ns and τ_2 = 3.78 ns.

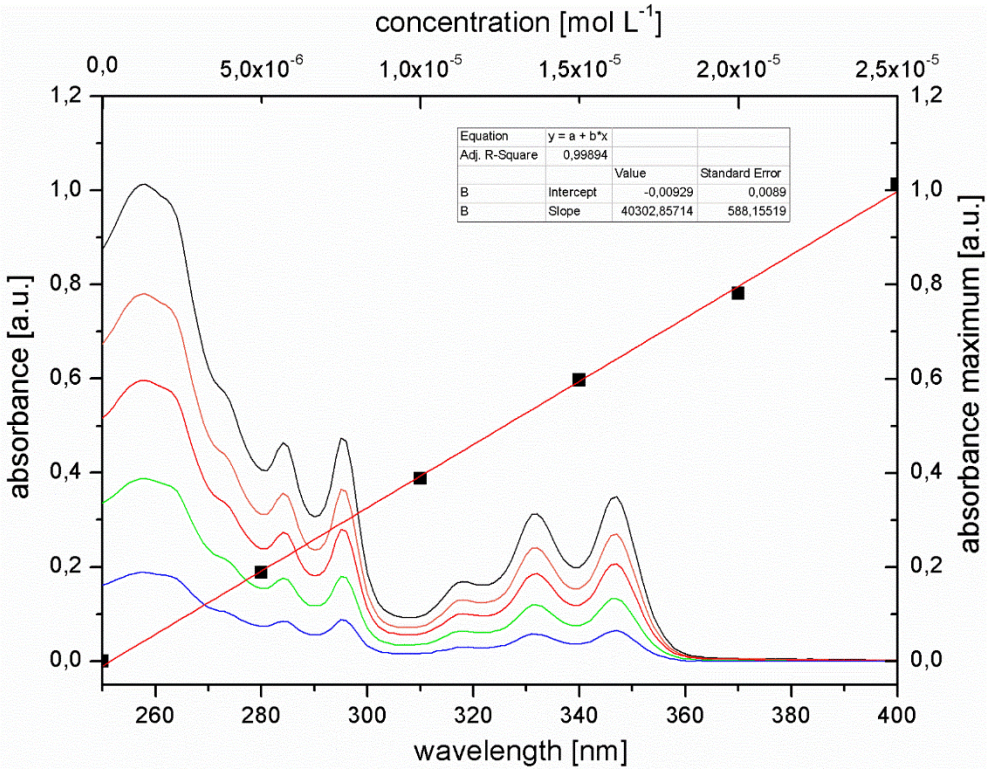

Fig. 11 Absorption spectra of ***BN*-PAH2** in different concentrations (5.0×10^{-6} to 2.5×10^{-5} mol L^{-1}) in chloroform and linear fitting according to Lambert-Beer law.

3.3. 10-Hydro-9-mesityl-10,9-azaborabenzo*[h]*quinoline (*BN*-PAH3)

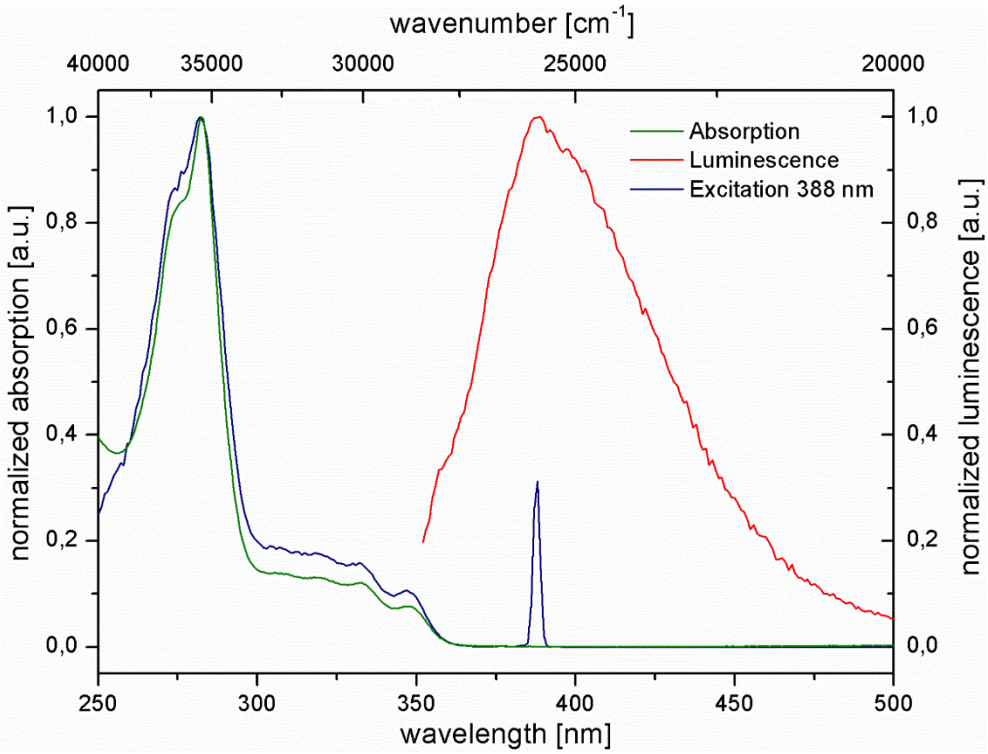

Fig. 12 Normalized absorption (green), luminescence (red) and excitation (blue, emission monochromator set to λ = 388 nm) spectra of ***BN*-PAH3** in chloroform solution. The concentration was 2×10^{-5} mol L^{-1}.

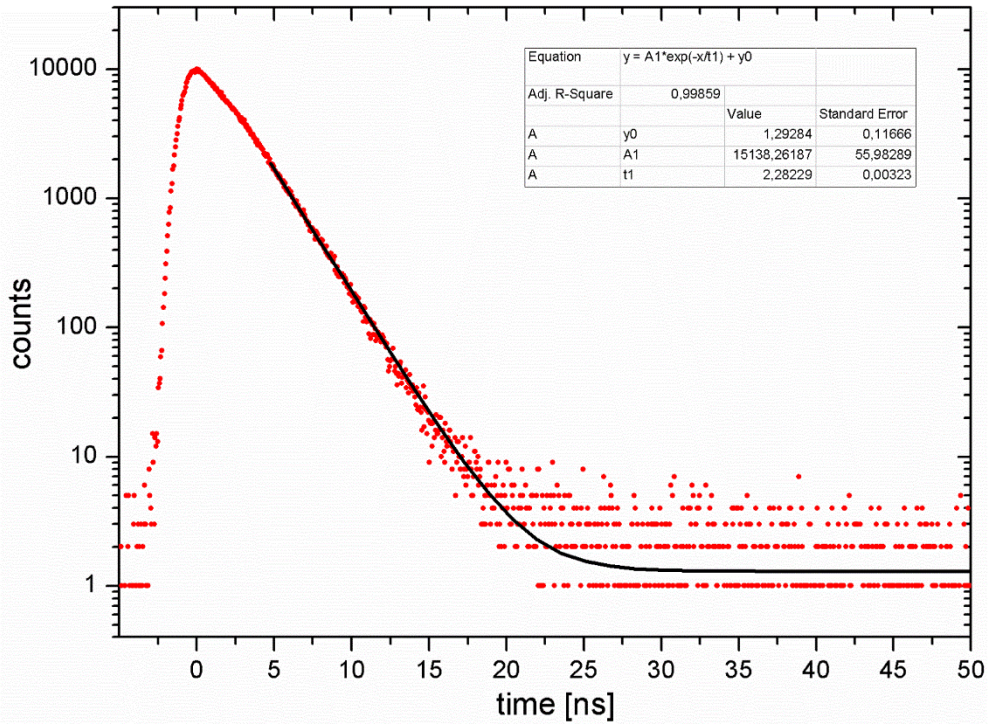

Fig. 13 Luminescence decay curve of ***BN*-PAH3** at an excitation wavelength of λ = 390 nm, measured in chloroform. An exponential fitting gives τ = 2.28 ns.

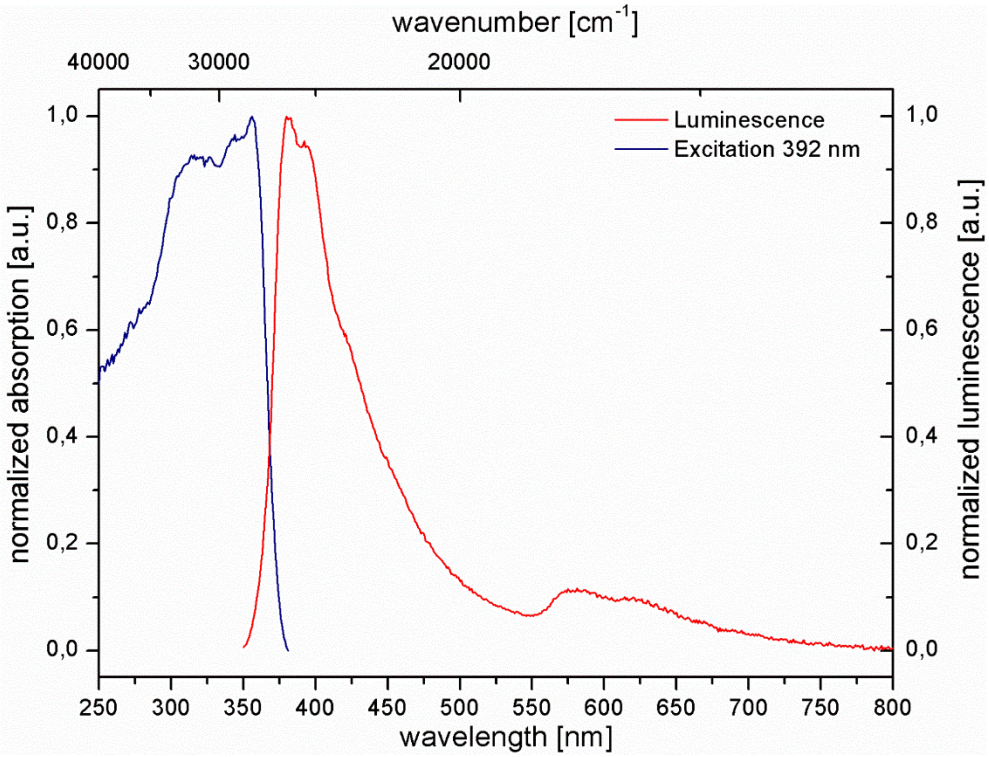

Fig. 14 Luminescence (red) and excitation (blue, emission monochromator set to λ = 392 nm) spectra of ***BN*-PAH3** in solid state. The excitation spectrum is cut from 383 nm to 800 nm because of an intense signal deriving from irradiation in the excitation wavelength.

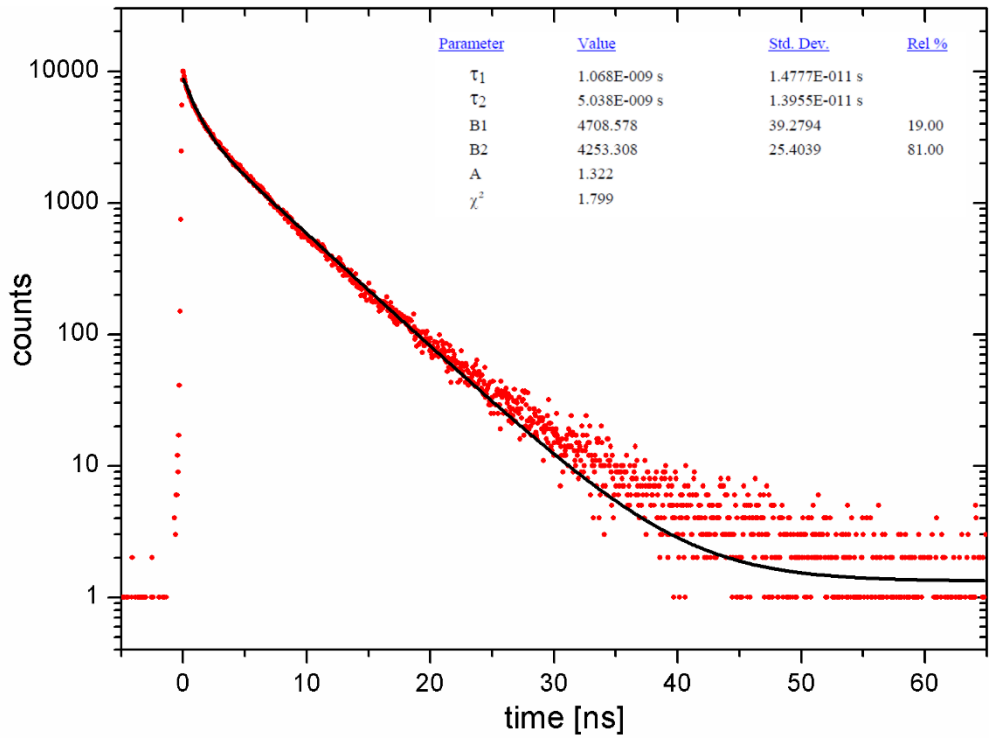

Fig. 15 Luminescence decay curve of ***BN*-PAH3** at an excitation wavelength of = 392 nm, measured in chloroform. An exponential fitting gives τ_1 = 1.07 ns and τ_2 = 5.04 ns.

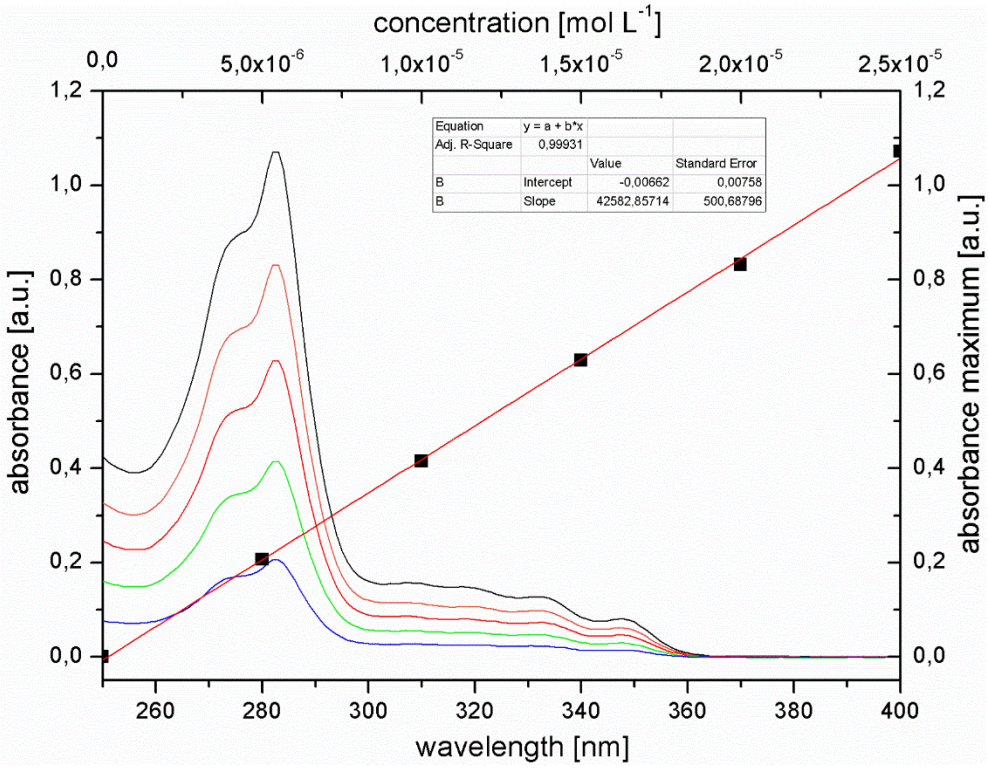

Fig. 16 Absorption spectra of ***BN*-PAH3** in different concentrations (5.0×10^{-6} to 2.5×10^{-5} mol L^{-1}) and linear fitting according to Lambert-Beer law.

3.4. 1,3-Dihydro-2,12-dimesityl-1,13-diaza-2,12-diboradibenz[*a,j*]anthracene (*BN*-PAH4)

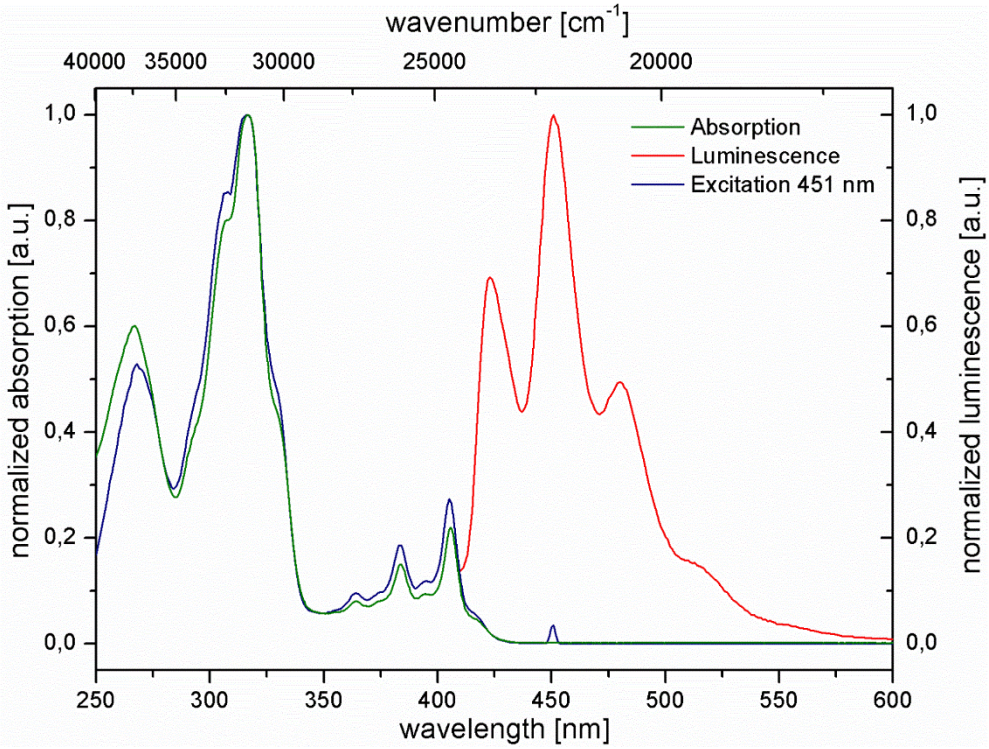

Fig. 17 Normalized absorption (green), luminescence (red) and excitation (blue, emission monochromator set to λ = 451 nm) spectra of ***BN*-PAH4** in chloroform solution. The concentration was 1×10^{-5} mol L^{-1}.

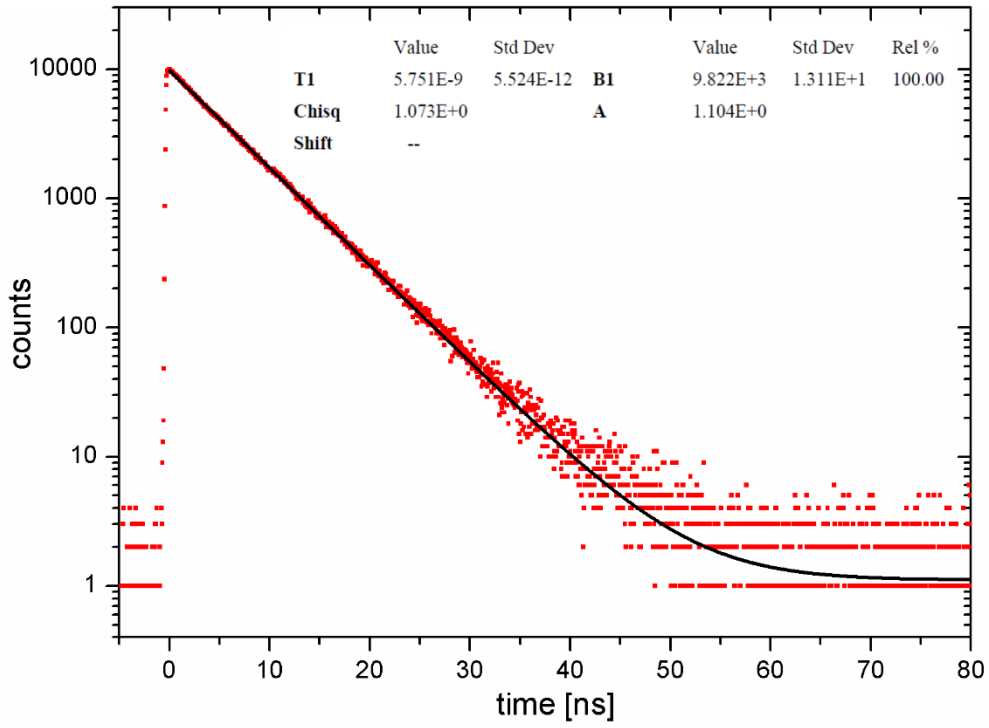

Fig. 18 Luminescence decay curve of ***BN*-PAH4** at an excitation wavelength of λ = 451 nm, measured in chloroform. An exponential fitting gives τ = 5.7 ns.

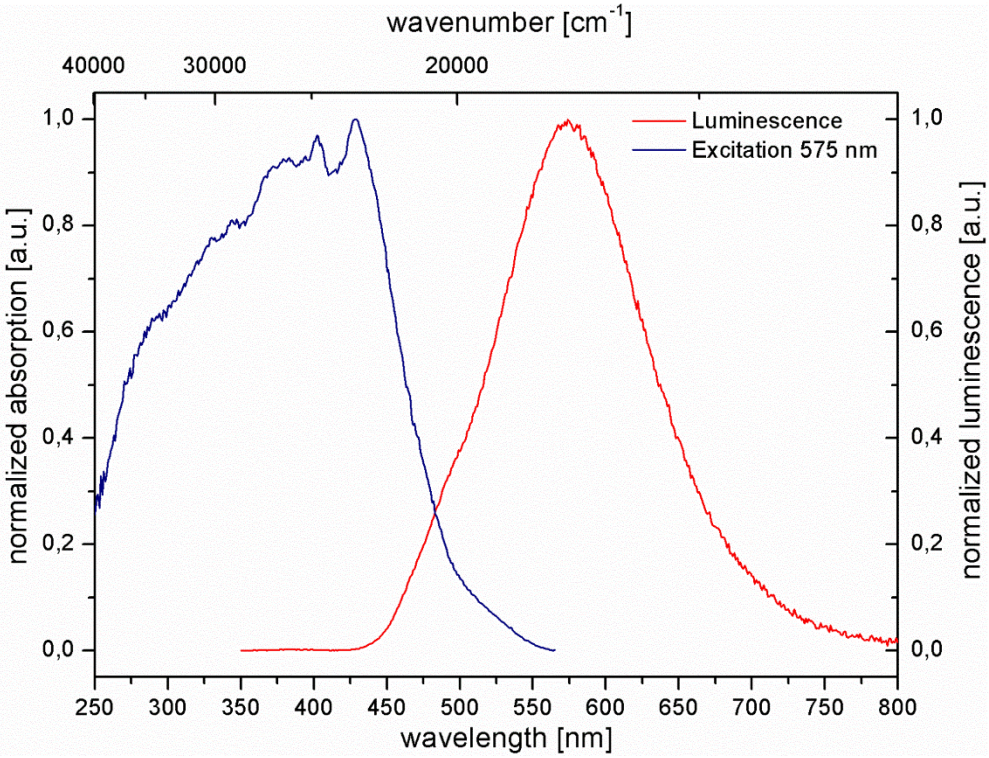

Fig. 19 Luminescence (red) and excitation (blue, emission monochromator set to λ = 575 nm) spectra of ***BN*-PAH4** in solid state. The excitation spectrum is cut from 566 nm to 800 nm because of an intense signal deriving from irradiation in the excitation wavelength.

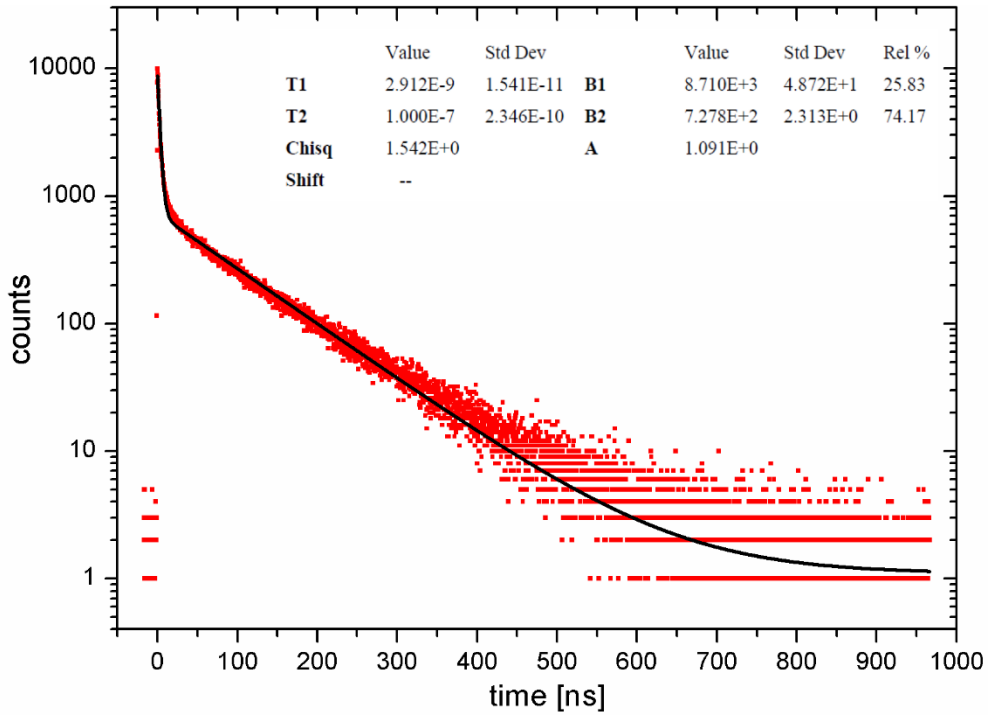

Fig. 20 Luminescence decay curve of ***BN*-PAH4** at an excitation wavelength of λ = 575 nm, measured in chloroform. An exponential fitting gives τ_1 = 2.91 ns and τ_2 = 100 ns.

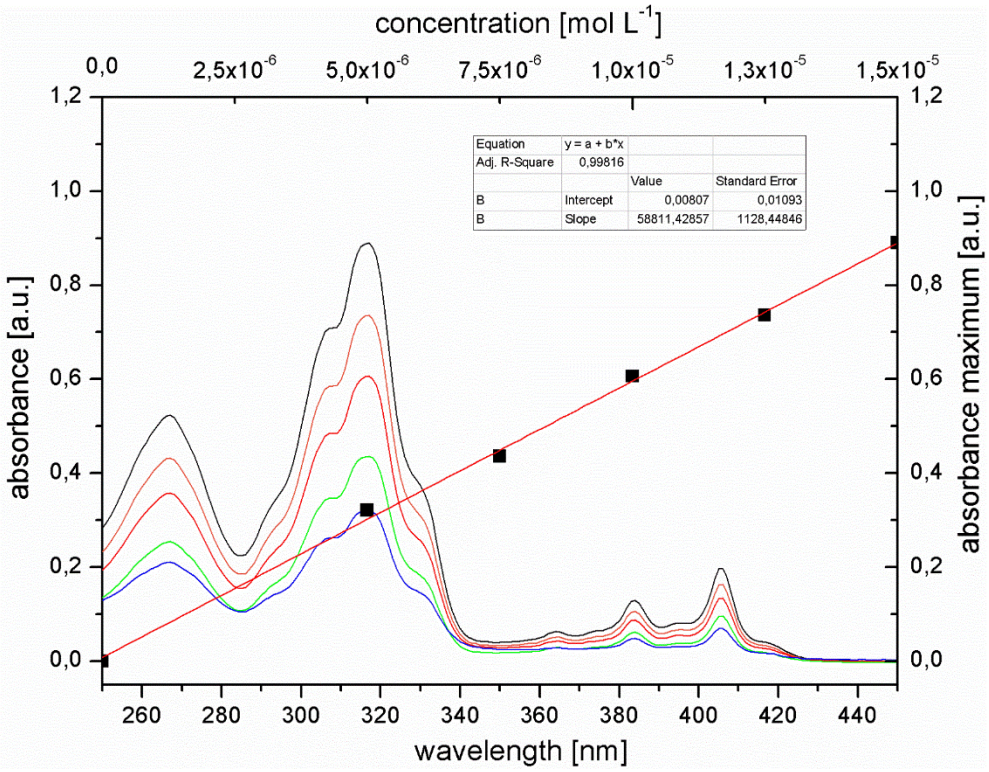

Fig. 21 Absorption spectra of ***BN*-PAH4** in different concentrations (5.0×10^{-6} to 1.5×10^{-5} mol L^{-1}) and linear fitting according to Lambert-Beer law.

3.5. 1,8-Dihydro-2,9-dimesityl-1,8-diaza-2,9-diboradibenz[*a,h*]anthracene (*BN*-PAH5)

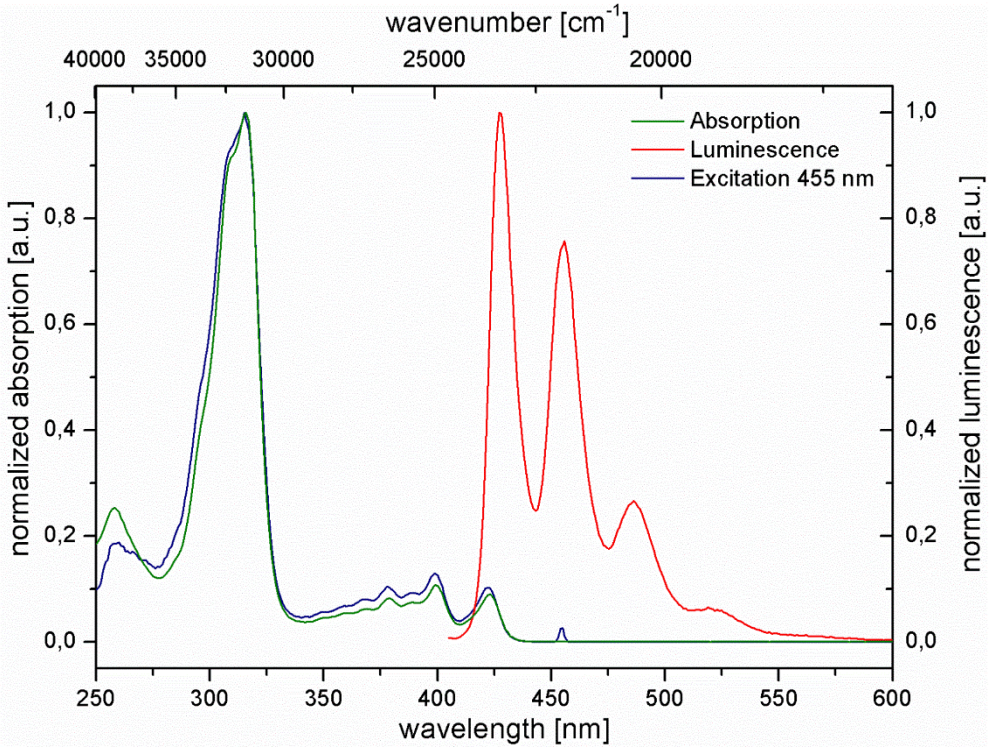

Fig. 22 Normalized absorption (green), luminescence (red) and excitation (blue, emission monochromator set to λ = 455 nm) spectra of ***BN*-PAH5** in chloroform solution. The concentration was 5×10^{-6} mol L^{-1}.

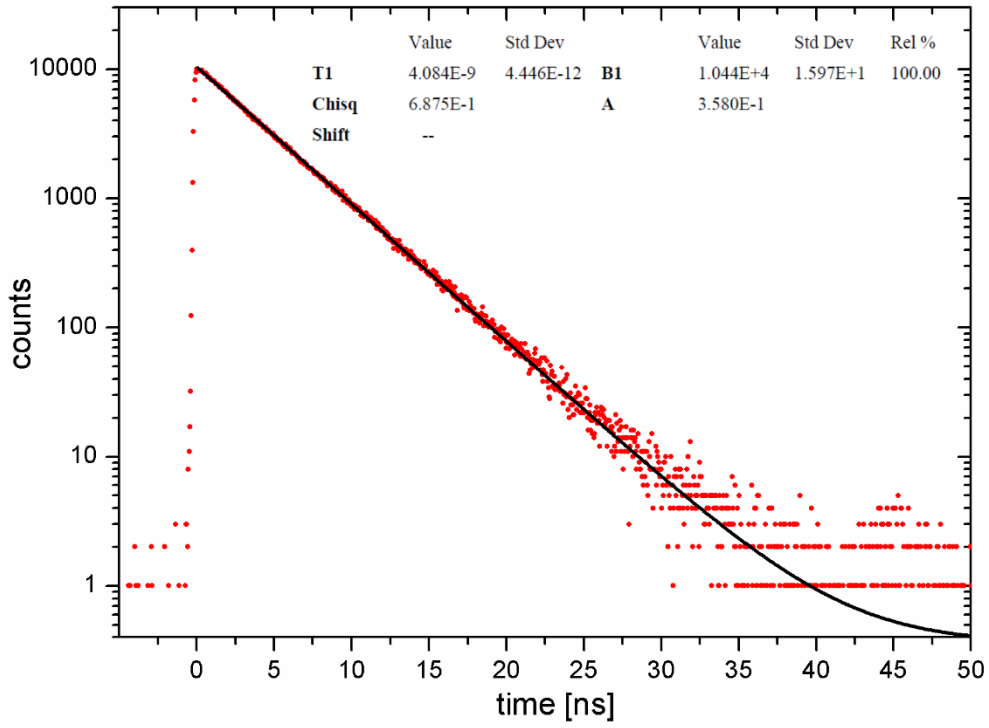

Fig. 23 Luminescence decay curve of ***BN*-PAH5** at an excitation wavelength of λ = 455 nm, measured in chloroform. An exponential fitting gives τ = 4.08 ns.

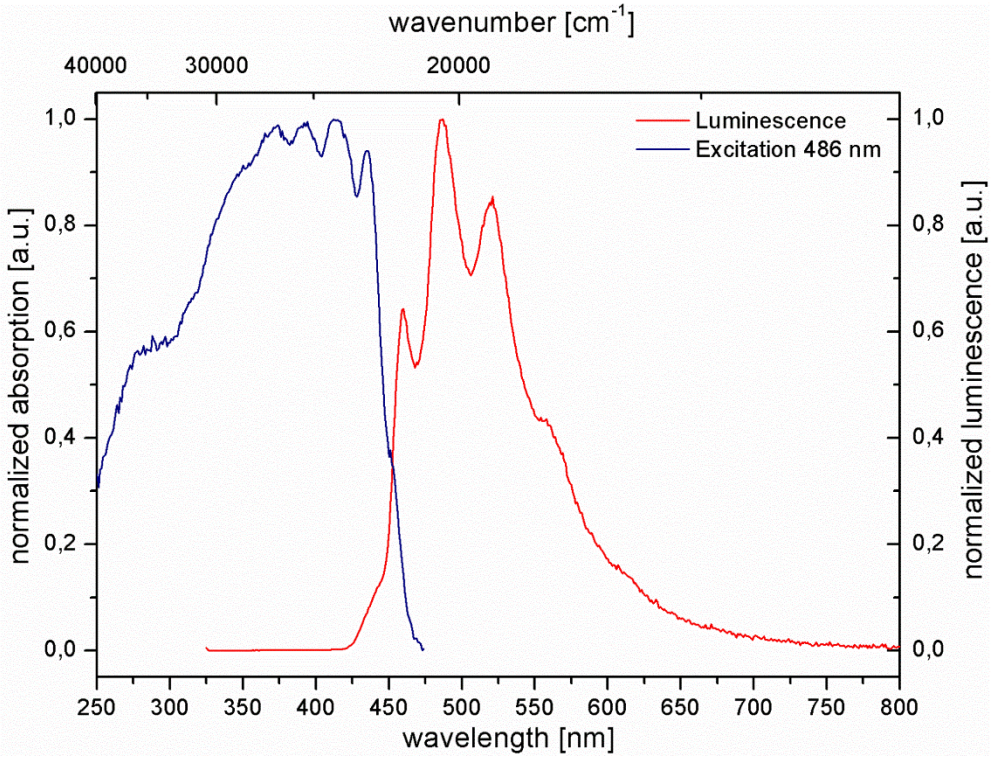

Fig. 24 Luminescence (red) and excitation (blue, emission monochromator set to λ = 486 nm) spectra of ***BN*-PAH5** in solid state. The excitation spectrum is cut from 475 nm to 800 nm because of an intense signal deriving from irradiation in the excitation wavelength.

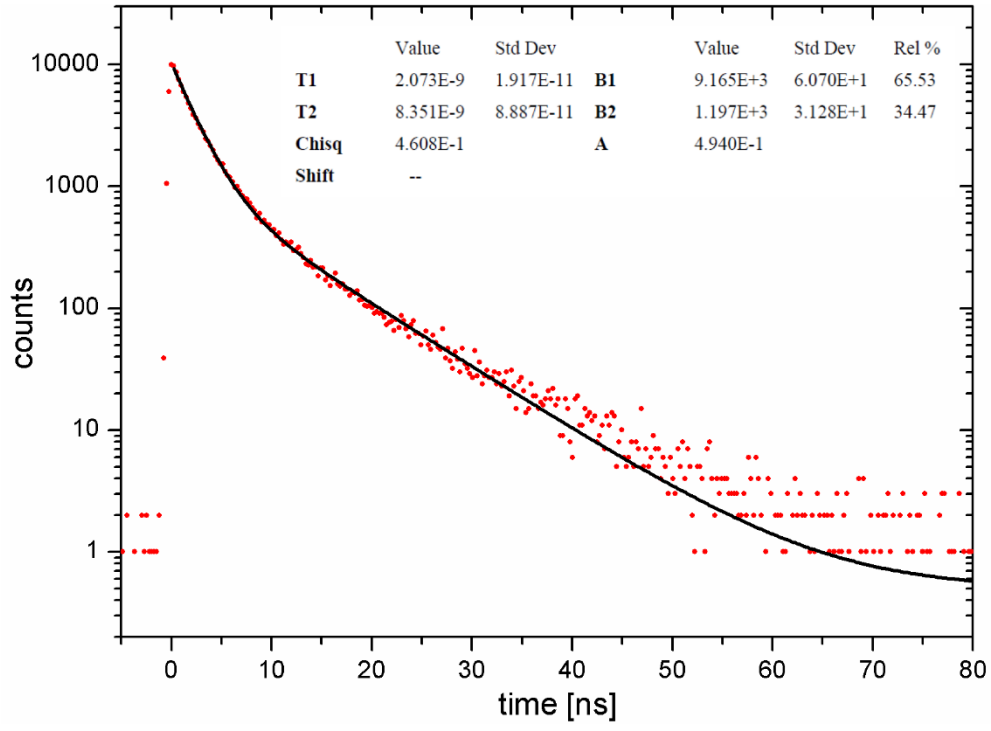

Fig. 25 Luminescence decay curve of ***BN*-PAH5** at an excitation wavelength of λ = 486 nm, measured in chloroform. An exponential fitting gives τ_1 = 2.07 ns and τ_2 = 8.35 ns.

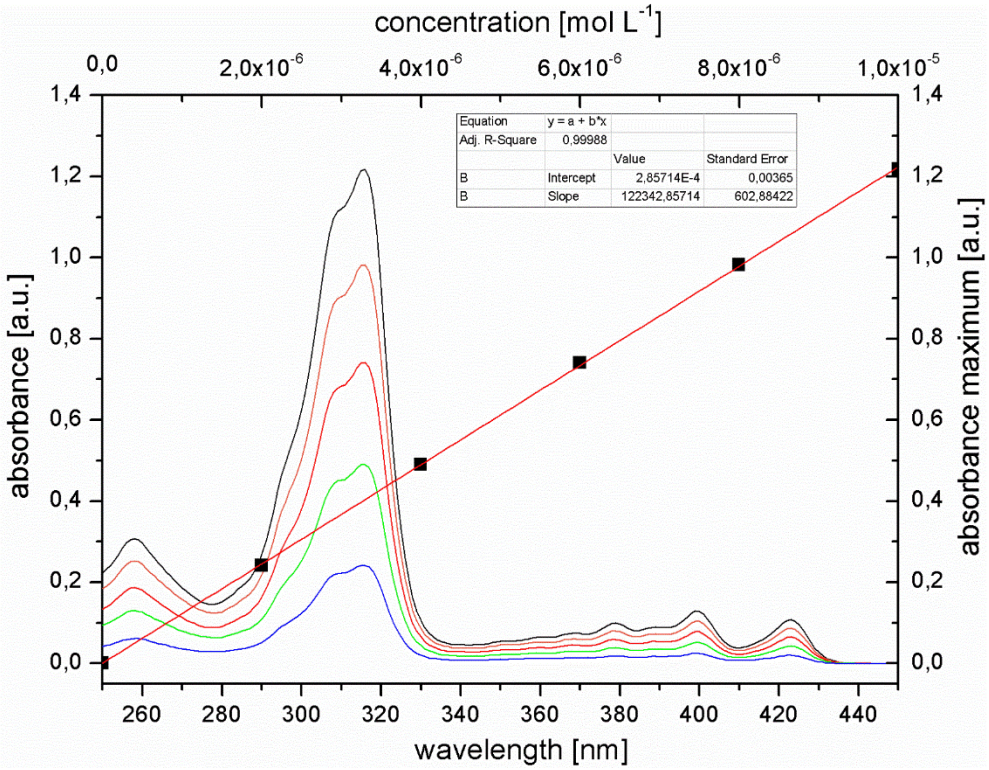

Fig. 26 Absorption spectra of ***BN*-PAH5** in different concentrations (2.0×10^{-6} to 1.0×10^{-5} mol L^{-1}) and linear fitting according to Lambert-Beer law.

3.6. 1,12-Dihydro-2,11-dimesityl-1,12-diaza-2,11-diborapicene (*BN*-PAH6)

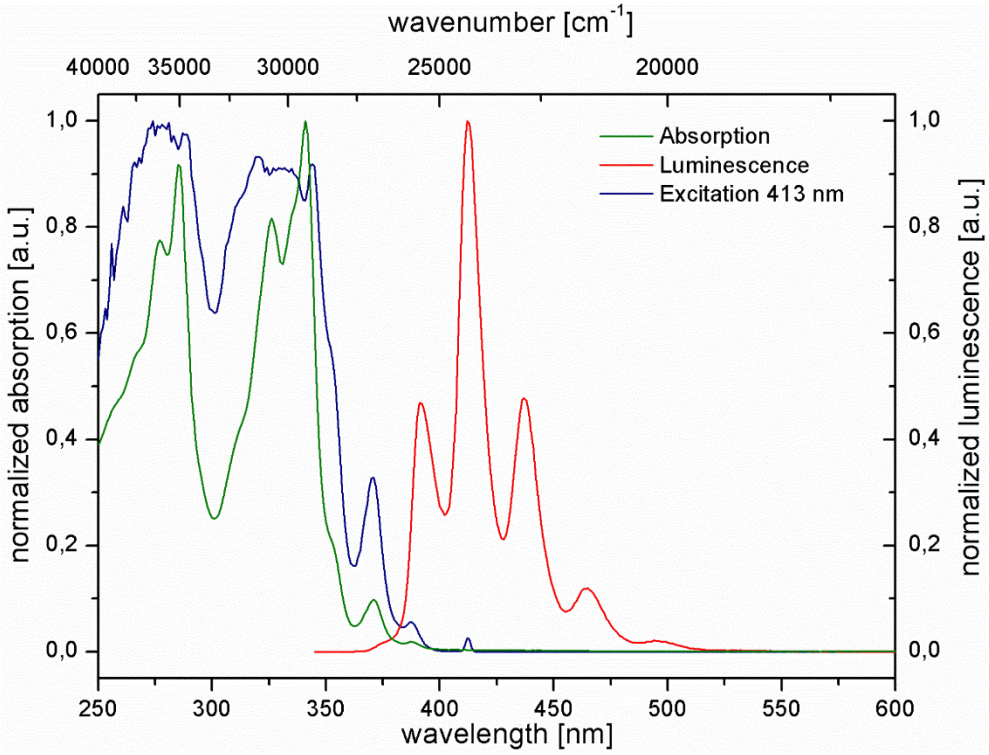

Fig. 27 Normalized absorption (green), luminescence (red) and excitation (blue, emission monochromator set to λ = 413 nm) spectra of ***BN*-PAH6** in chloroform solution. The concentration was 5×10^{-6} mol L^{-1}.

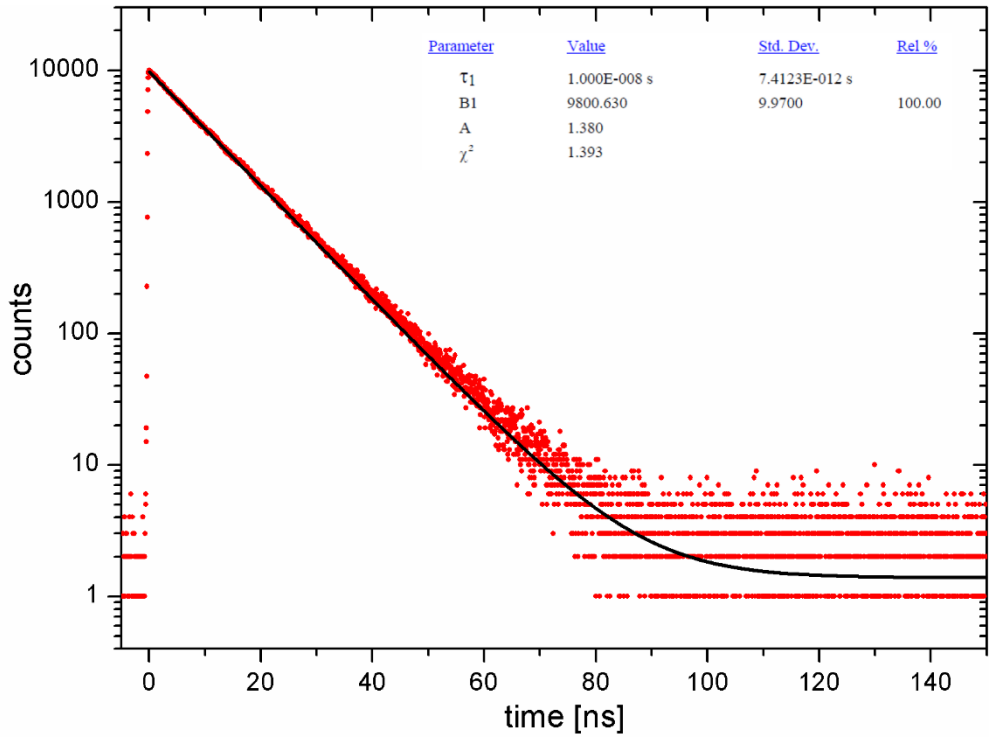

Fig. 28 Luminescence decay curve of ***BN*-PAH6** at an excitation wavelength of λ = 413 nm, measured in chloroform. An exponential fitting gives τ = 10.0 ns.

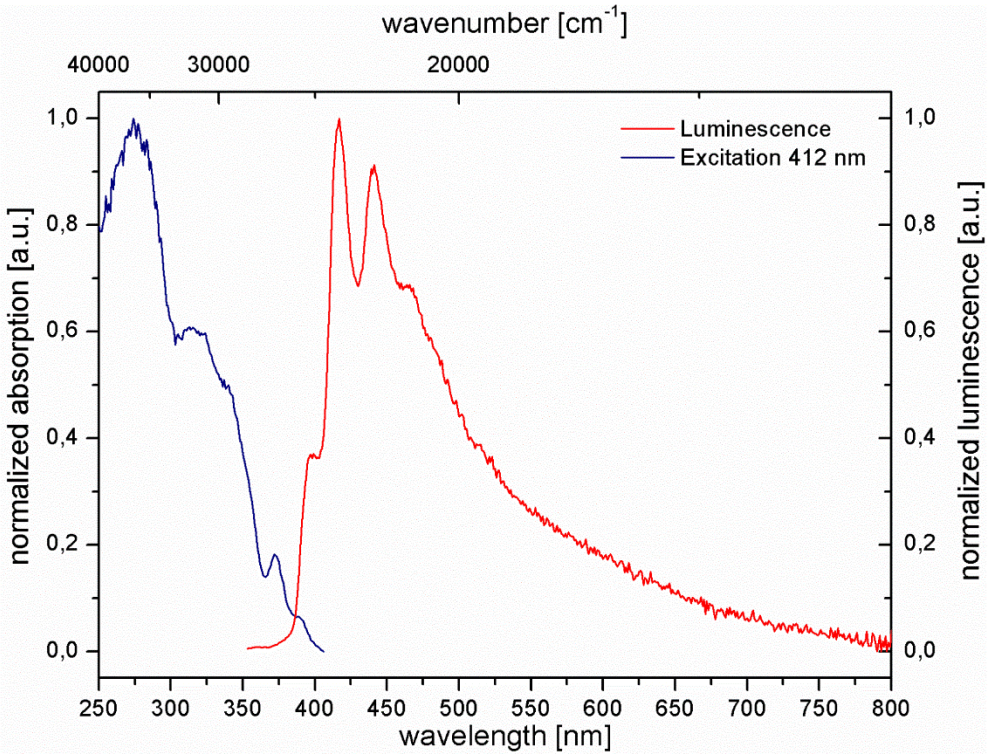

Fig. 29 Luminescence (red) and excitation (blue, emission monochromator set to λ = 412 nm) spectra of ***BN*-PAH6** in solid state. The excitation spectrum is cut from 408 nm to 800 nm because of an intense signal deriving from irradiation in the excitation wavelength.

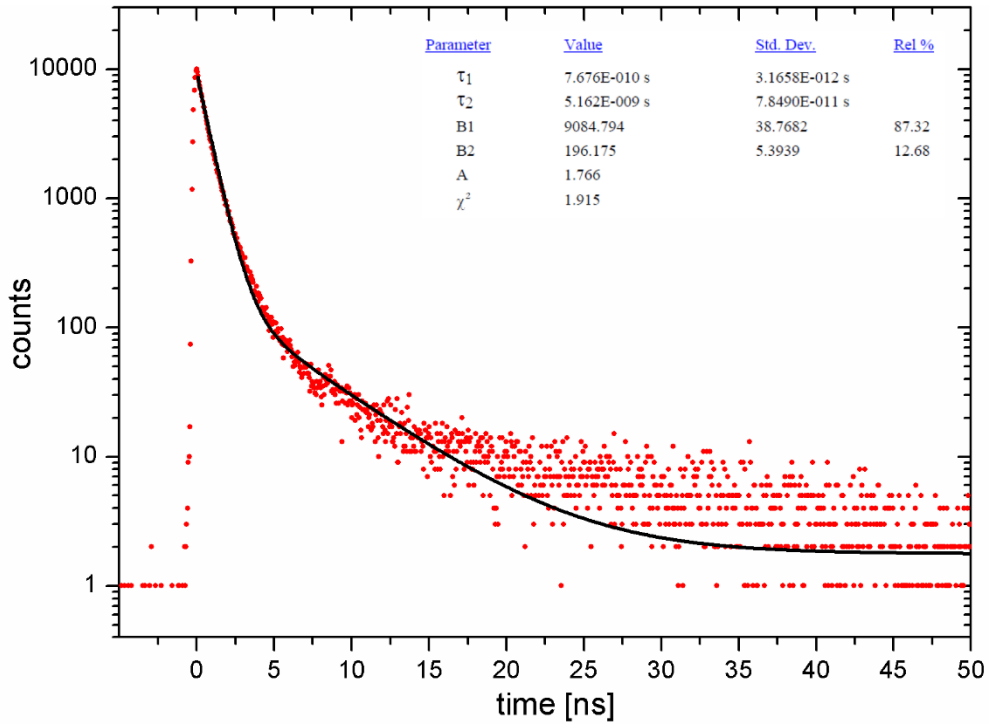

Fig. 30 Luminescence decay curve of ***BN*-PAH6** at an excitation wavelength of λ = 412 nm, measured in chloroform. An exponential fitting gives τ_1 = 0.77 ns and τ_2 = 5.16 ns.

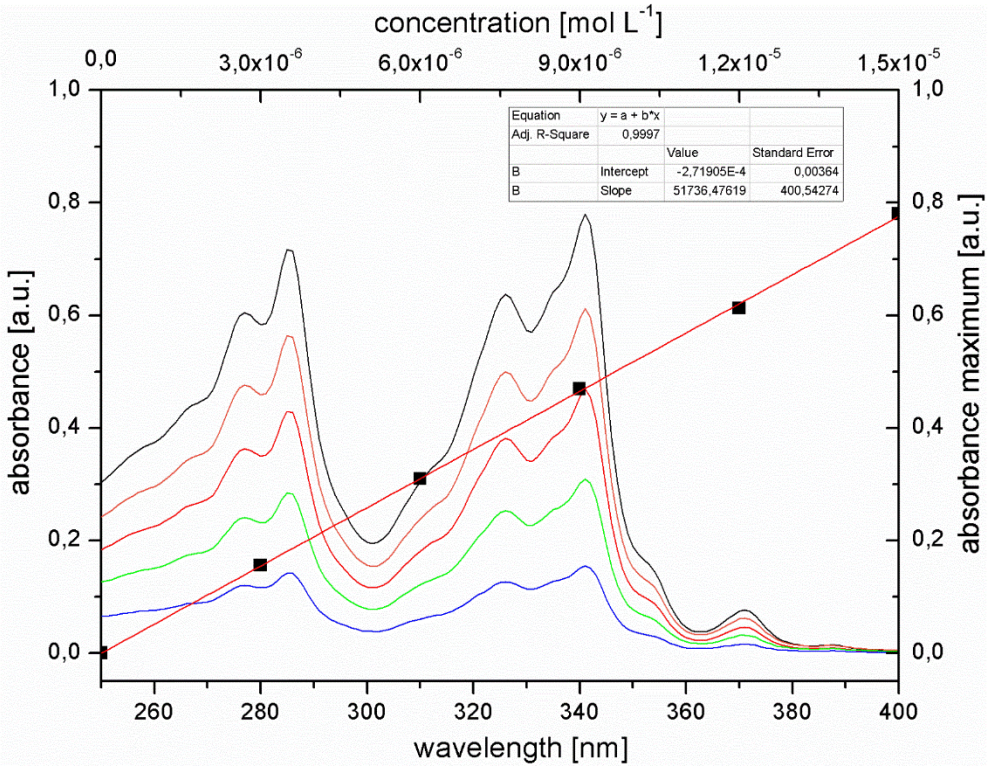

Fig. 31 Absorption spectra of ***BN*-PAH6** in different concentrations (3.0×10^{-6} to 1.5×10^{-5} mol L^{-1}) and linear fitting according to Lambert-Beer law.

3.7. Investigation of the Optical Properties in Different Solvents

Besides chloroform, which was used as the solvent in all optical measurements so far (Fig. 32), the emission and excitation spectra for all ***BN*-PAHs** were also measured in the more polar solvents ethyl acetate and DMF (Fig. 33-34 and Table 1).

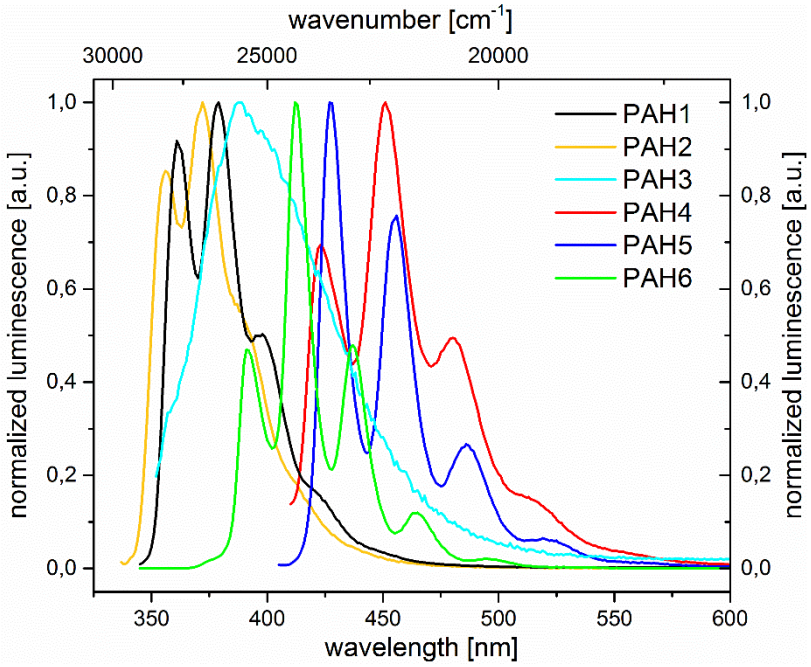

Fig. 32 Normalized photoluminescence spectra of ***BN*-PAH1-6** in chloroform solution.

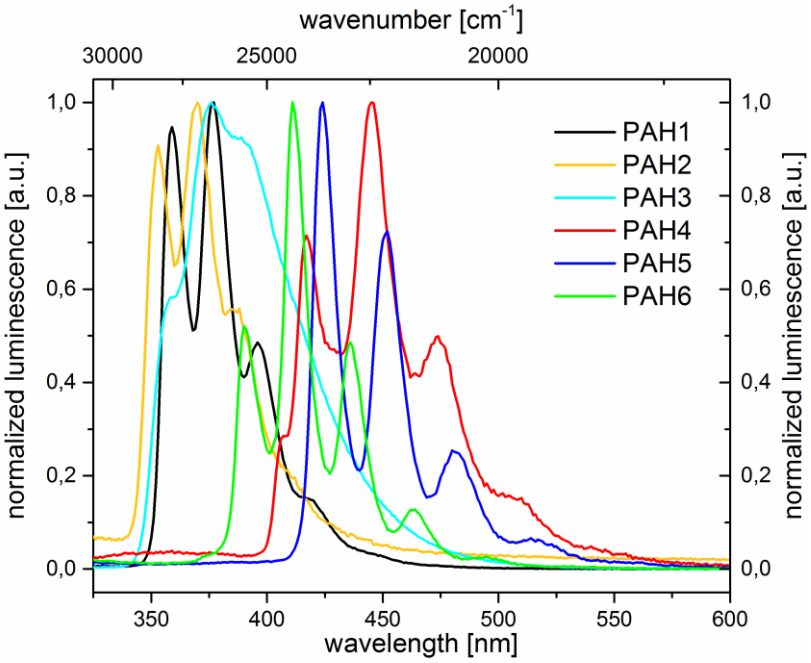

Fig. 33 Normalized photoluminescence spectra of ***BN*-PAH1-6** in ethyl acetate solution.

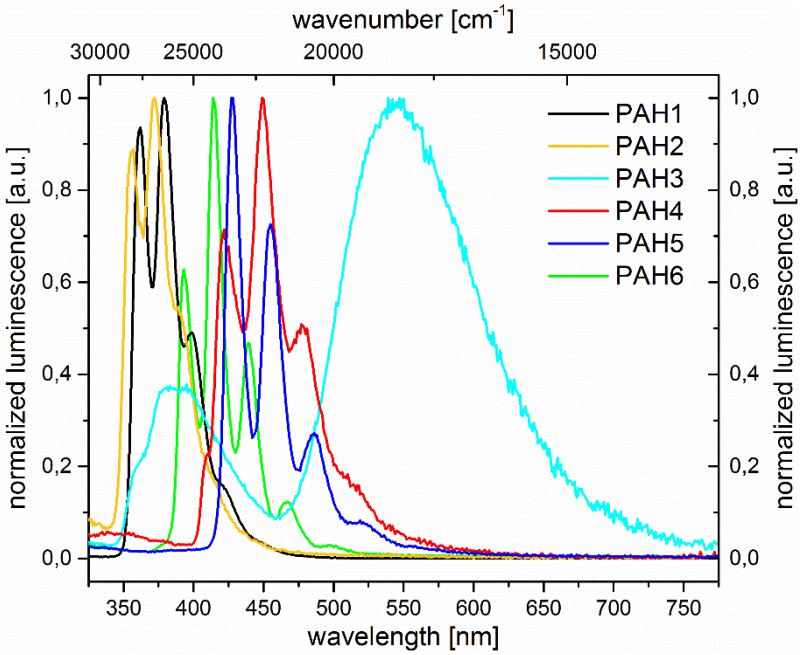

Fig. 34 Normalized photoluminescence spectra of ***BN*-PAH1-6** in DMF solution.

Table 1 Photoluminescence maxima of ***BN*-PAH1-6** in chloroform, ethyl acetate and DMF.

Compound	$\lambda_{lum\ max}$ ($CHCl_3$) [nm]	$\lambda_{lum\ max}$ (EtOAc) [nm]	$\lambda_{lum\ max}$ (DMF) [nm]	Max. $\Delta\ \lambda_{lum\ max}$ [nm]
***BN*-PAH1**	379	377	379	2
***BN*-PAH2**	372	370	372	2
***BN*-PAH3**	389	376	(383), 547	(13), 171
***BN*-PAH4**	451	445	449	6
***BN*-PAH5**	427	424	427	3
***BN*-PAH6**	412	411	414	3

As discussed in the manuscript, almost all *BN*-PAHs consist of three major emission bands and two less intense minor emission bands, independent of the solvent. The compounds mostly exhibited almost non-solvatochromic behavior, with emission maxima differing only 2 nm (***BN*-PAH1** and ***BN*-PAH2**) to 6 nm (***BN*-PAH2**) in the tested solvents, which indicates no or very little interaction with the solvents.

***BN*-PAH3**, as the only molecule in this sequence, showed a significantly broadened band shape and the lack of fine-structuring in chloroform. In the solvents chloroform, ethyl acetate and DMF, the emission maxima of ***BN*-PAH3** differ by 13 nm, which implies slightly increased solvatochromism. A slight fine-structuring into three bands became apparent when measuring the emission in ethyl acetate, however the bands' separation was still clearly less pronounced than for the other *BN*-PAHs. Most remarkably, the emission spectrum in DMF gained a second, strongly bathochromically shifted emission band with a maximum of 547 nm and the emission band below 400 nm being still present. Presumably, a charge transfer complex (exciplex) with a solvent molecule is formed, which emits at much lower energy. To represent the discussed, special behavior of ***BN*-PAH3** compared to other *BN*-PAHs, it was compared to ***BN*-PAH1** in Fig. 35. The band shapes and maxima of ***BN*-PAH1** did not change in different solvents; which was very different from ***BN*-PAH3**.

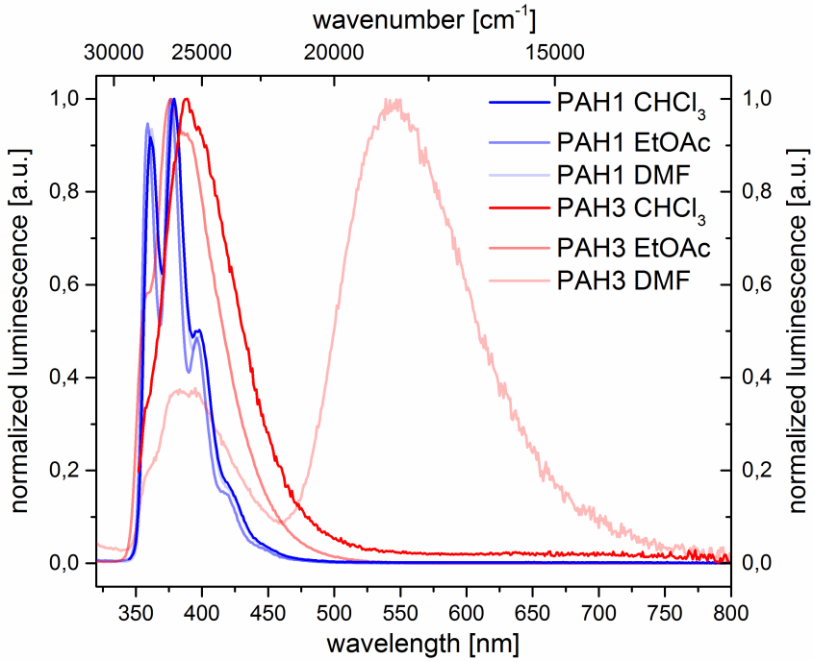

Fig. 35 Normalized photoluminescence spectra of ***BN*-PAH1** (blue) and ***BN*-PAH3** (red) in chloroform, ethyl acetate and DMF.

The absence of line broadening and solvatochromic behavior in all other *BN*-PAHs except ***BN*-PAH3** can indicate two things: First, the pyridyl-unit with its lone pair character in ***BN*-PAH3** could be involved in dipolar interactions with the solvents, but only in case of DMF, a charge transfer occurs. Alternatively, despite the *B-N* interaction, the boron atom may keep some of its Lewis acidity and interact with DMF as a Lewis base.

As depicted in Table 31 in the section Calculations, ***BN*-PAH3** in its excited state geometry has a strongly increased dipole moment and shows the highest absolute increase in the dipole moment upon excitation among all *BN*-PAHs. Presumably, this causes the decreased resolution of the different vibronic states. Opposed to the common finding that large, flat and delocalized aromatic systems often exhibit fine-structuring in their emission spectra, ***BN*-PAH3** in the excited state geometry seems to meet these attributes to a lesser extent.

Compound	$\lambda_{lum\ max}$ ($CHCl_3$) [nm]	$\lambda_{lum\ max}$ (EtOAc) [nm]	$\lambda_{lum\ max}$ (DMF) [nm]	Max. $\Delta\ \lambda_{lum\ max}$ [nm]
***BN*-PAH1**	379	377	379	2
***BN*-PAH2**	372	370	372	2
***BN*-PAH3**	389	376	(383), 547	(13), 171
***BN*-PAH4**	451	445	449	6
***BN*-PAH5**	427	424	427	3
***BN*-PAH6**	412	411	414	3

As expected, the excitation spectra were not dependent on the solvent to a considerable extent (Fig. 36).

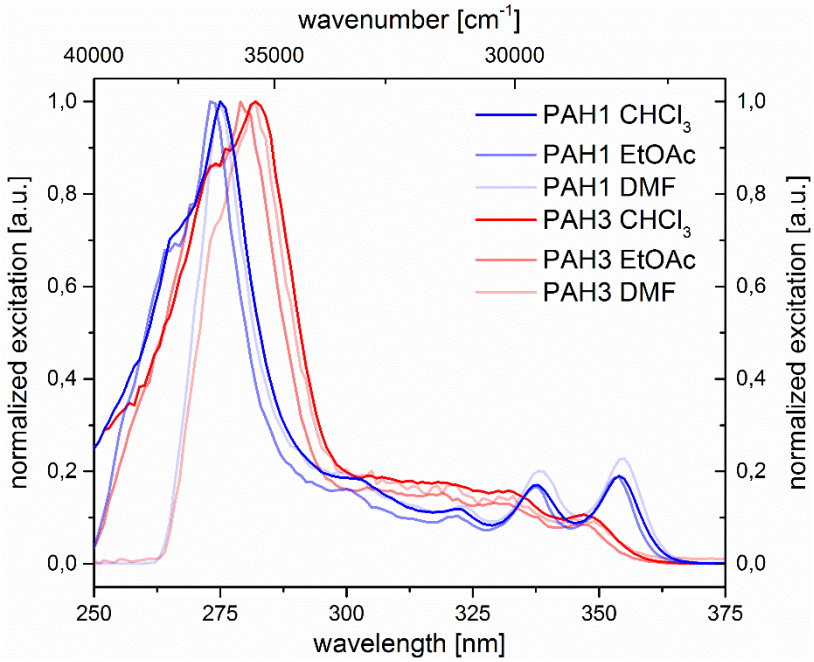

Fig. 36 Normalized excitation spectra of ***BN*-PAH1** (blue) and ***BN*-PAH3** (red) in chloroform, ethyl acetate and DMF. The excitation wavelengths were 377 – 390 nm.

4. Cyclic Voltammetry

Cyclic voltammetry (CV) experiments were performed with a Metrohm potentiostat running the NOVA 2.1 software package using an RHD Instruments electrochemical cell TSC 1600 Closed. Tetrabutylammonium hexafluorophosphate ([TBA]PF_6) was used as the conducting salt as a 0.1 M solution in DCM. The setup contained a Pt working electrode, Ag/AgCl pseudo reference electrode, and Pt counter electrode. Measurements were performed at 298 K. The results are shown in Fig. 37.

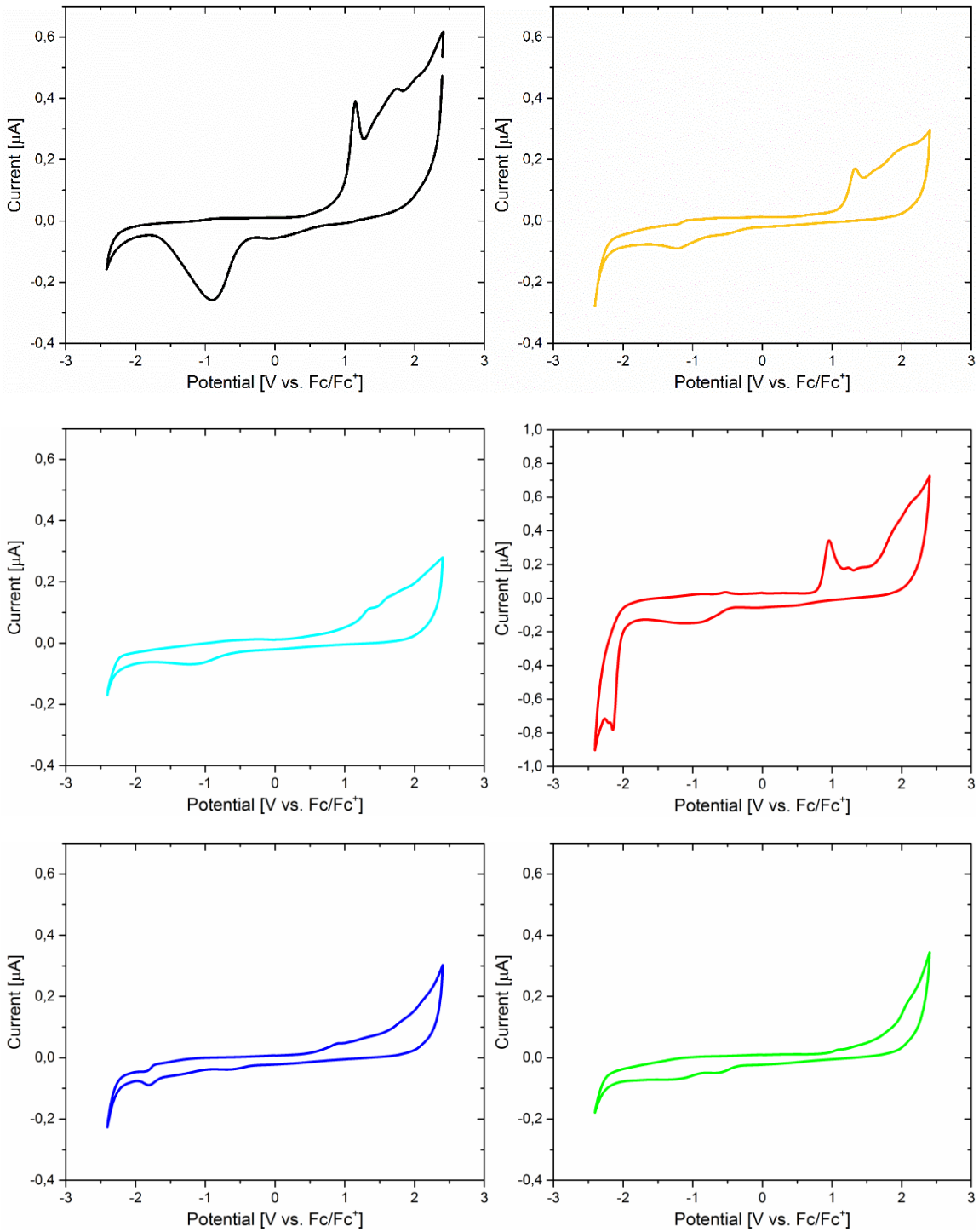

Fig. 37 Voltammograms of ***BN*-PAH1** (black), ***BN*-PAH2** (yellow), ***BN*-PAH3** (cyan), ***BN*-PAH4** (red), ***BN*-PAH5** (blue) and ***BN*-PAH6** (green).

As it becomes apparent, the *BN*-PAHs throughout undergo an irreversible oxidation at a potential of ca. 1.0 V or slightly above. For some *BN*-PAHs like small ***BN*-PAH1-3** it seems that secondary oxidation processes occur when the potential is further increased (potential > 1.5 V). Reduction processes appear considerably less pronounced at ca. −1.0 V. Because a less pronounced return wave is visible for some *BN*-PAHs, it is possible that the reduction is reversible to a certain extent. Large ***BN*-PAH5** and ***BN*-PAH6** exhibit much less distinct potentials for both the reduction and oxidation processes.

5. NMR Spectra

Triallylborane (27)

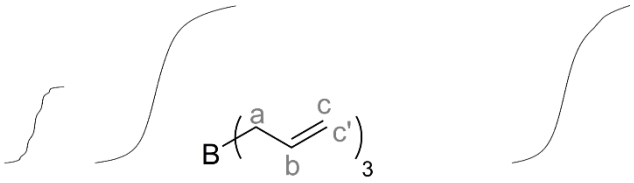

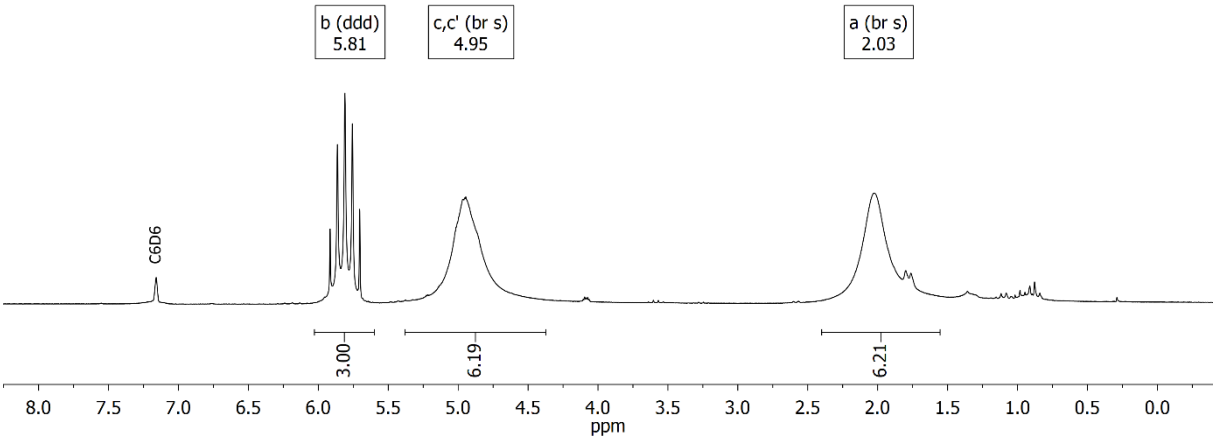

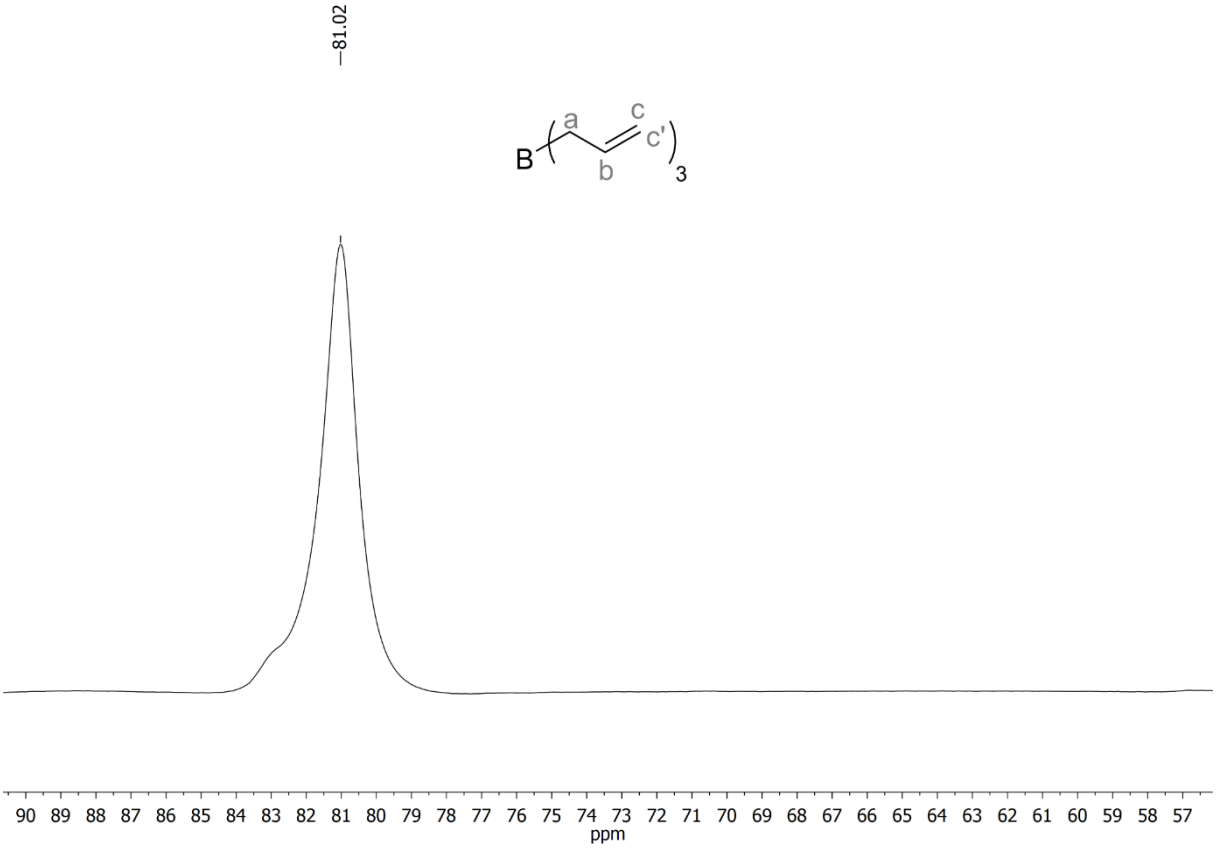

***N*-Allyl-1-(*tert*-butyl)-1,1-dimethylsilanamine (28)**

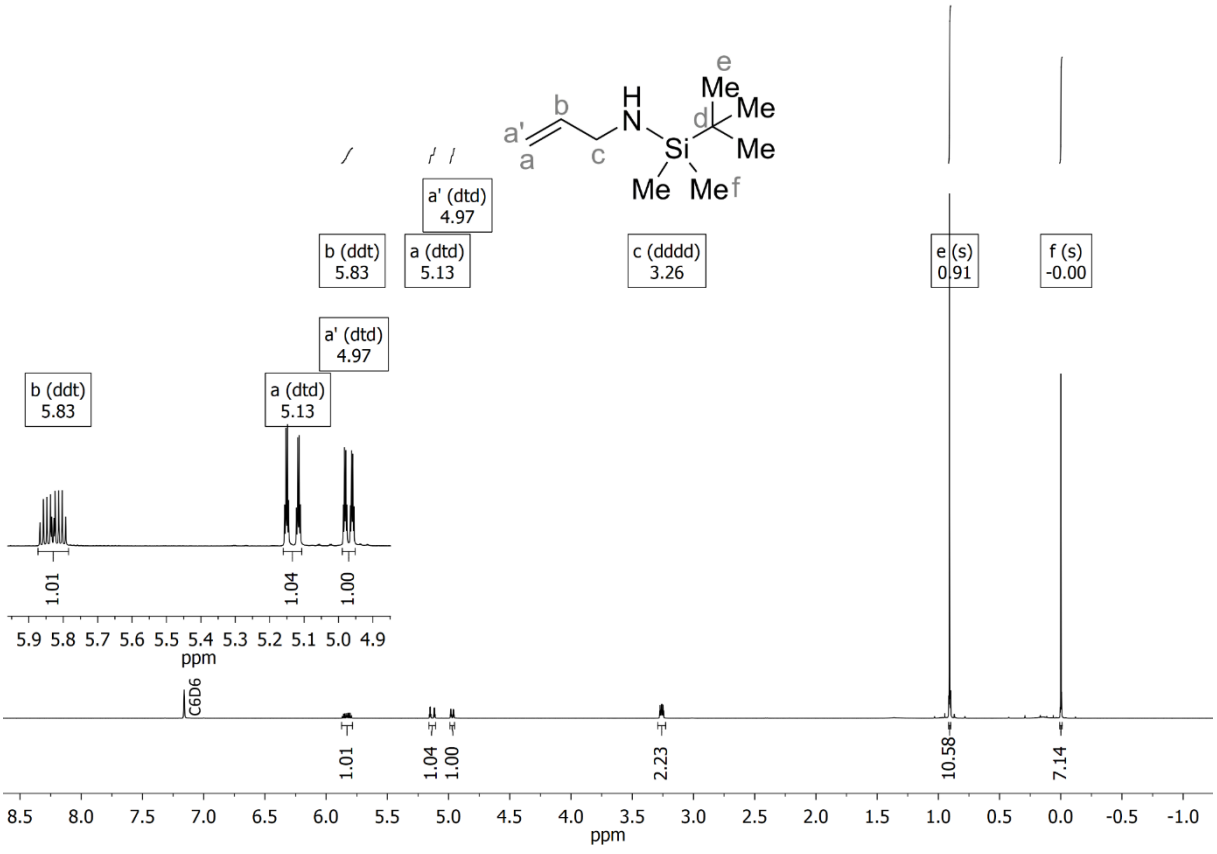

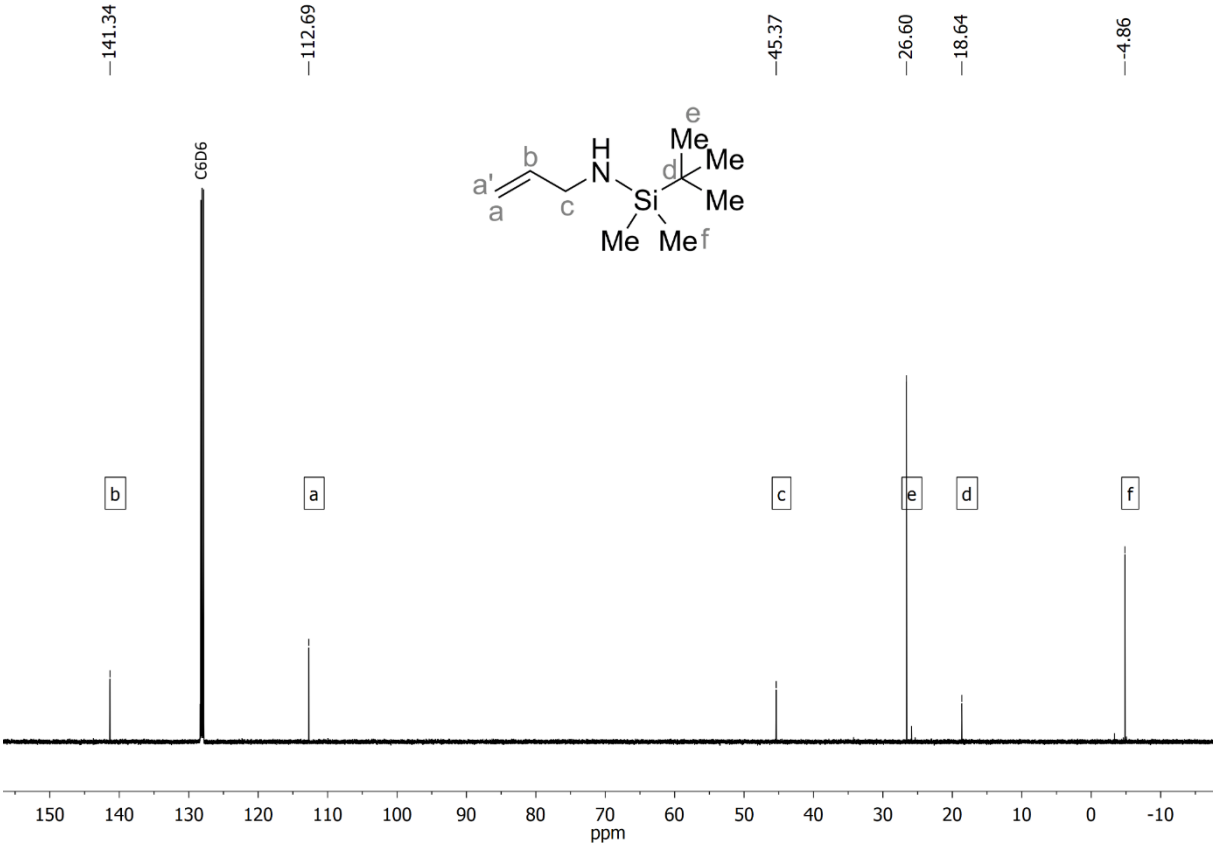
141.34
112.69
45.37
26.60
18.64
4.86
C6D6
b
a
c
e
d
f
150 140 130 120 110 100 90 80 70 60 50 40 30 20 10 0 -10
ppm

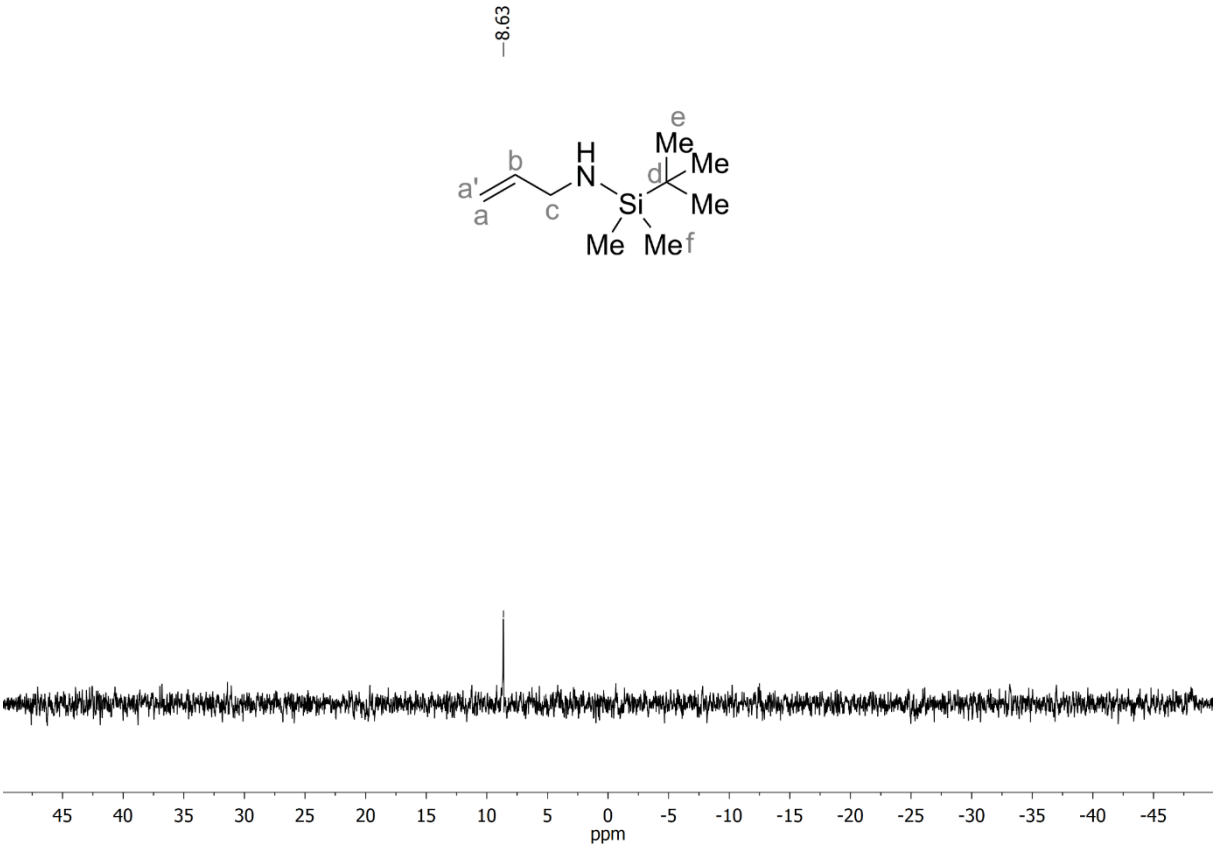
8.63
45 40 35 30 25 20 15 10 5 0 -5 -10 -15 -20 -25 -30 -35 -40 -45
ppm

***N*-Allyl-*N*-(allylchloroboryl)-1-(*tert*-butyl)-1,1-dimethylsilanamine (29)**

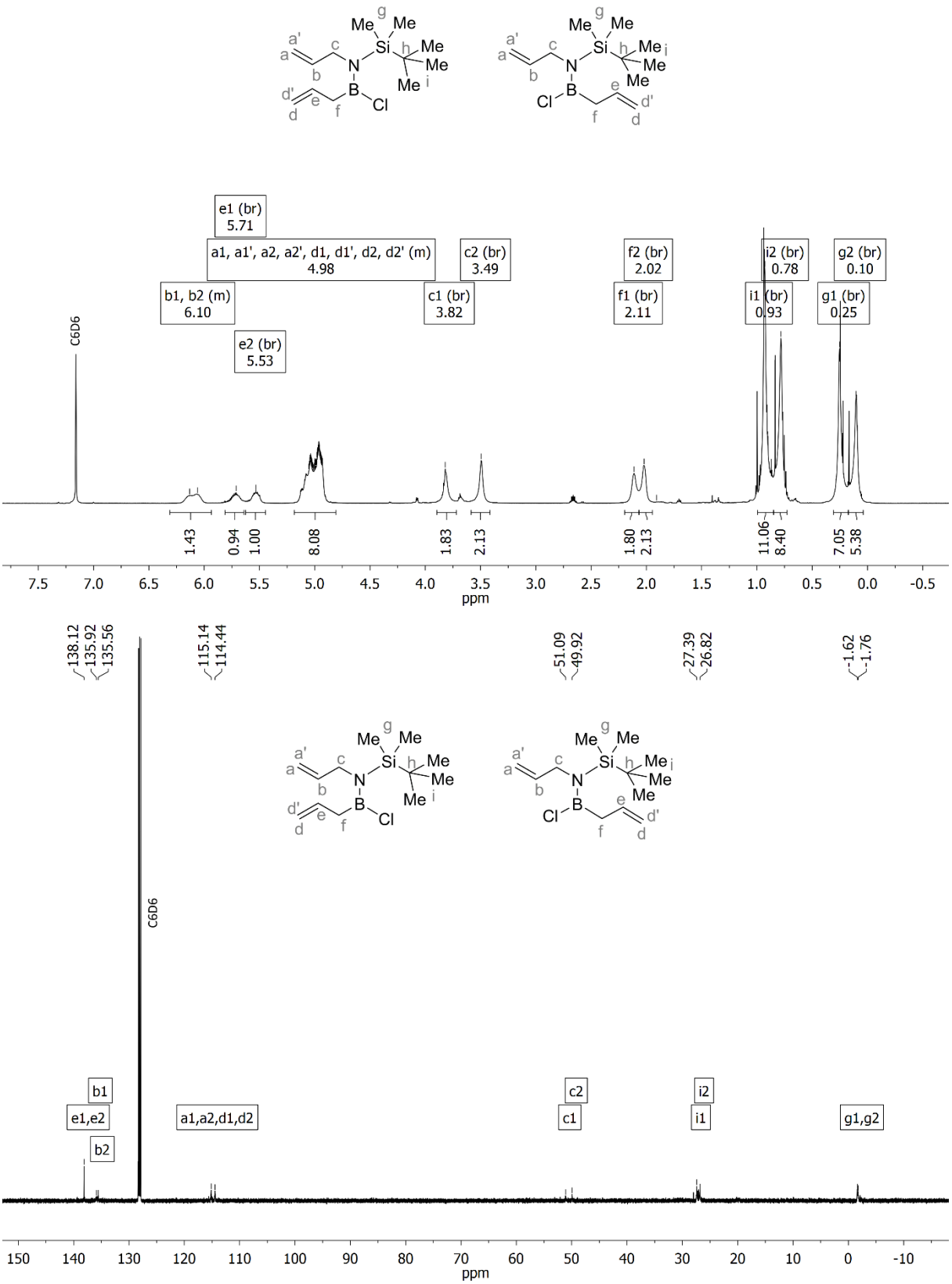

43.41

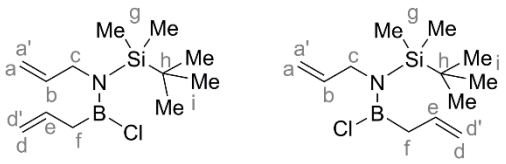
g
Me
Me
a'
c
Si
h
Me
a
N
Me
b
Me
i
d'
e
B
Cl
d
f
g
Me
Me
a'
c
Si
h
Me
i
a
N
Me
b
Me
e
B
Cl
d'
f
d

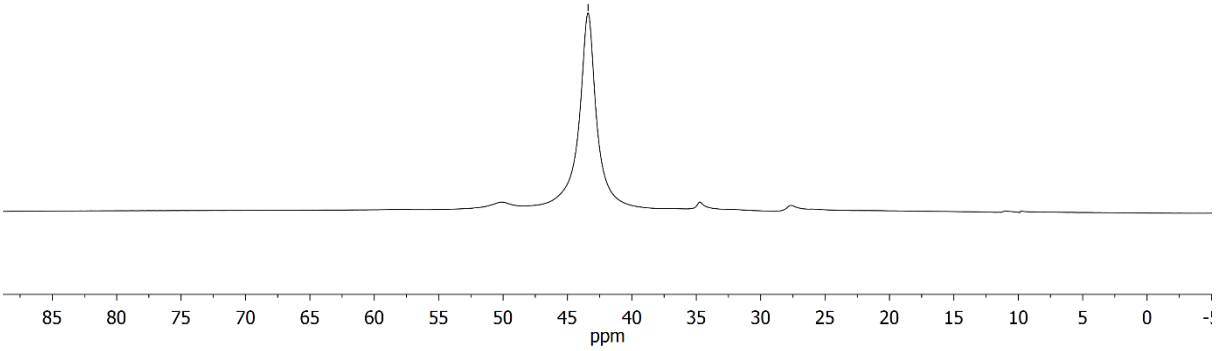
85
80
75
70
65
60
55
50
45
40
35
30
25
20
15
10
5
0
ppm

13.57

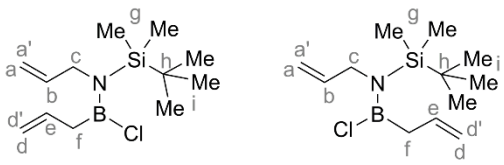
g
Me
Me
a'
c
Si
h
Me
a
N
Me
b
Me
i
d'
e
B
Cl
d
f
g
Me
Me
a'
c
Si
h
Me
i
a
N
Me
b
Me
e
B
Cl
d'
f
d

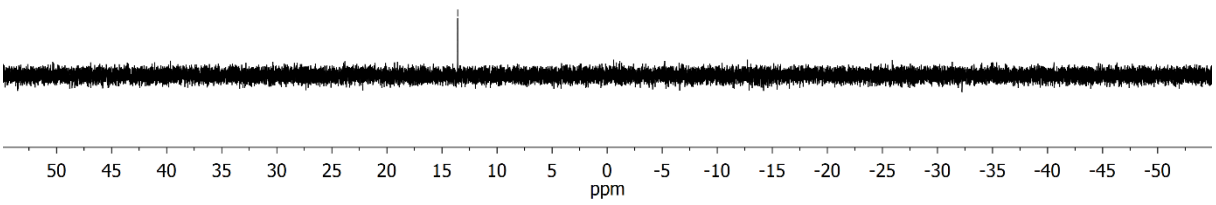
50
45
40
35
30
25
20
15
10
5
0
-5
-10
-15
-20
-25
-30
-35
-40
-45
-50
ppm

1-(*tert*-Butyldimethylsilyl)-2-chloro-3,6-dihydro-1,2-azaborinine (30)

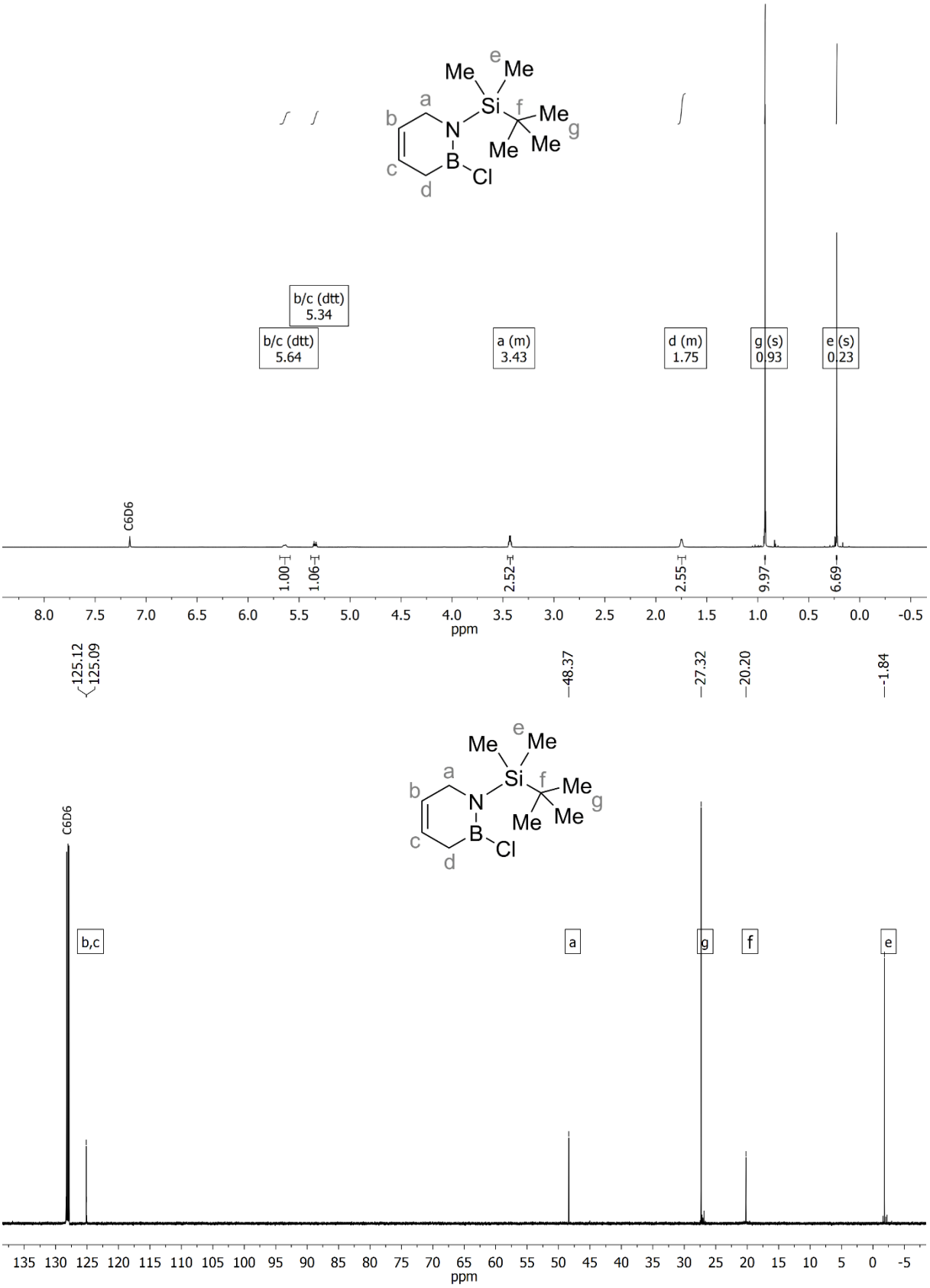

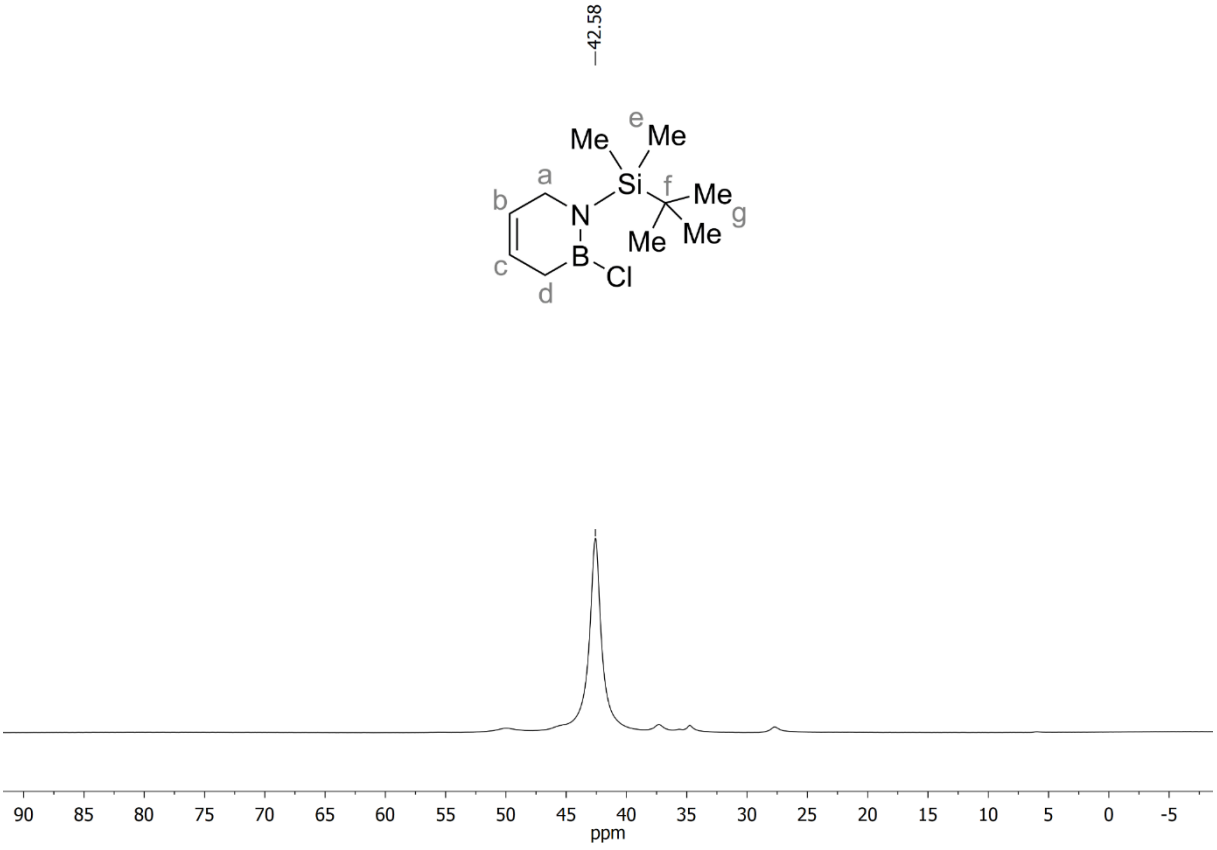
42.58
e
Me
Me
a
Si
f
Me
b
N
g
Me
Me
c
B
Cl
d
90 85 80 75 70 65 60 55 50 45 40 35 30 25 20 15 10 5 0 -5
ppm


18.02
e
Me
Me
a
Si
f
Me
b
N
g
Me
Me
c
B
Cl
d
0 65 60 55 50 45 40 35 30 25 20 15 10 5 0 -5 -10 -15 -20 -25 -30
ppm

Mesityllithium (31)

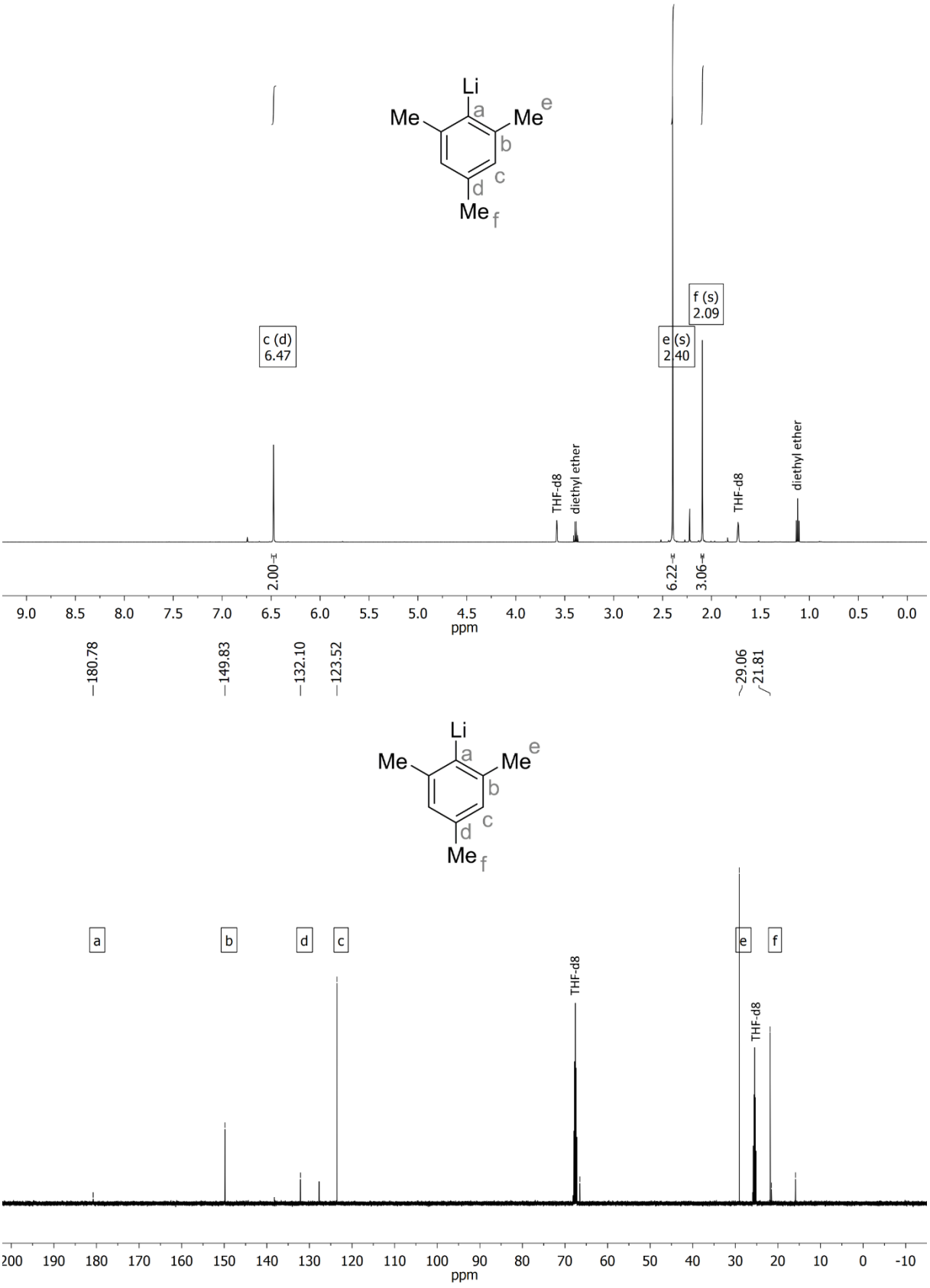

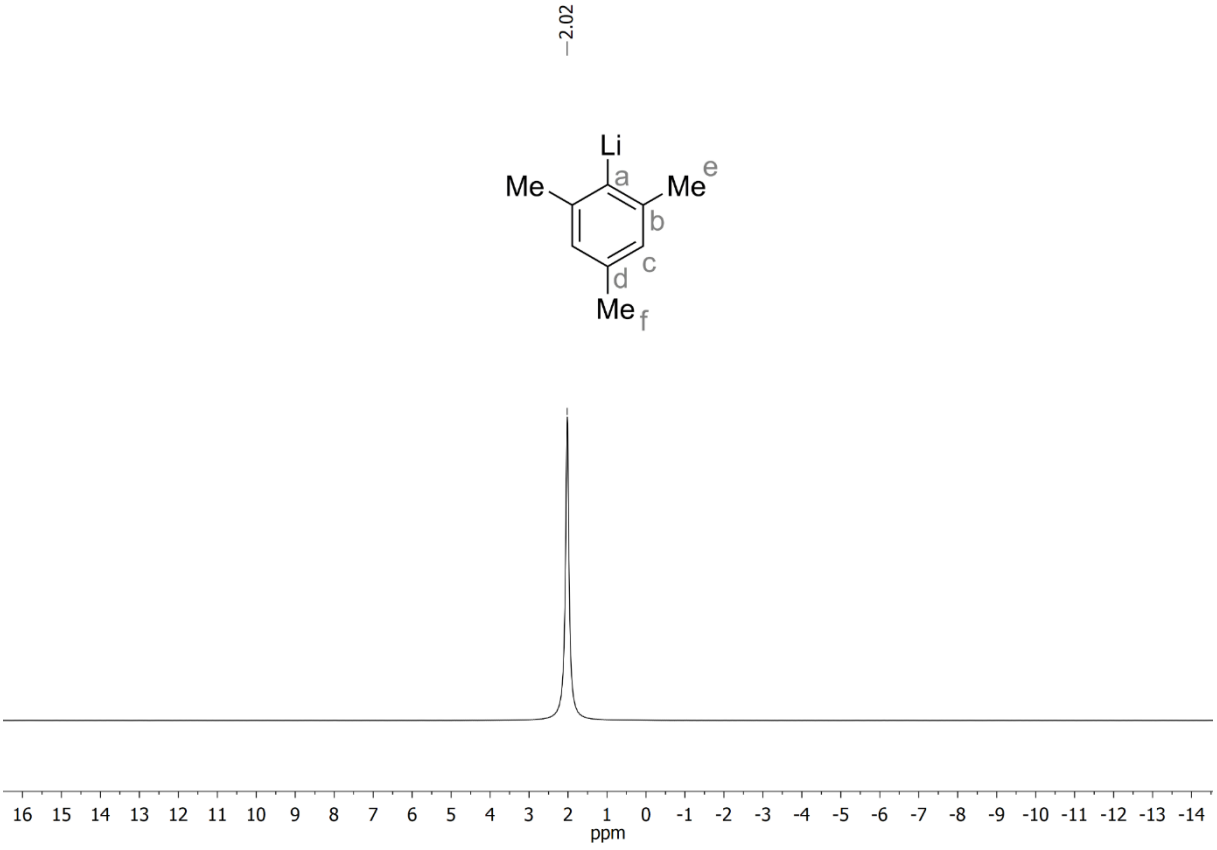

1-(*tert*-Butyldimethylsilyl)-2-mesityl-3,6-dihydro-1,2-azaborinine (32)

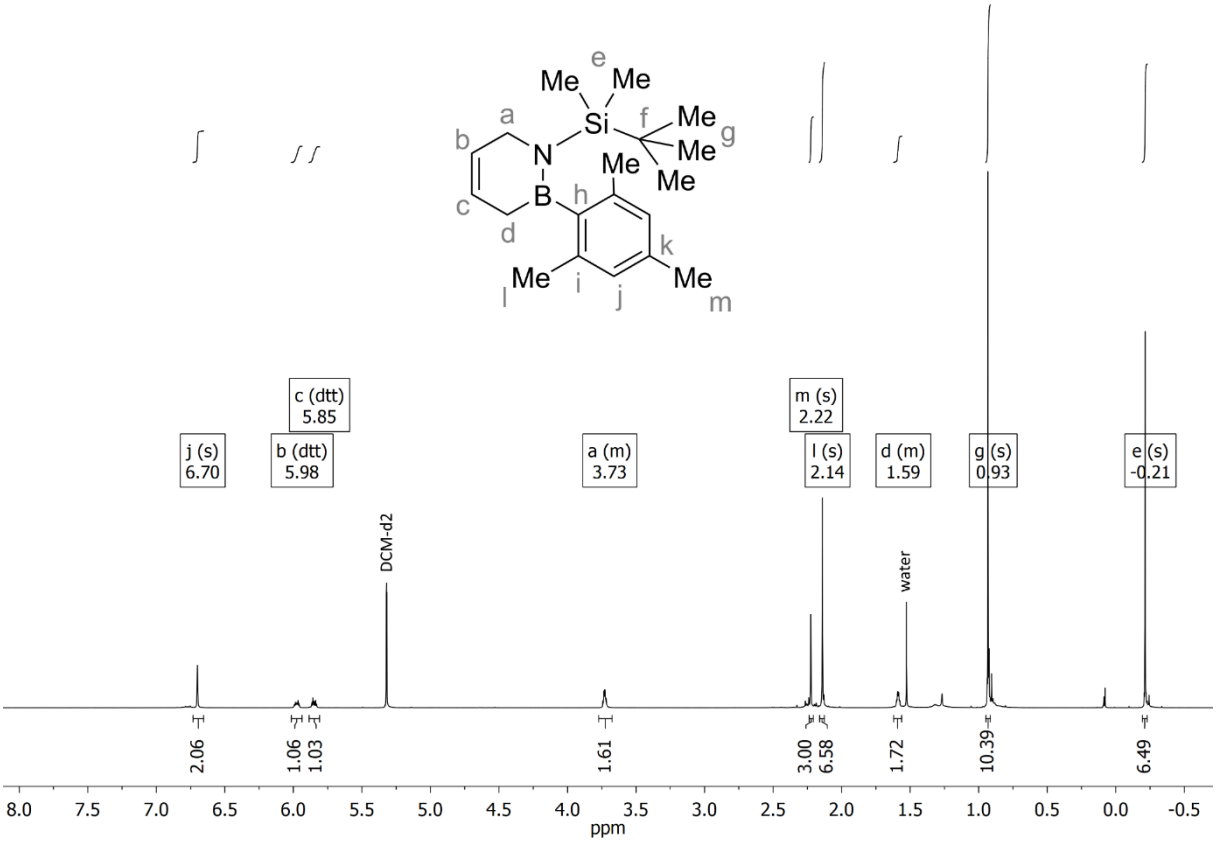

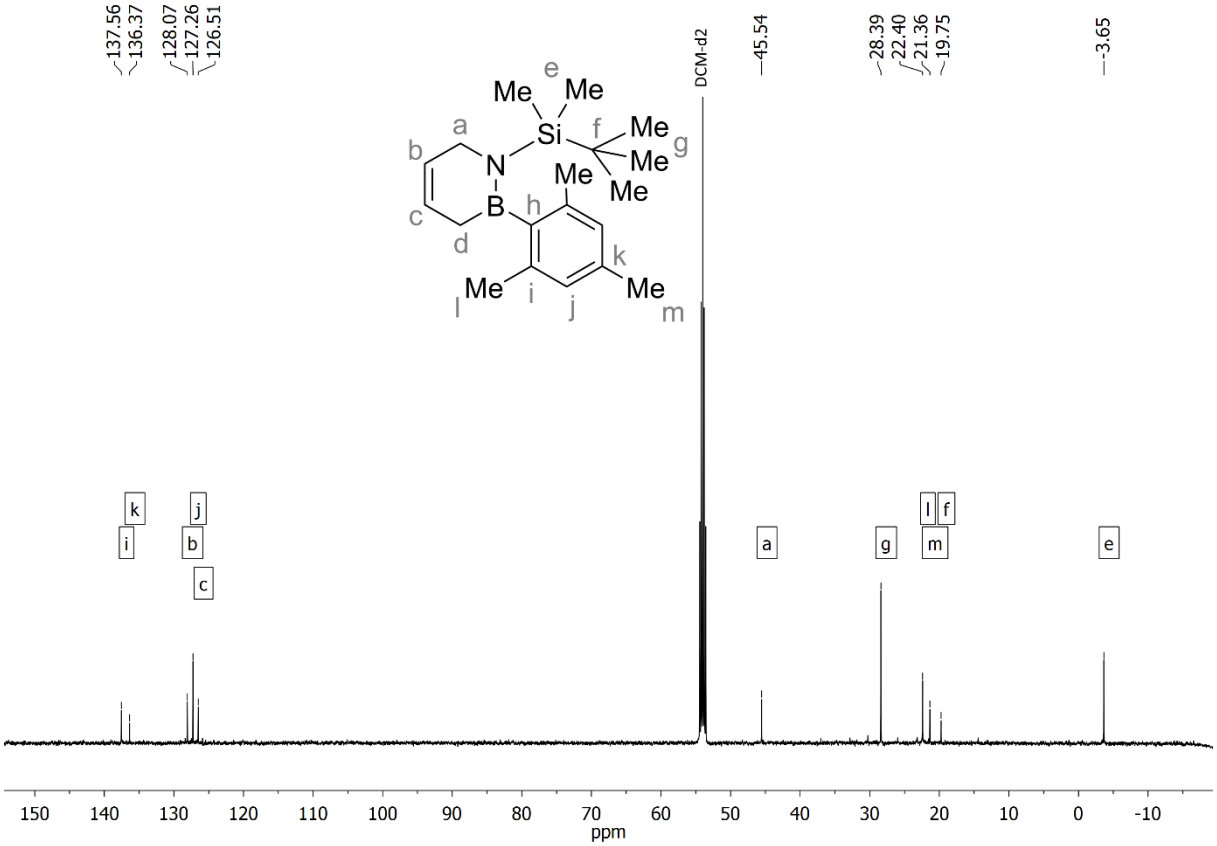
137.56
136.37
128.07
127.26
126.51
DCM-d2
45.54
28.39
22.40
21.36
19.75
-3.65
Me
Si
N
B
a
b
c
d
e
f
g
h
i
j
k
l
m
150
140
130
120
110
100
90
80
70
60
50
40
30
20
10
0
-10
ppm

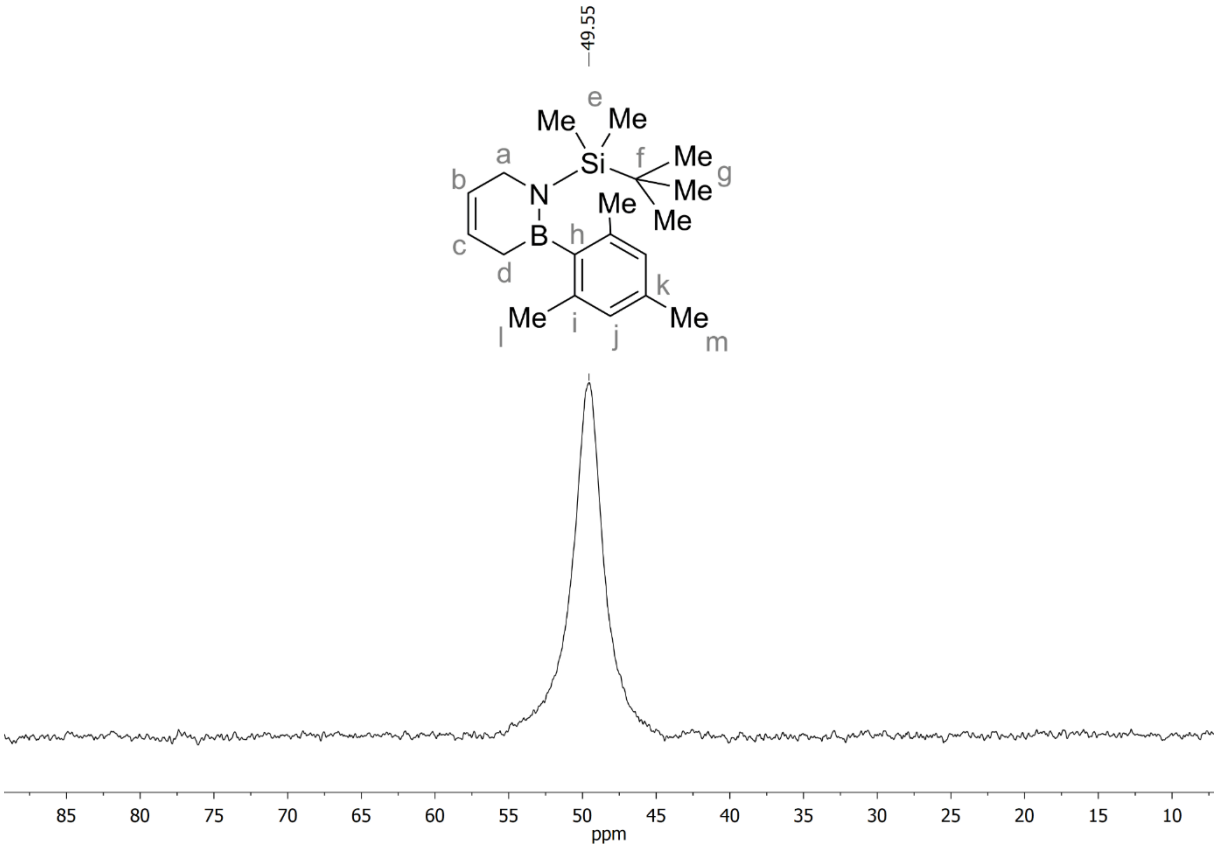
49.55
Me
Si
N
B
a
b
c
d
e
f
g
h
i
j
k
l
m
85
80
75
70
65
60
55
50
45
40
35
30
25
20
15
10
ppm

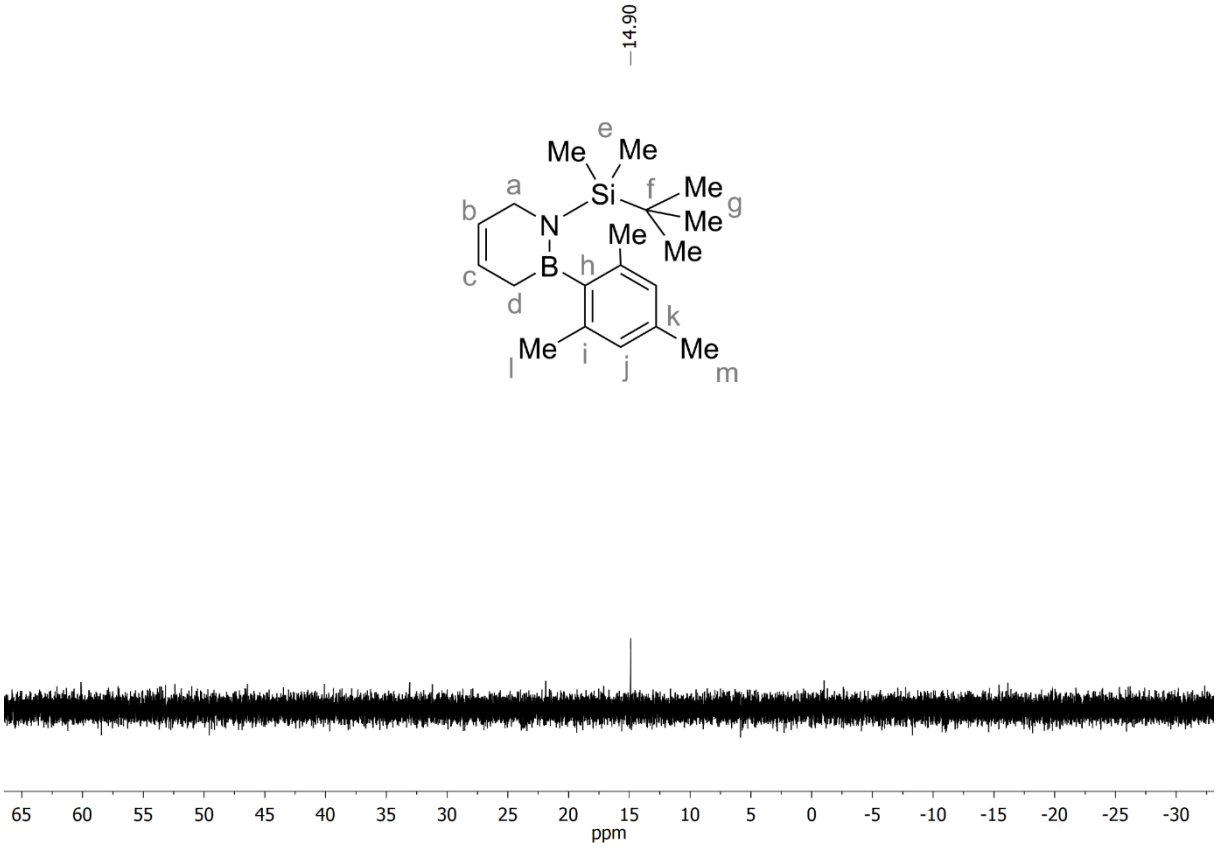

1-(*tert*-Butyldimethylsilyl)-2-mesityl-1,2-azaborinine (33)

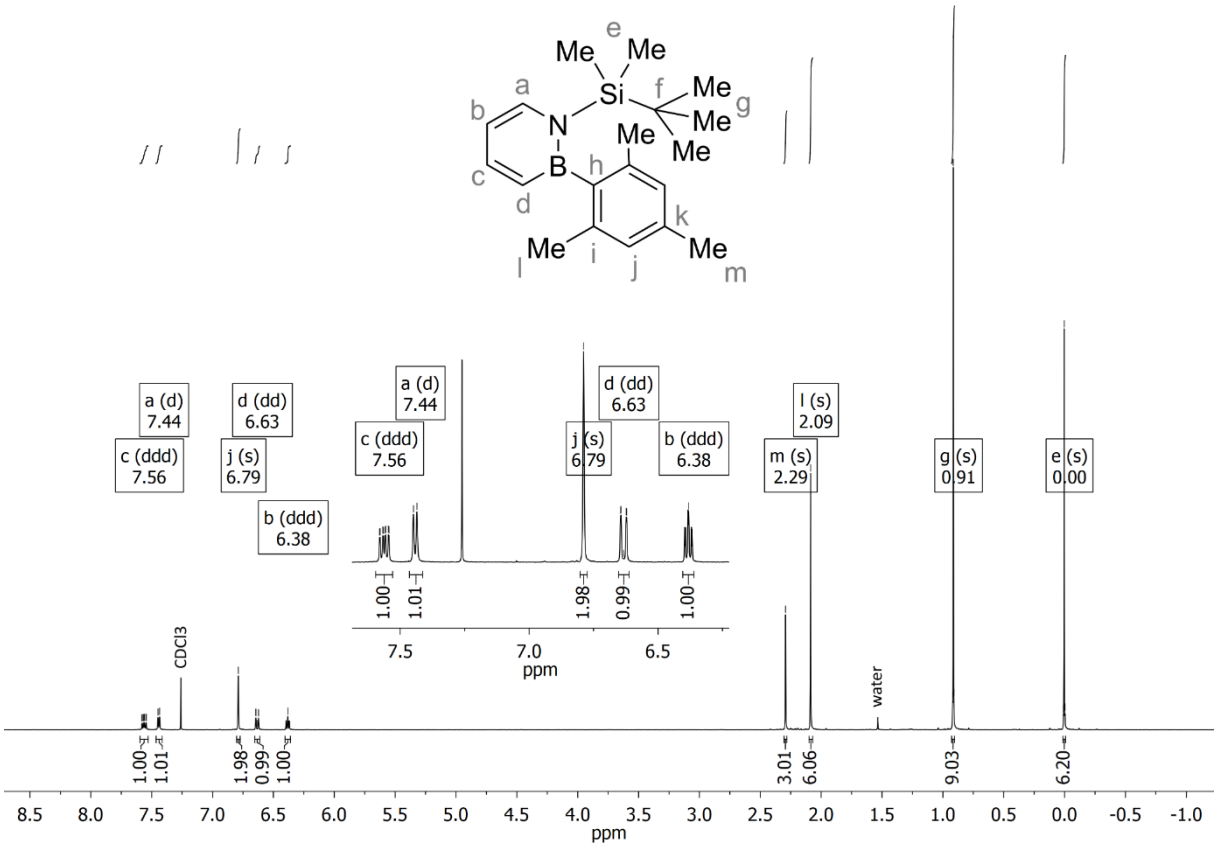

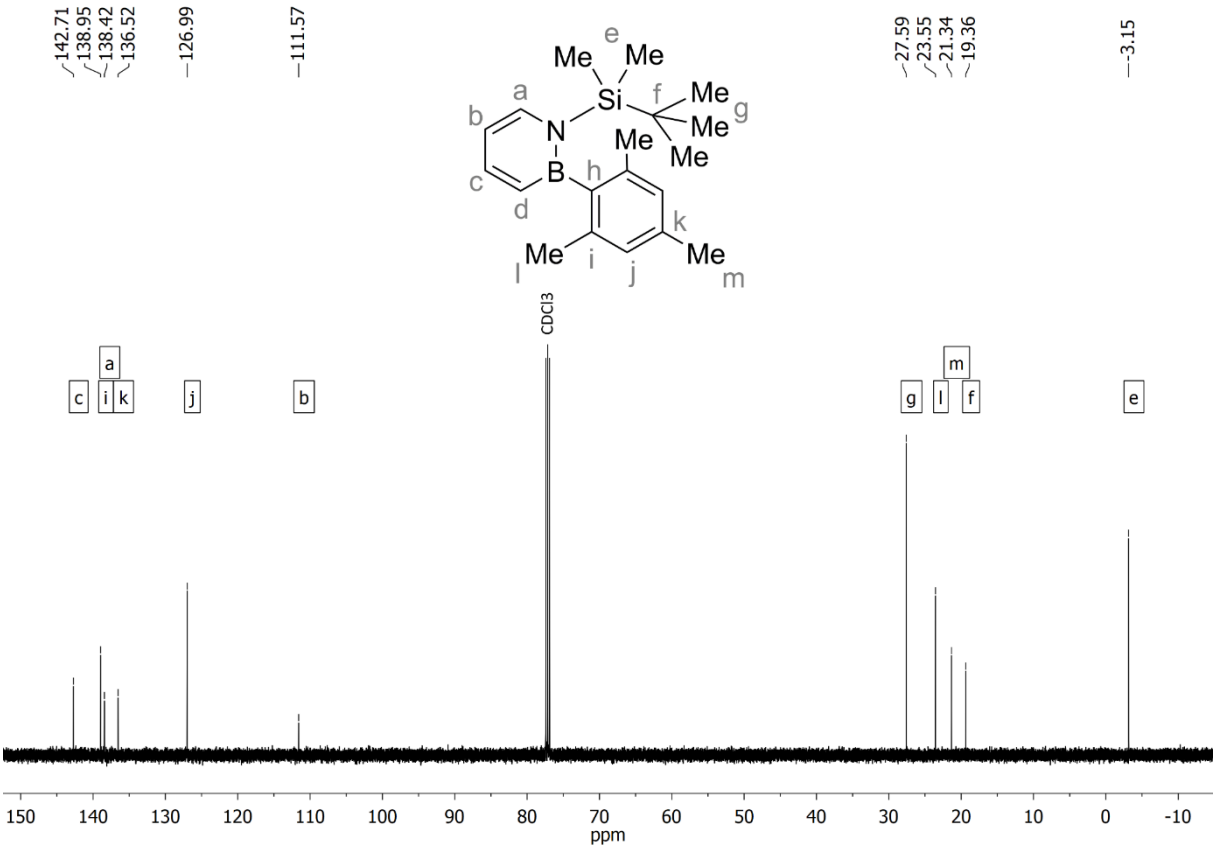
142.71
138.95
138.42
136.52
126.99
111.57
27.59
23.55
21.34
19.36
3.15
CDCl3
a
c i k
j
b
g l m f
e
150 140 130 120 110 100 90 80 70 60 50 40 30 20 10 0 -10
ppm

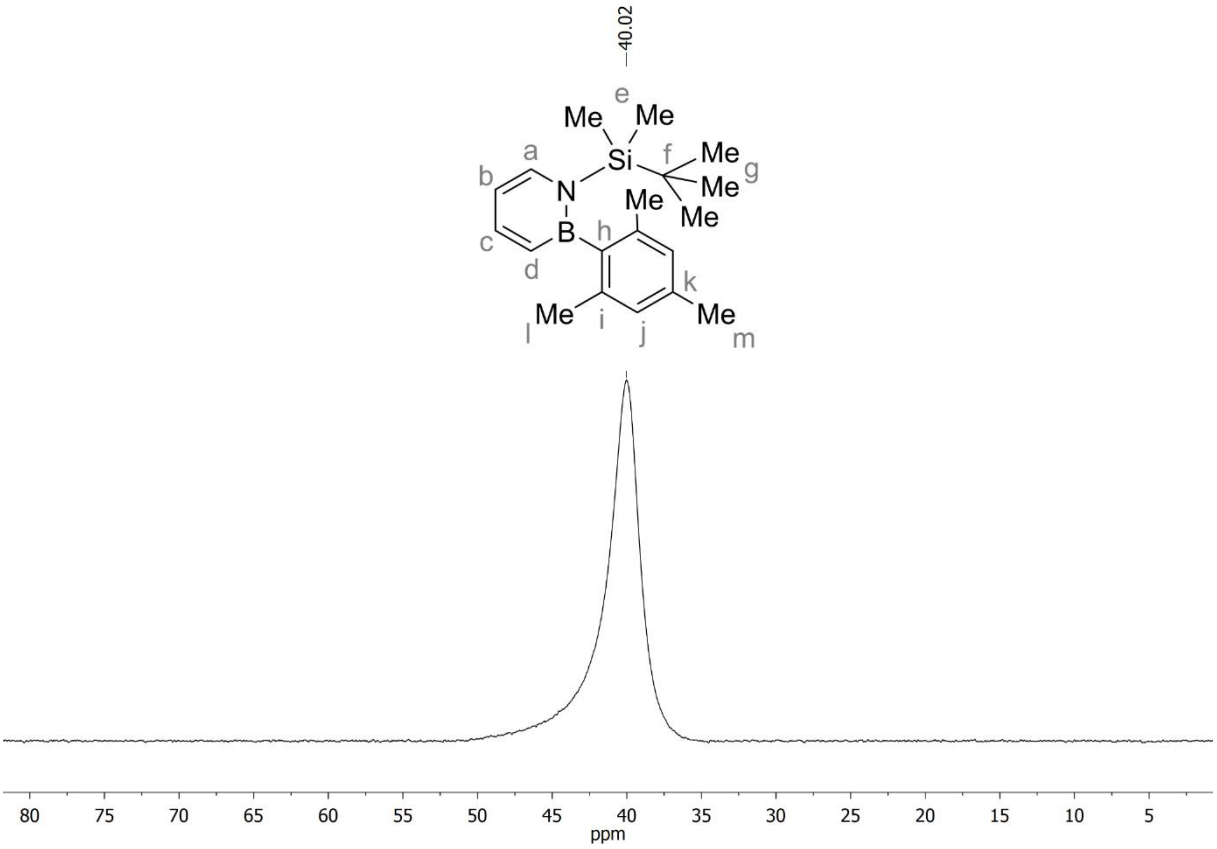
40.02
80 75 70 65 60 55 50 45 40 35 30 25 20 15 10 5
ppm

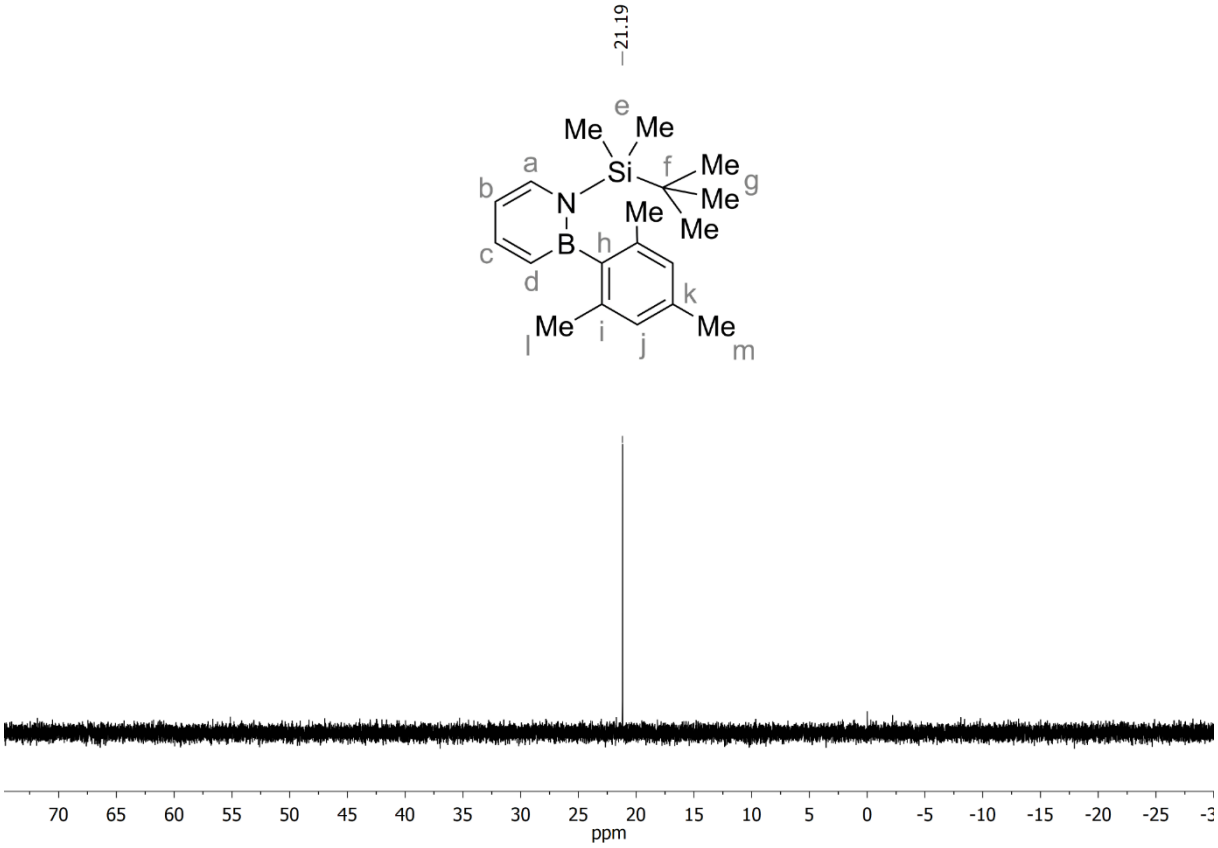

1-Hydro-2-mesityl-1,2-azaborinine (34)

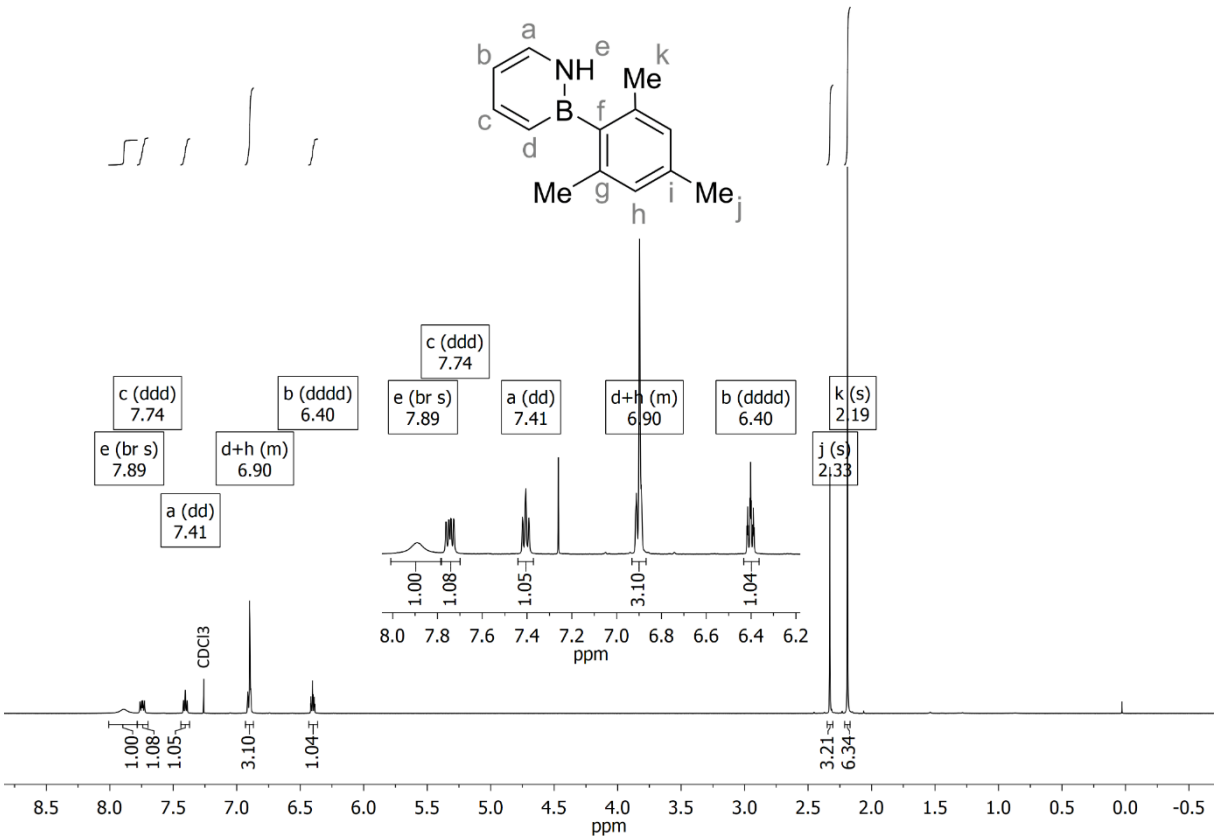

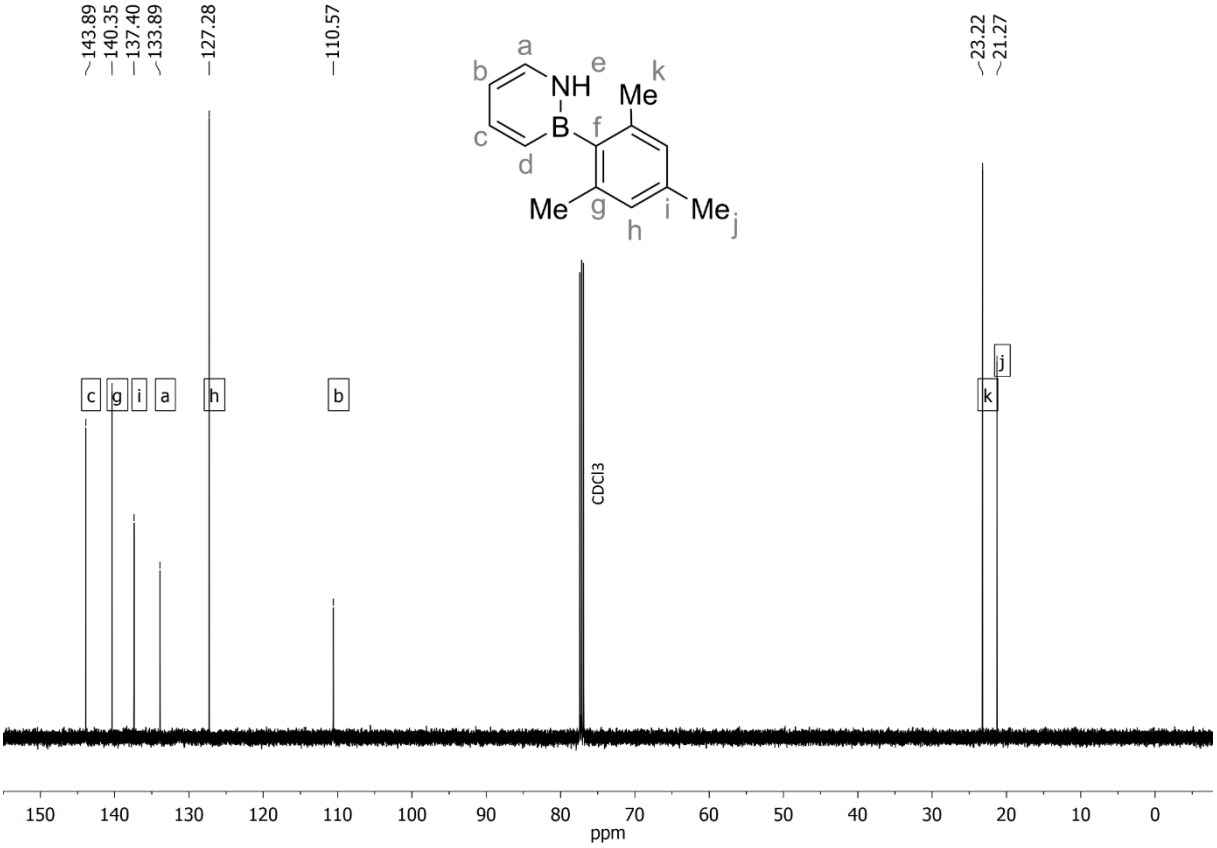
143.89
140.35
137.40
133.89
127.28
110.57
23.22
21.27
a
b
c
d
e
f
g
h
i
j
k
NH
B
Me
CDCl3
150
140
130
120
110
100
90
80
70
60
50
40
30
20
10
0
ppm

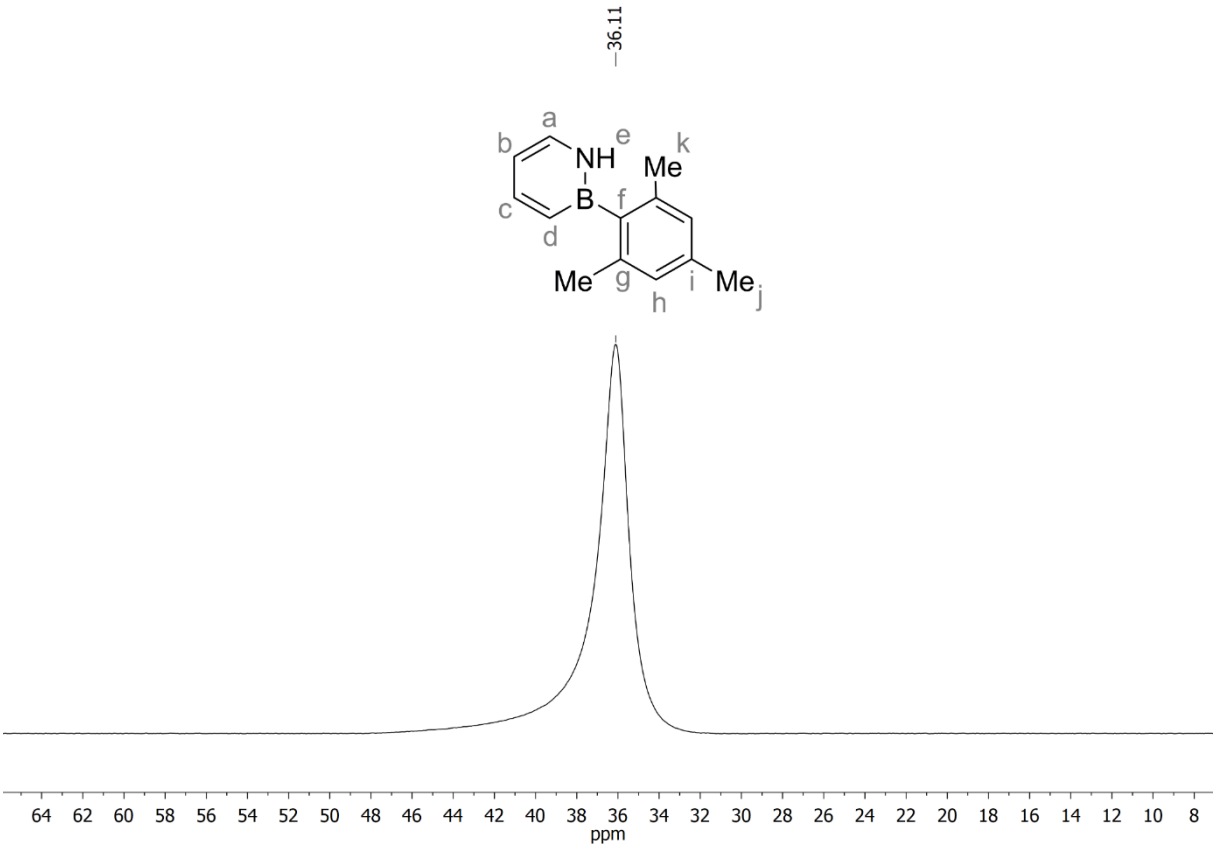
36.11
a
b
c
d
e
f
g
h
i
j
k
NH
B
Me
64
62
60
58
56
54
52
50
48
46
44
42
40
38
36
34
32
30
28
26
24
22
20
18
16
14
12
10
8
ppm

1-Hydro-2-mesityl-6-(4,4,5,5-tetramethyl-1,3,2-dioxaborolan-2-yl)-1,2-azaborinine (1)

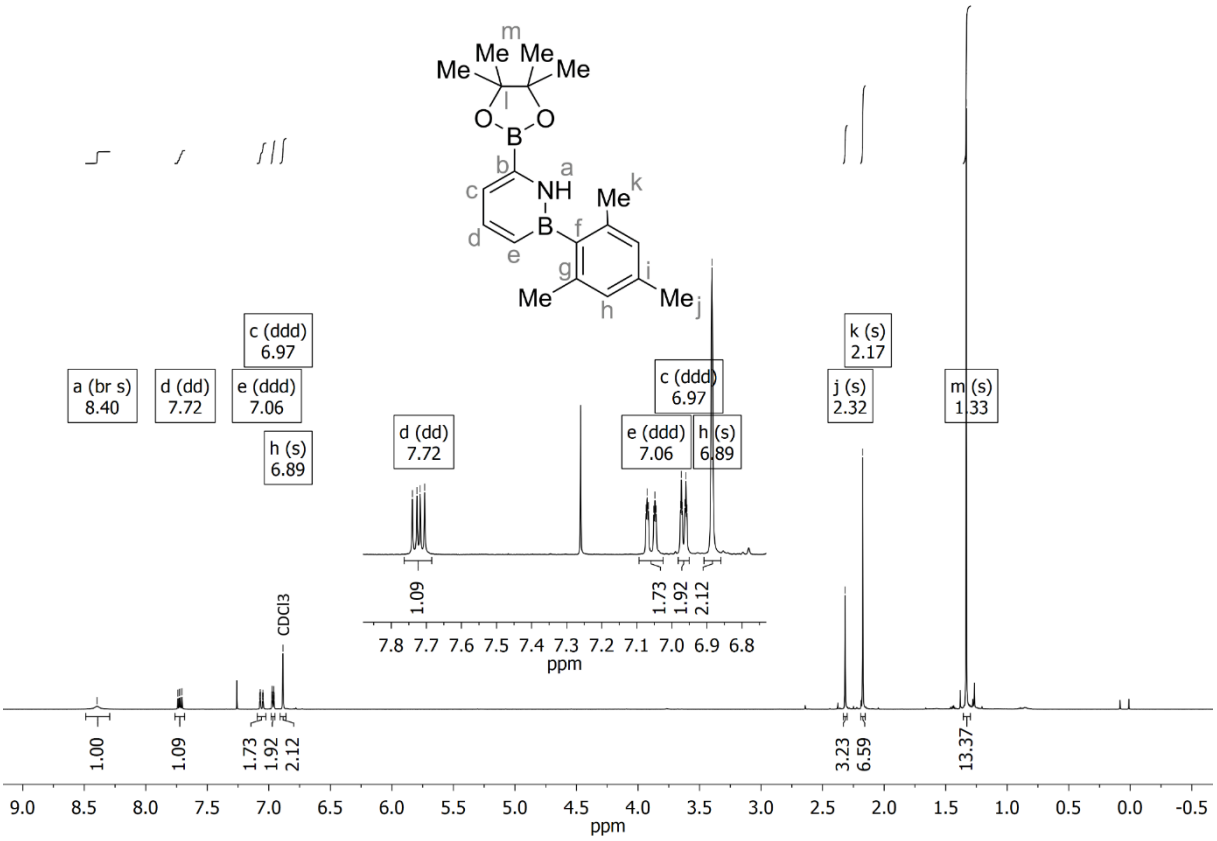

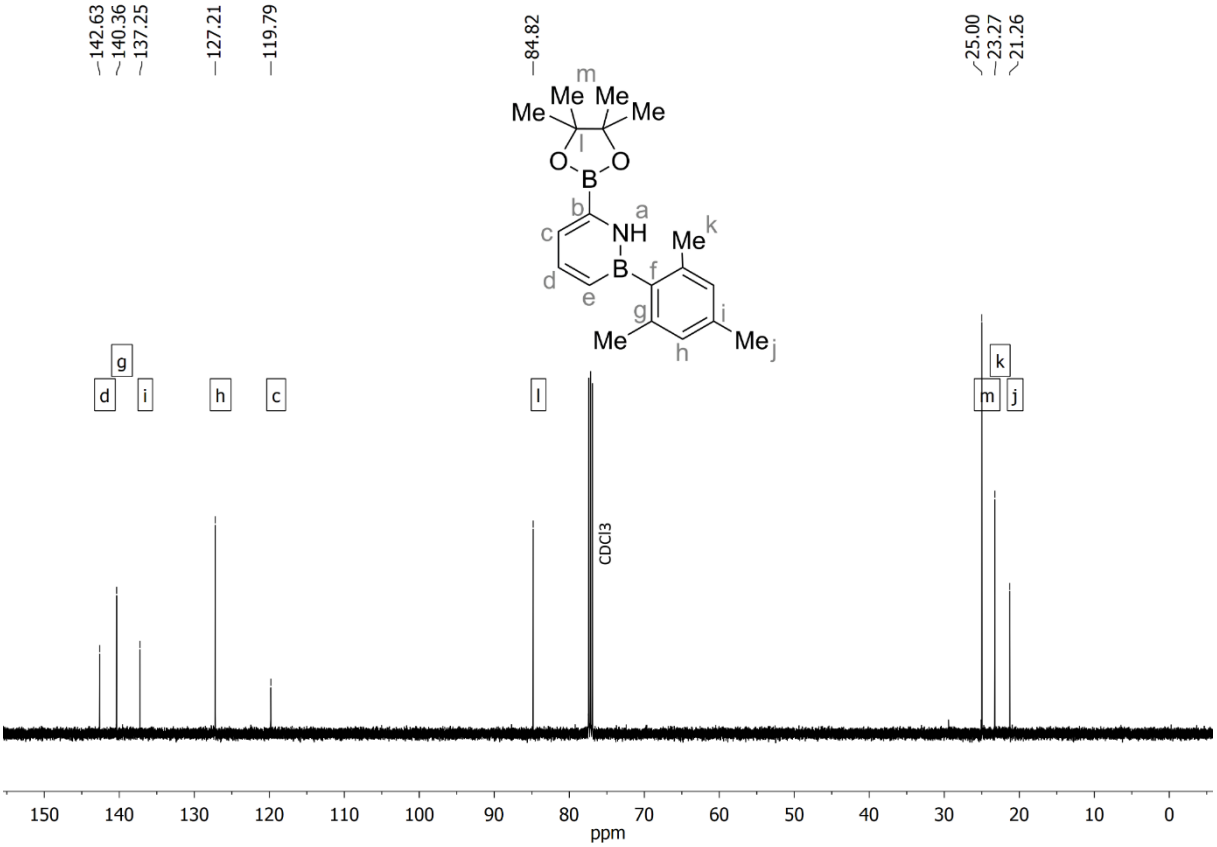

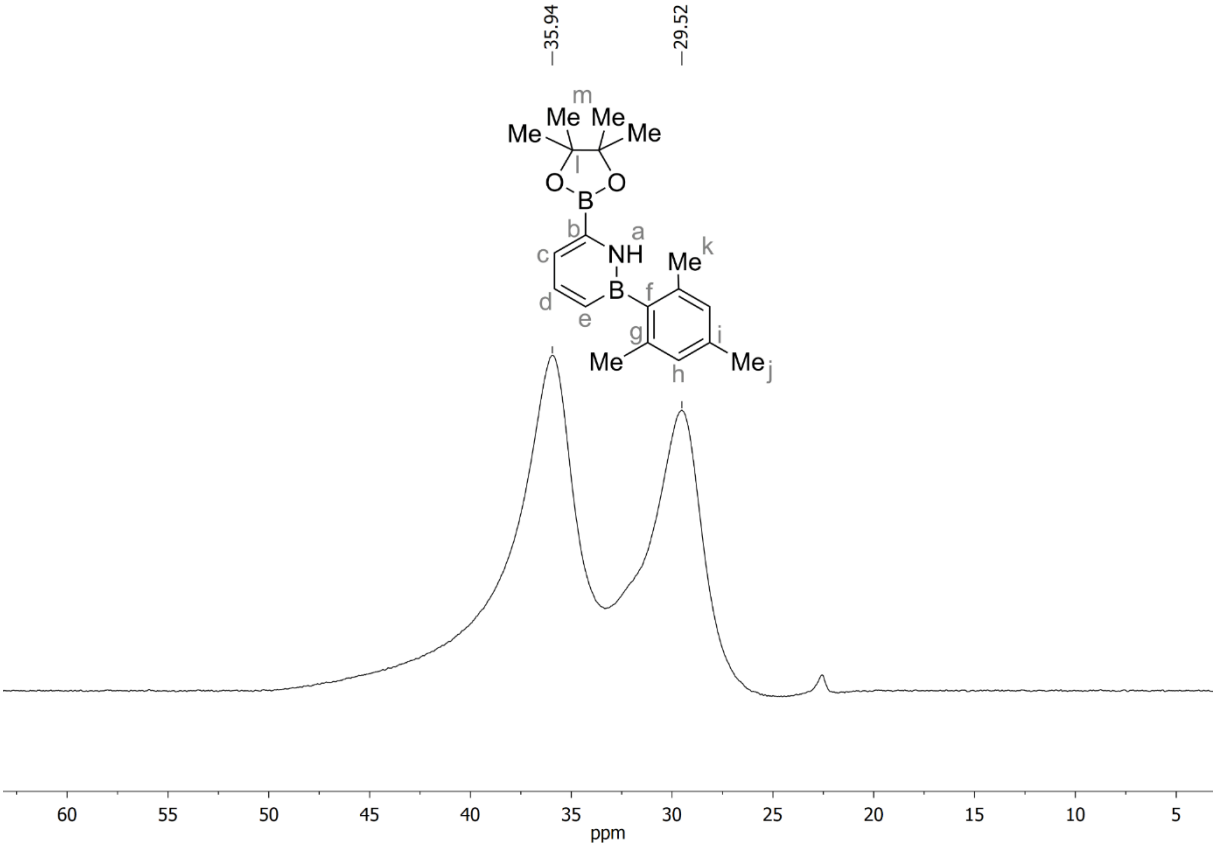

2,2'-Dimesityl-1,1'-dihydro-6,6'-bis(1,2-azaborinine) (20)

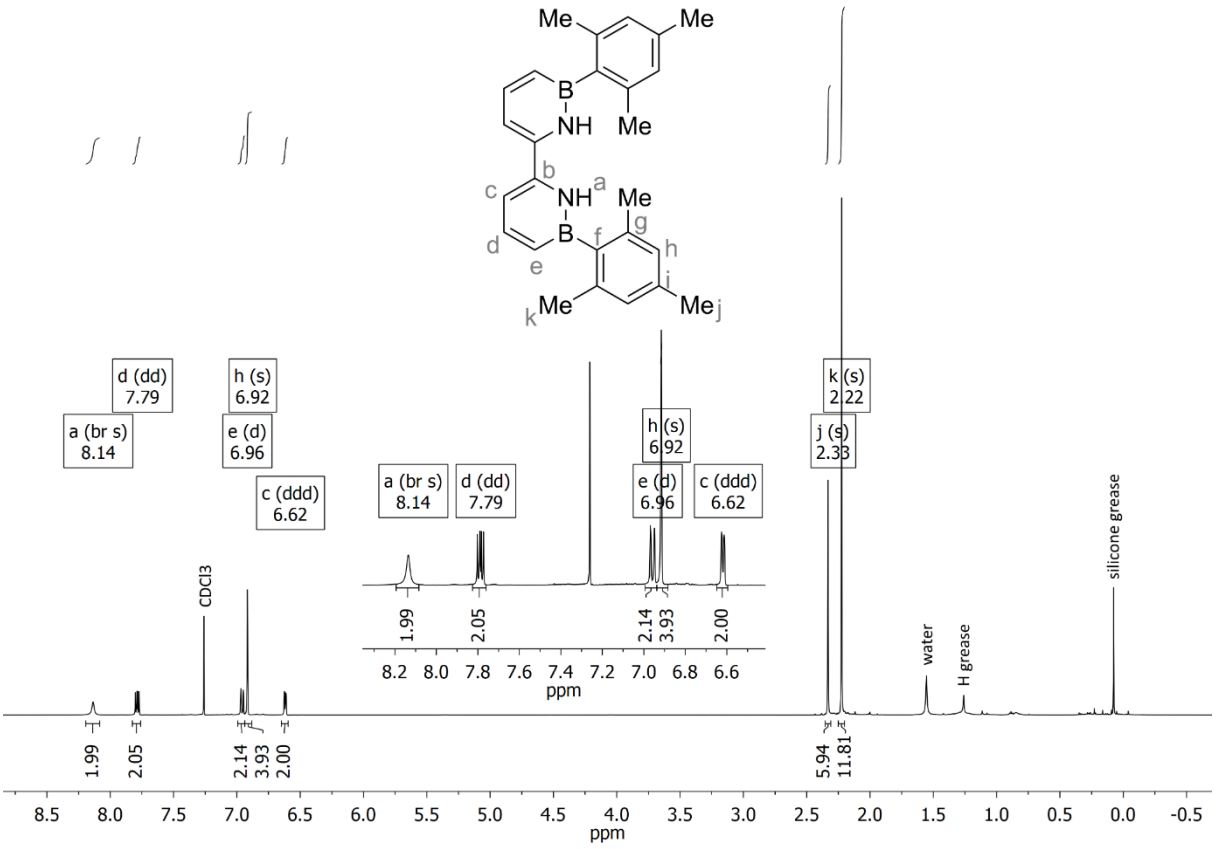

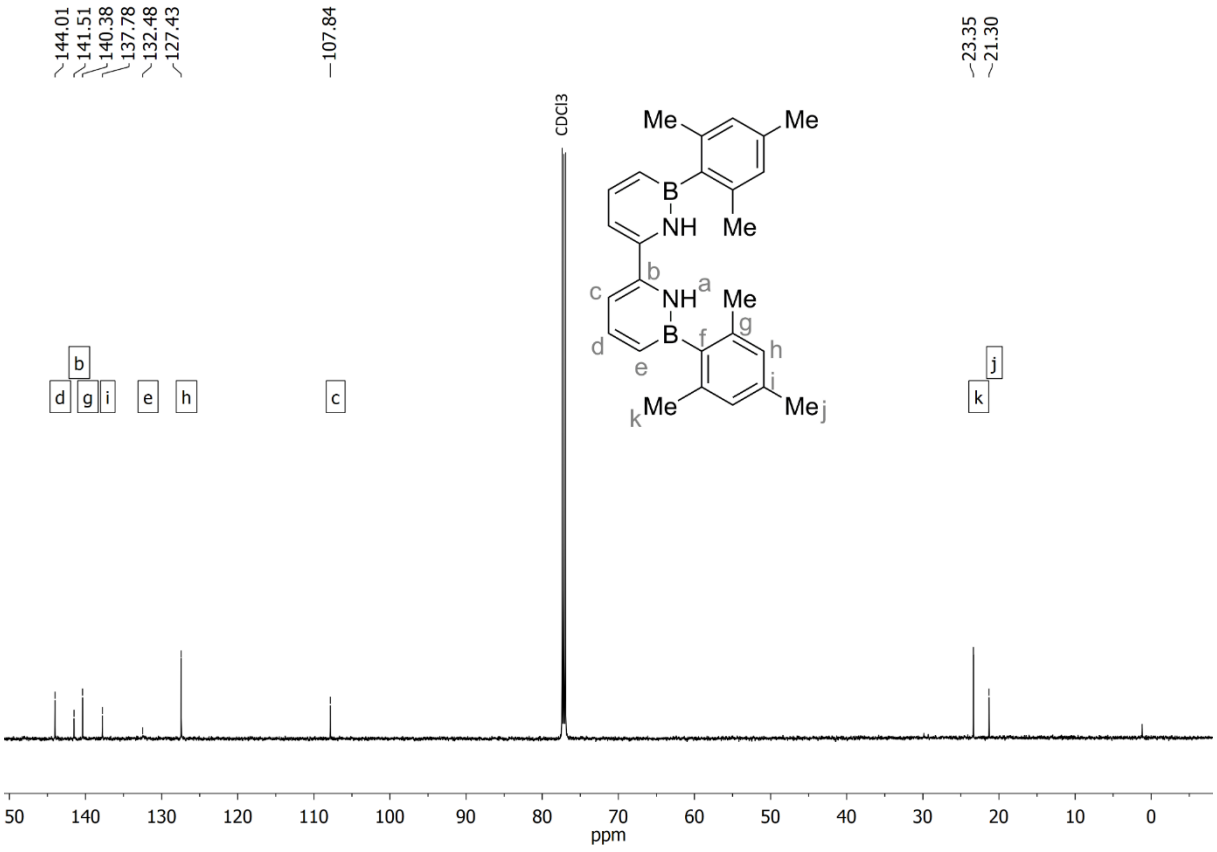
144.01
141.51
140.38
137.78
132.48
127.43
107.84
CDCl3
23.35
21.30
b
d g i e h
c
j
k
Me
Me
B
NH
Me
a
b
c
d
e
f
g
h
i
Me
Me
k
Me
j
50 140 130 120 110 100 90 80 70 60 50 40 30 20 10 0
ppm

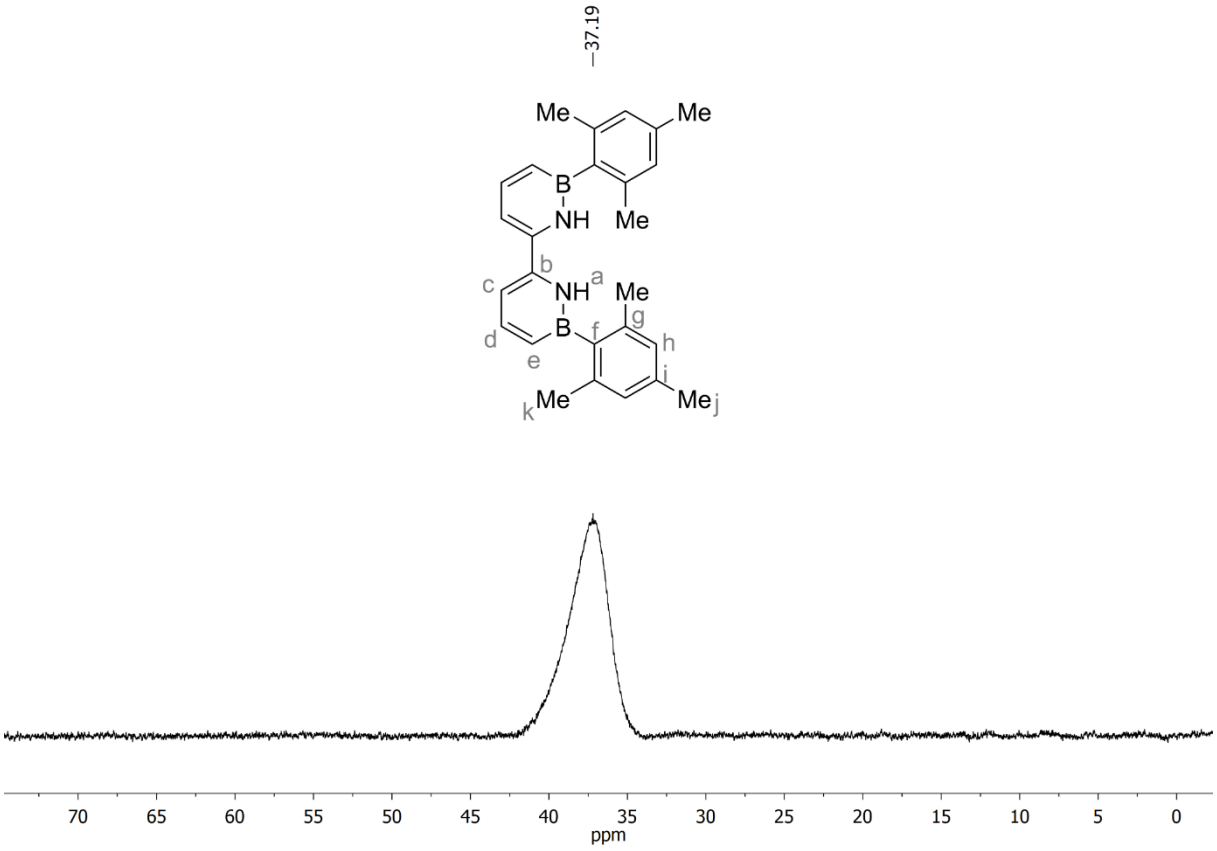
37.19
Me
Me
B
NH
Me
a
b
c
d
e
f
g
h
i
Me
Me
k
Me
j
70 65 60 55 50 45 40 35 30 25 20 15 10 5 0
ppm

1-Bromo-2-(2-(trimethylsilyl)ethynyl)benzene (8)

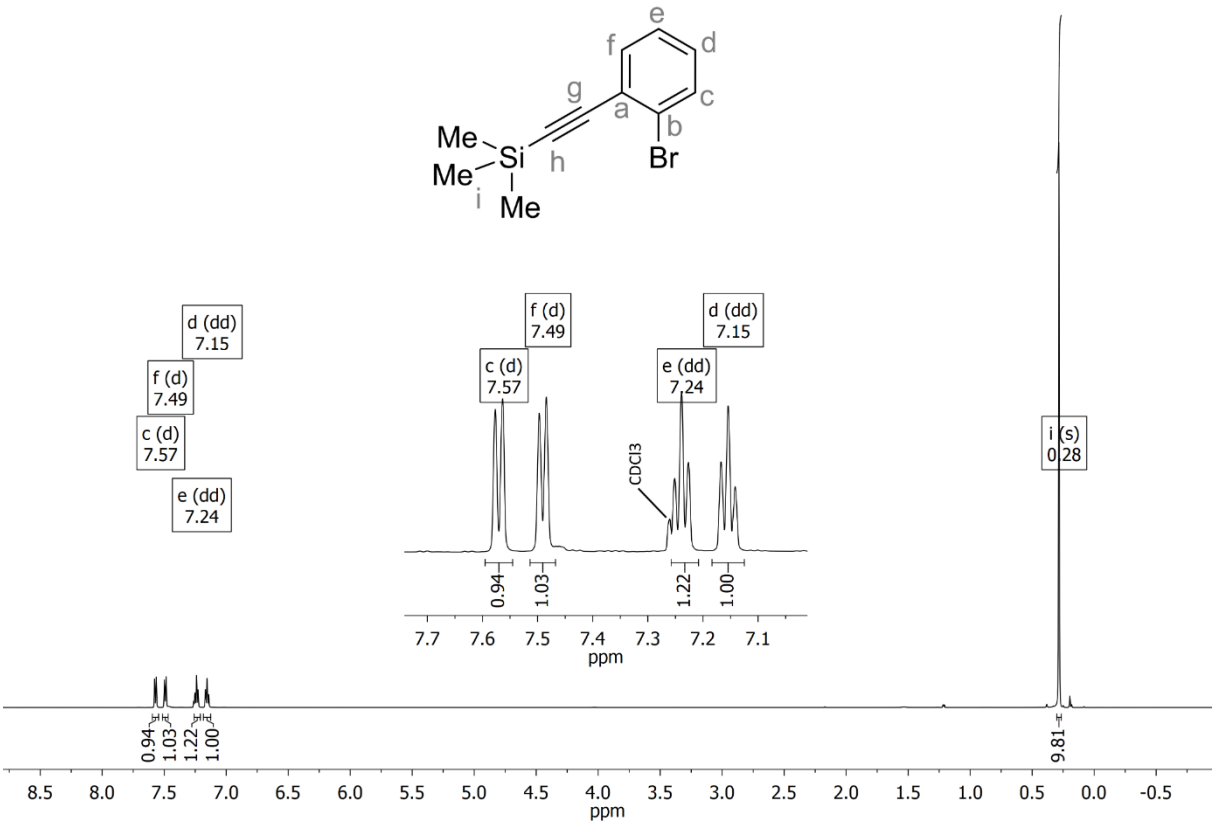

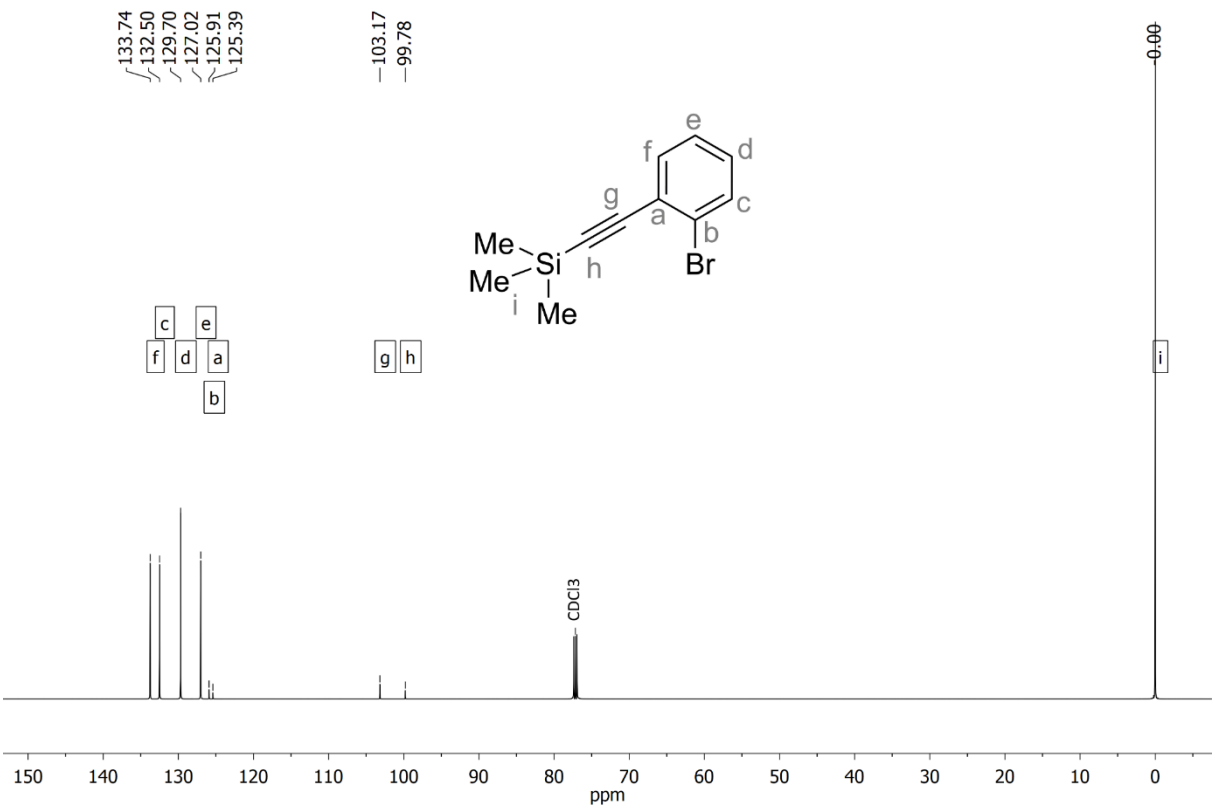

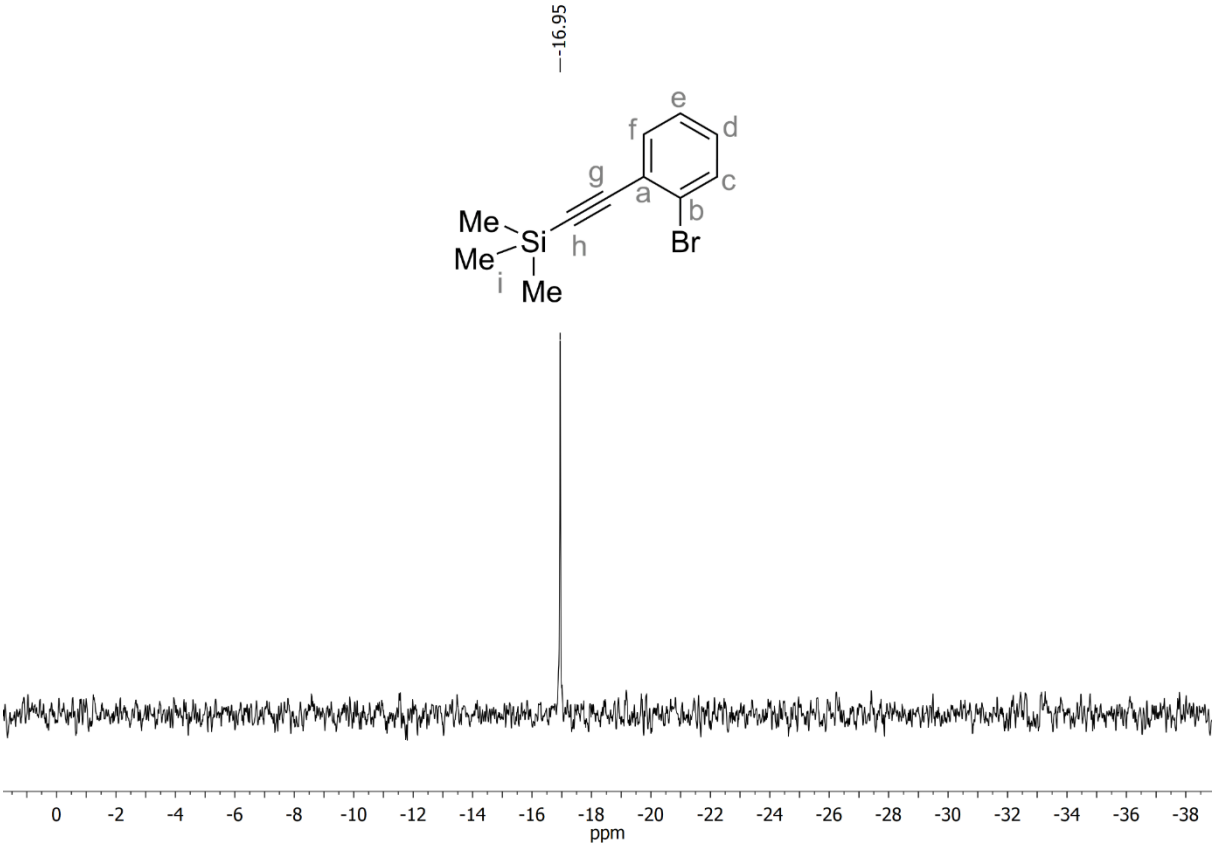

1-Hydro-2-mesityl-6-(2-((trimethylsilyl)ethynyl)phenyl)-1,2-azaborinine (14)

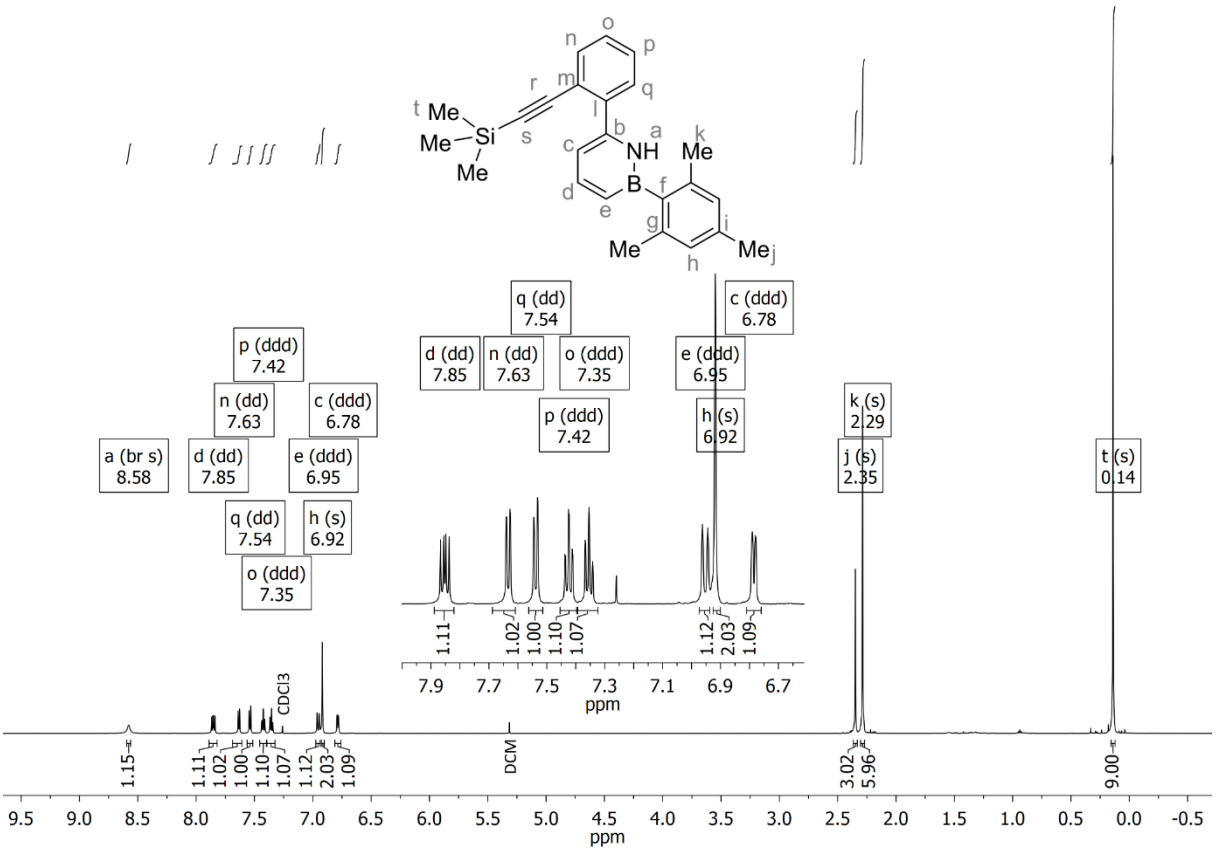

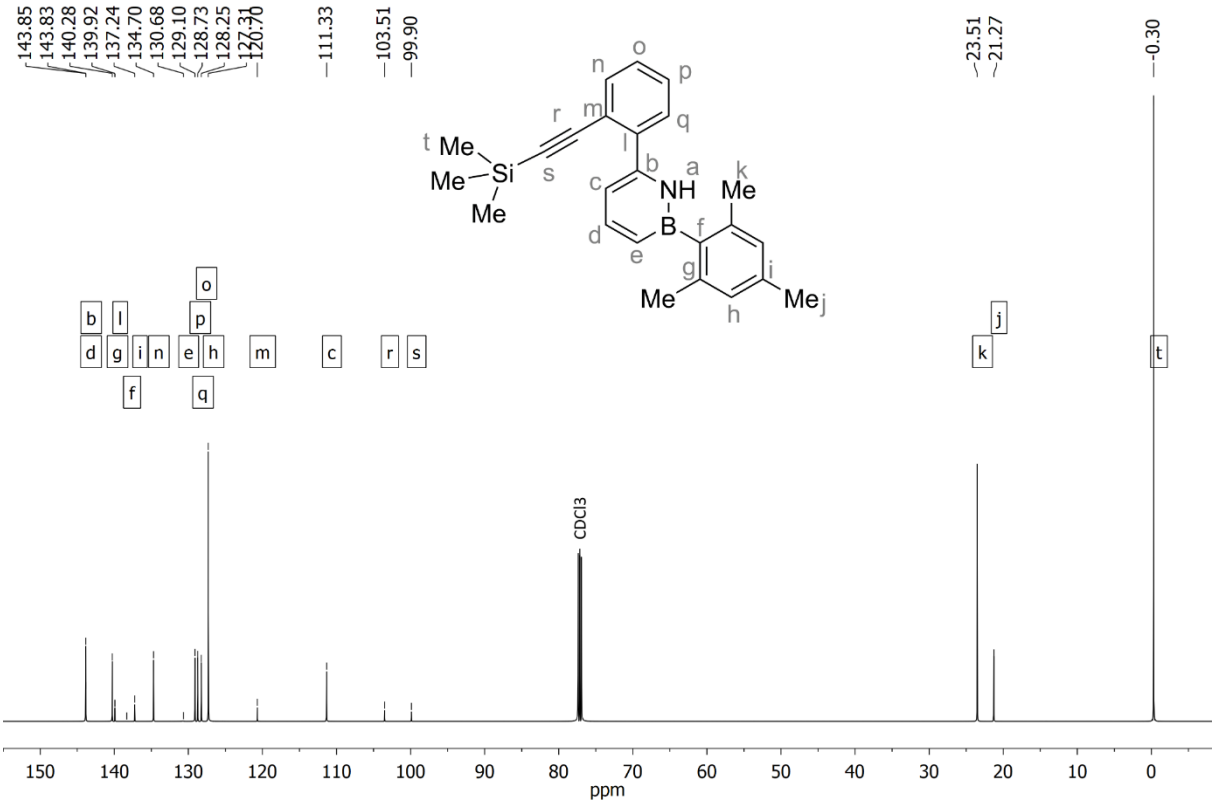
143.85
143.83
140.28
139.92
137.24
134.70
130.68
129.10
128.73
128.25
127.31
120.70
111.33
103.51
99.90
23.51
21.27
0.30
CDCl3
Me
Si
NH
B
ppm

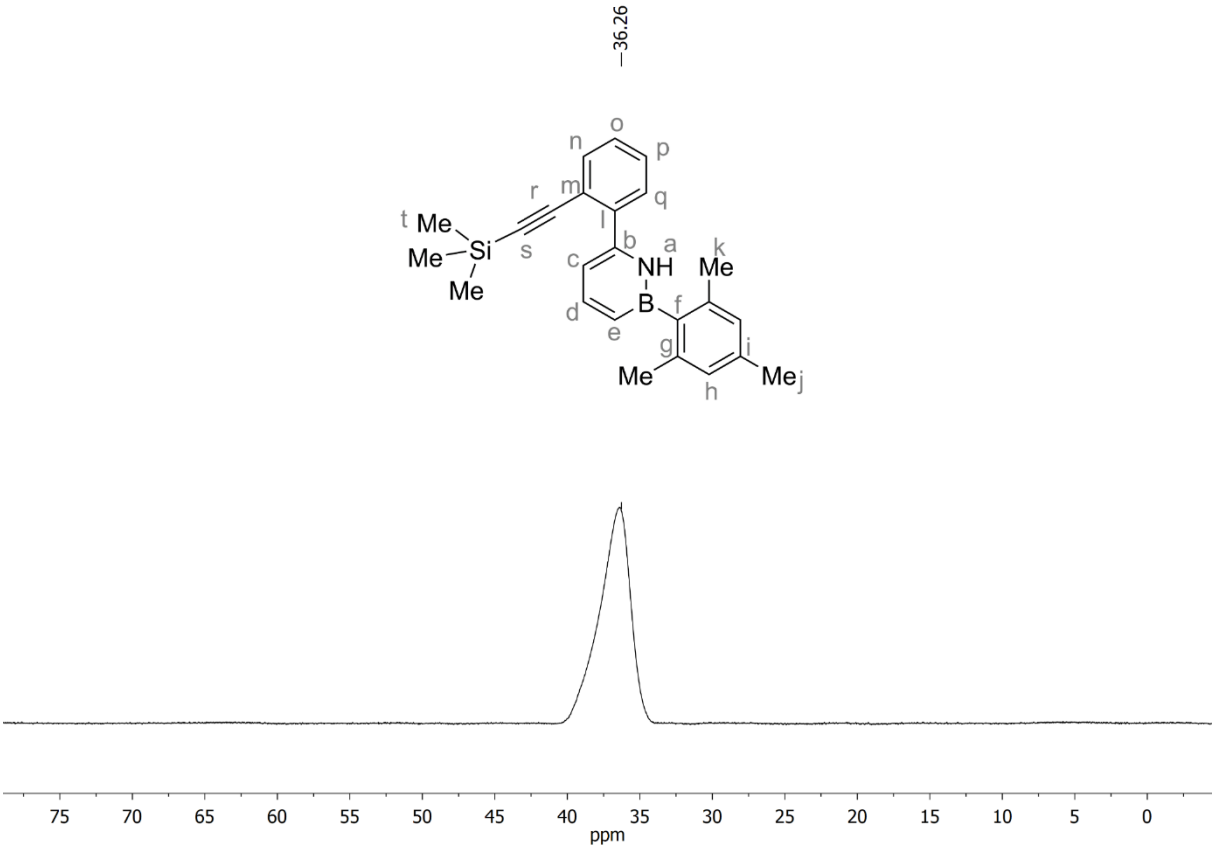
36.26
Me
Si
NH
B
ppm

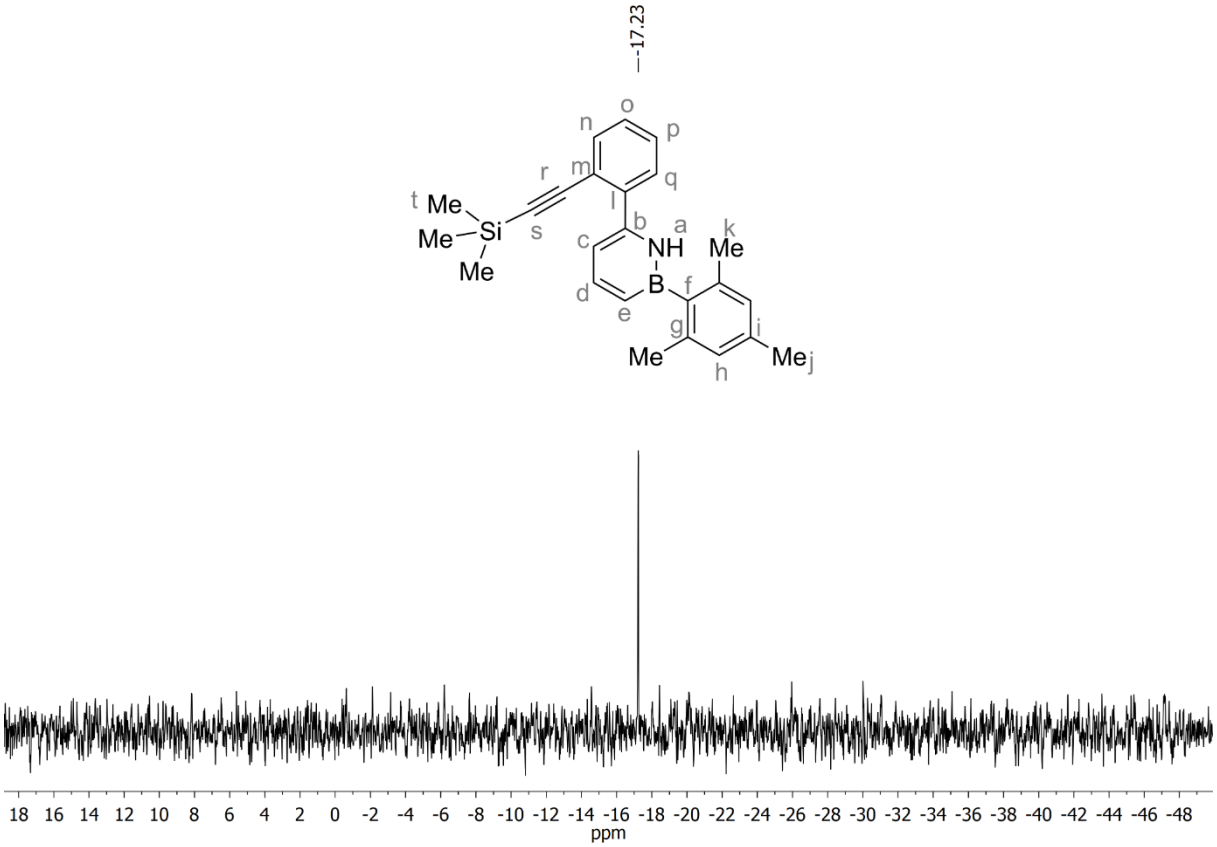

4-Hydro-3-mesityl-4,3-azaboraphenanthrene (*BN*-PAH1)

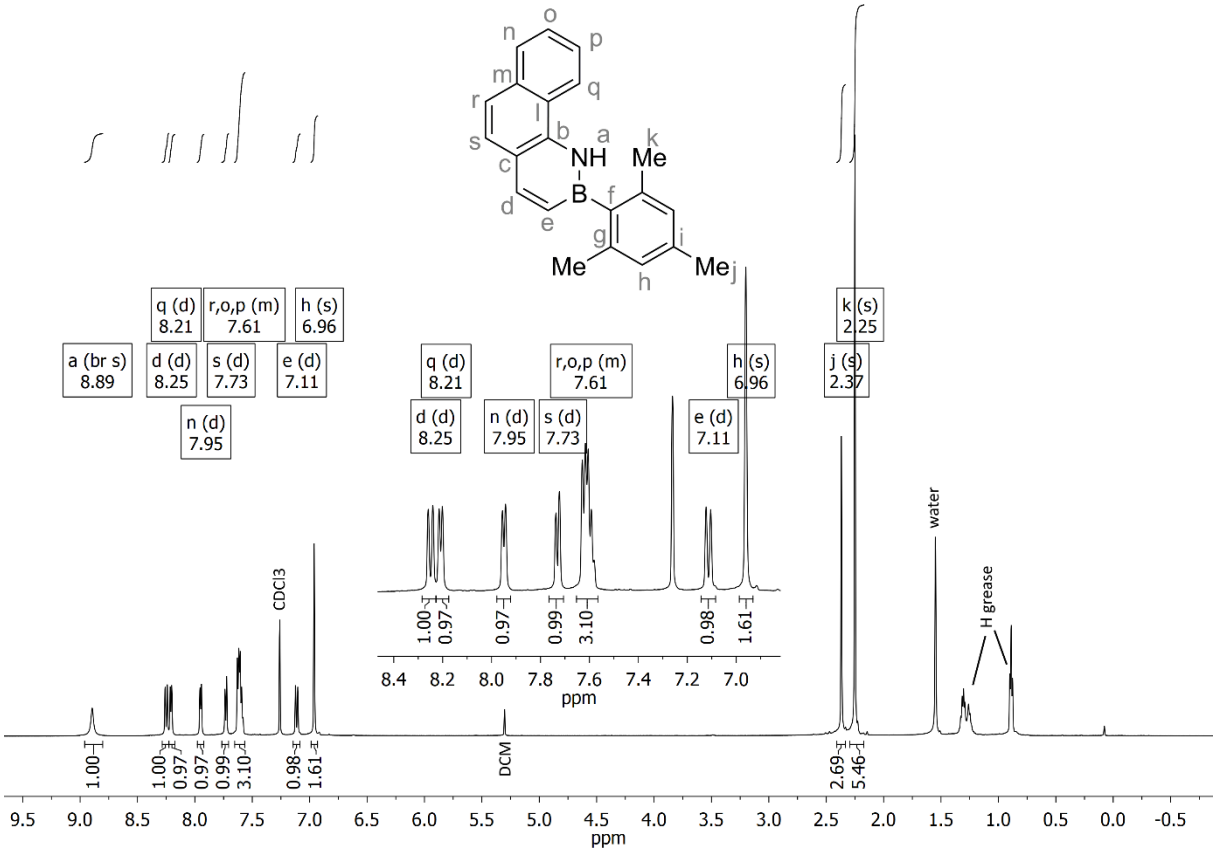

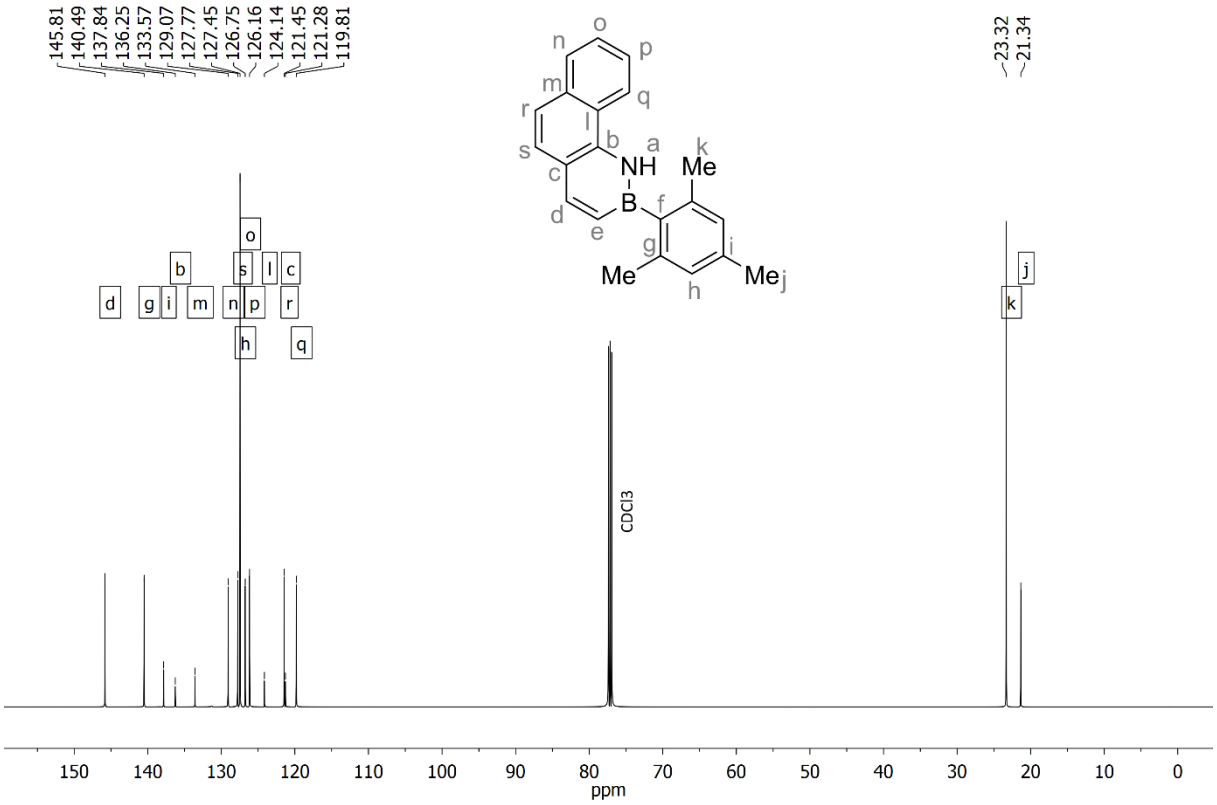
145.81
140.49
137.84
136.25
133.57
129.07
127.77
127.45
126.75
126.16
124.14
121.45
121.28
119.81
23.32
21.34
CDCl3
NH
Me
B
Me
Me
ppm

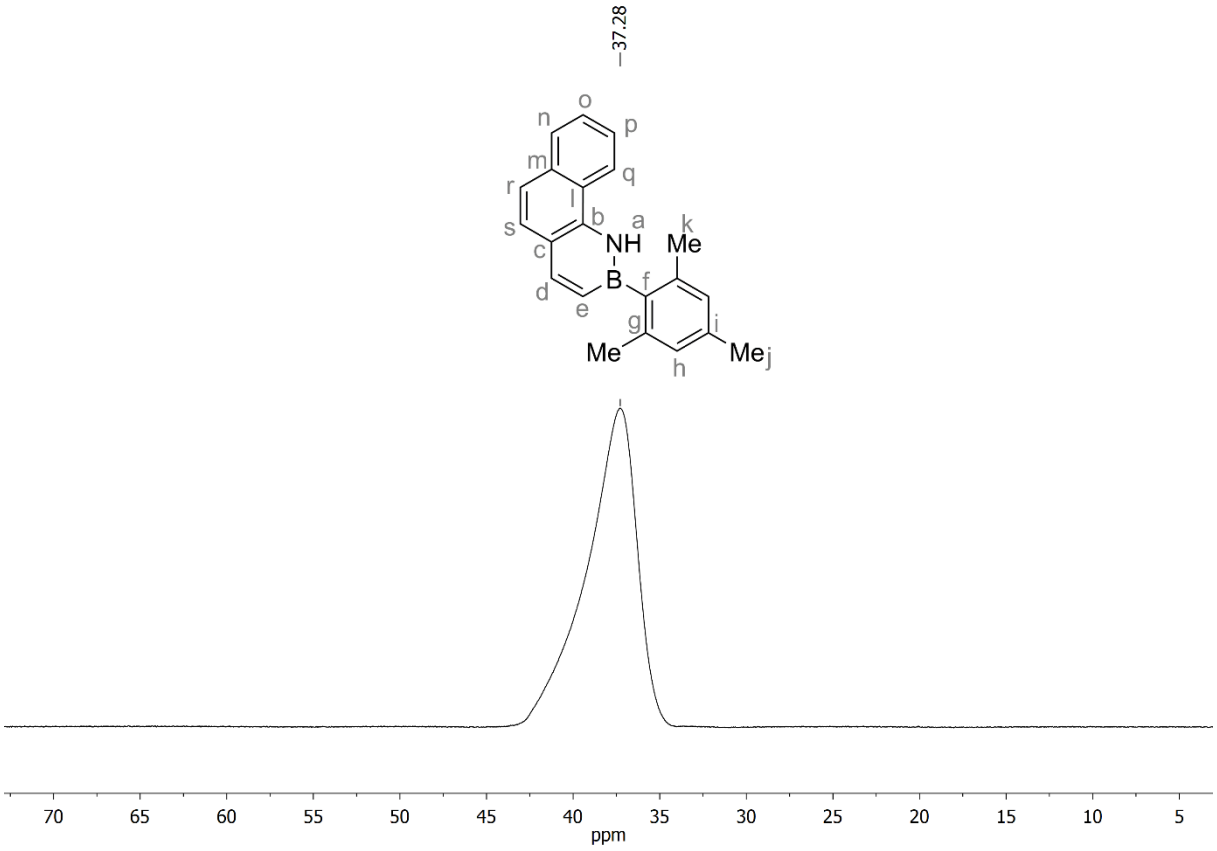
37.28
NH
Me
B
Me
Me
ppm

2-Bromo-3-iodothiophene (35)

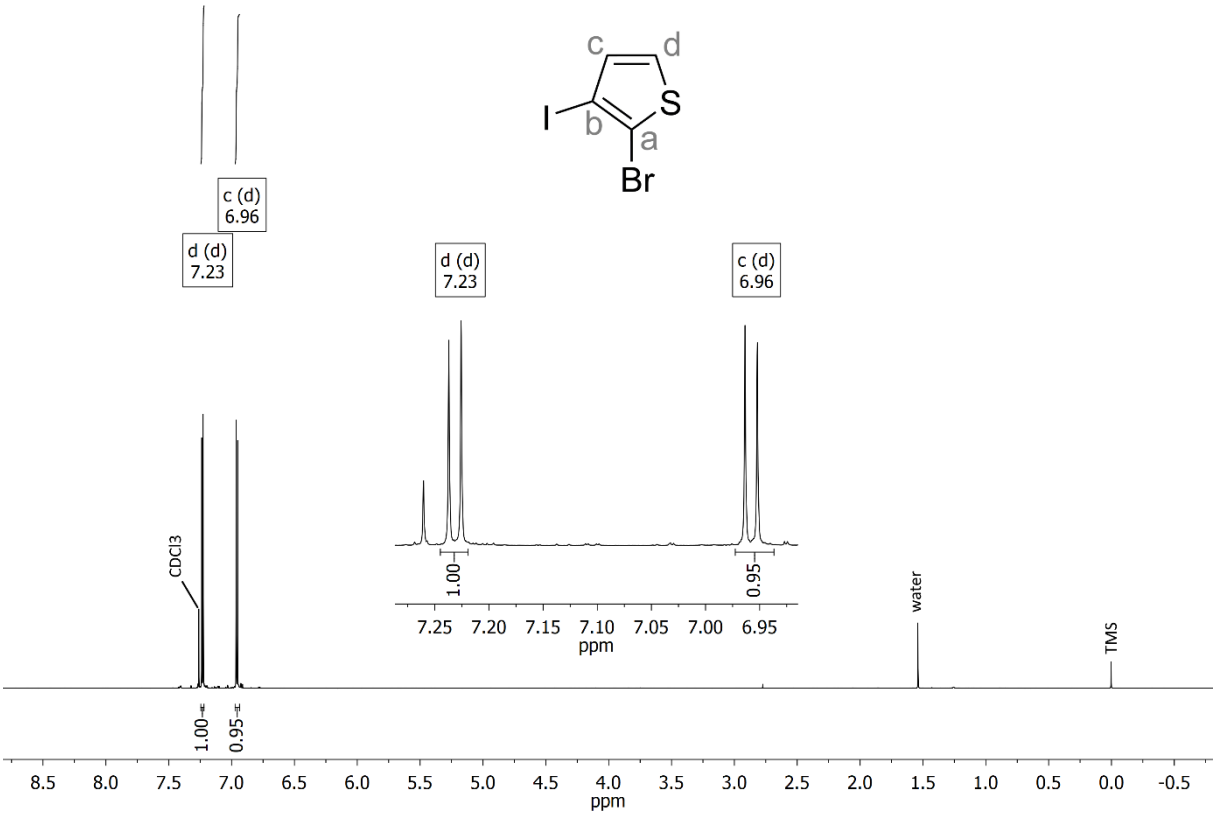

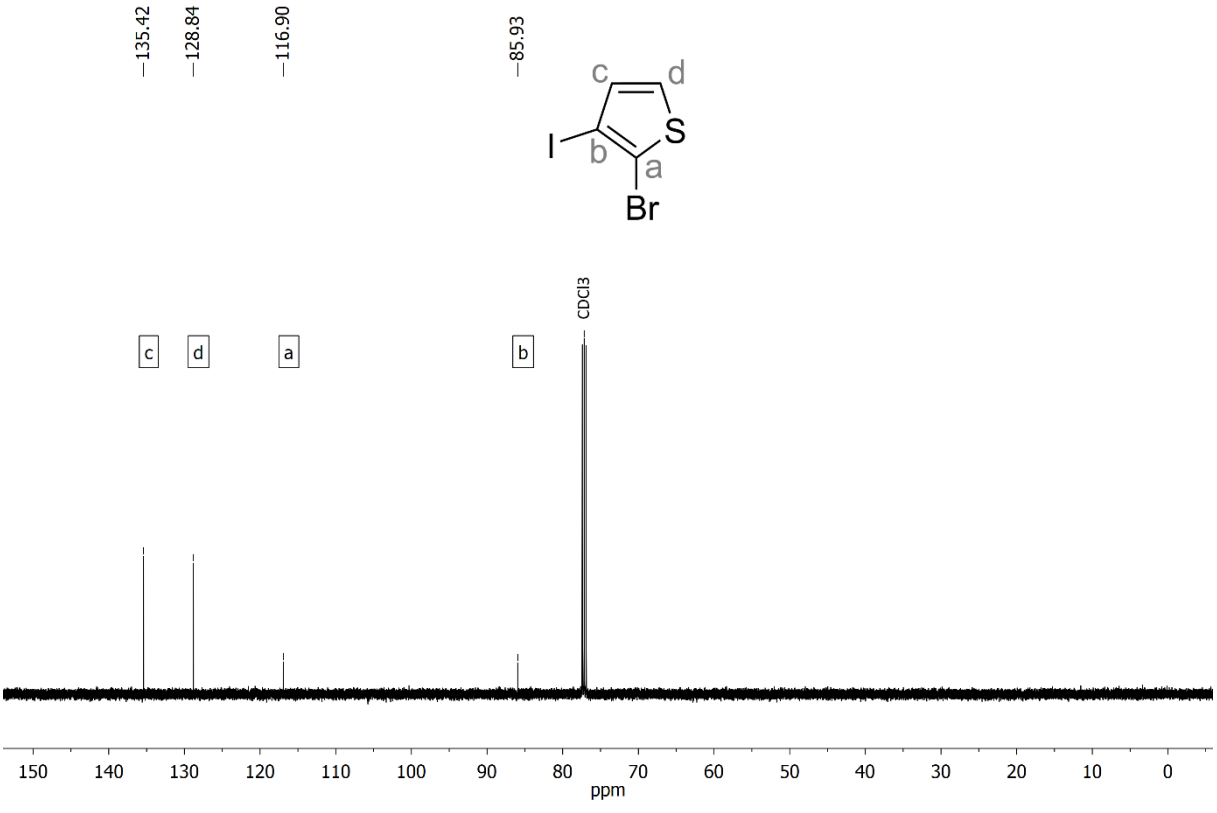

2-Bromo-3-(2-(trimethylsilyl)ethynyl)thiophene (9)

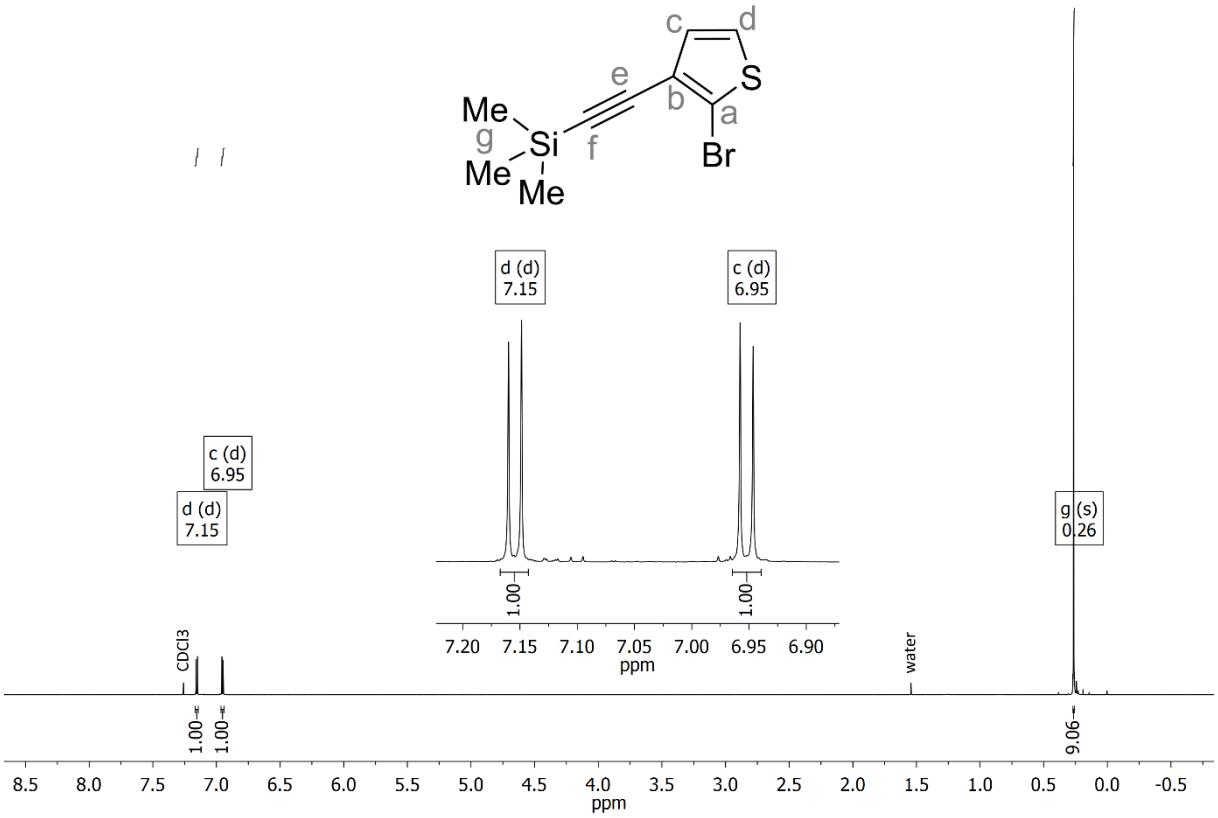

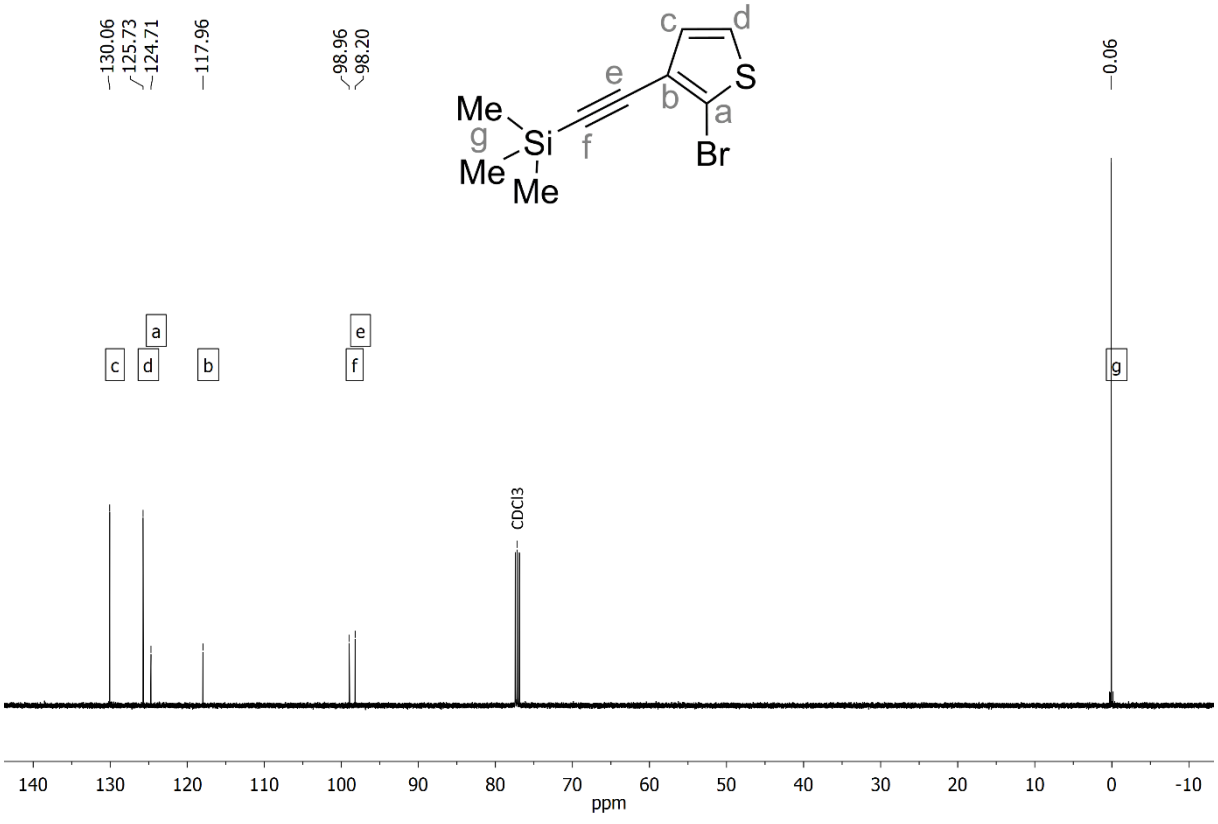

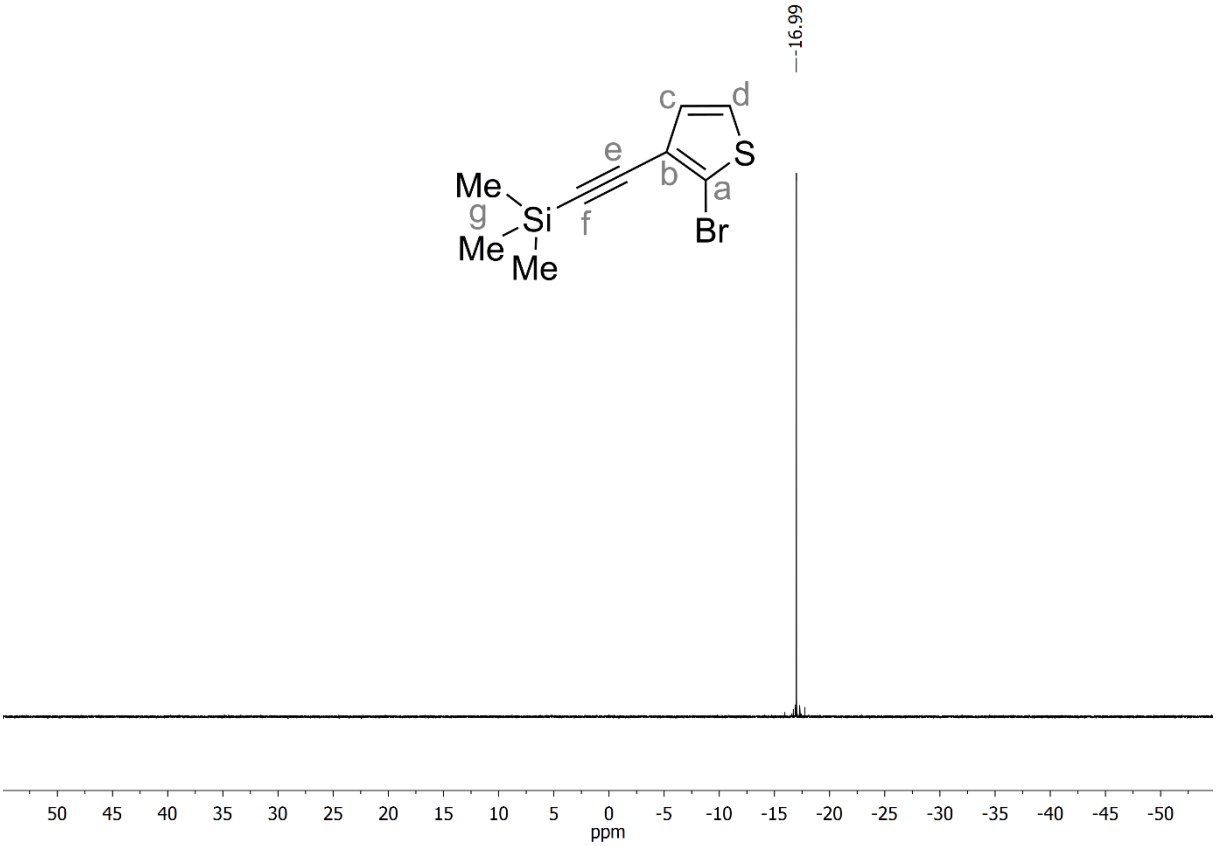

1-Hydro-2-mesityl-6-(3-((trimethylsilyl)ethynyl)thiophen-2-yl)-1,2-azaborinine (15)

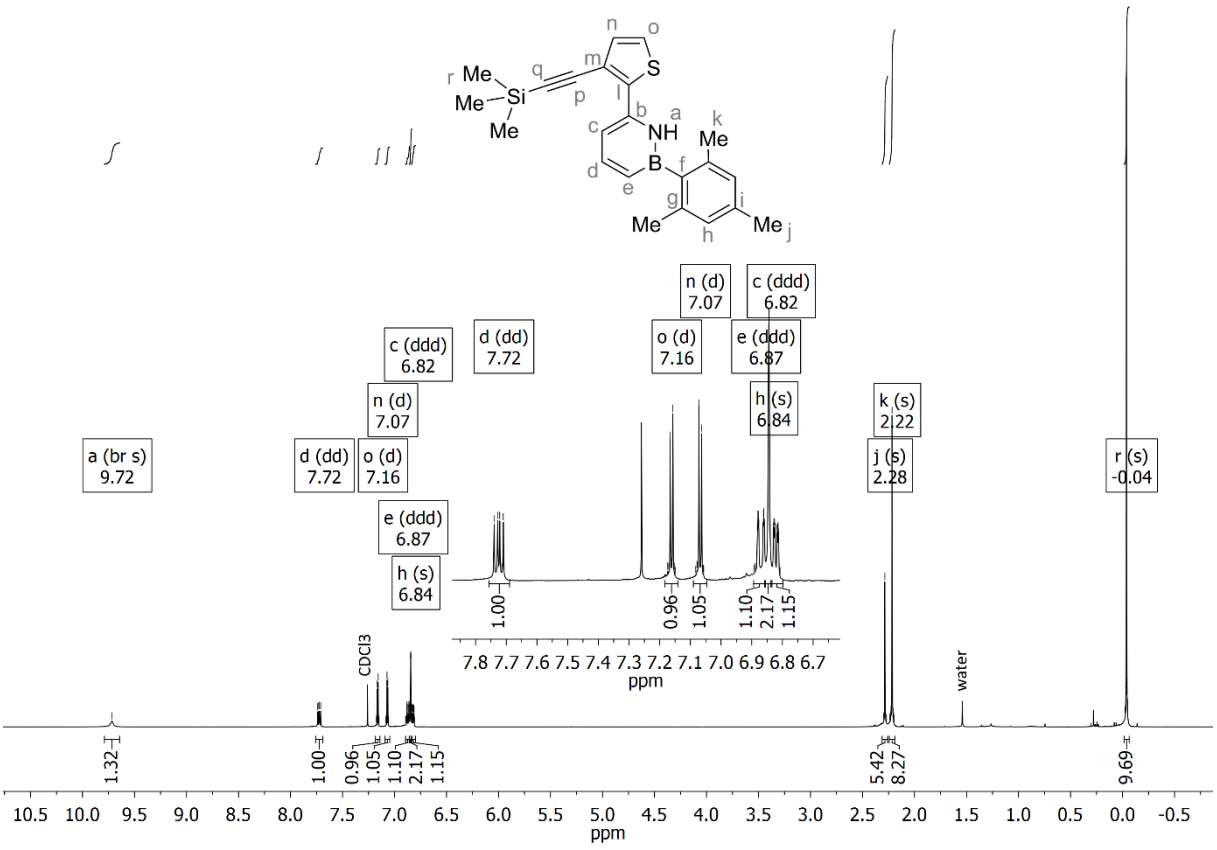

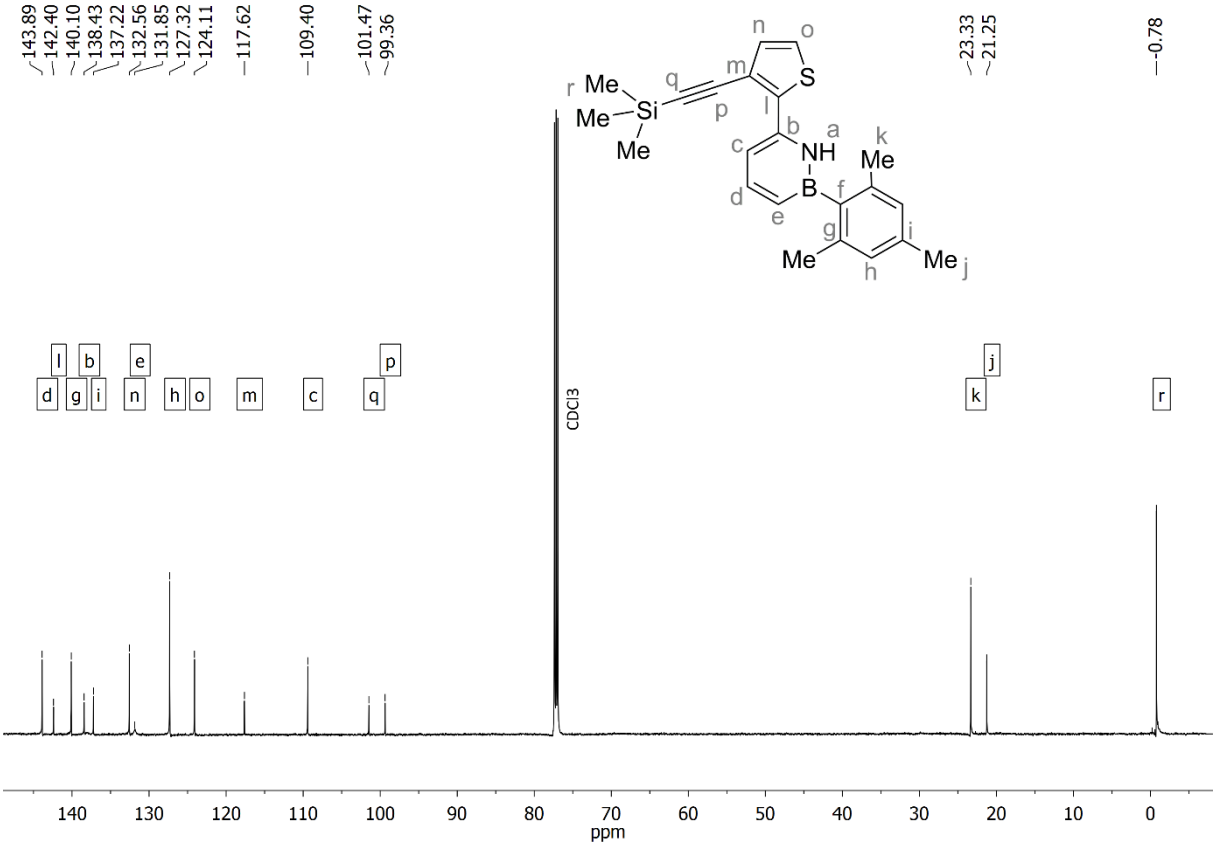
143.89
142.40
140.10
138.43
137.22
132.56
131.85
127.32
124.11
117.62
109.40
101.47
99.36
23.33
21.25
-0.78
CDCl3
ppm

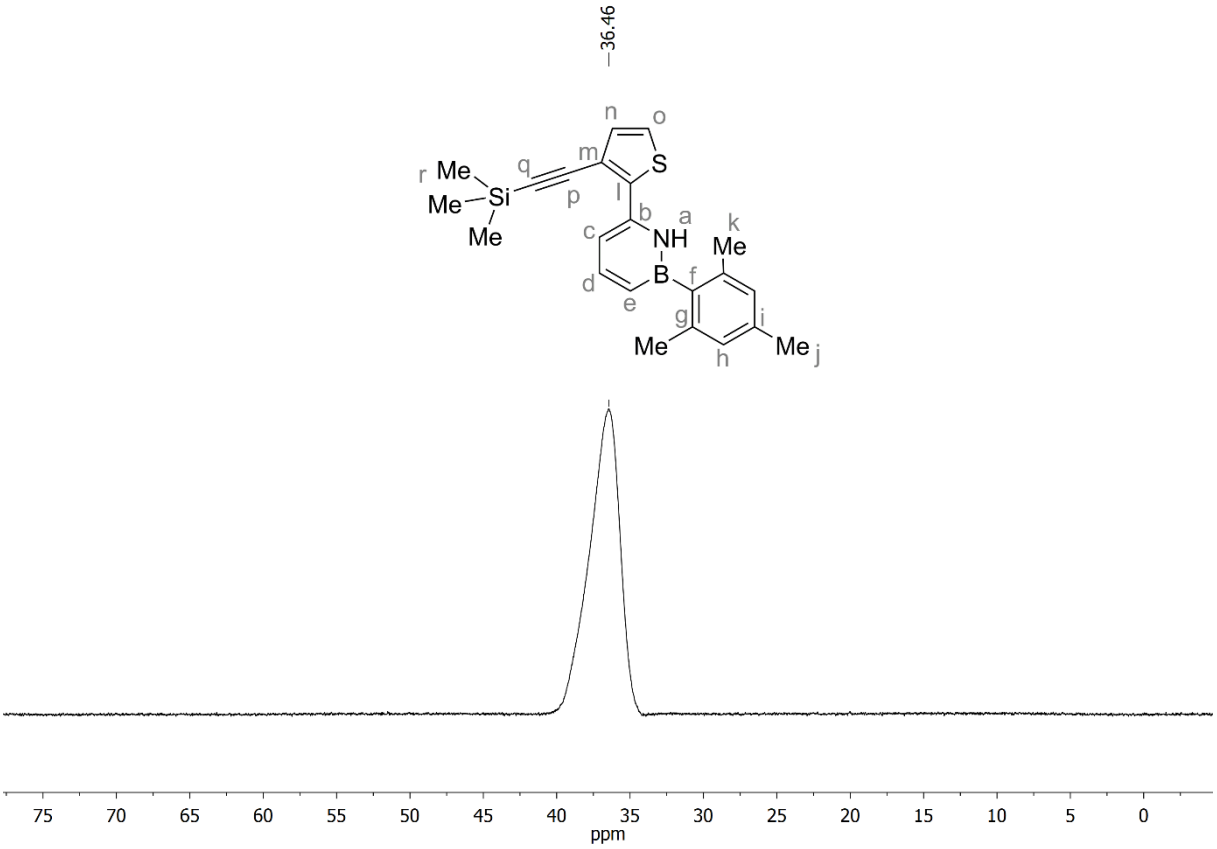
36.46
ppm

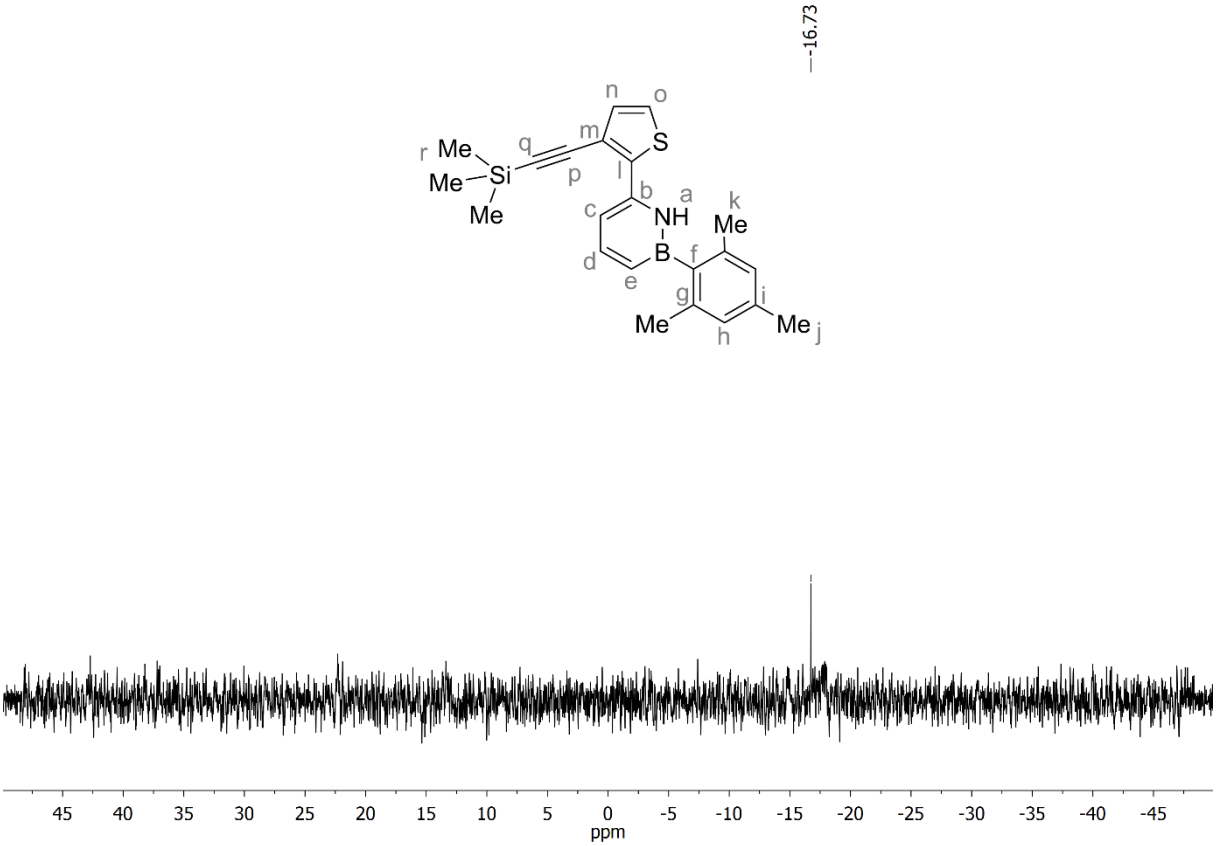

9-Hydro-8-mesityl-9,8-azaboranaphtho[1,2-*b*]thiophene (*BN*-PAH2)

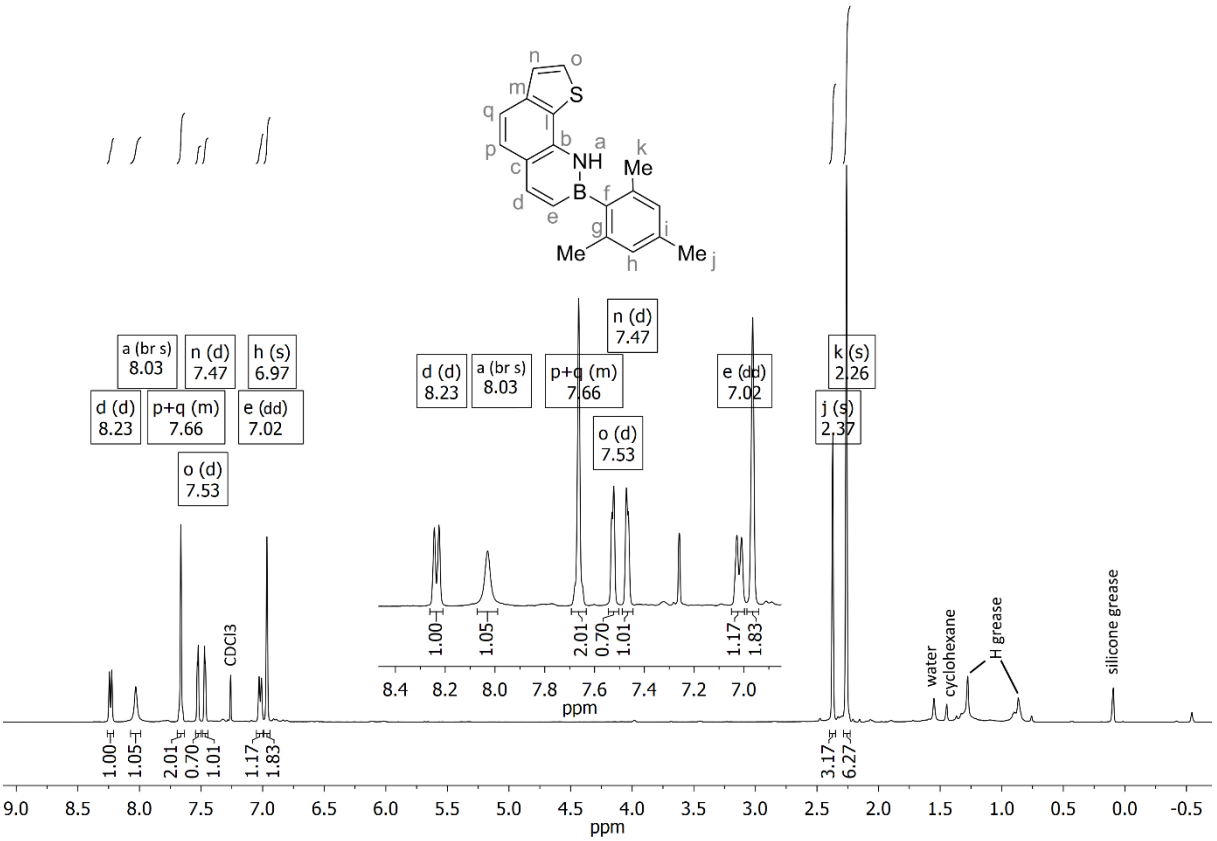

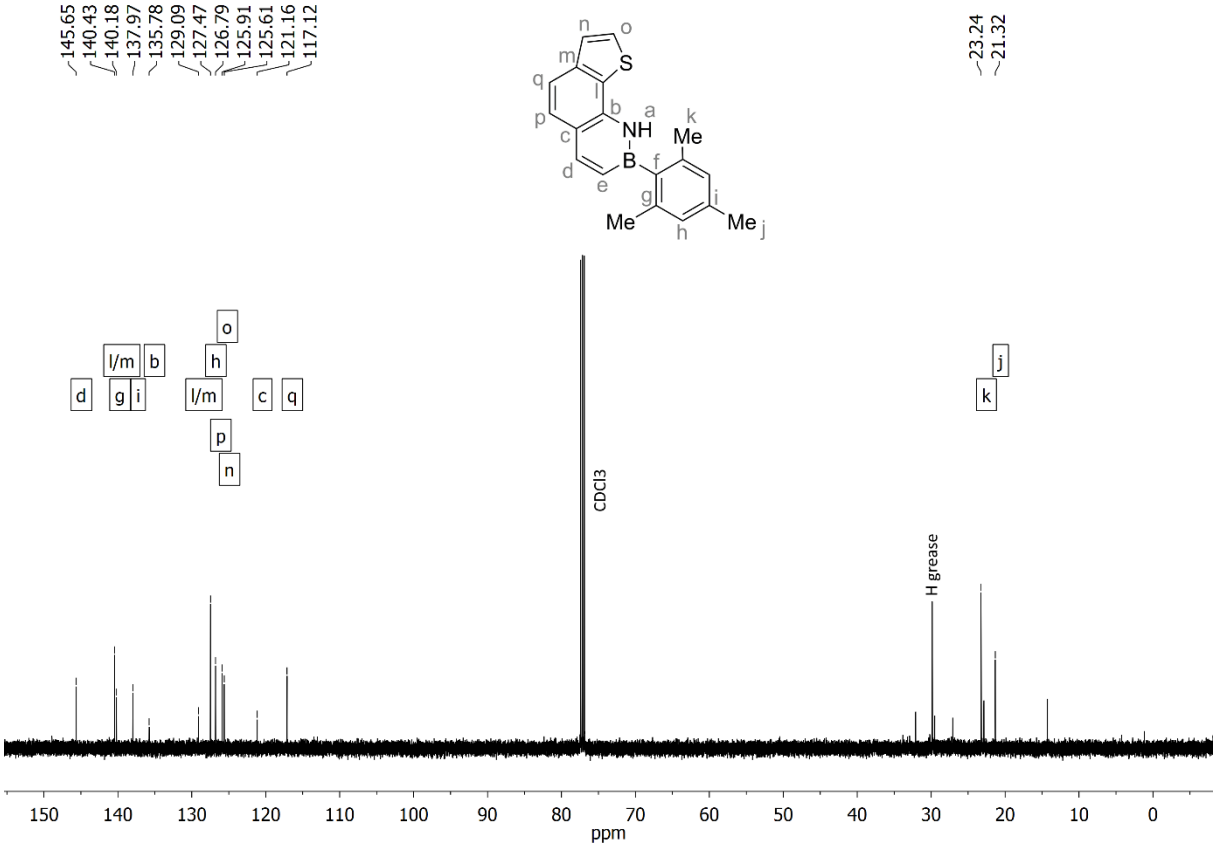
145.65
140.43
140.18
137.97
135.78
129.09
127.47
126.79
125.91
125.61
121.16
117.12
23.24
21.32
CDCl3
H grease
ppm

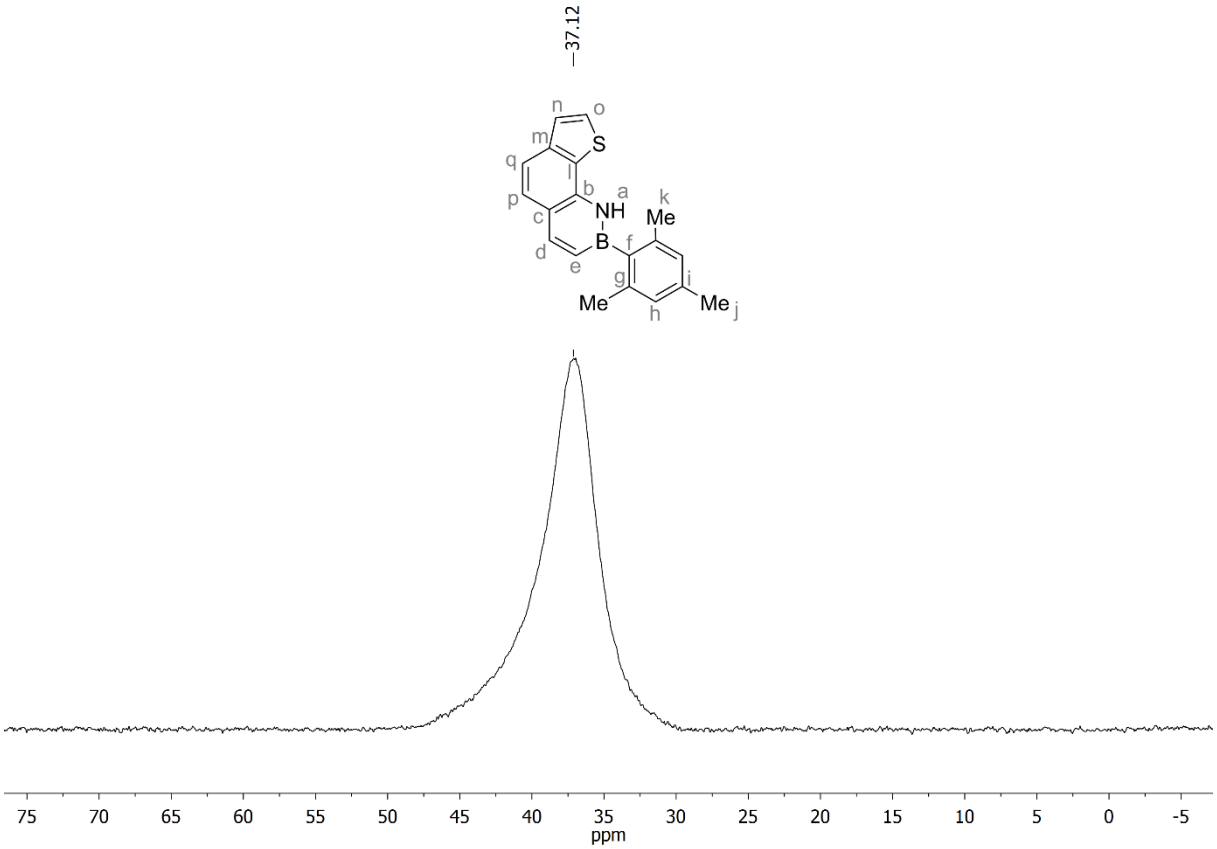
37.12
ppm

2-Bromo-3-(2-(trimethylsilyl)ethynyl)pyridine (10)

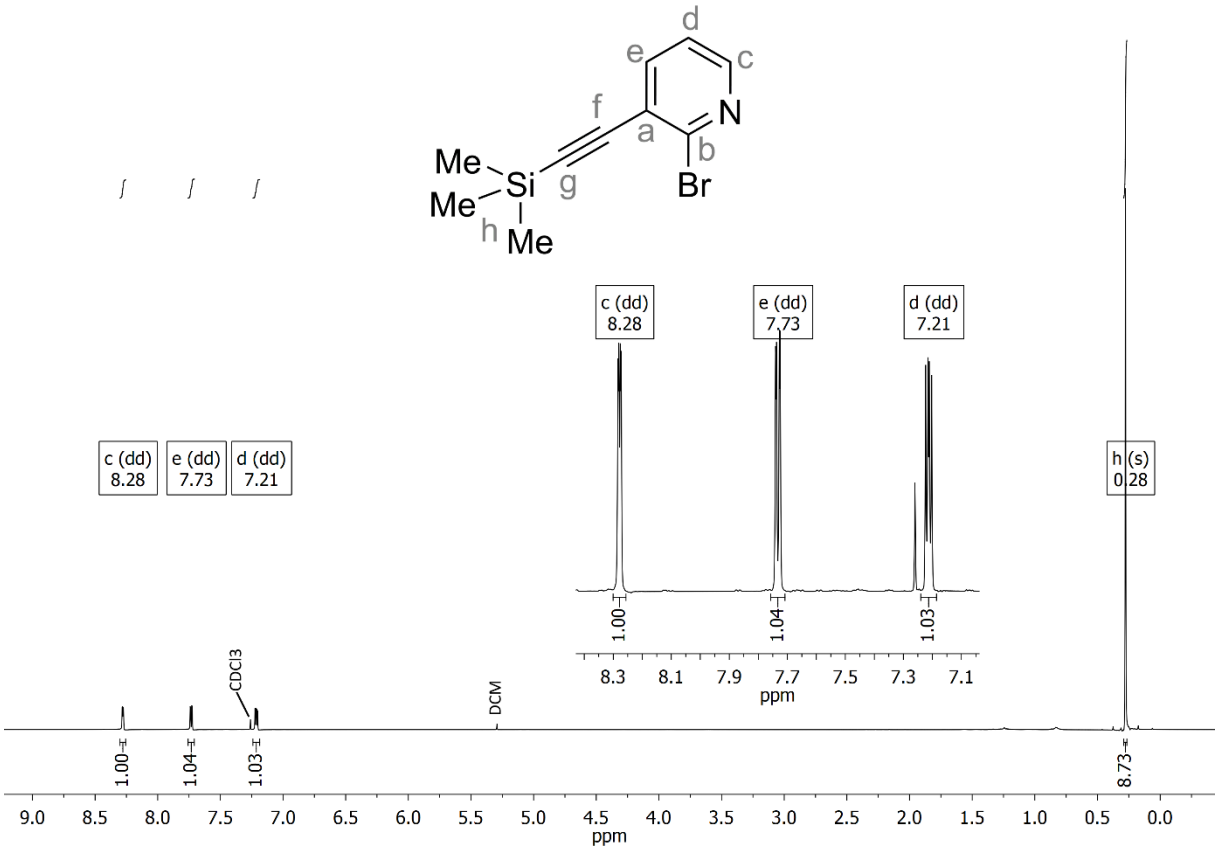

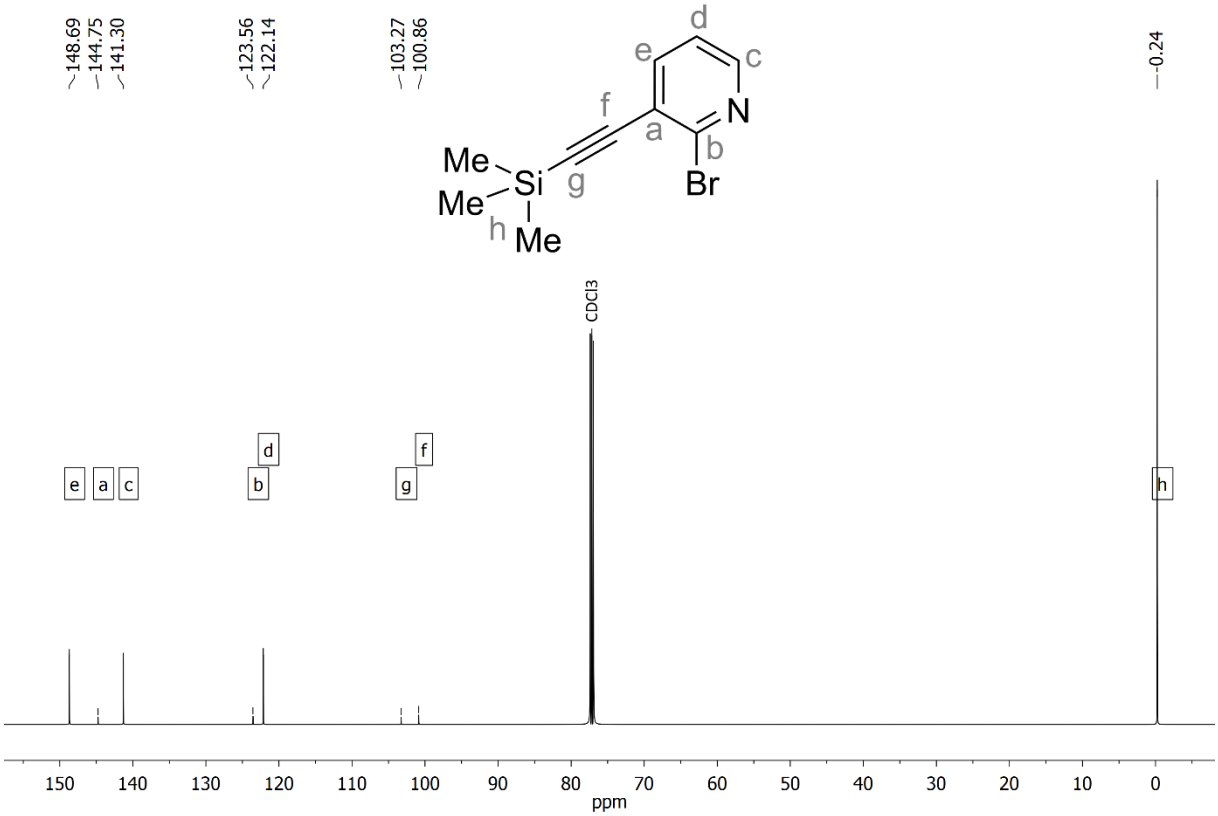

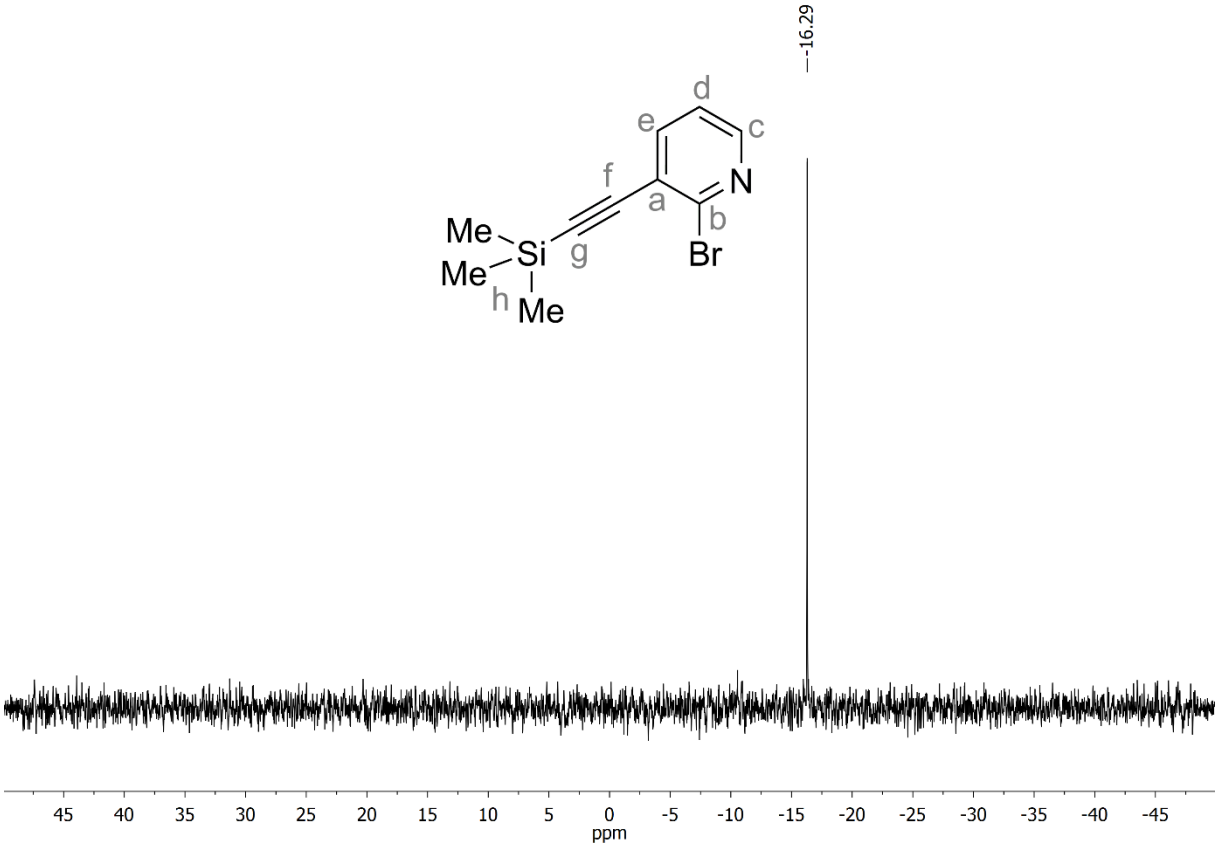

1-Hydro-2-mesityl-6-(3-((trimethylsilyl)ethynyl)pyridin-2-yl)-1,2-azaborinine (16)

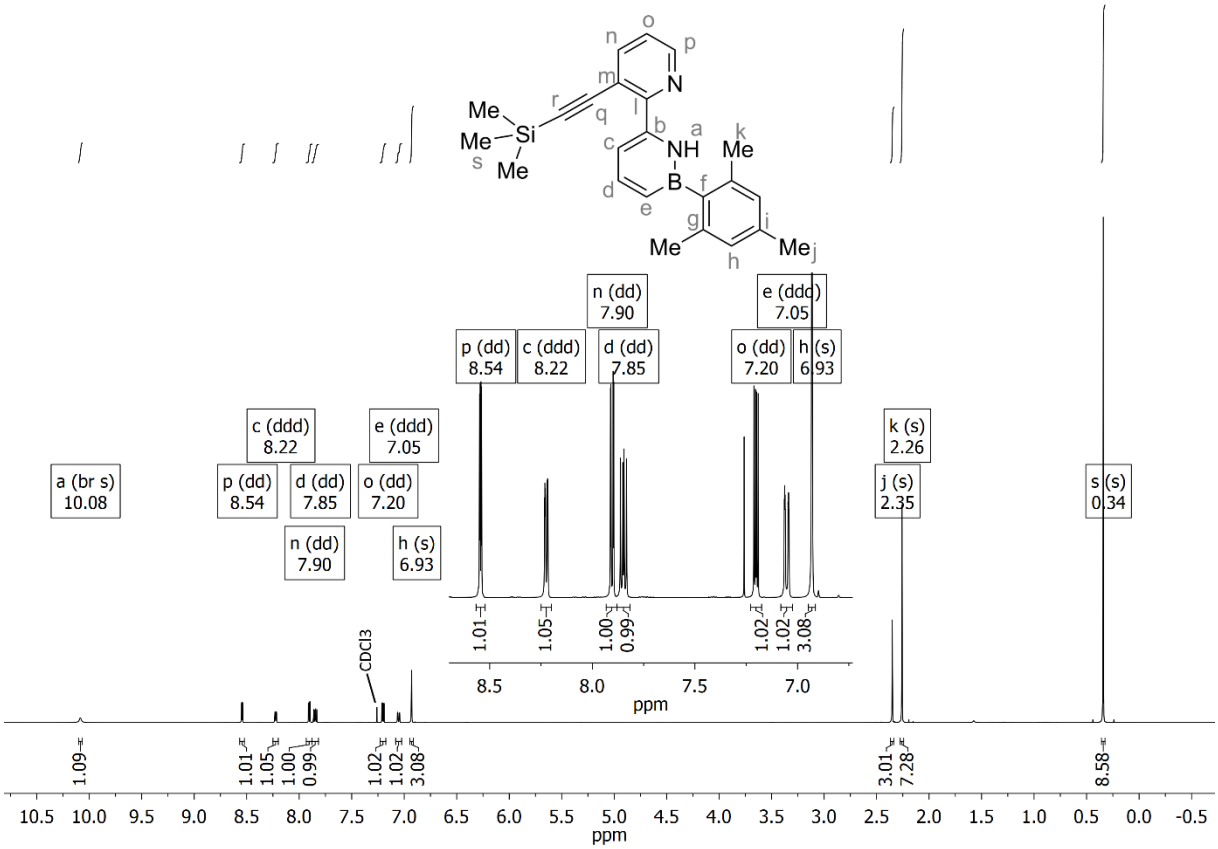

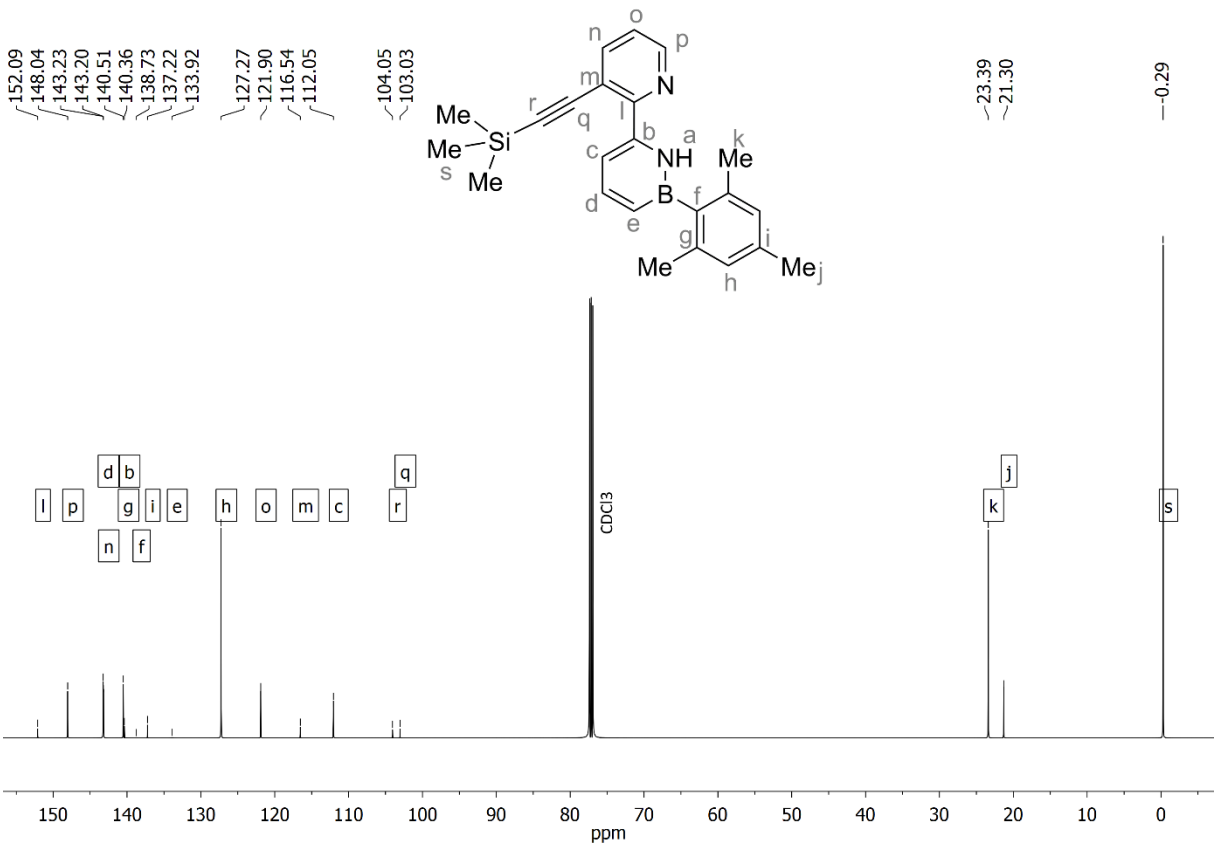
152.09
148.04
143.23
143.20
140.51
140.36
138.73
137.22
133.92
127.27
121.90
116.54
112.05
104.05
103.03
23.39
21.30
-0.29
CDCl3
ppm

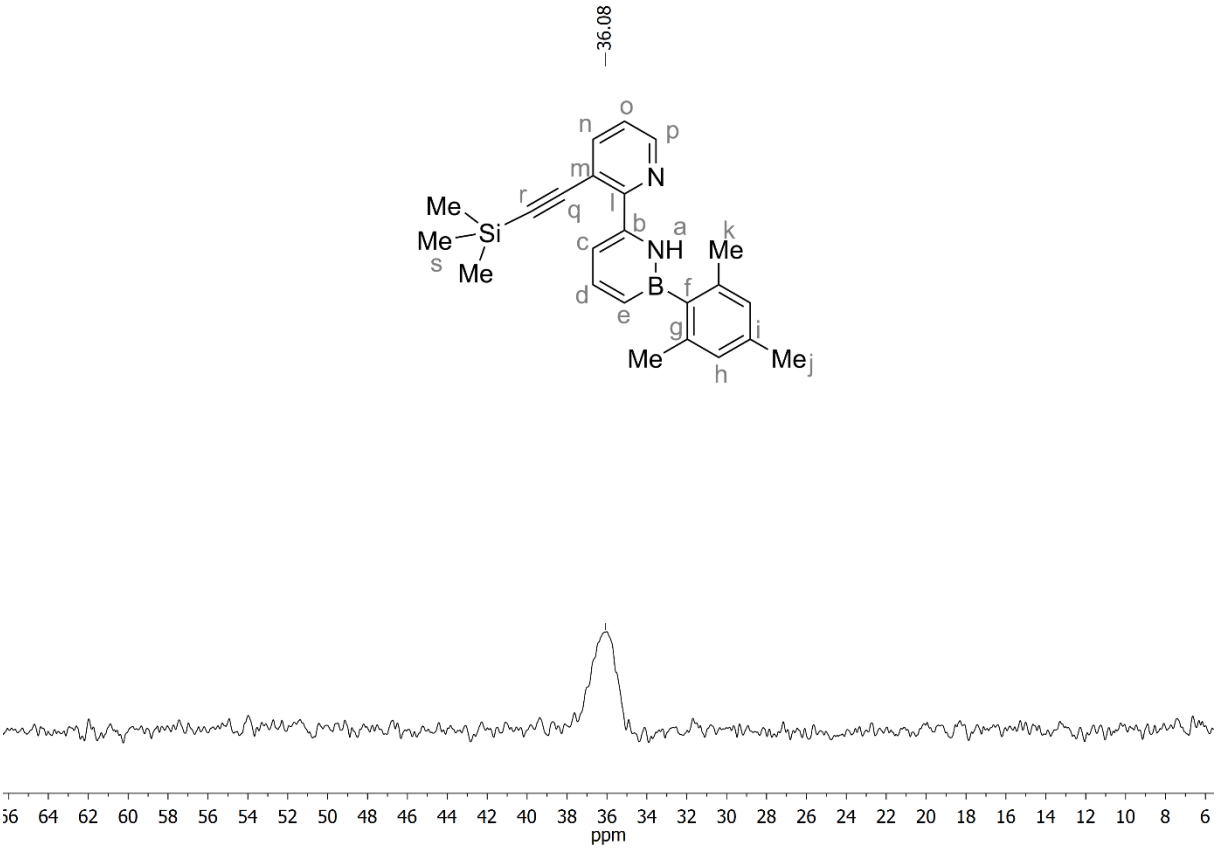
36.08
ppm

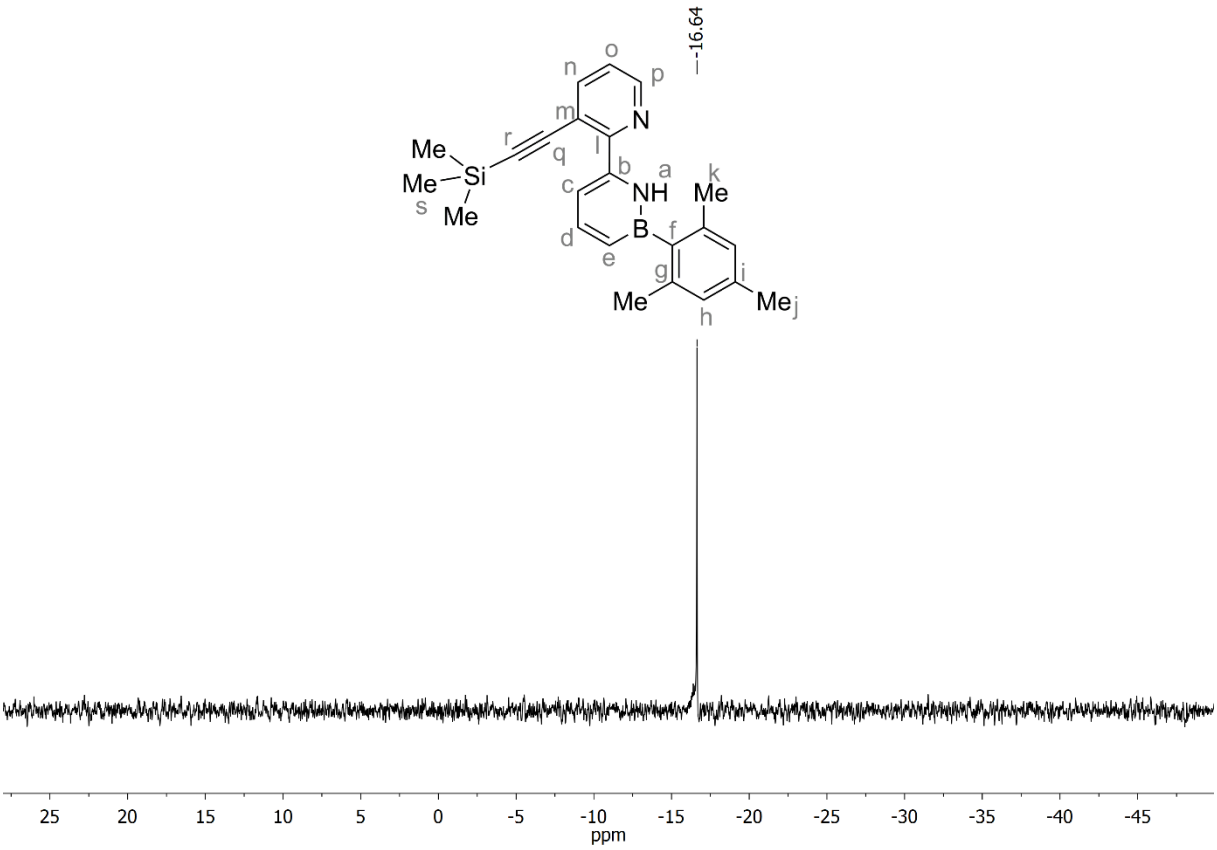

10-Hydro-9-mesityl-10,9-azaborabenzo*[h]*quinoline (*BN*-PAH3)

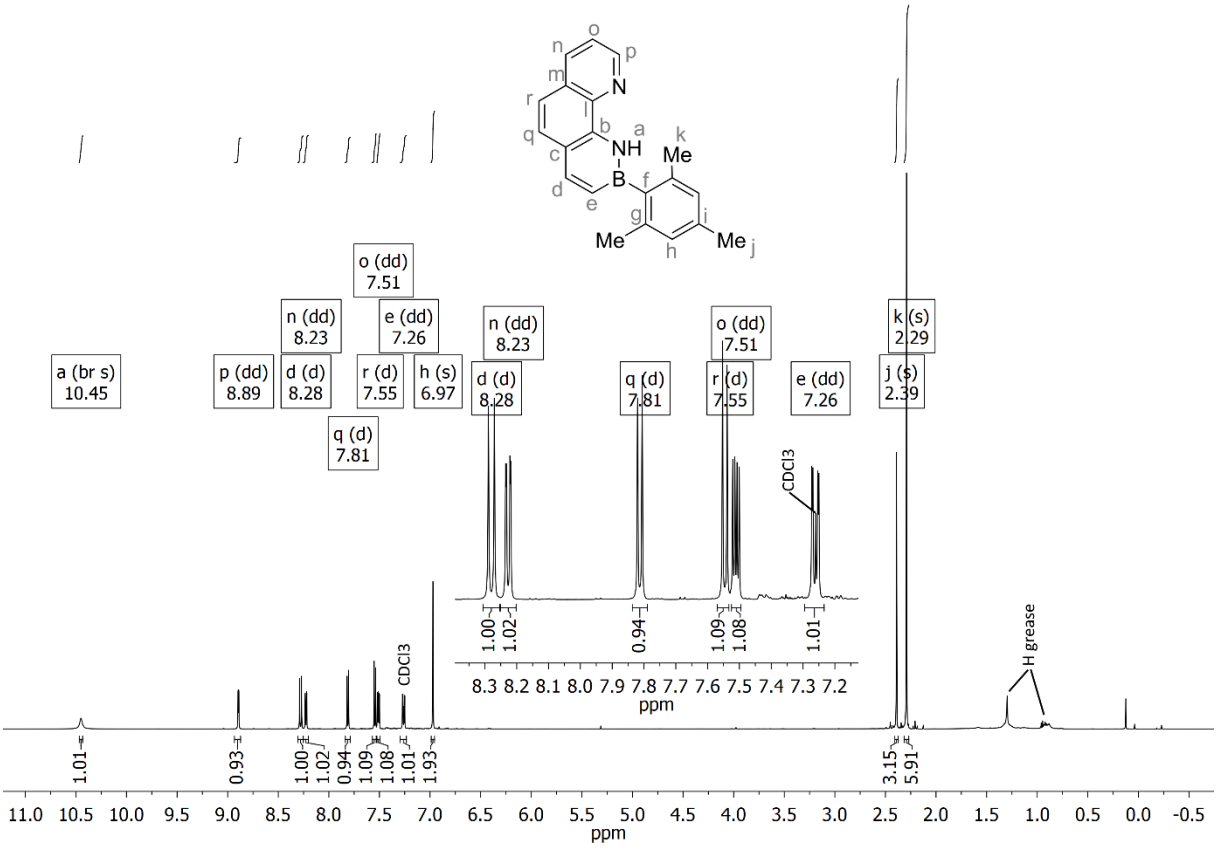

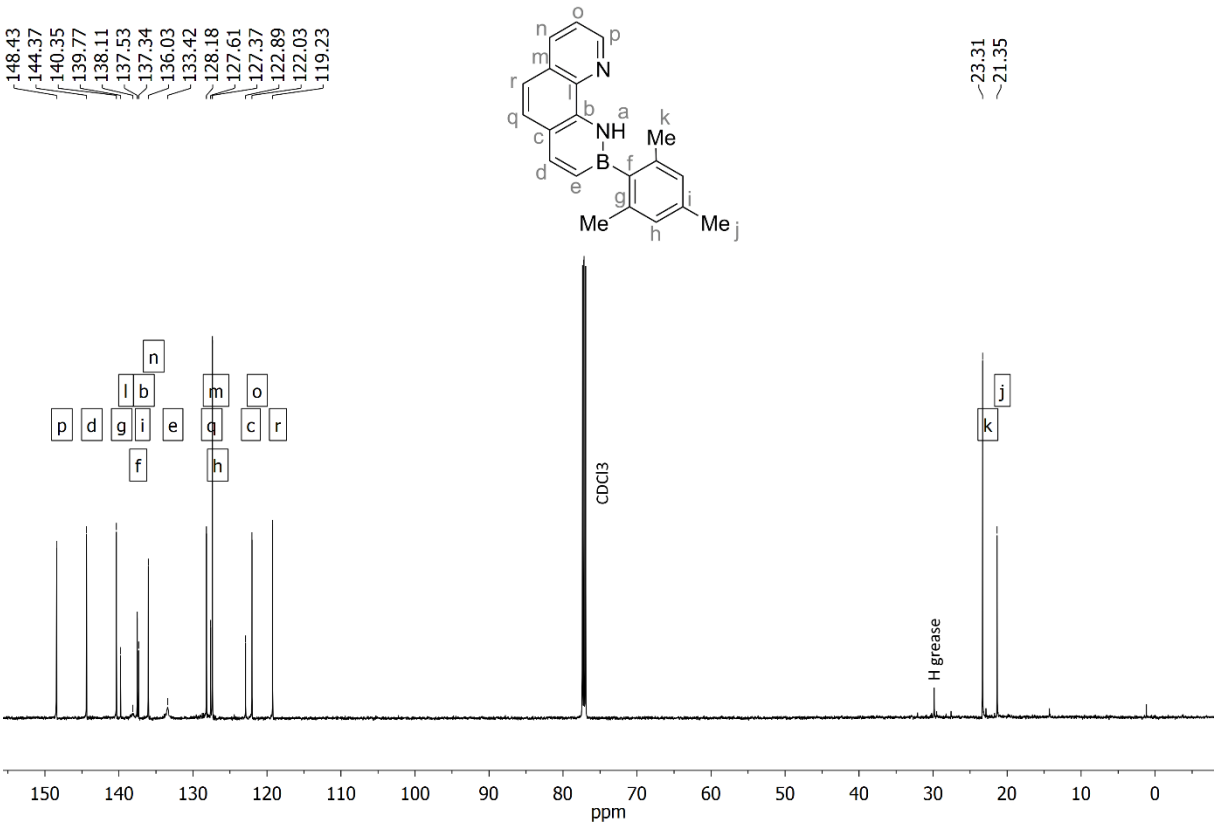
148.43
144.37
140.35
139.77
138.11
137.53
137.34
136.03
133.42
128.18
127.61
127.37
122.89
122.03
119.23
23.31
21.35
CDCl3
H grease
ppm

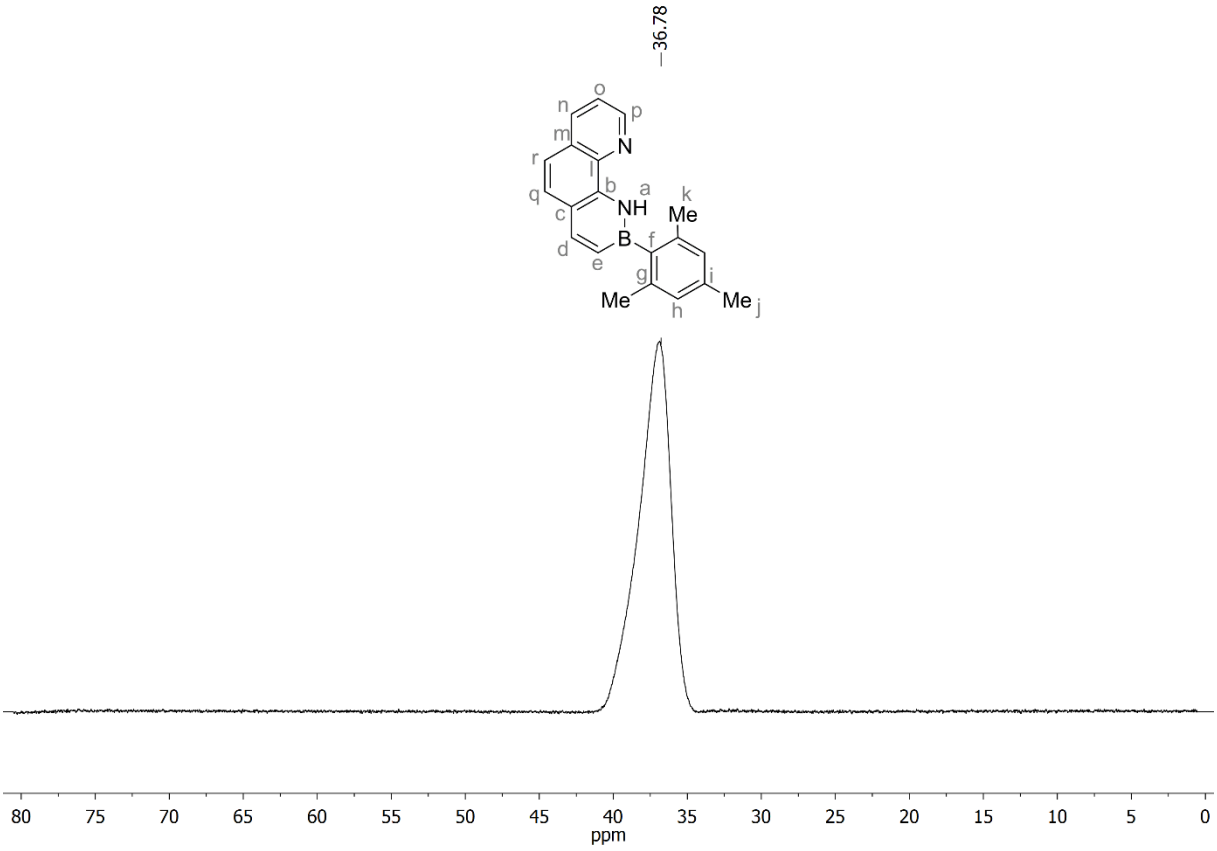
36.78
ppm

1,5-Dibromo-2,4-diiodobenzene (36)

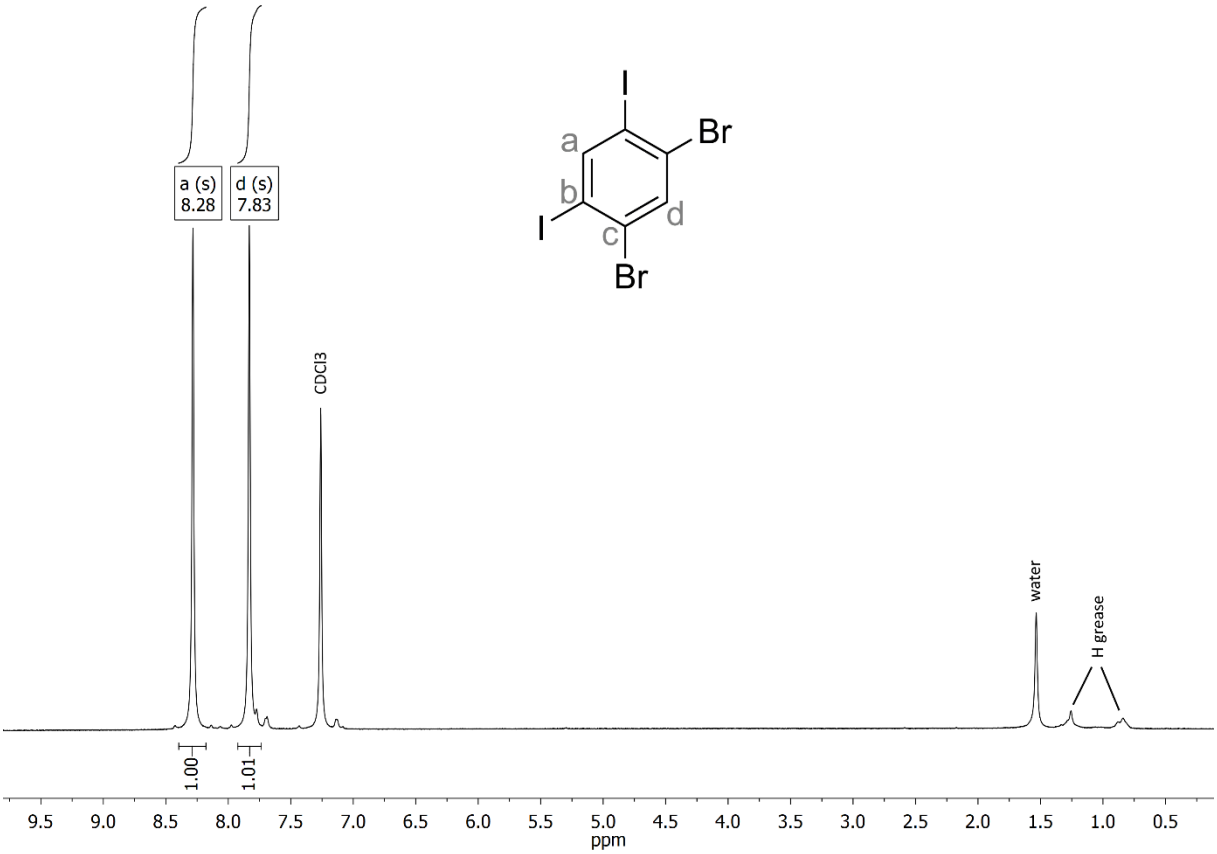

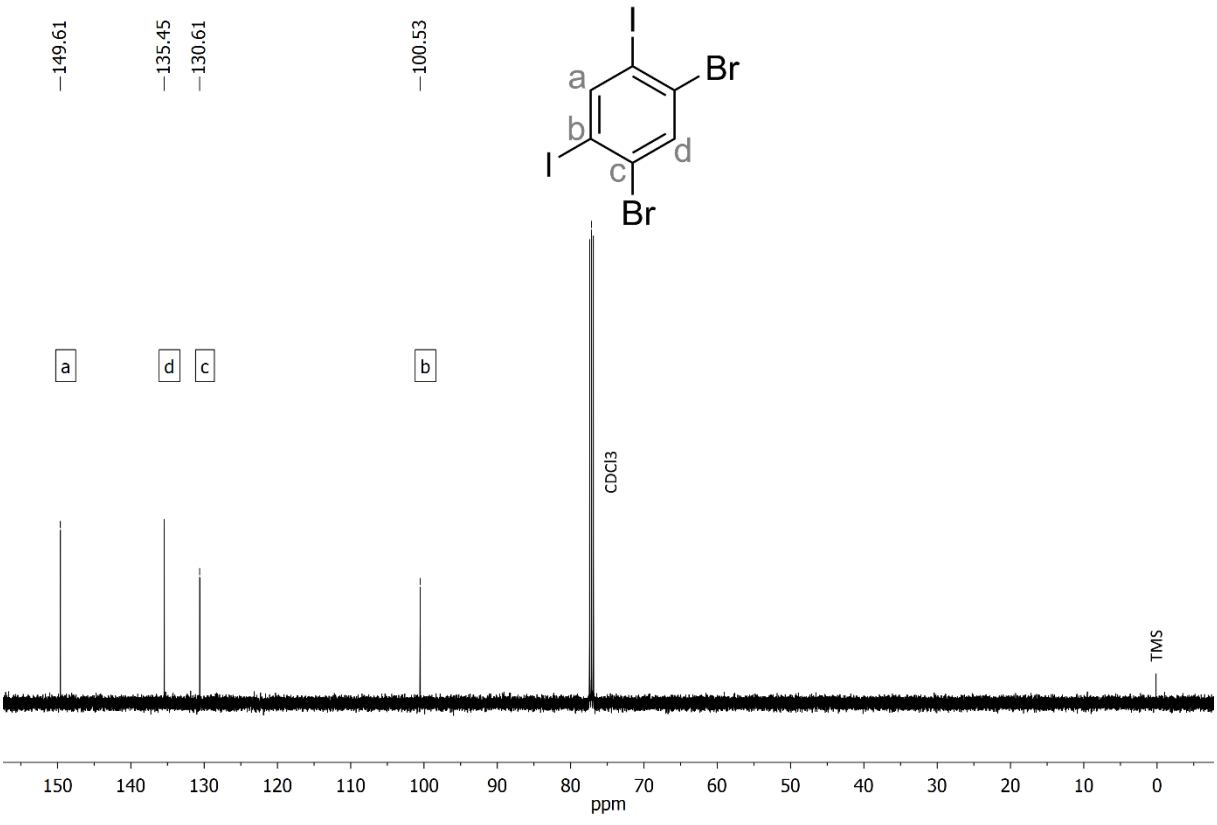

1,5-Dibromo-2,4-bis(2-(trimethylsilyl)ethynyl)benzene (11)

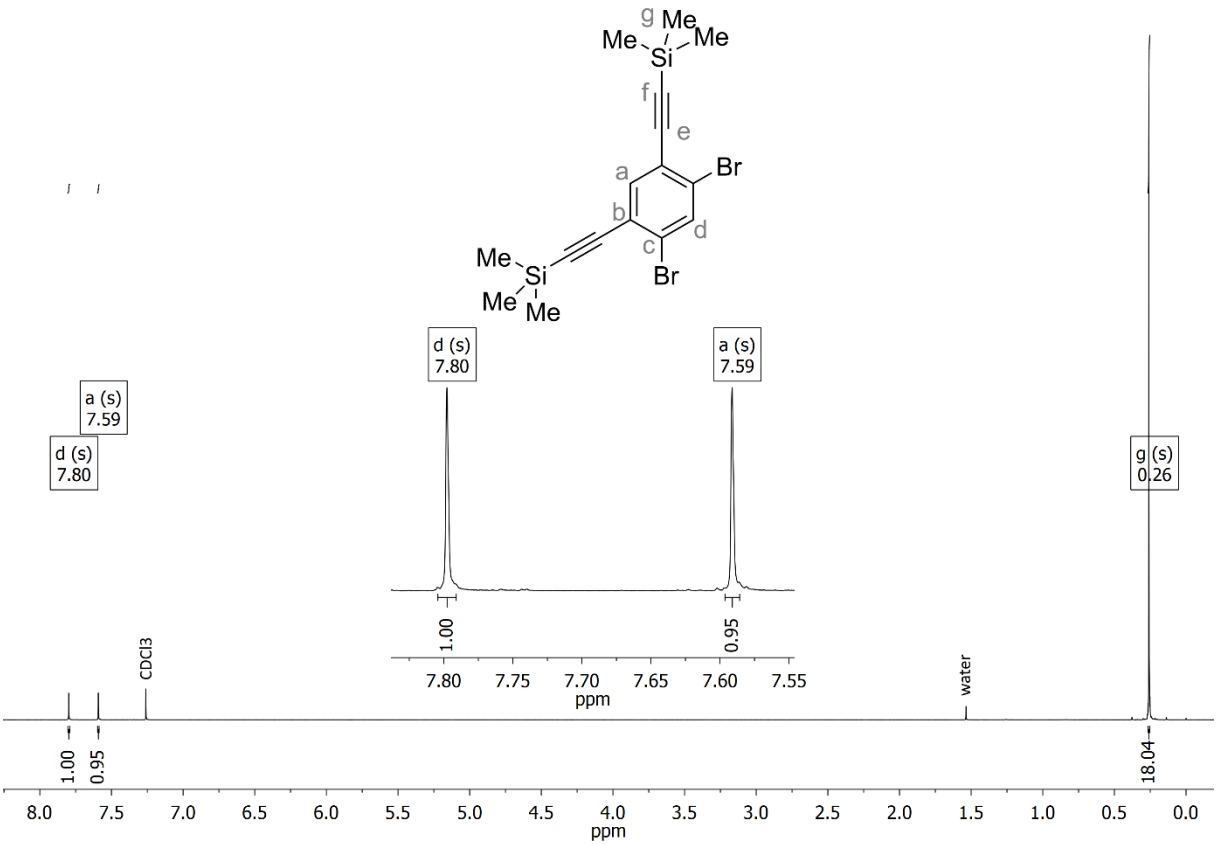

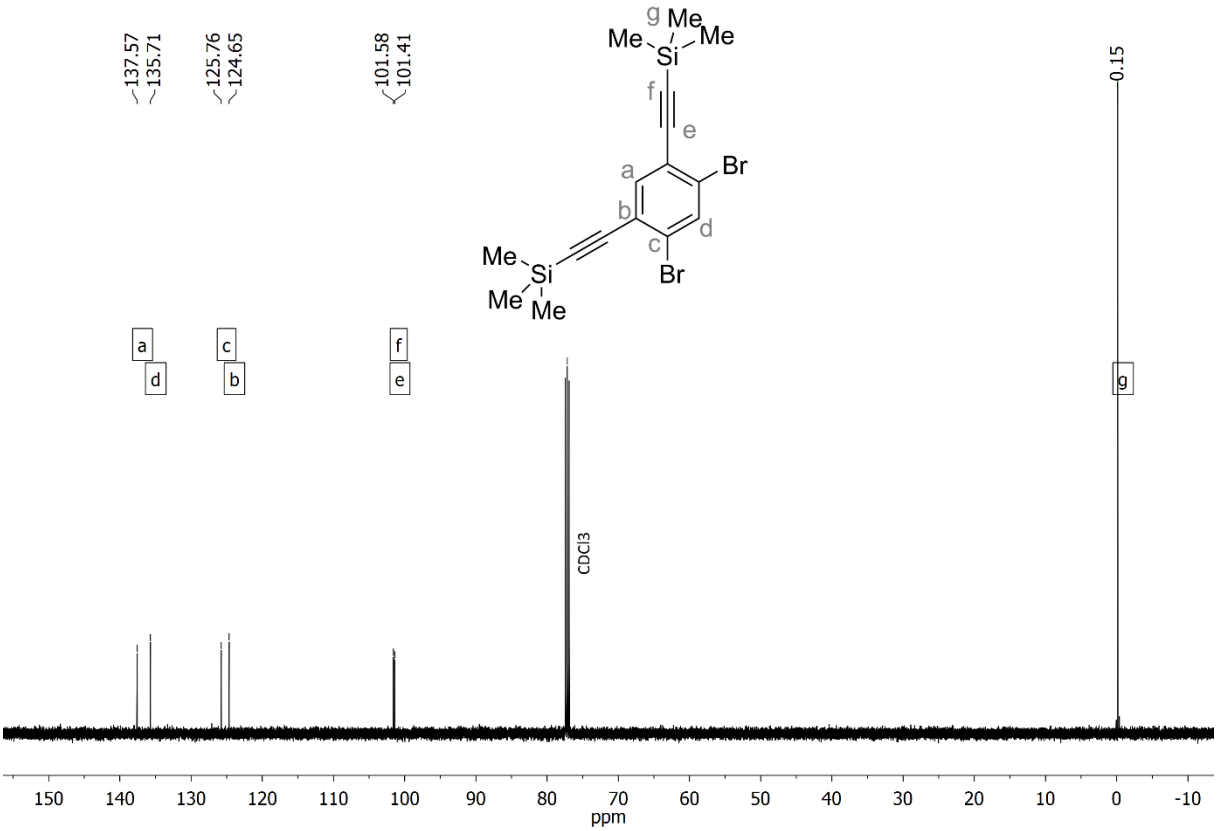

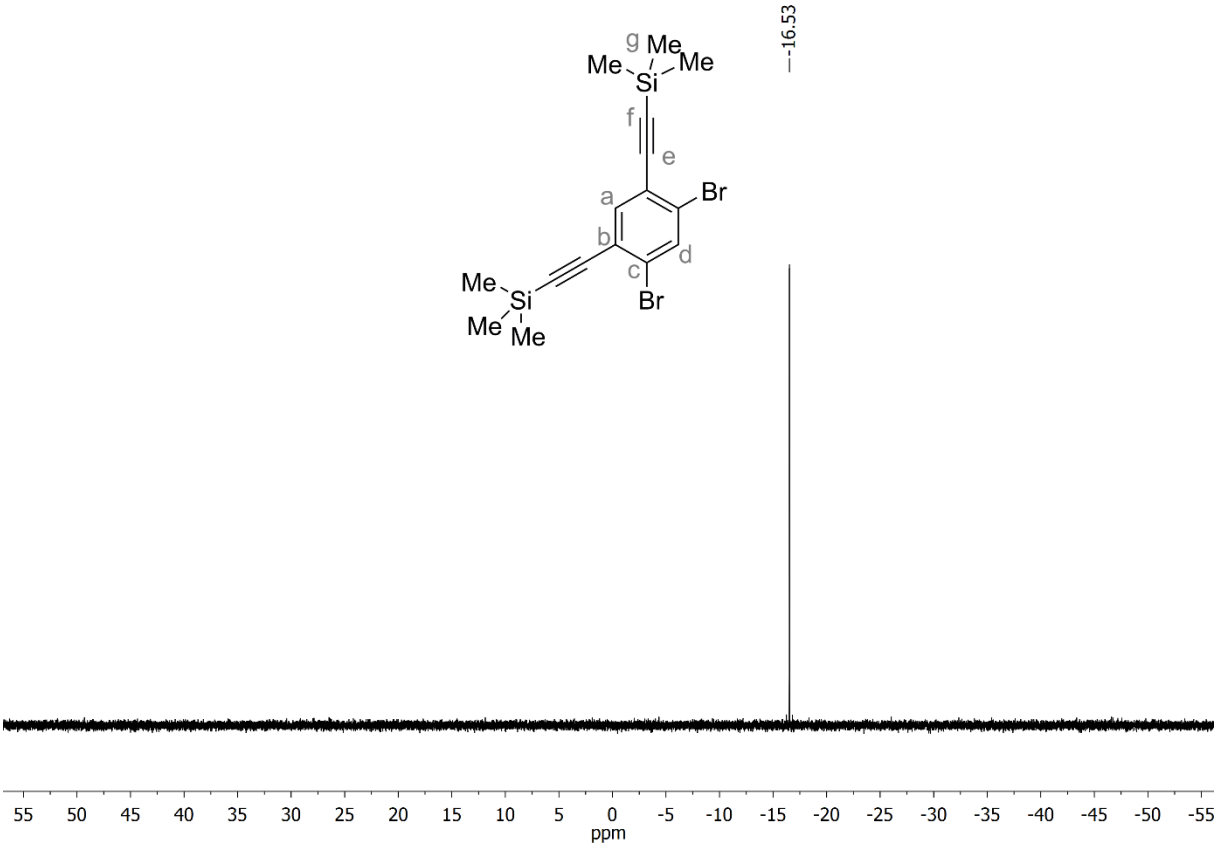

6,6'-(4,6-bis((Trimethylsilyl)ethynyl)-1,3-phenylene)bis(1-hydro-2-mesityl-1,2-azaborinine) (17)

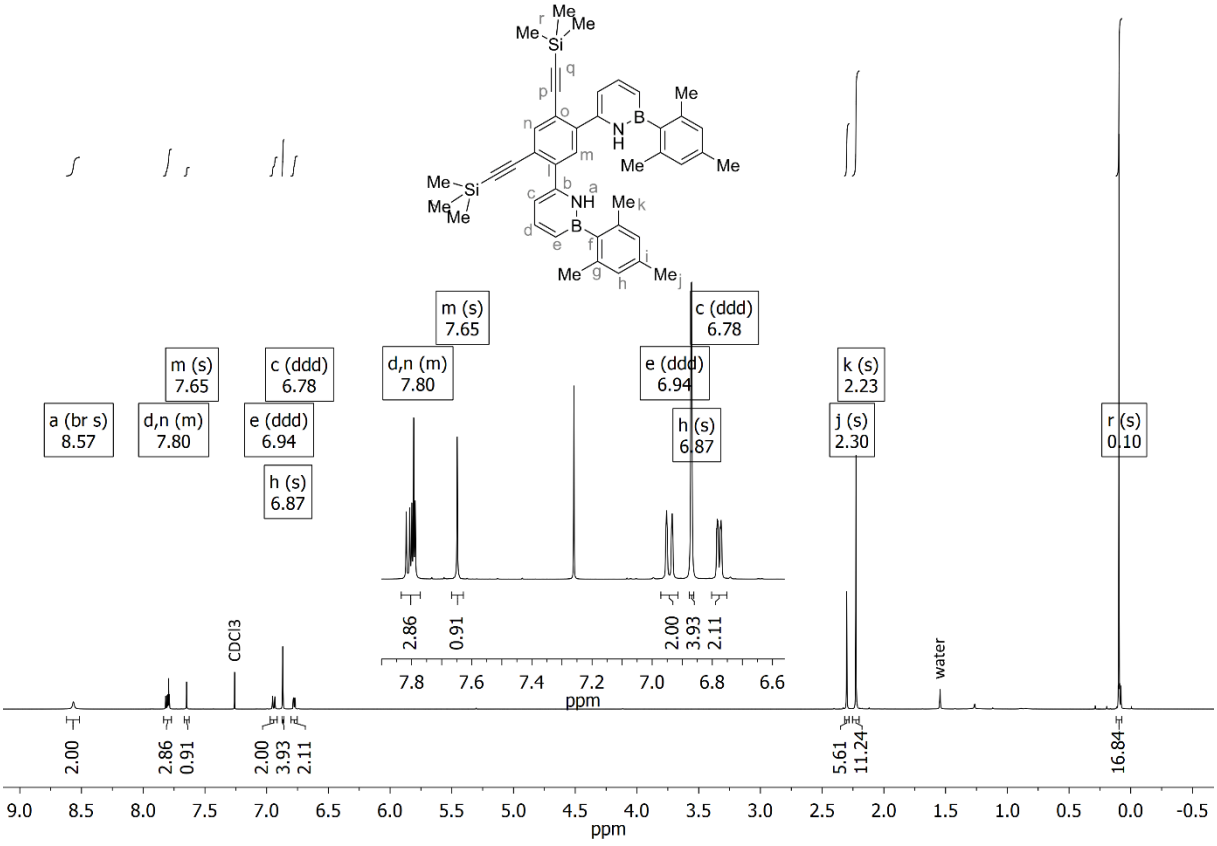

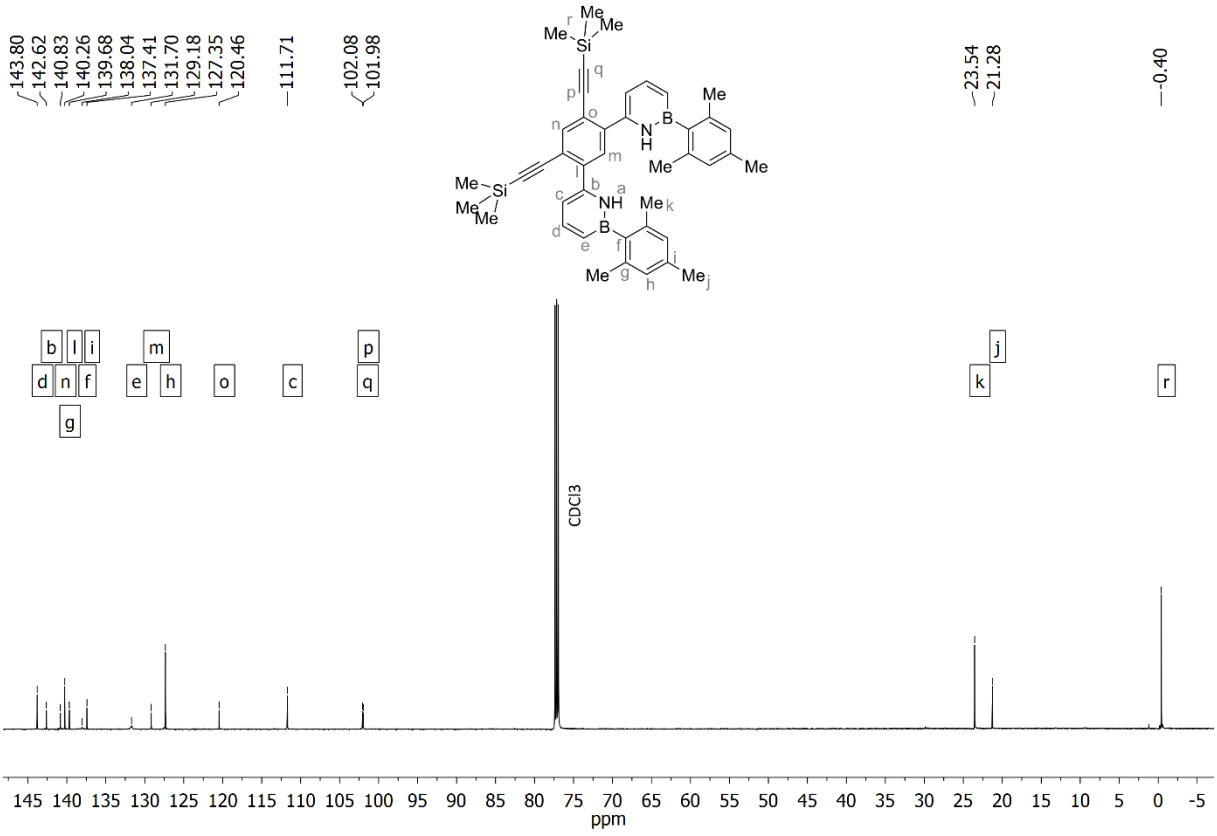
143.80
142.62
140.83
140.26
139.68
138.04
137.41
131.70
129.18
127.35
120.46
111.71
102.08
101.98
23.54
21.28
0.40
CDCl3
ppm

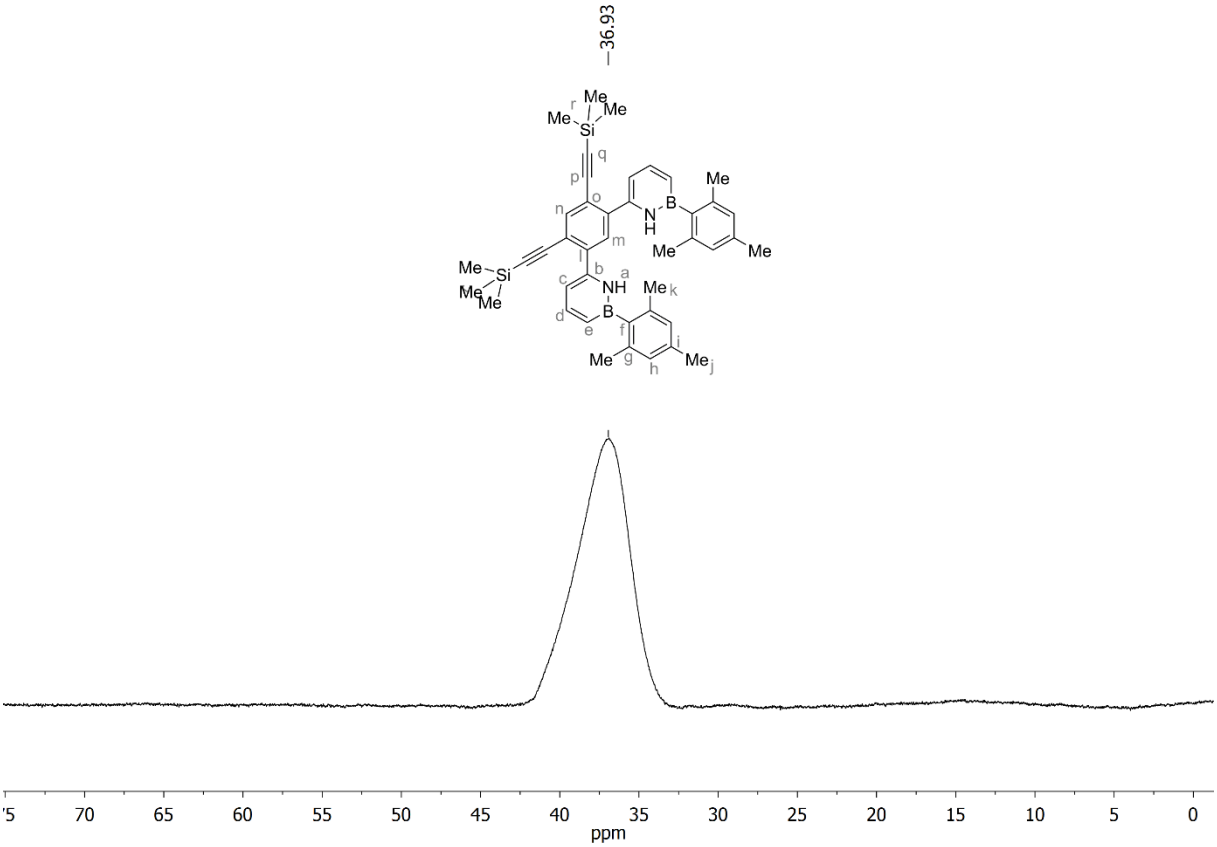
36.93
ppm

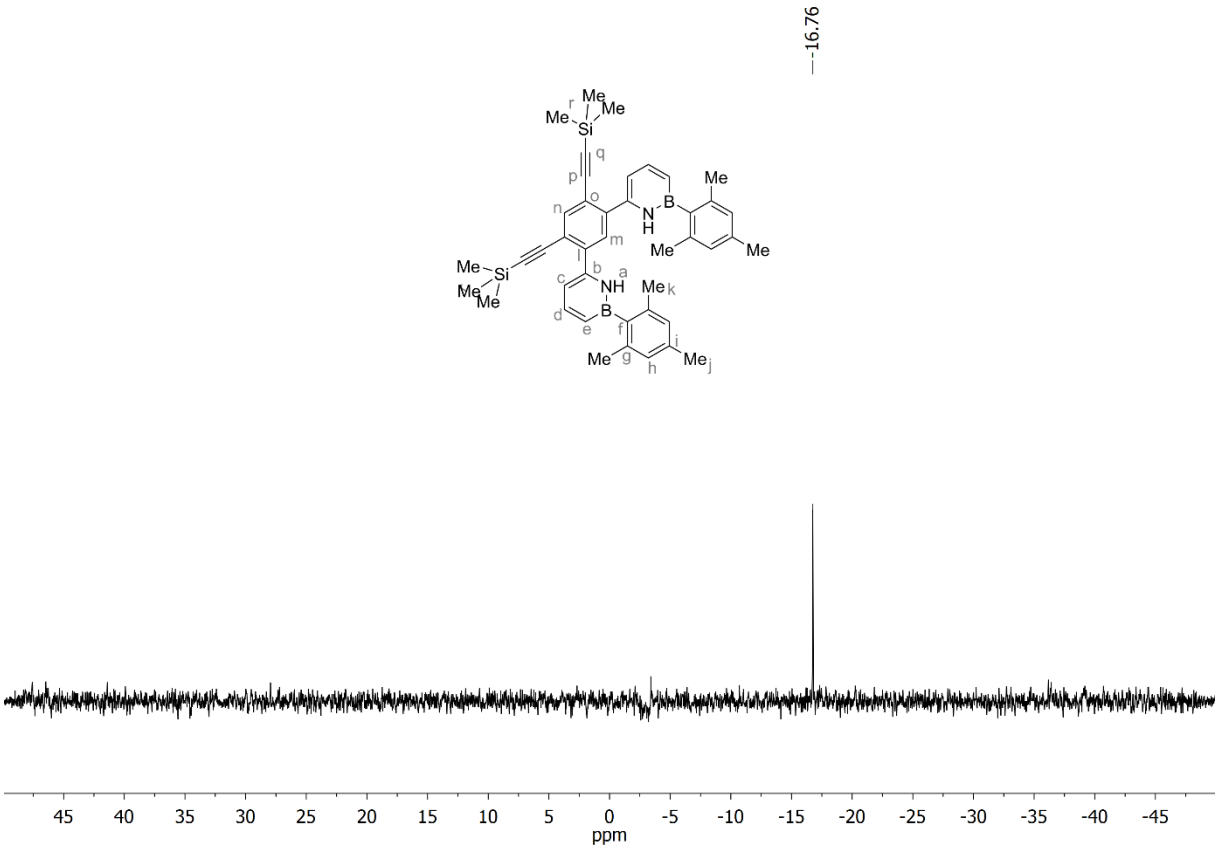

1,13-Dihydro-2,12-dimesityl-1,13-diaza-2,12-diboradibenz[*a,j*]anthracene (*BN*-PAH4)

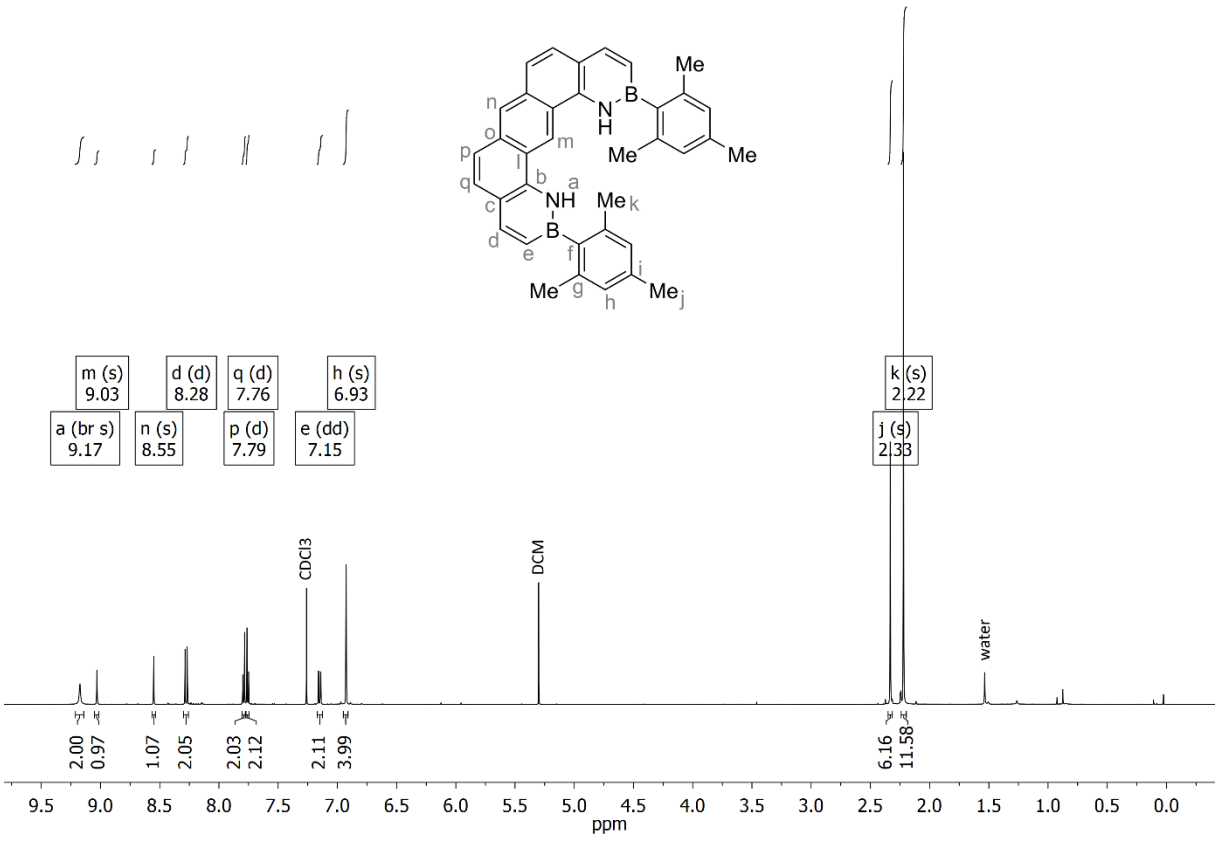

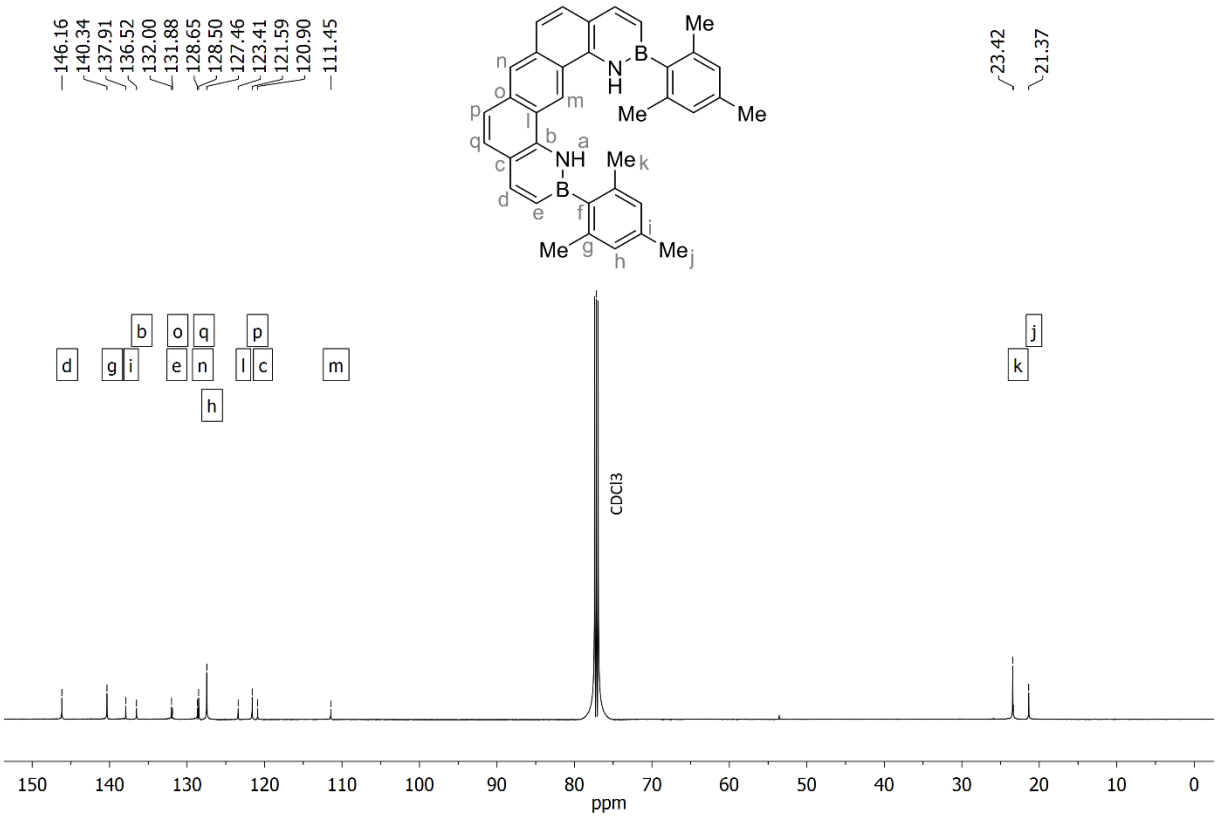
146.16
140.34
137.91
136.52
132.00
131.88
128.65
128.50
127.46
123.41
121.59
120.90
111.45
23.42
21.37
CDCl3
ppm

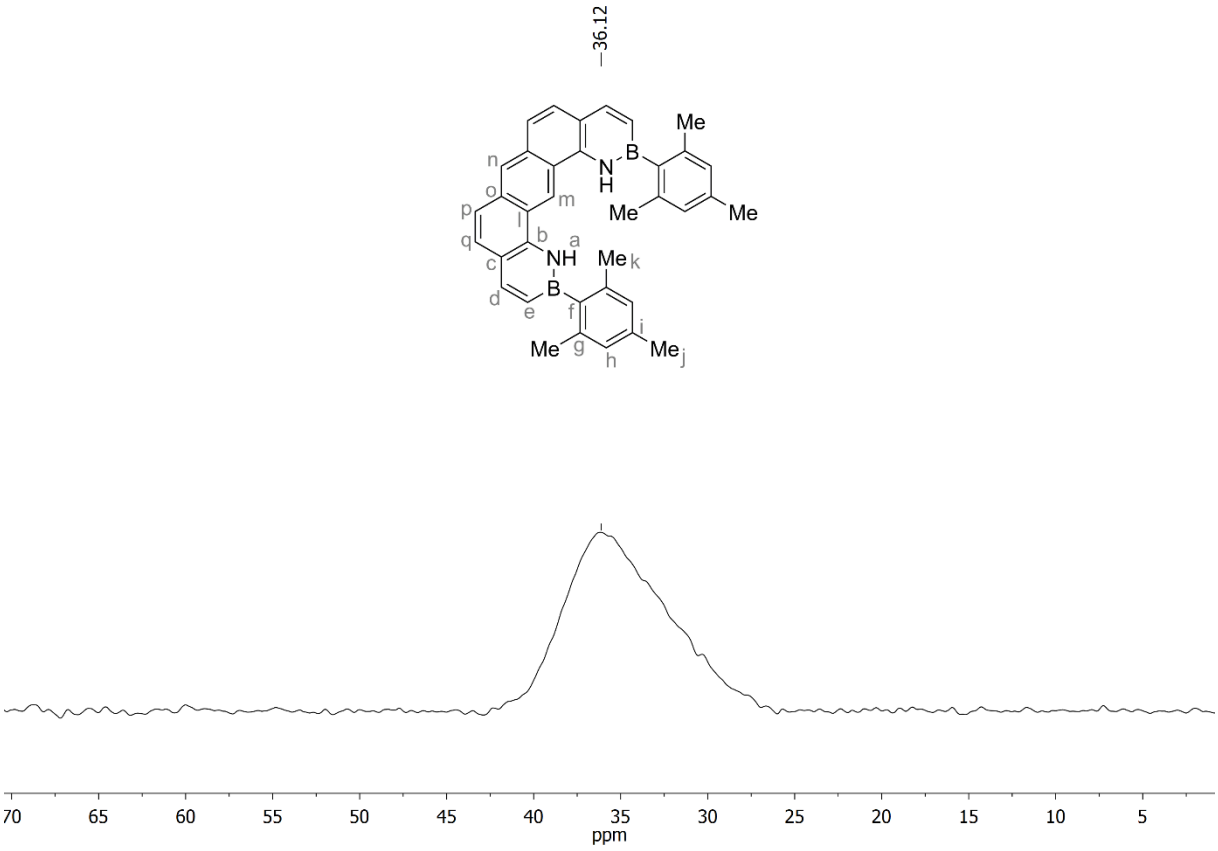
36.12
ppm

1,4-Dibromo-2,5-diiodobenzene (37)

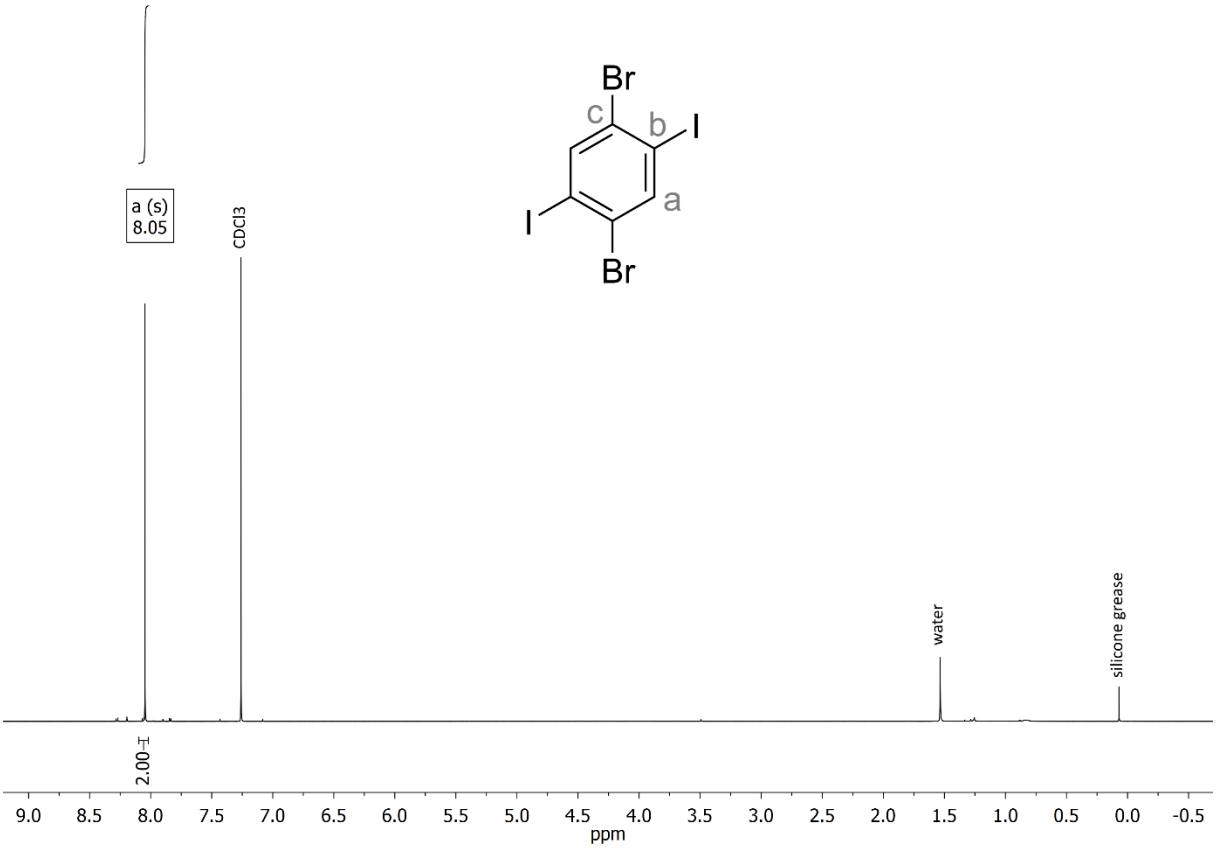

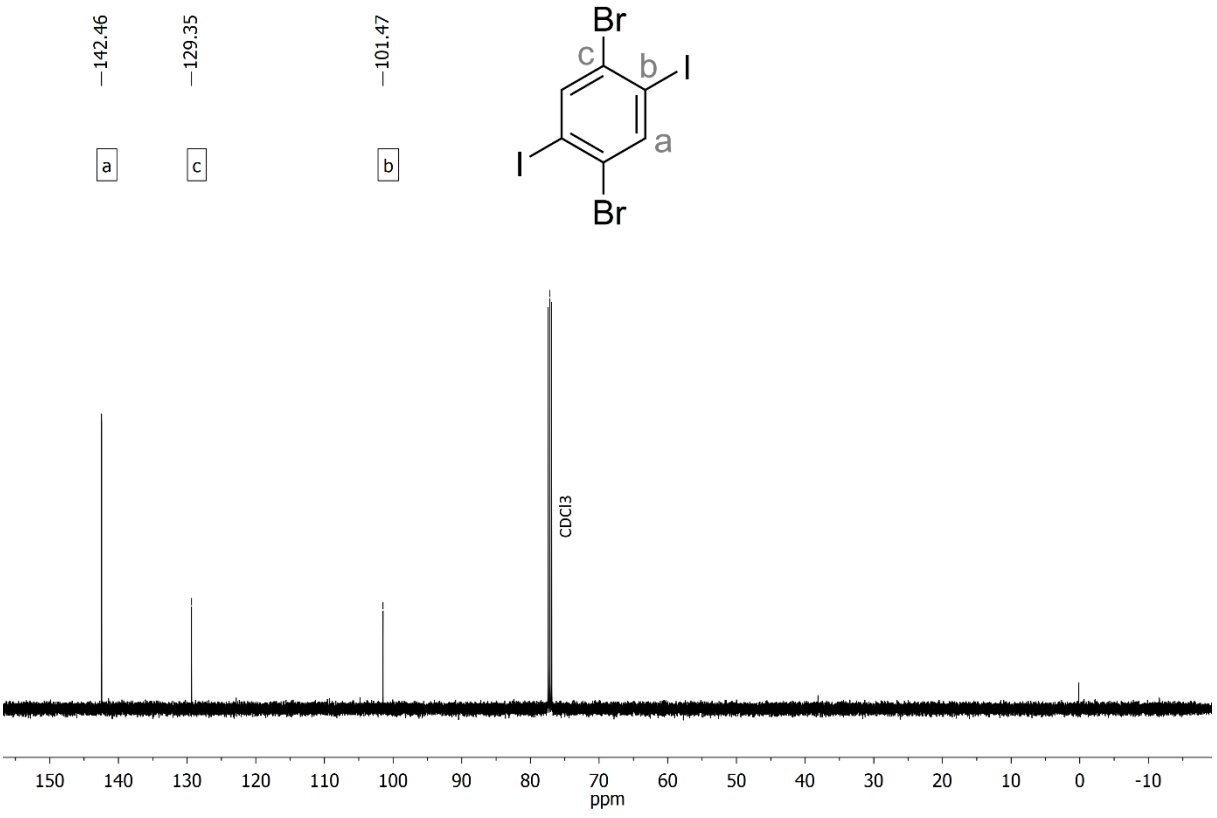

1,4-Dibromo-2,5-bis(2-(trimethylsilyl)ethynyl)benzene (12)

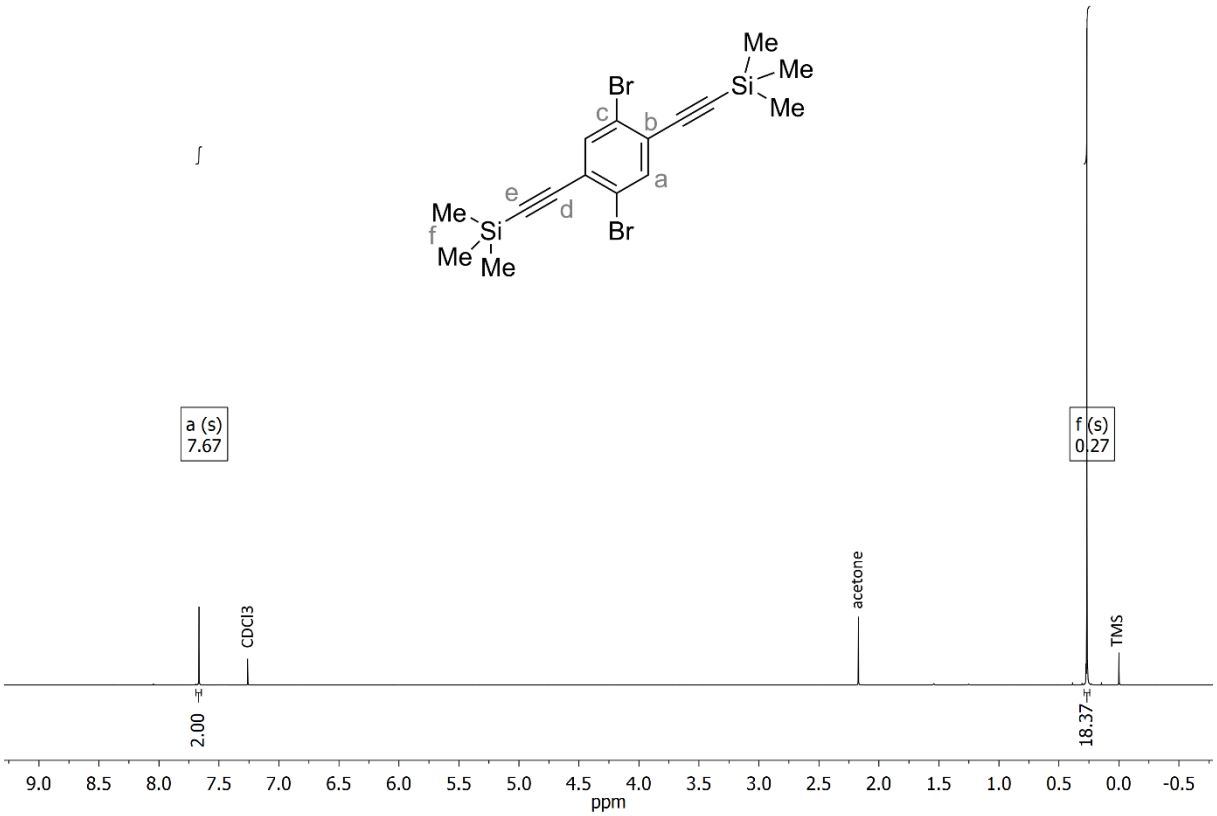

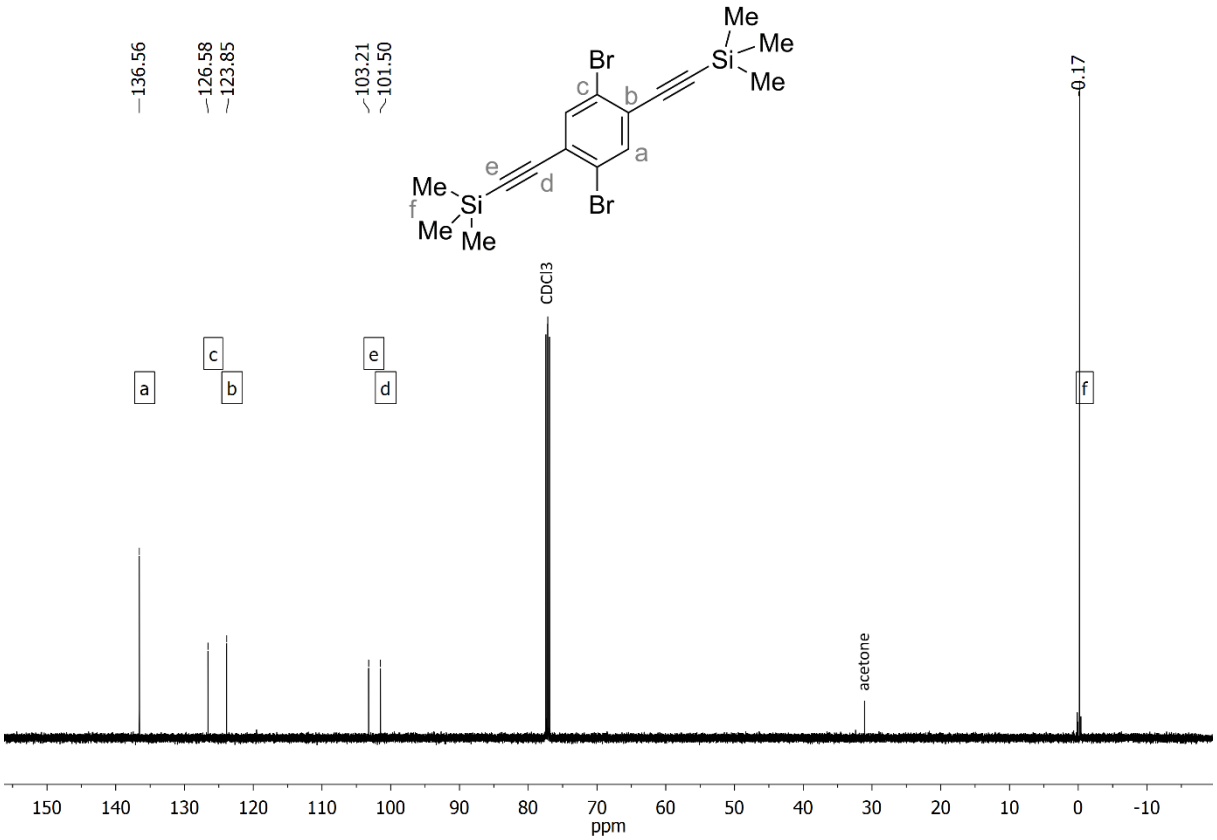

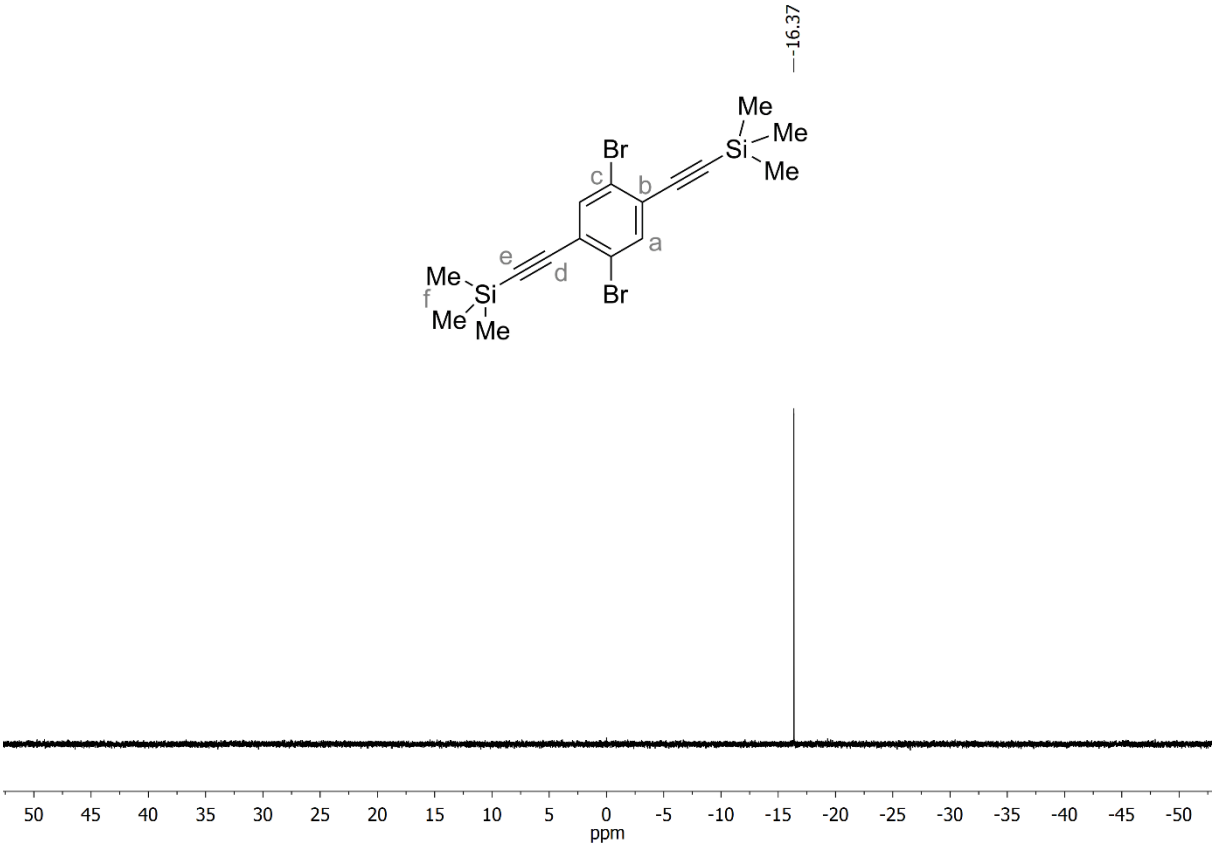

6,6'-(2,5-bis((Trimethylsilyl)ethynyl)-1,4-phenylene)bis(1-hydro-2-mesityl-1,2-azaborinine) (18)

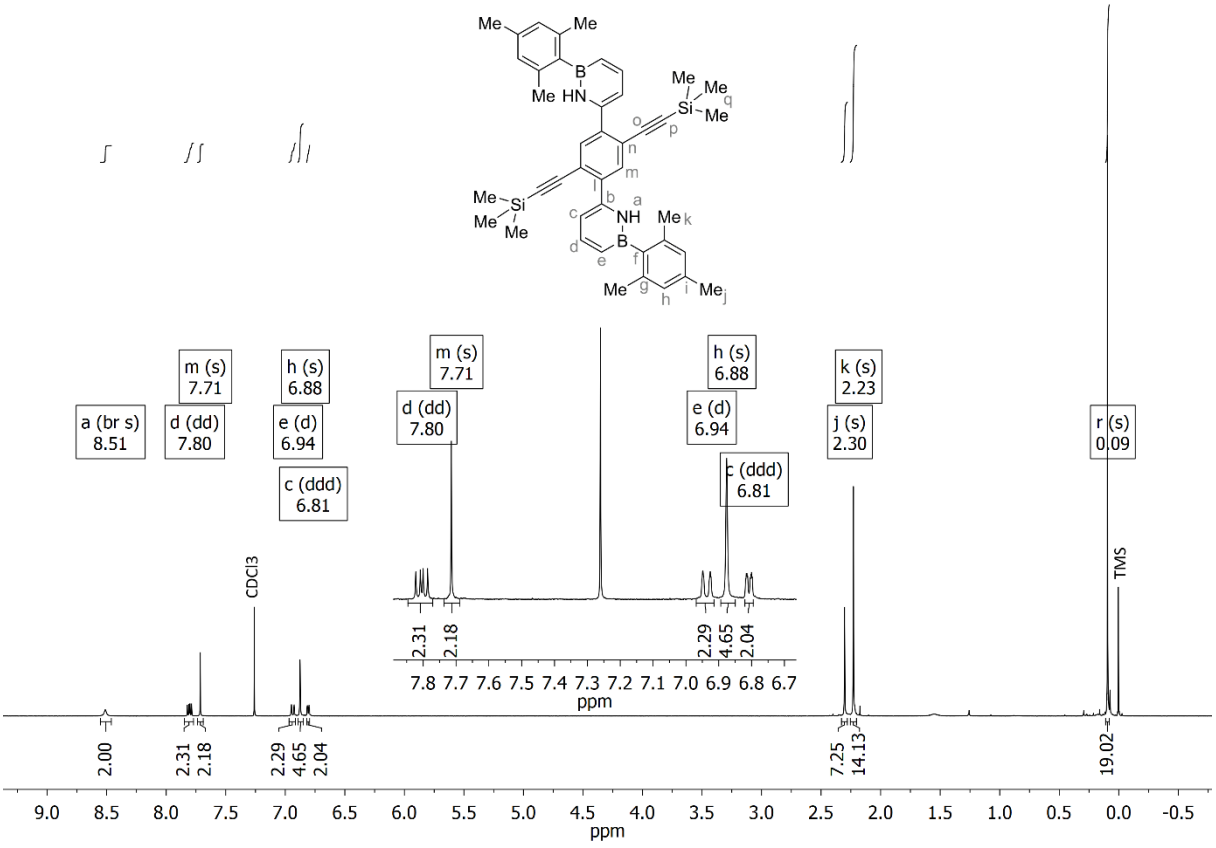

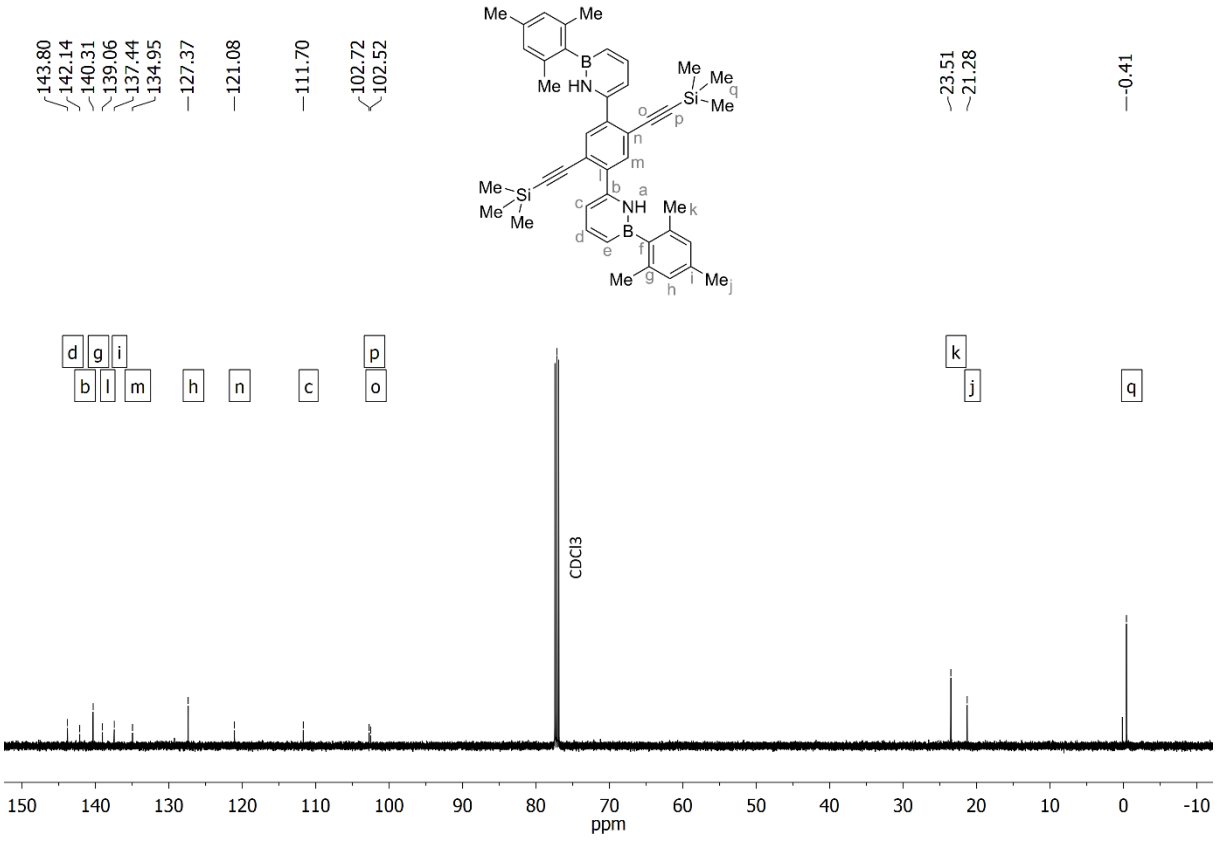
143.80
142.14
140.31
139.06
137.44
134.95
127.37
121.08
111.70
102.72
102.52
23.51
21.28
-0.41
CDCl3
150
140
130
120
110
100
90
80
70
60
50
40
30
20
10
0
-10
ppm

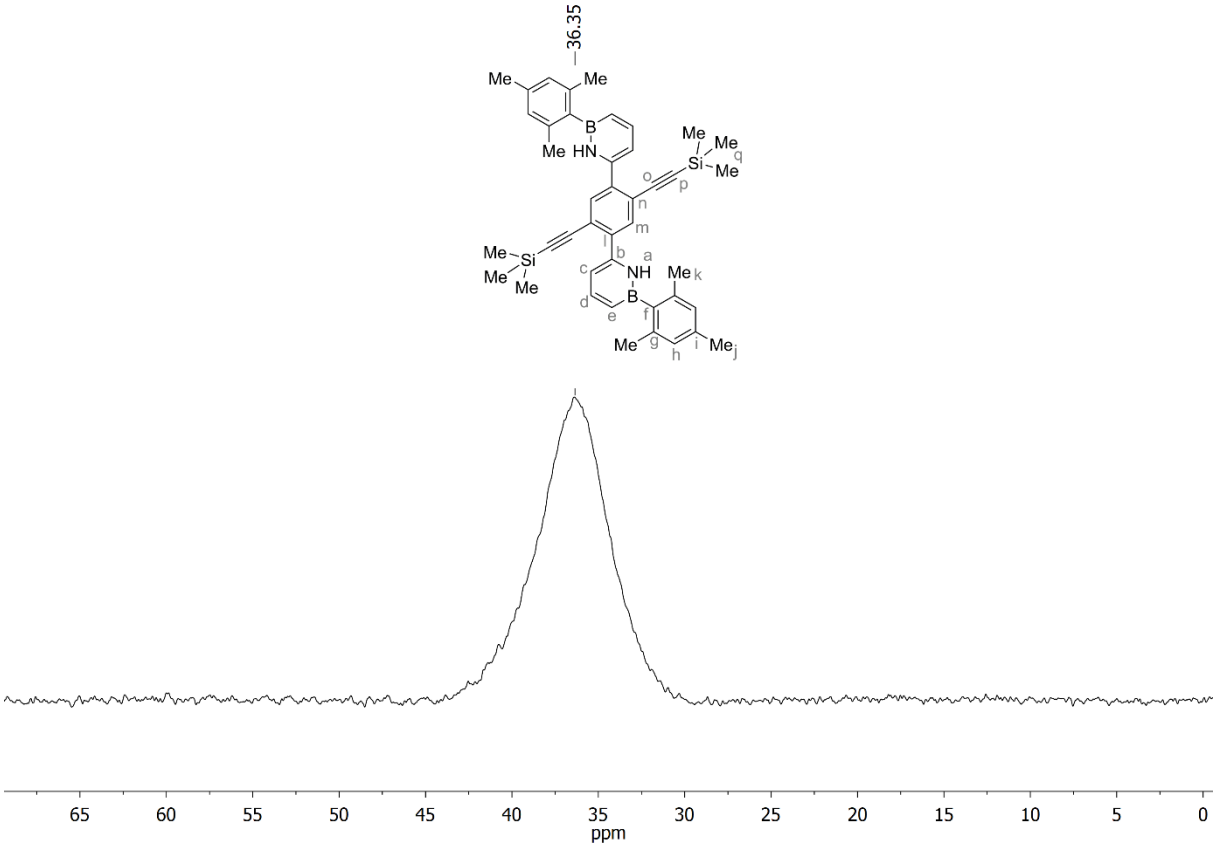
36.35
65
60
55
50
45
40
35
30
25
20
15
10
5
0
ppm

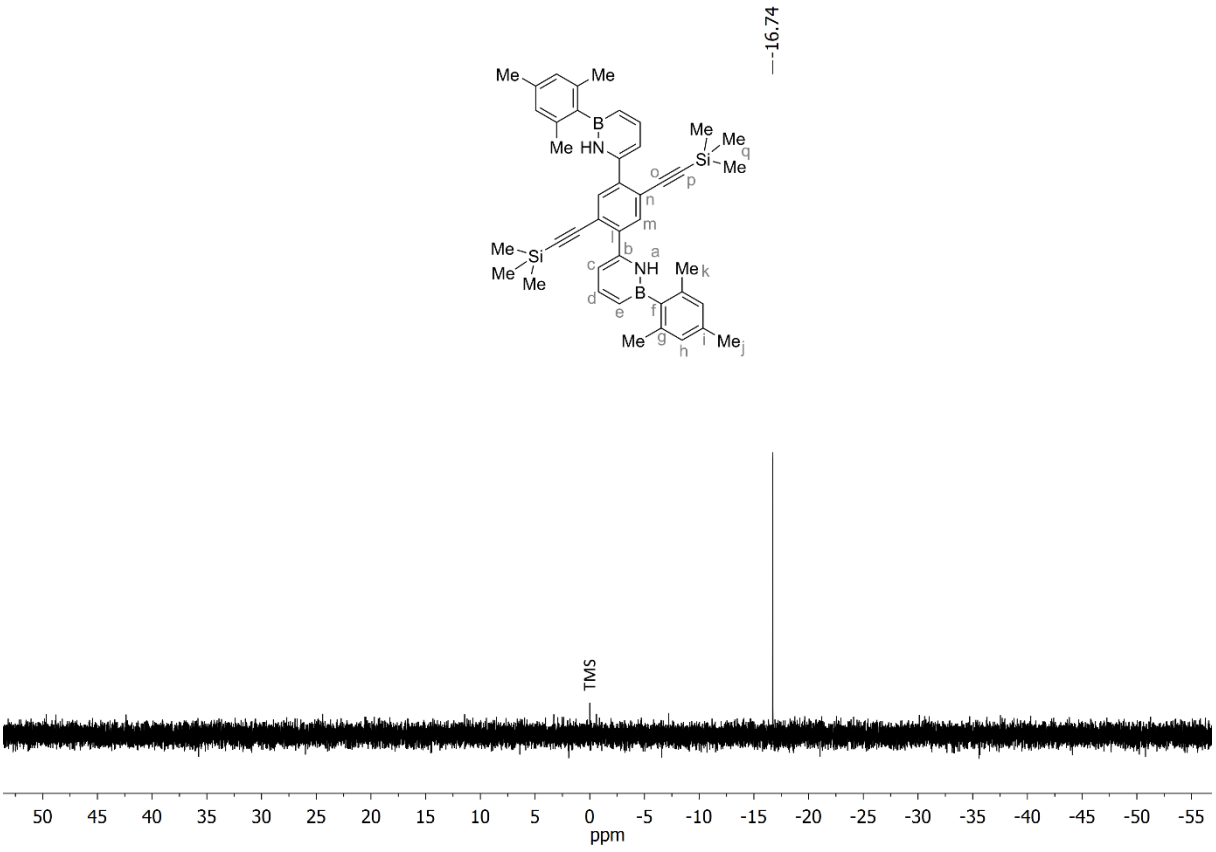

1,8-Dihydro-2,9-dimesityl-1,8-diaza-2,9-diboradibenz[*a,h*]anthracene (*BN*-PAH5)

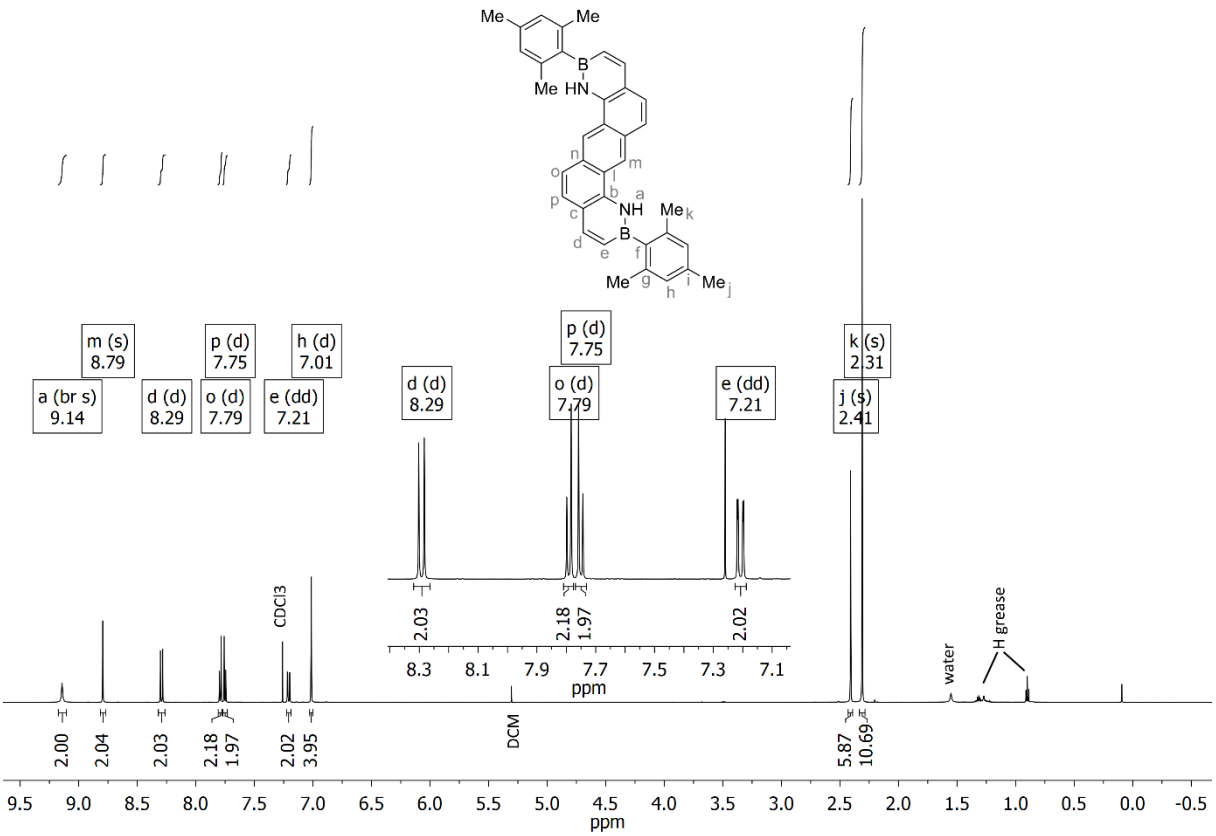

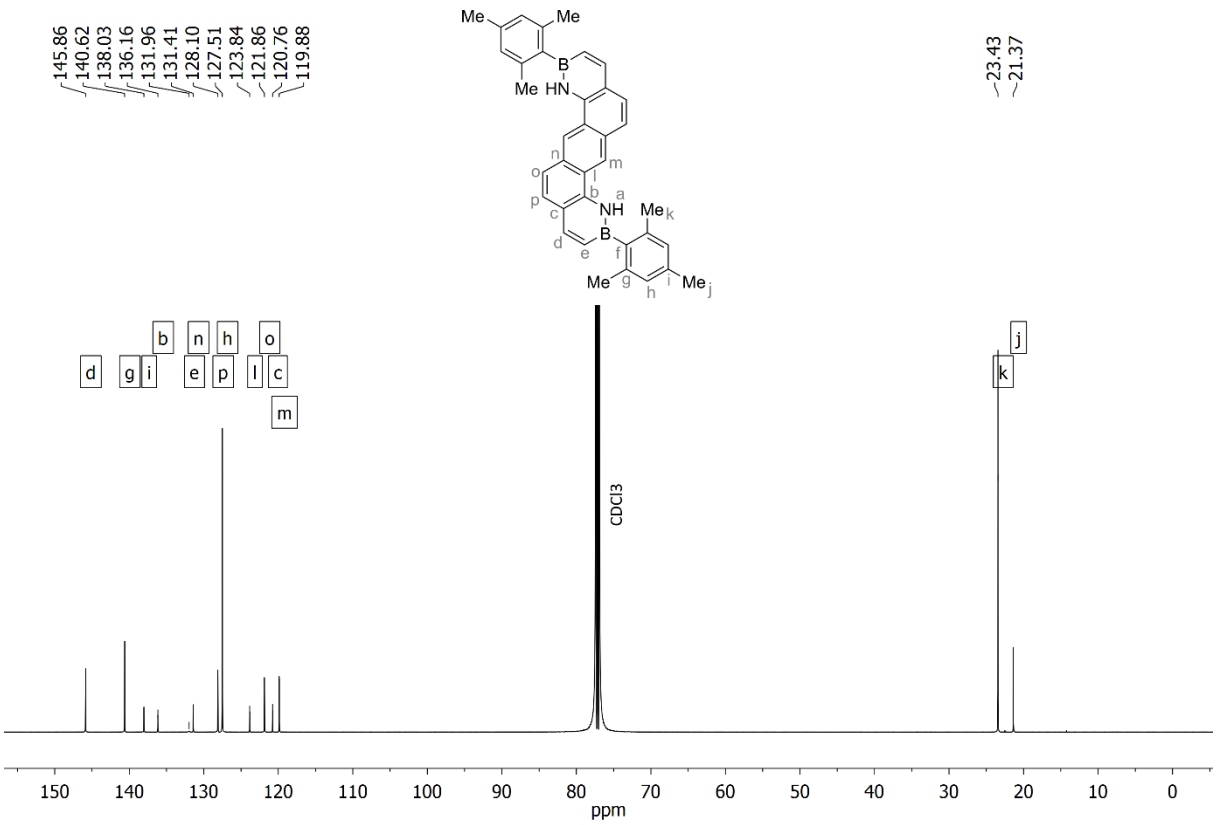
145.86
140.62
138.03
136.16
131.96
131.41
128.10
127.51
123.84
121.86
120.76
119.88
23.43
21.37
CDCl3
ppm

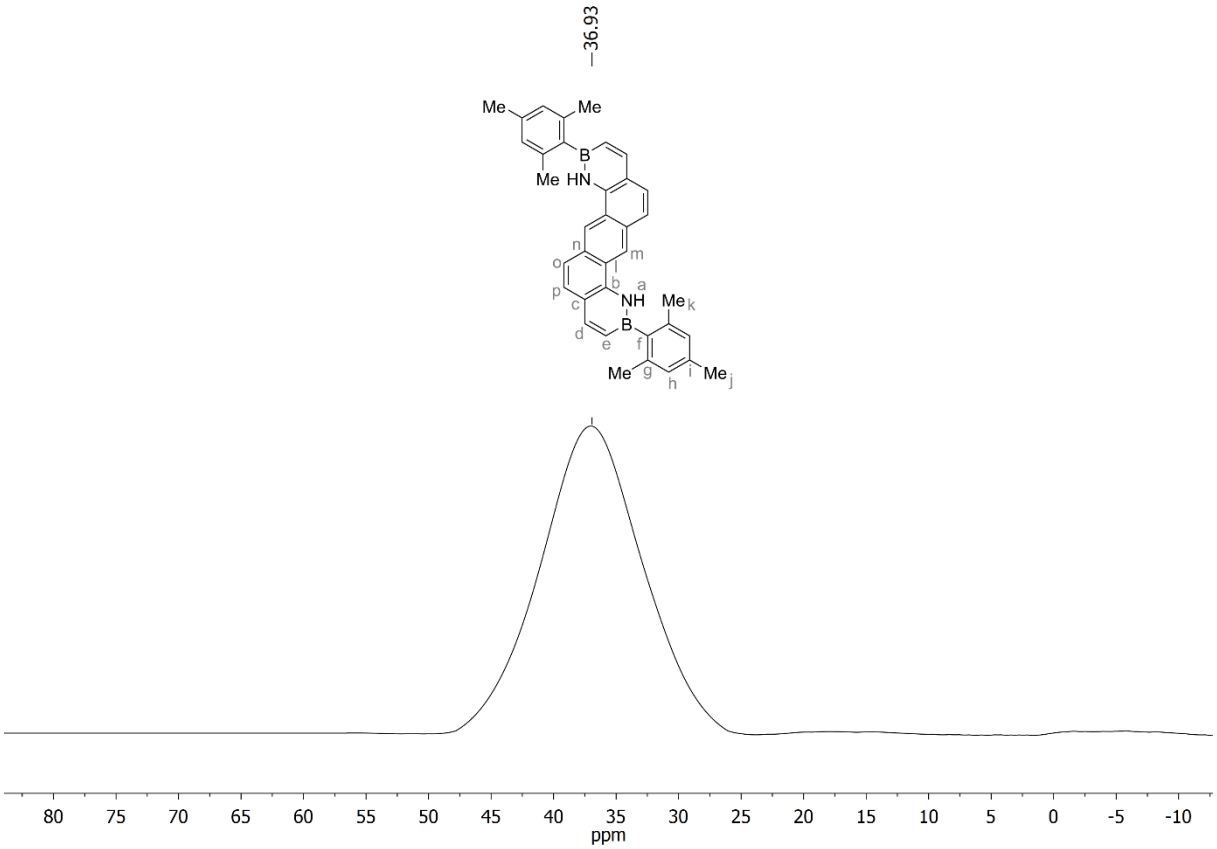
36.93
ppm

(2,5-Dibromophenyl)-2-(hydroxyimino)acetamide (38)

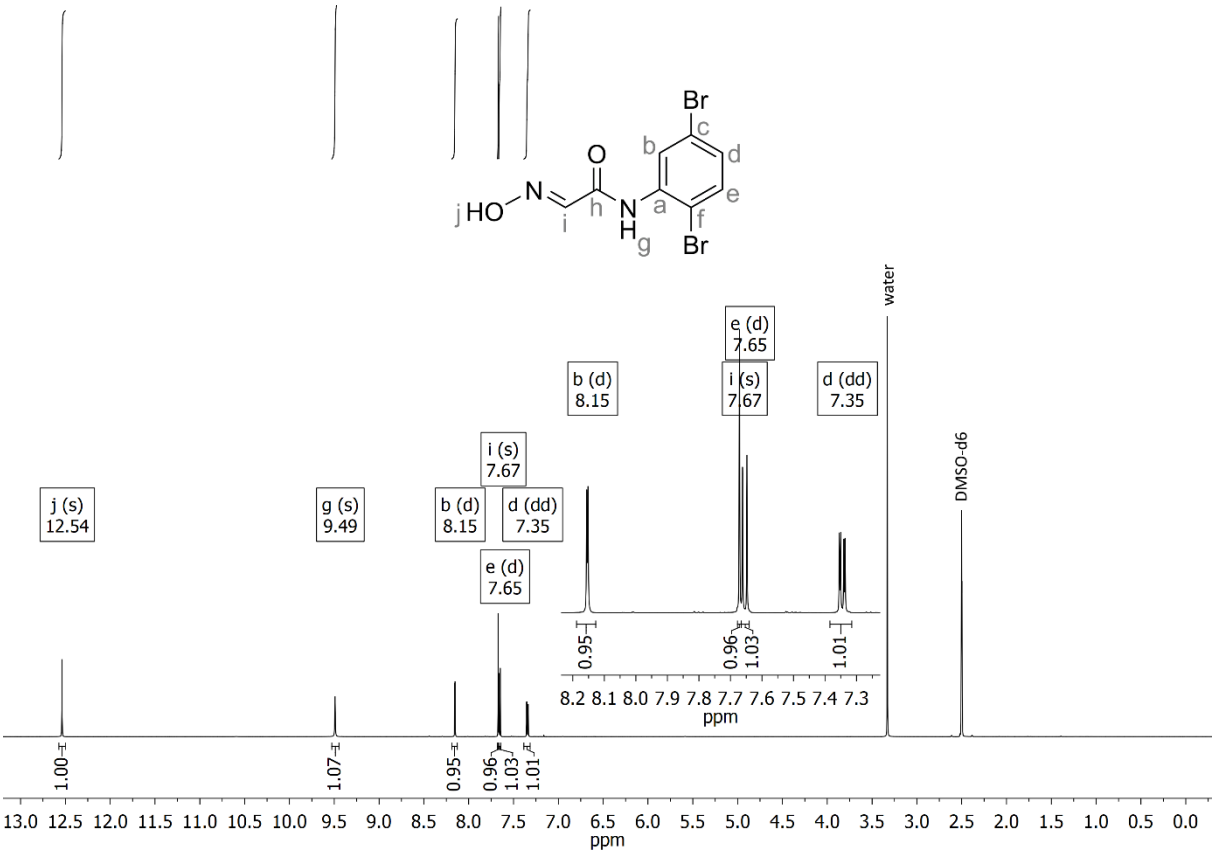

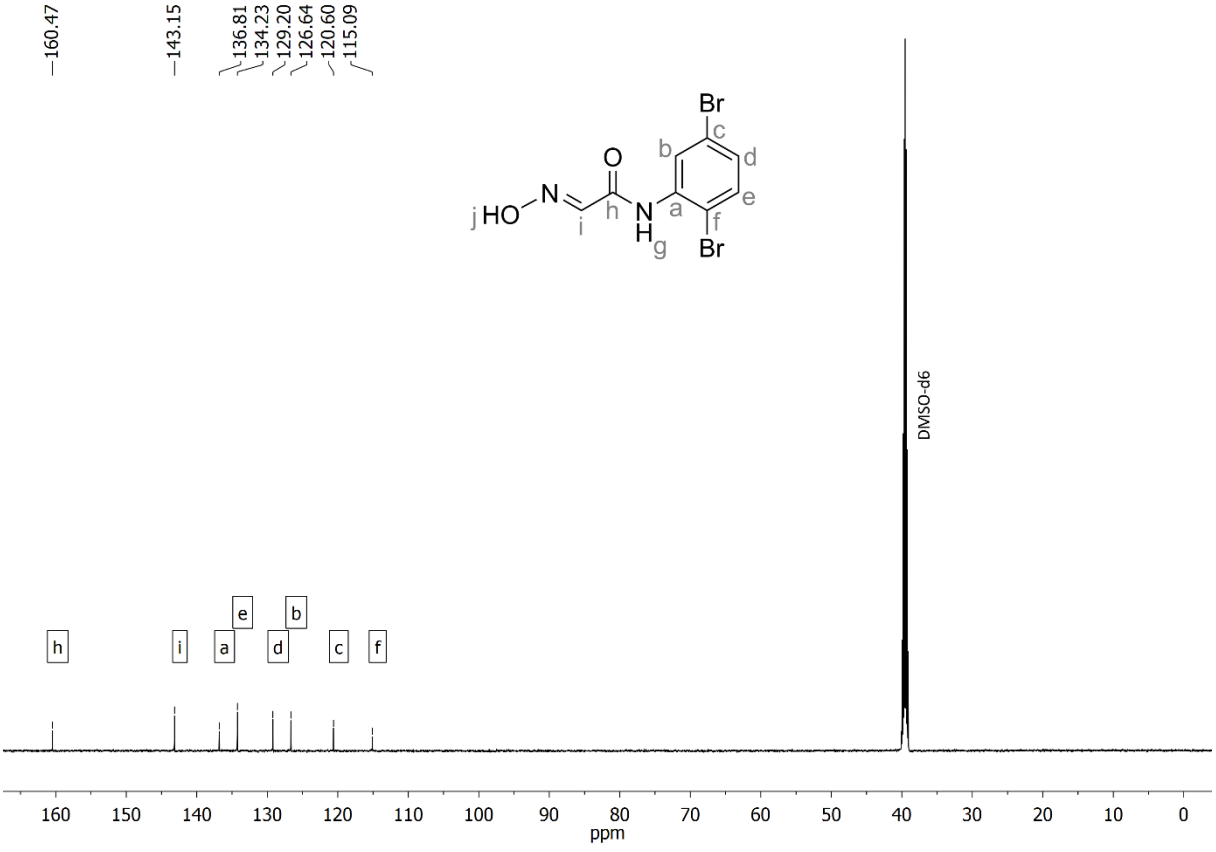

4,7-Dibromoindolin-2,3-dione (39)

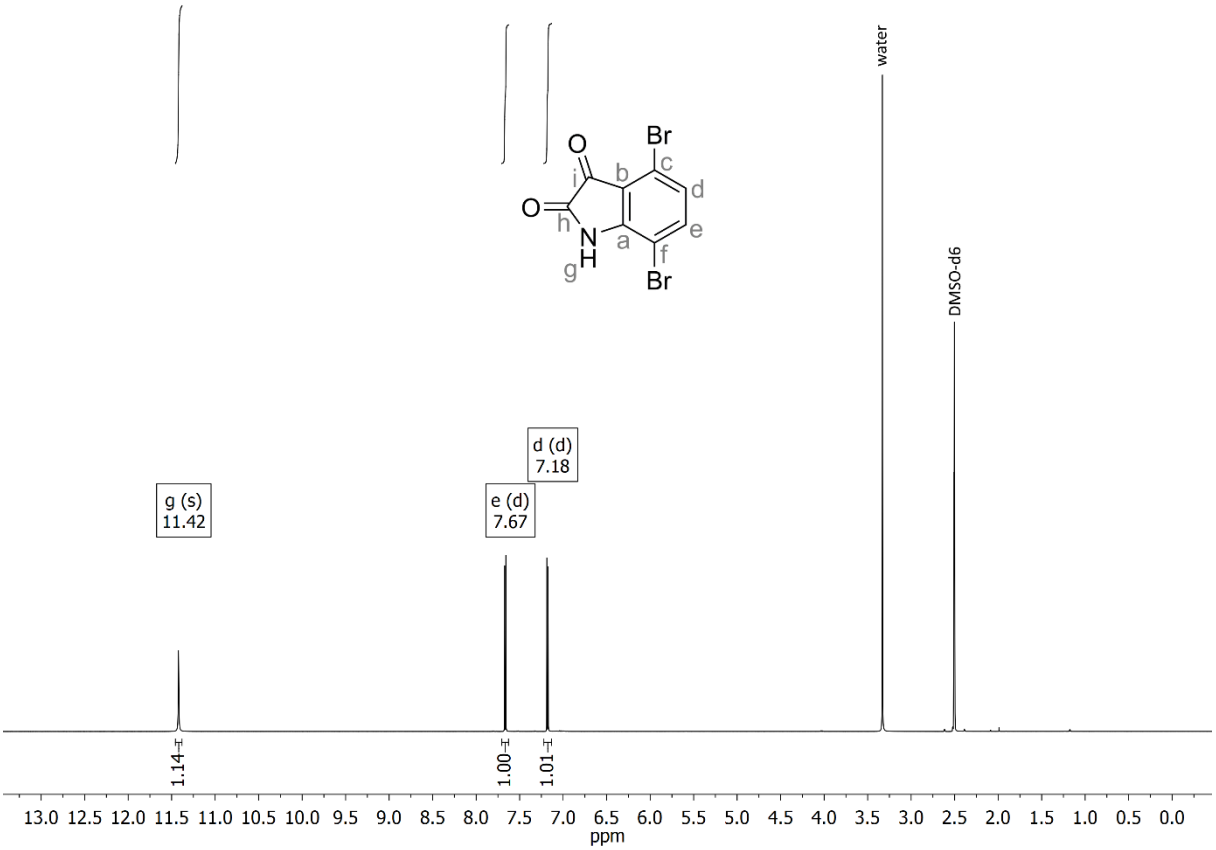

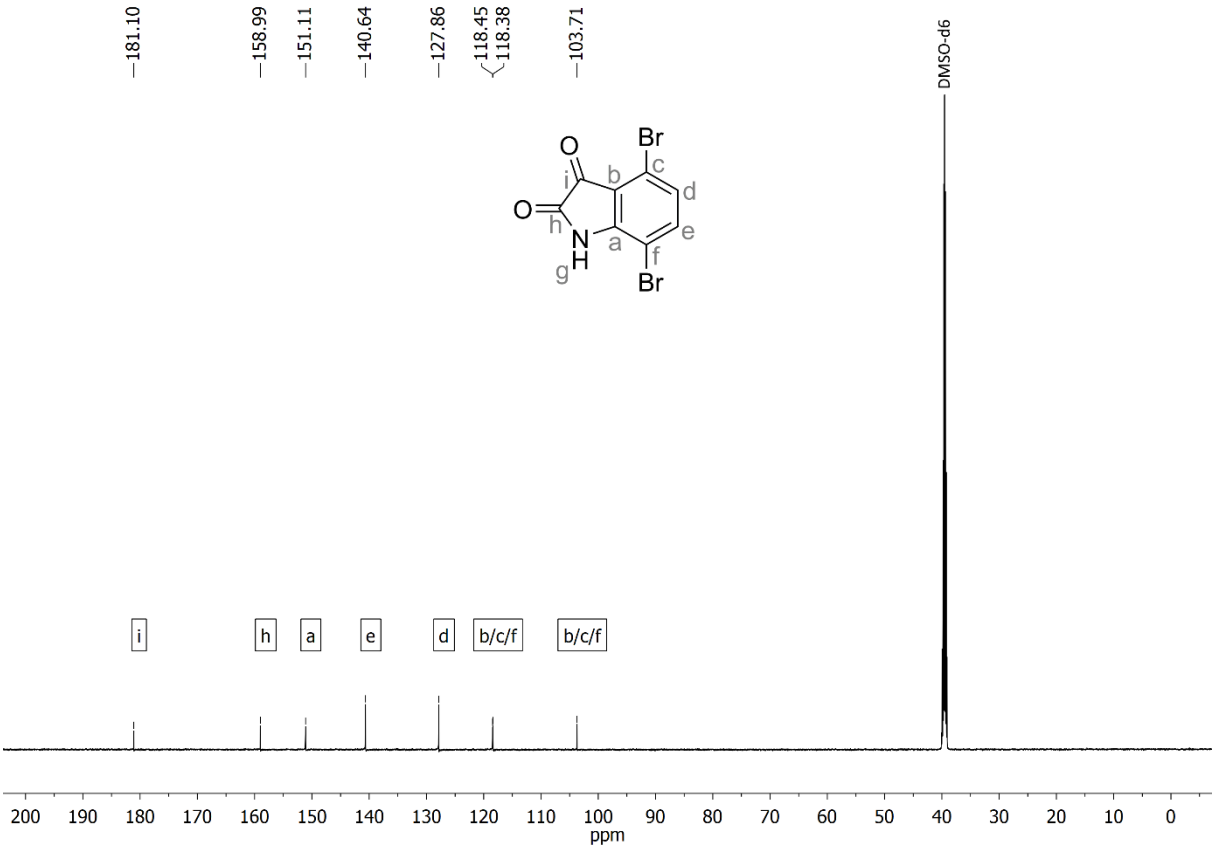

2-Amino-3,6-dibromobenzoic acid (40)

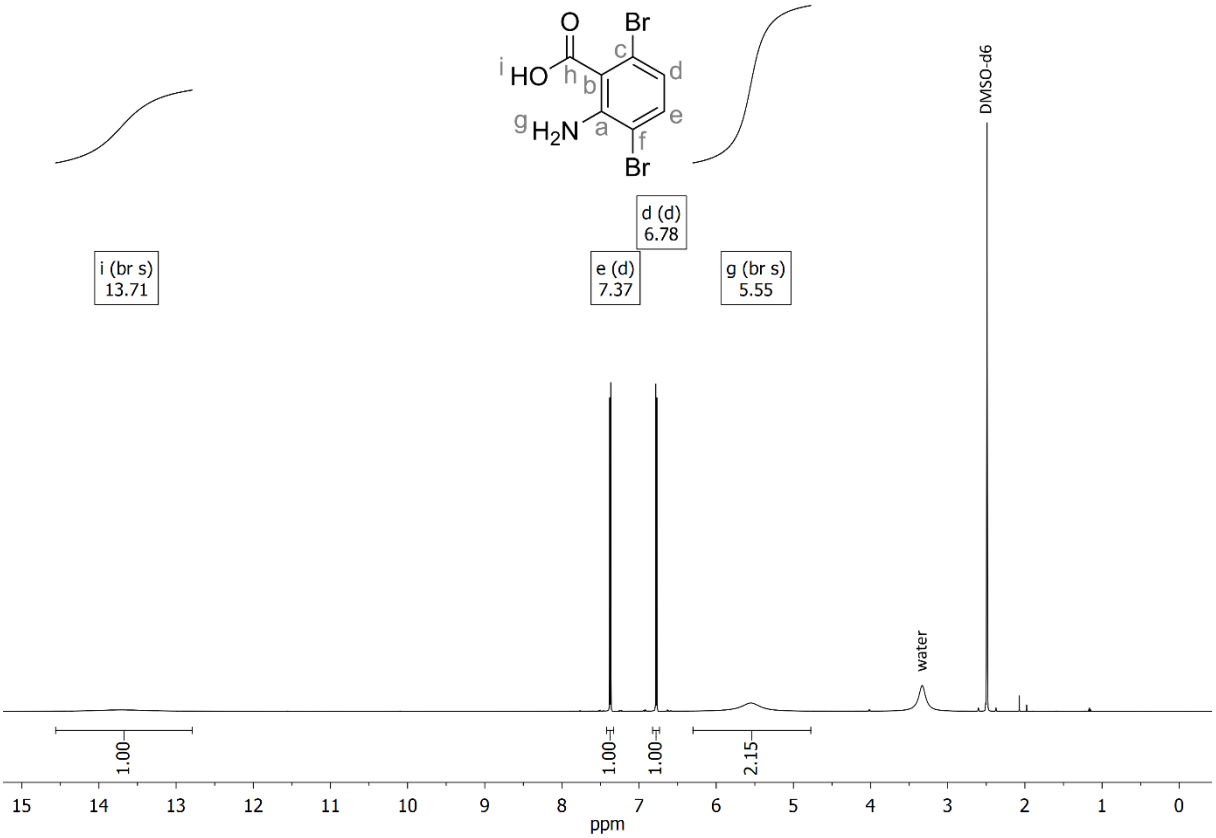

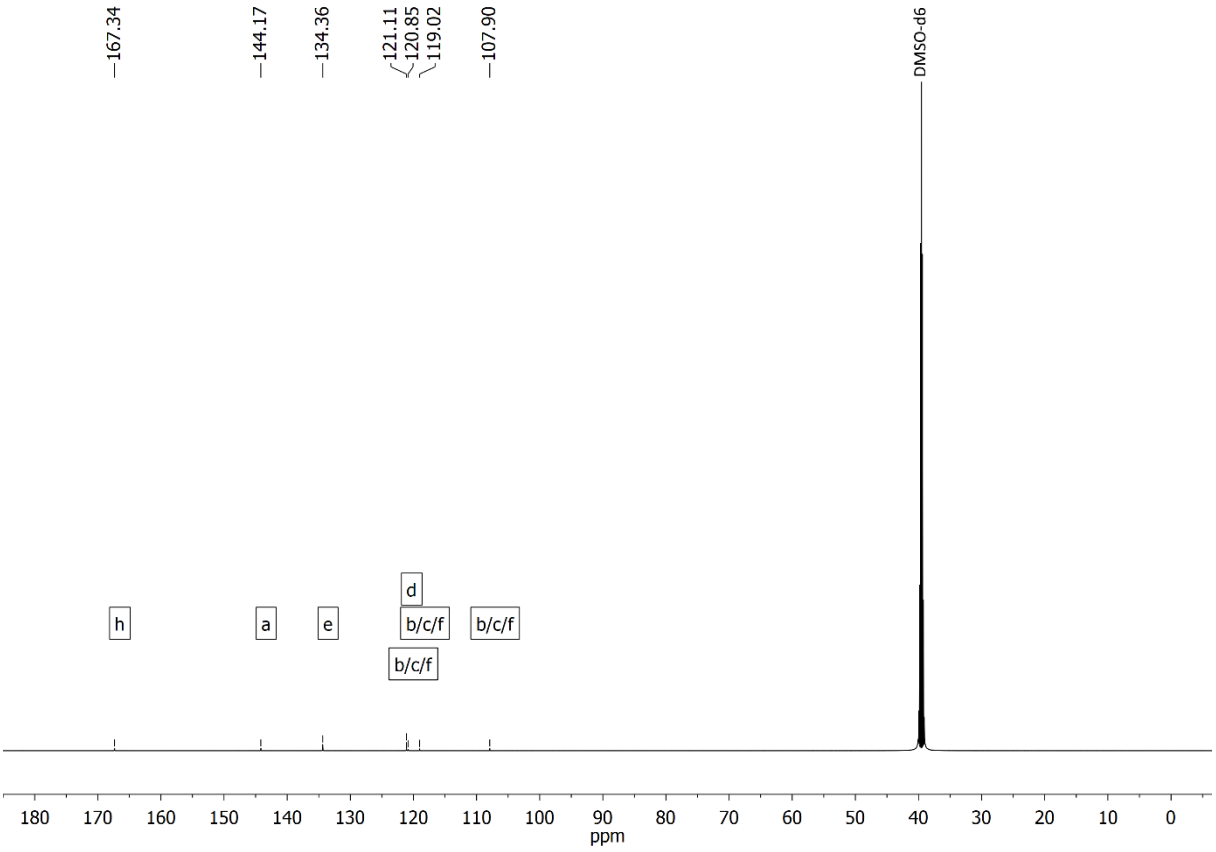

1,4-Dibromo-2,3-diiodobenzene (41)

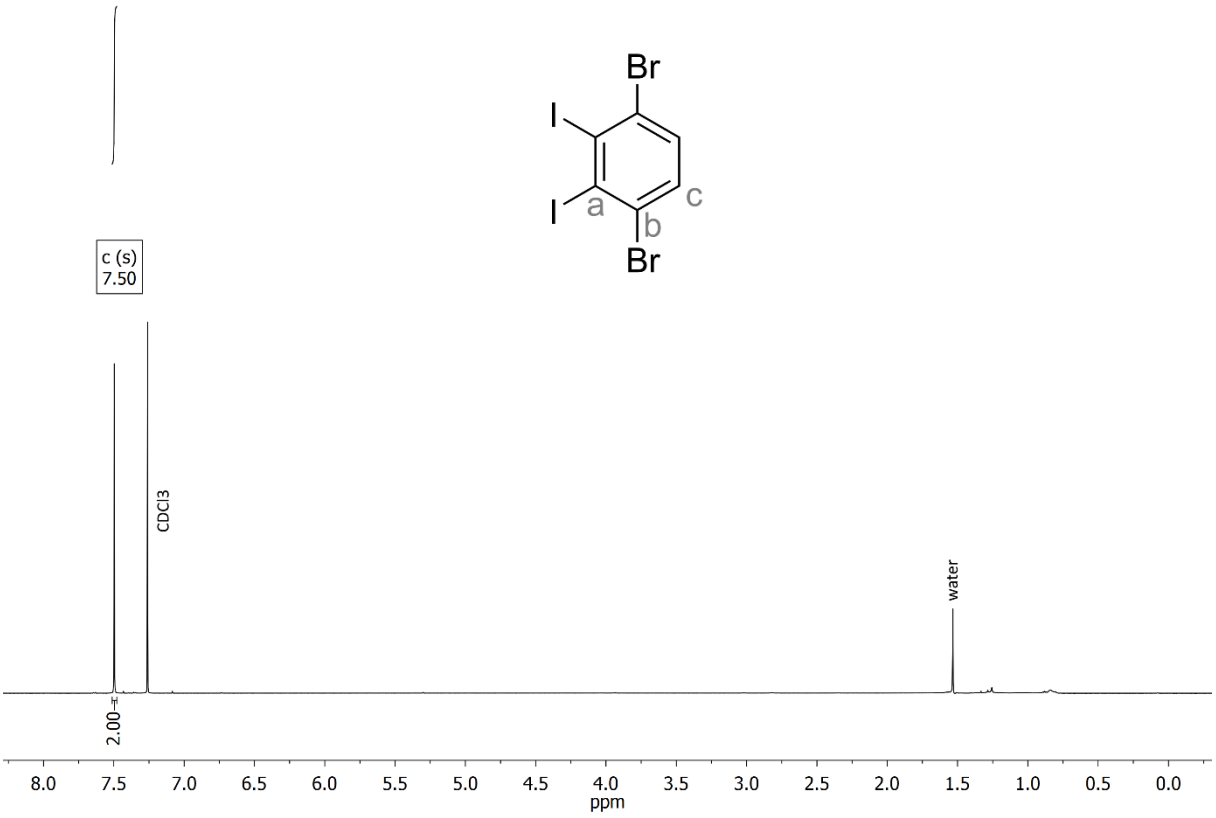

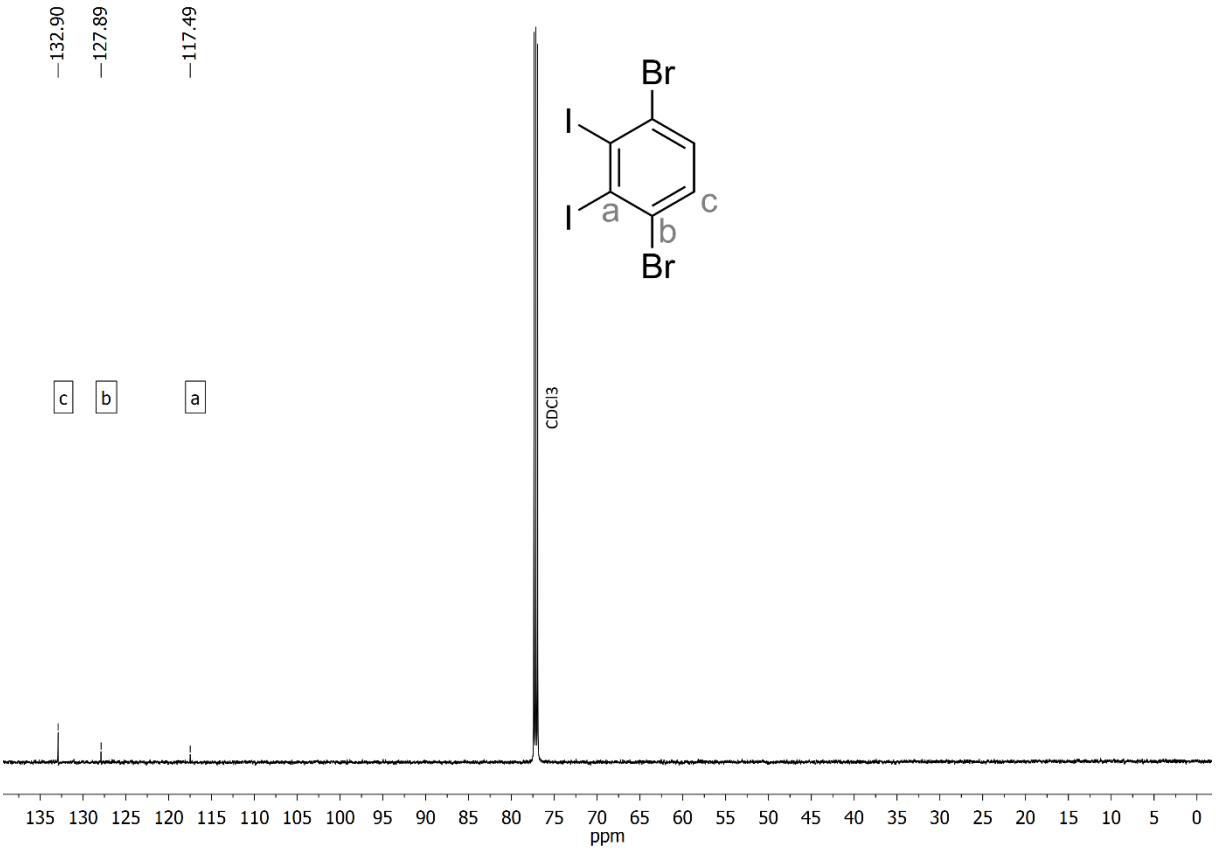

1,4-Dibromo-2,3-bis(2-(trimethylsilyl)ethynyl)benzene (13)

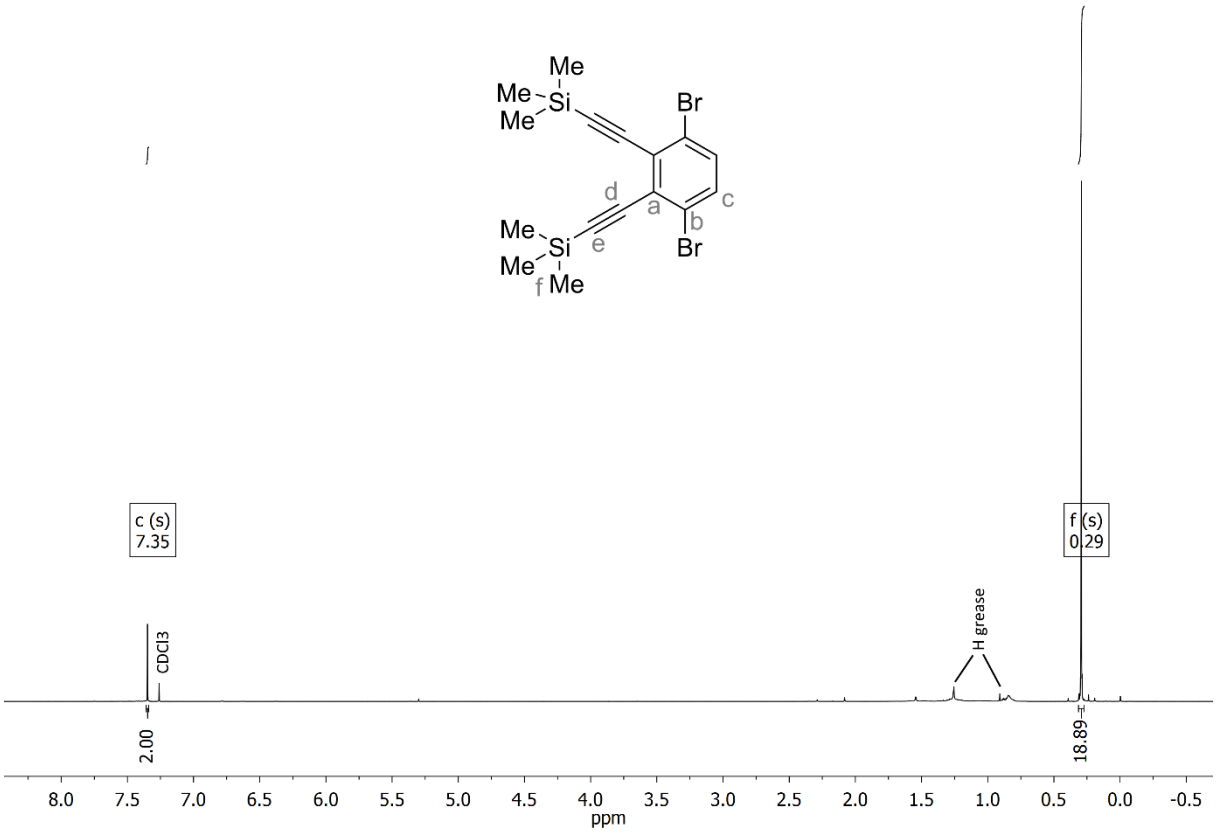

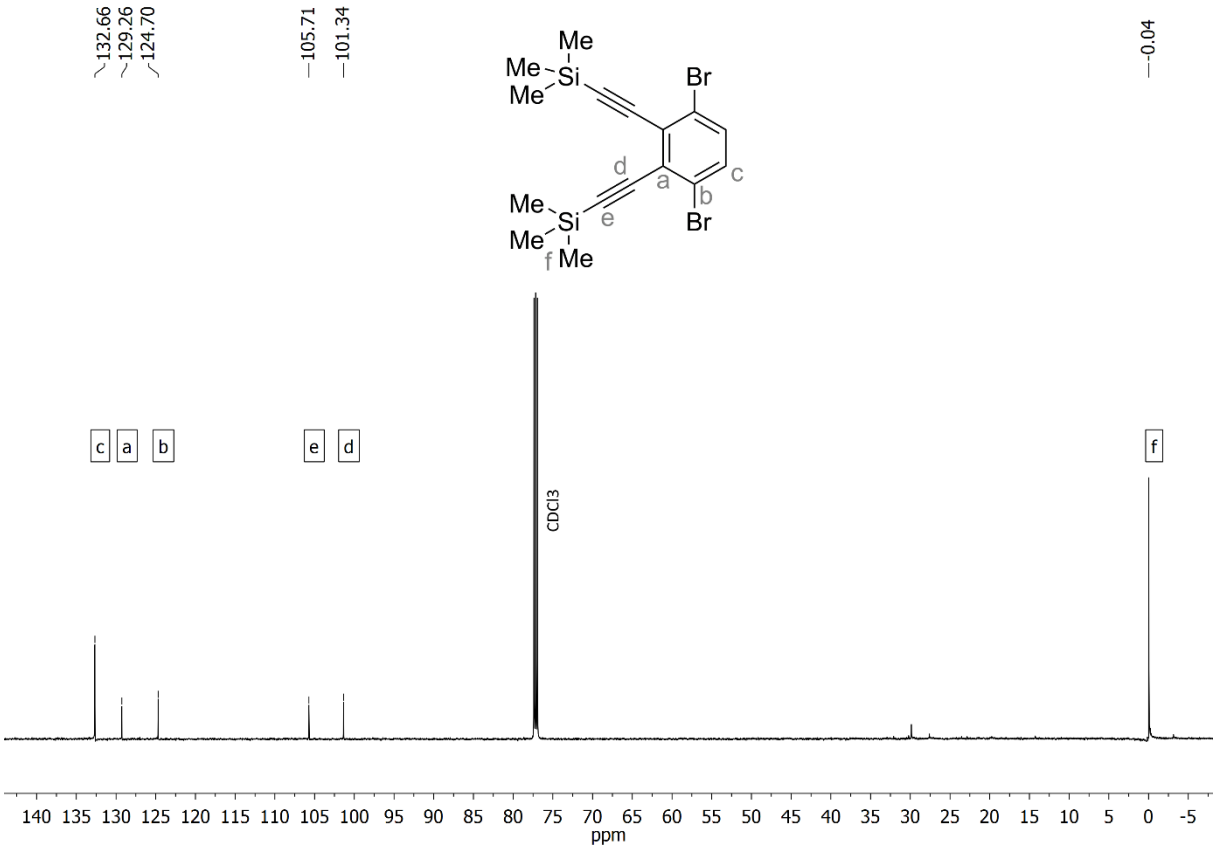

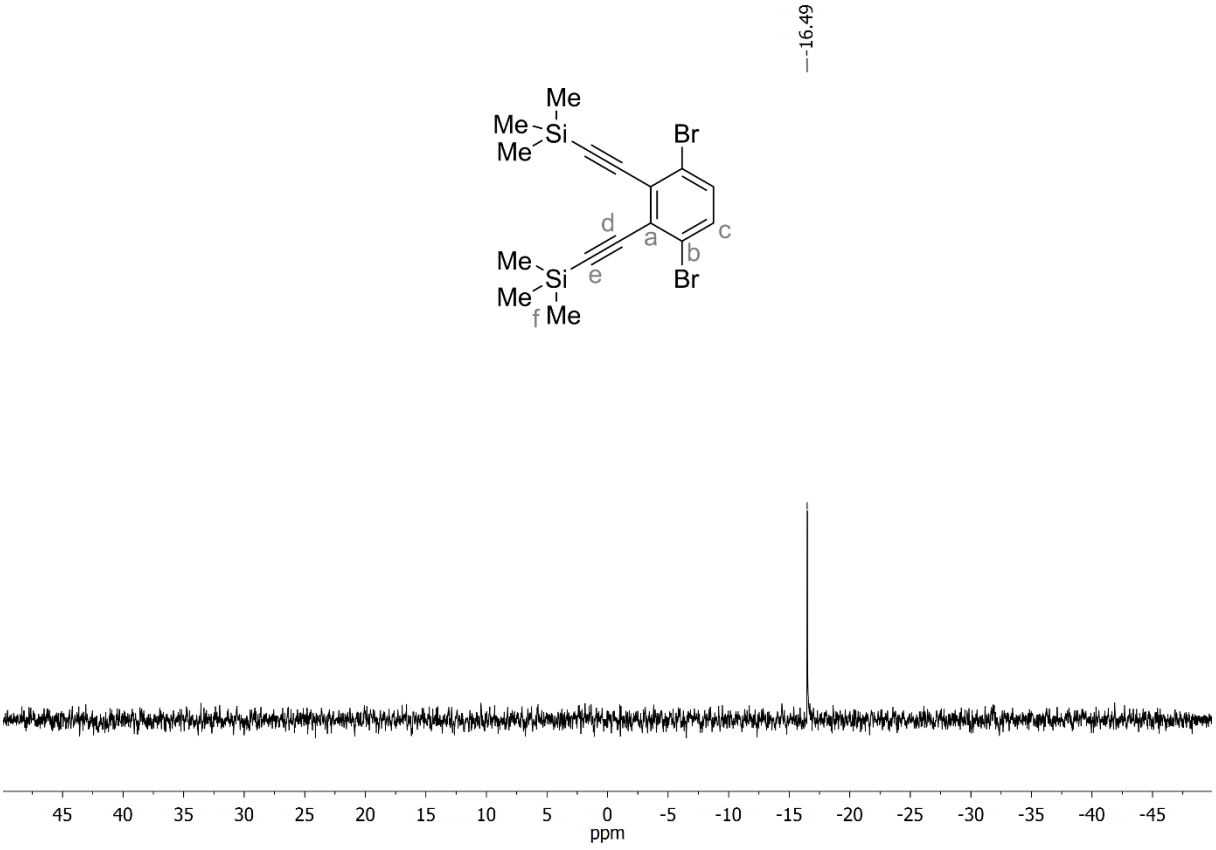

6,6'-(2,3-bis((Trimethylsilyl)ethynyl)-1,4-phenylene)bis(1-hydro-2-mesityl-1,2-azaborinine) (19)

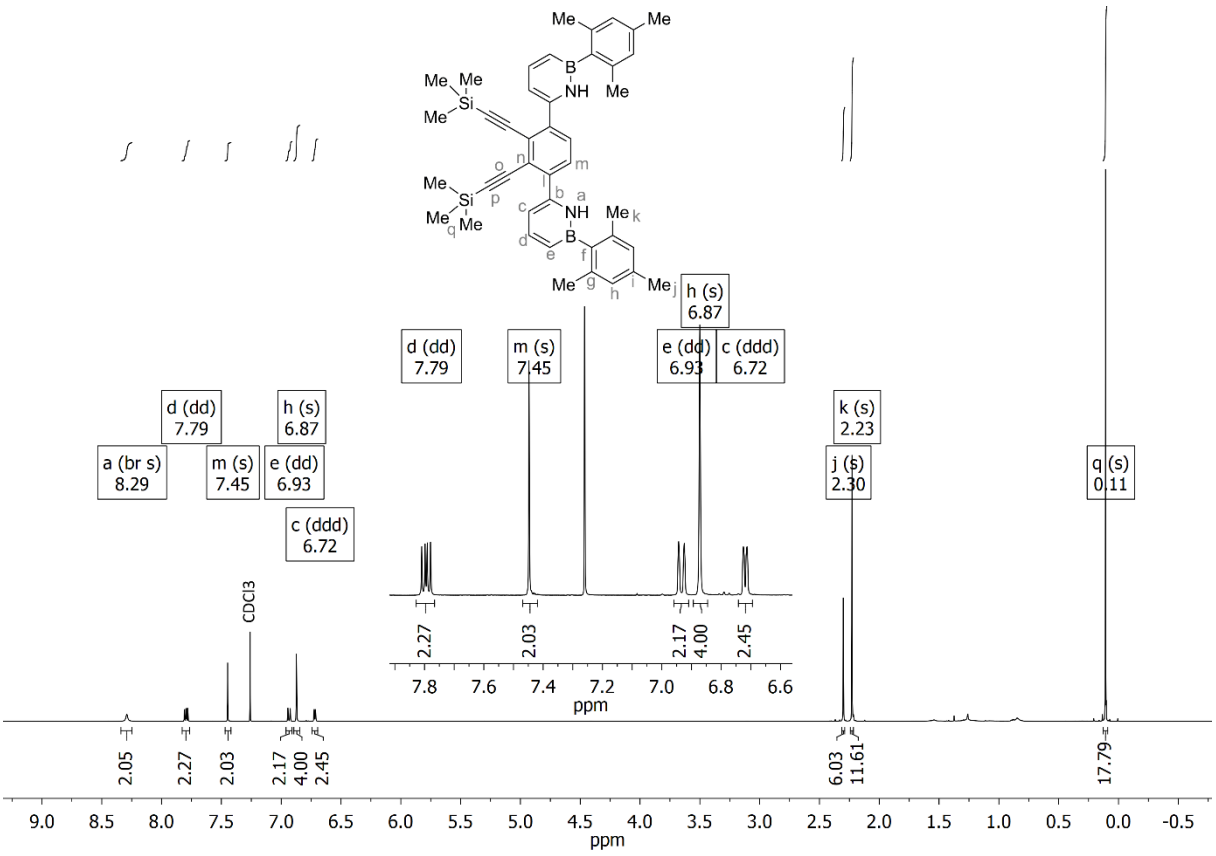

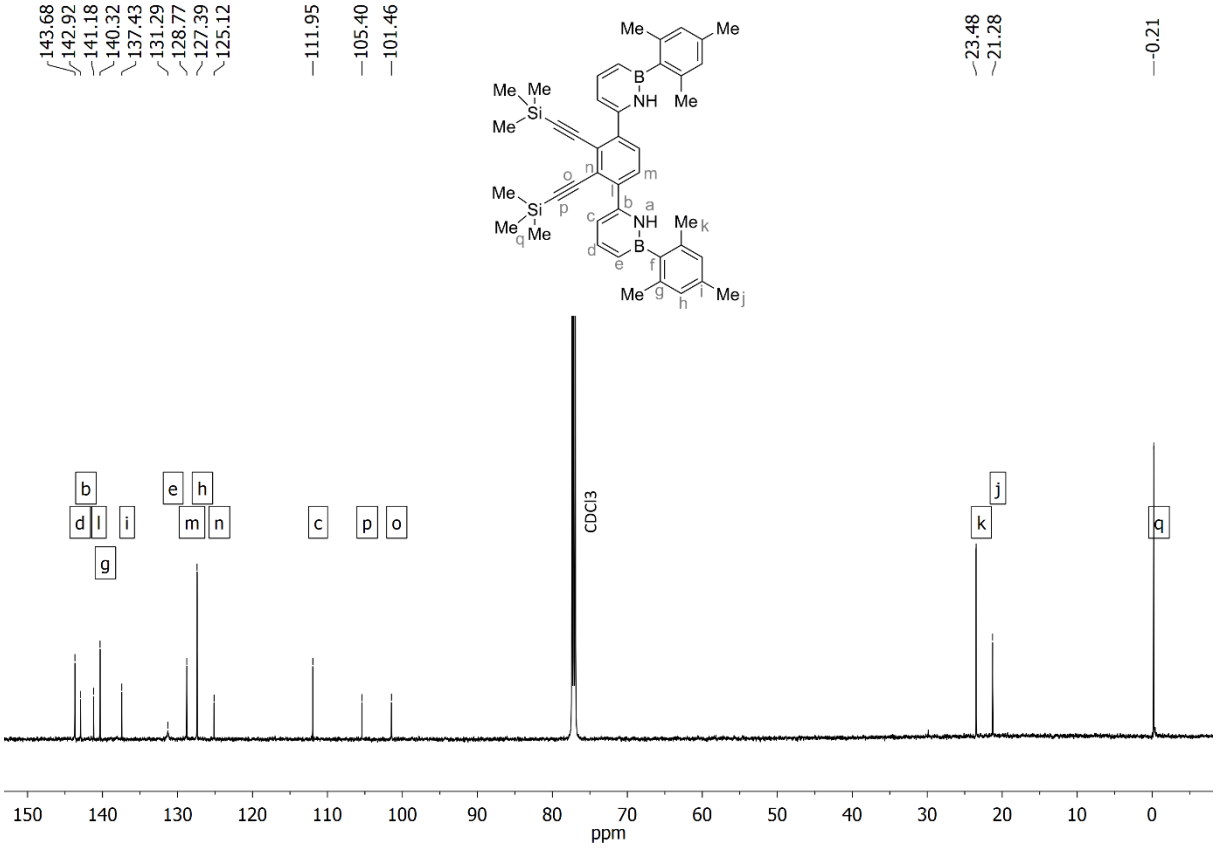
143.68
142.92
141.18
140.32
137.43
131.29
128.77
127.39
125.12
111.95
105.40
101.46
23.48
21.28
0.21
CDCl3
ppm

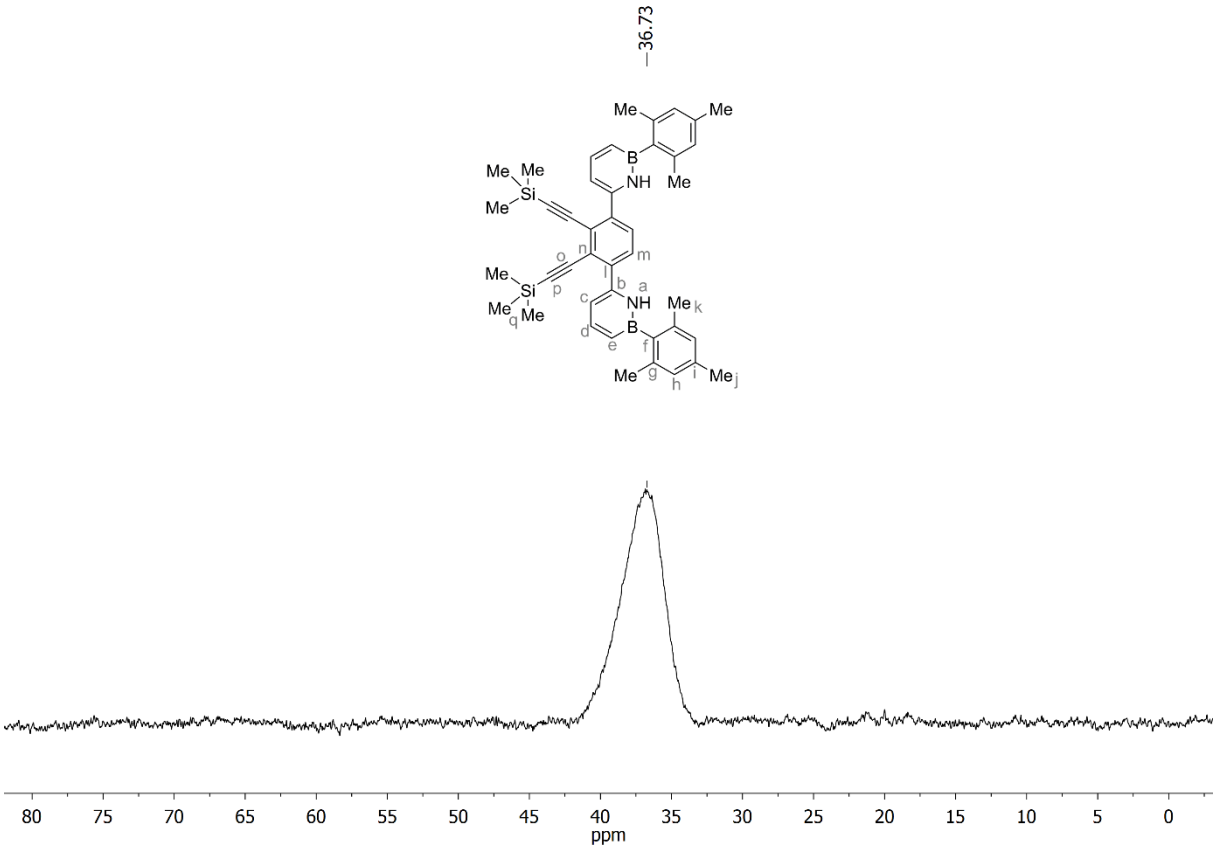
36.73
ppm

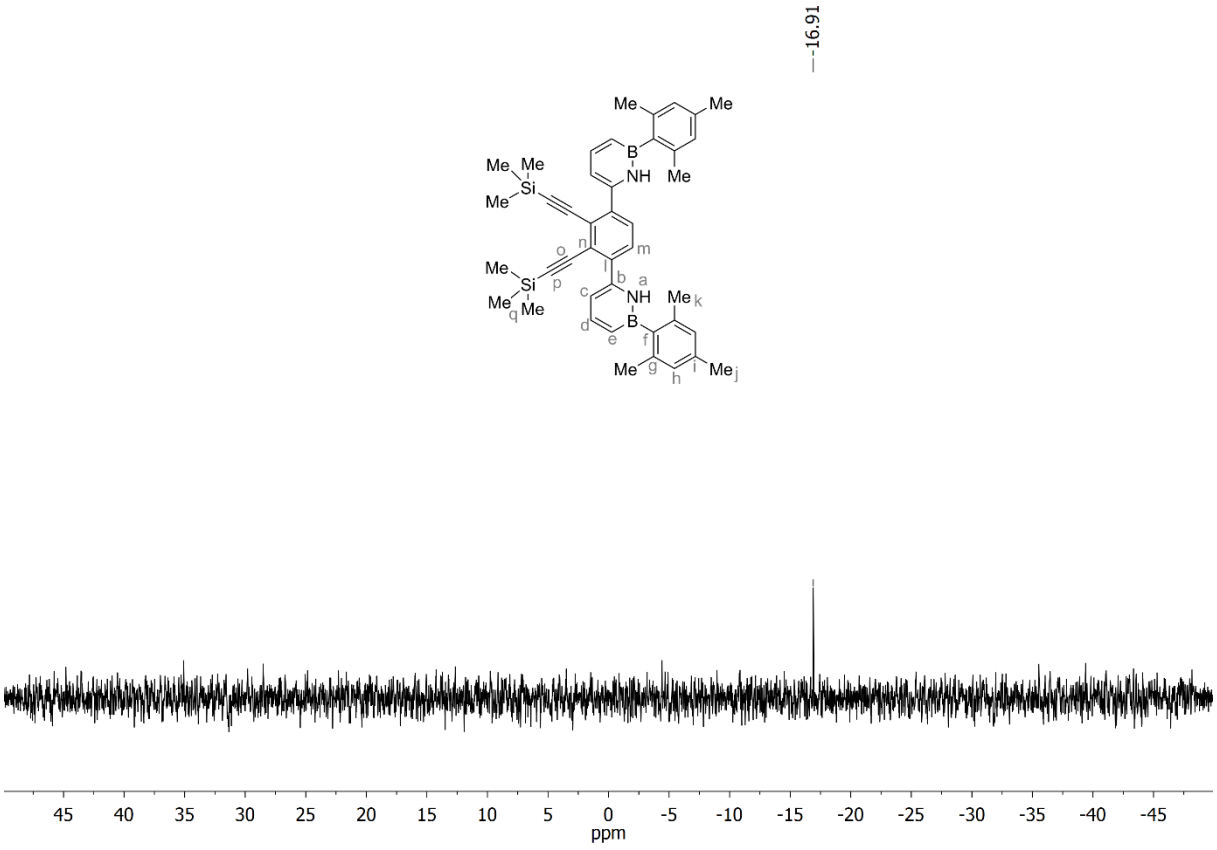

1,12-Dihydro-2,11-dimesityl-1,12-diaza-2,11-diborapicene (*BN*-PAH6)

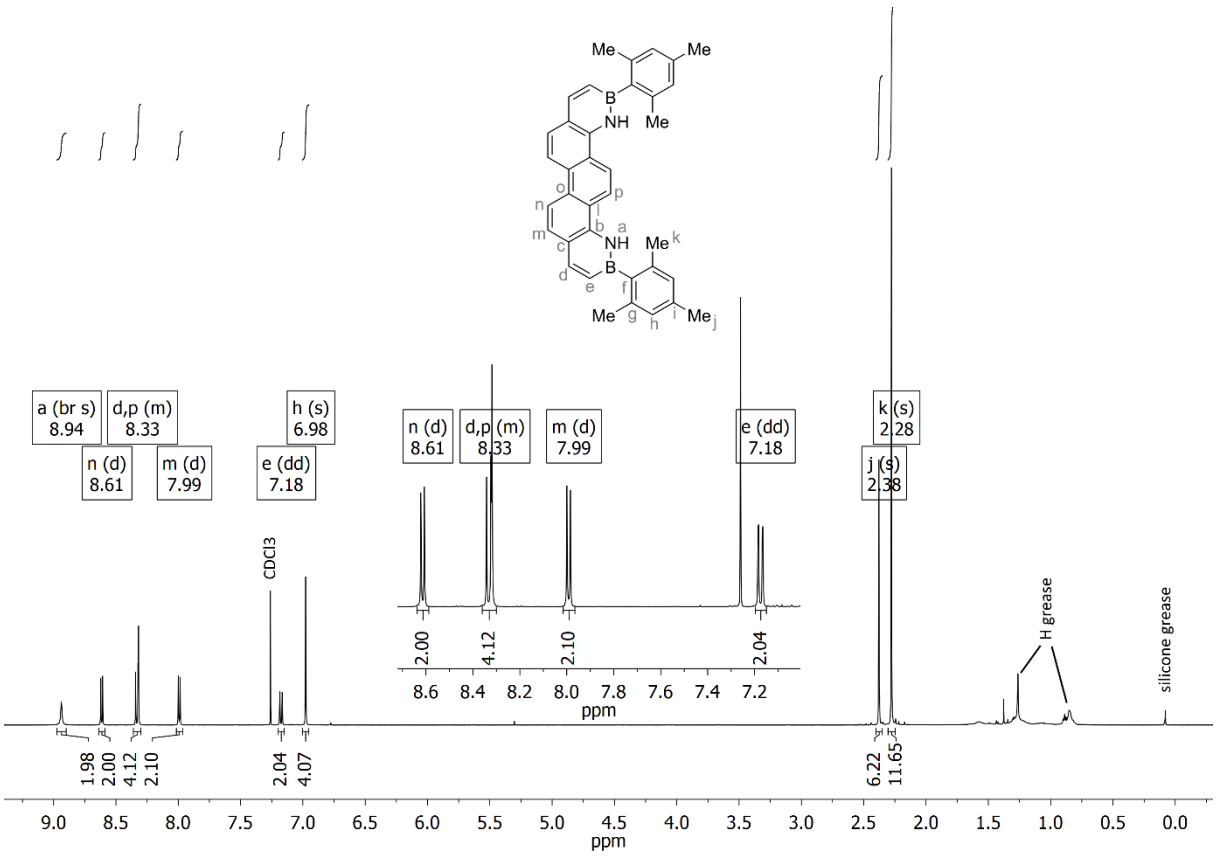

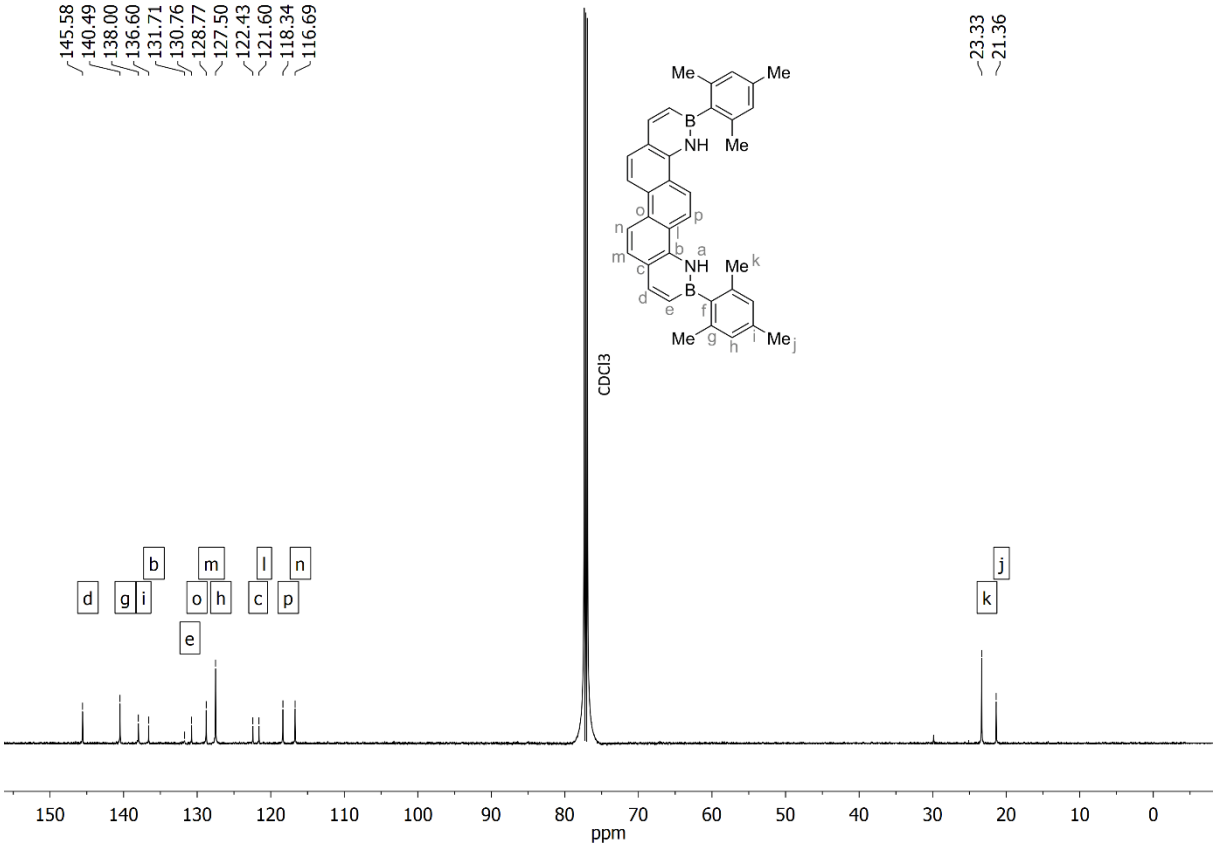
145.58
140.49
138.00
136.60
131.71
130.76
128.77
127.50
122.43
121.60
118.34
116.69
23.33
21.36
CDCl3
Me
Me
B
NH
Me
Me
Me
Me
Me
Me
d
g
i
b
o
h
e
m
c
l
p
n
k
j
150
140
130
120
110
100
90
80
70
60
50
40
30
20
10
0
ppm

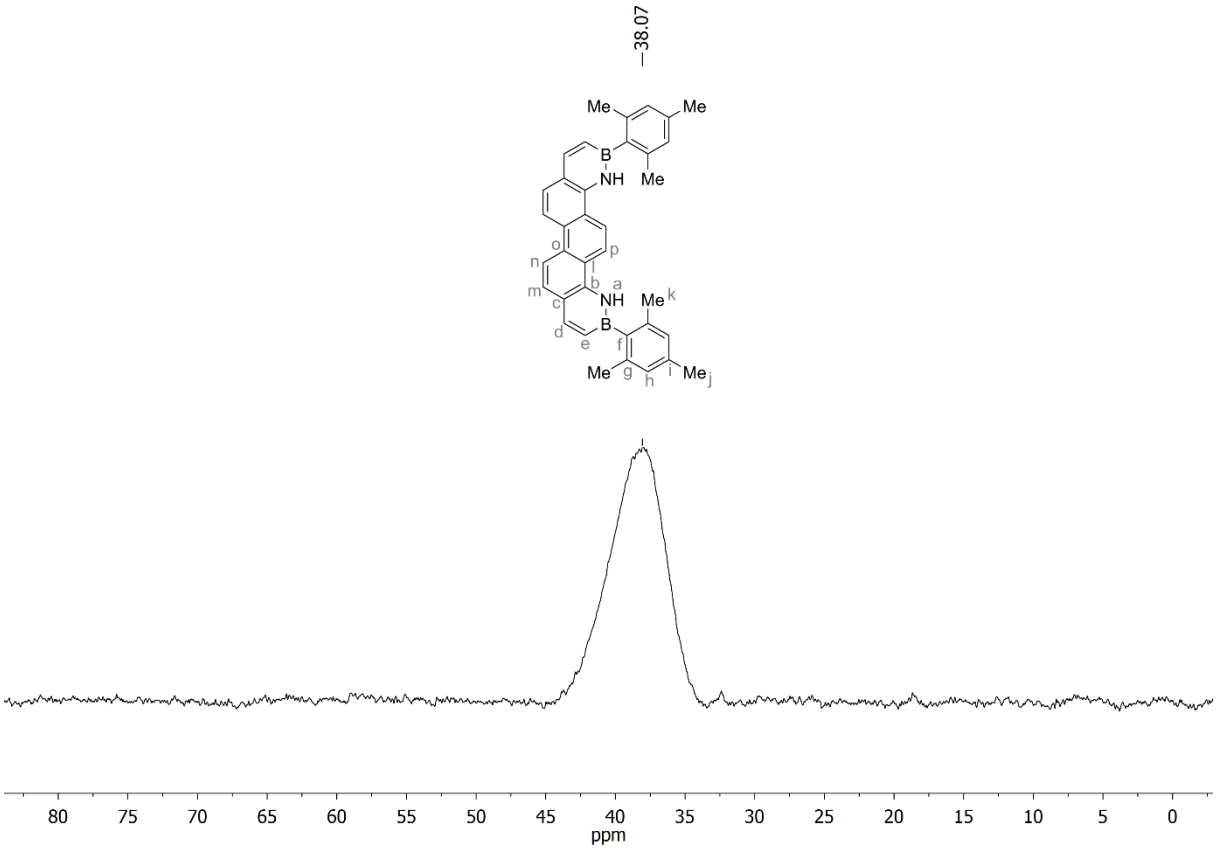
38.07
Me
Me
B
NH
Me
Me
Me
Me
Me
Me
80
75
70
65
60
55
50
45
40
35
30
25
20
15
10
5
0
ppm

6. Mass Spectra

6.1. 4-Hydro-3-mesityl-4,3-azaboraphenanthrene (*BN*-PAH1)

The GC-MS chromatograms of ***BN*-PAH1** after filtration over silica (eluents: 5% diethyl ether in *n*-pentane) but before silica gel chromatography show the formation of two isomers with close retention times. While the most intense signal at t_R = 24.82 min represents ***BN*-PAH1**, the by-product at t_R = 25.21 min could not be characterized due to its low share. It is possible that this signal represents the product of a 5-exo-dig cyclization, leading to a newly formed five-membered ring with an exocyclic double bond. Another possibility is the formation of a new six-membered ring via the azaborinine nitrogen atom. The formation of differently ring-closed isomers was observed in almost all approaches, though in different amounts.

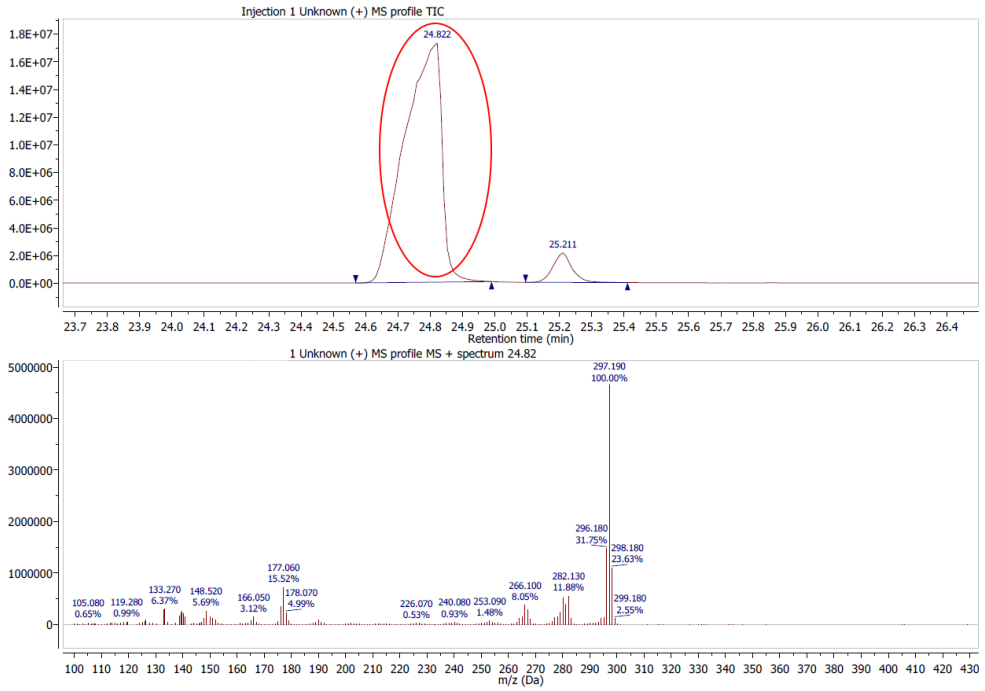

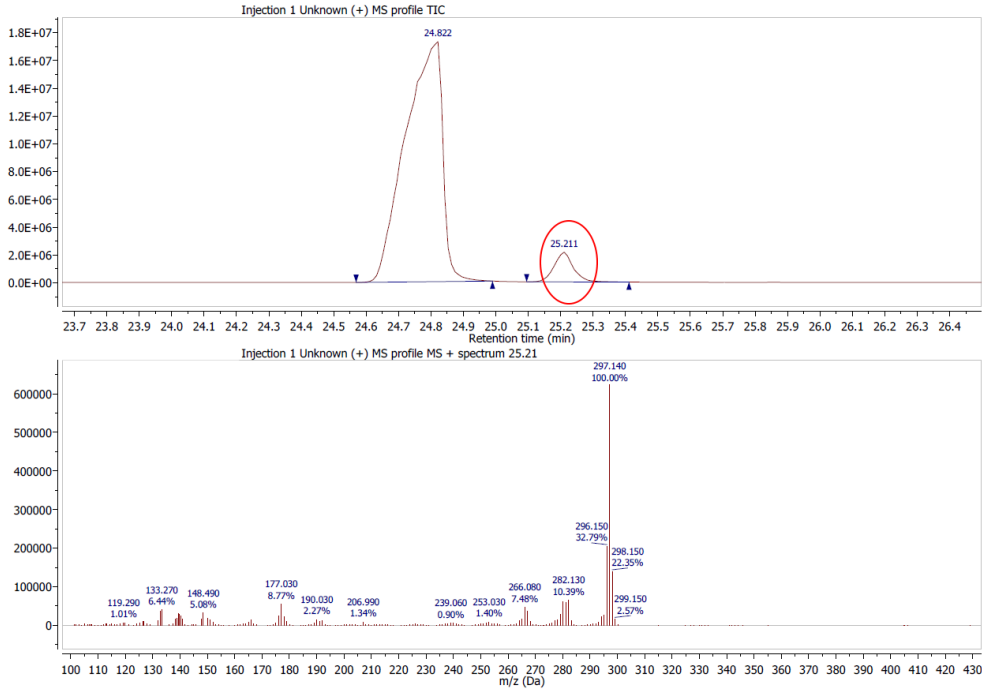

7. Single Crystal Data

7.1. 4-Hydro-3-mesityl-4,3-azaboraphenanthrene (*BN*-PAH1)

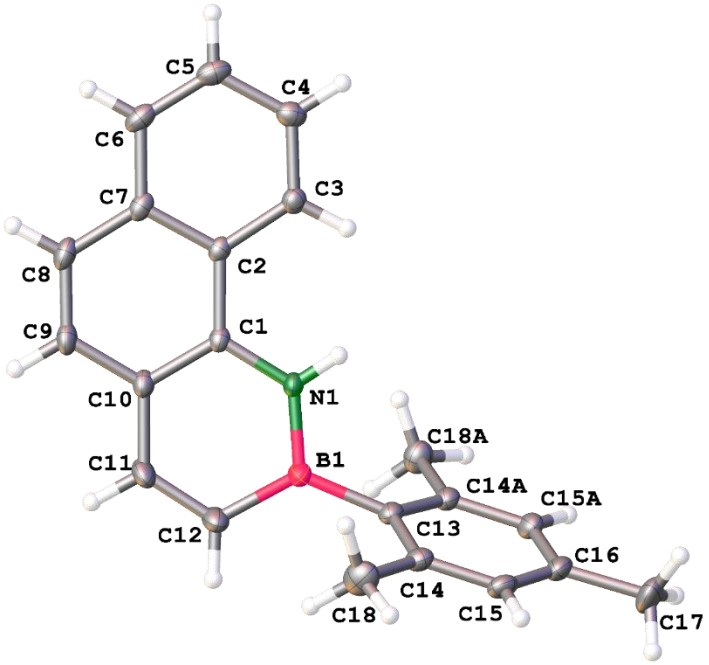

Single crystals of $C_{21}H_{20}BN$ (***BN*-PAH1**) were grown by dissolving a small amount (ca. 5 mg) of the compound in chloroform (ca. 200 µL) in a snap cap sample vial. Ethanol (ca. 1 mL) was cautiously added on top of the solution to prevent mixing. Solvents were allowed to evaporate slowly at 25 °C by leaving the vial open for 7 d. CCDC Deposition Number: 1998253.

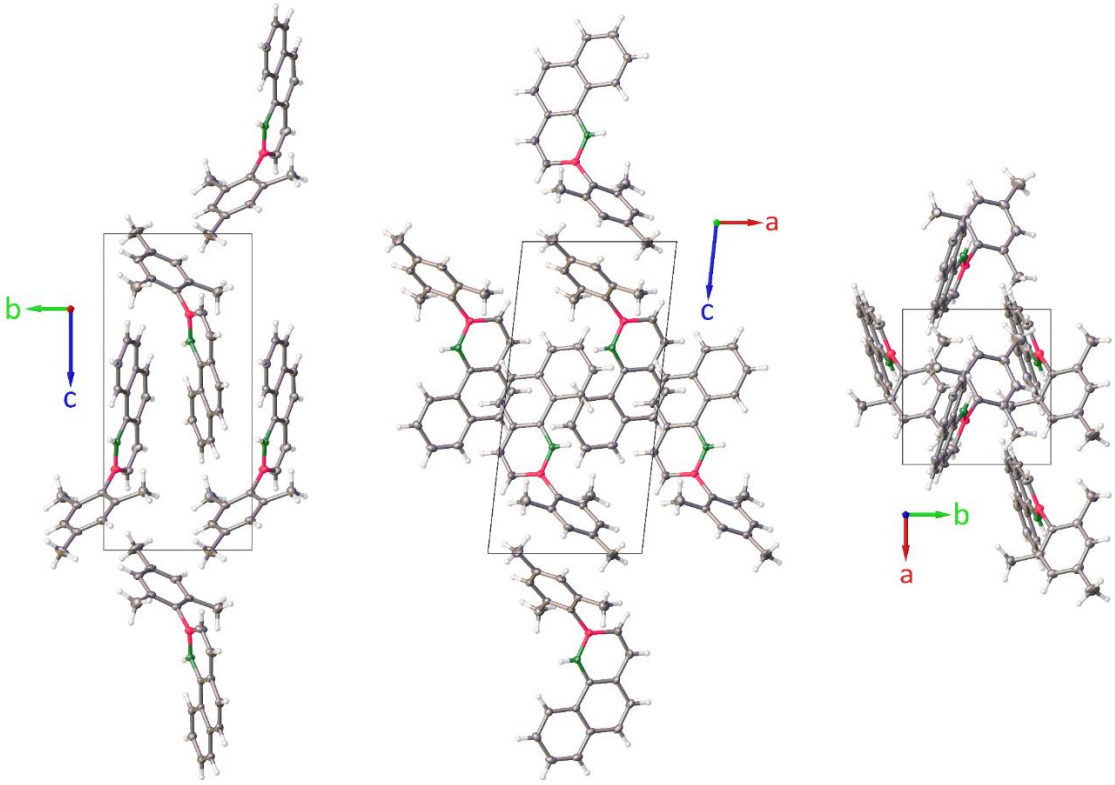

Fig. 38 Unit cell packing view of a ***BN*-PAH1** crystal along the *a, b* and *c*-axes.

Table 2 Crystal data and structure refinement for ***BN*-PAH1**.

Empirical formula	$C_{21}H_{20}BN$
Formula weight	297.19
Temperature/K	100.00
Crystal system	monoclinic
Space group	$P2_1$
a/Å	7.5758(3)
b/Å	7.1933(3)
c/Å	15.4440(6)
α/°	90
β/°	96.3710(10)
γ/°	90
Volume/Å^3	836.42(6)
Z	2
ρ_{calc}g/cm^3	1.180
μ/mm^{-1}	0.067
F(000)	316.0
Crystal size/mm^3	0.24 × 0.2 ×
Radiation	MoKα (λ =
2Θ range for data collection/°	5.308 to 66.51
Index ranges	-11 ≤ h ≤ 11, -
Reflections collected	29265
Independent reflections	6419 [R_{int} =
Data/restraints/parameters	6419/1/215
Goodness-of-fit on F^2	1.043
Final R indexes [I>=2σ (I)]	R_1 = 0.0445,
Final R indexes [all data]	R_1 = 0.0569,
Largest diff. peak/hole / e Å^{-3}	0.36/-0.21

Table 3 Fractional Atomic Coordinates (×10^4) and Equivalent Isotropic Displacement Parameters (Å^2×10^3) for ***BN*-PAH1**. U_{eq} is defined as 1/3 of of the trace of the orthogonalized U_{ij} tensor.

Atom	*x*	*y*	*z*	U(eq)
N_1	6563.9(15)	4138.7(17)	3403.8(7)	16.5(2)
C_1	7537.3(17)	3446.2(19)	4141.5(9)	15.5(2)
C_2	6845.3(18)	3442.6(19)	4968.5(9)	15.3(2)
C_3	5103.6(19)	4043(2)	5083.5(10)	18.4(3)
C_4	4499(2)	4023(2)	5889.8(10)	22.0(3)
C_5	5608(2)	3399(2)	6623.7(10)	24.0(3)
C_6	7300(2)	2799(2)	6534.6(9)	22.6(3)
C_7	7963.7(19)	2811.3(19)	5713.5(9)	18.1(3)
C_8	9726(2)	2208(2)	5622.5(10)	22.2(3)
C_9	10325.2(18)	2176(2)	4828.1(10)	22.1(3)
C_{10}	9249.7(18)	2770(2)	4064.8(9)	18.7(3)
C_{11}	9920.5(19)	2748(3)	3235.6(10)	24.9(3)
C_{12}	8990(2)	3417(3)	2498.2(10)	26.1(3)
C_{13}	5815.6(18)	5100(2)	1803.2(9)	18.7(3)
C_{14}	6193(2)	6813(2)	1421.3(9)	21.8(3)
C_{14A}	4177.2(18)	4234(2)	1528.0(9)	19.6(3)
C_{15}	4932(2)	7648(2)	817.1(9)	24.2(3)
C_{15A}	2938(2)	5121(2)	932.4(9)	23.1(3)
C_{16}	3285(2)	6843(3)	582.8(9)	25.3(3)
C_{17}	1911(3)	7810(4)	-42.9(12)	39.7(5)
C_{18}	7939(2)	7786(3)	1677.2(12)	33.7(4)
C_{18A}	3764(2)	2314(2)	1846.6(11)	27.6(3)
B_1	7138(2)	4211(2)	2552.0(10)	19.3(3)

Table 4 Anisotropic Displacement Parameters (Å^2×10^3) for ***BN*-PAH1**. The Anisotropic displacement factor exponent takes the form: $-2\pi^2[h^2a^{*2}U_{11}+2hka^*b^*U_{12}+\ldots]$.

Atom	U_{11}	U_{22}	U_{33}	U_{23}	U_{13}	U_{12}
N_1	14.4(5)	19.1(5)	15.4(5)	0.2(4)	-0.5(4)	3.6(4)
C_1	15.7(5)	14.5(5)	15.6(6)	-1.1(5)	-1.6(4)	1.8(5)
C_2	17.7(5)	12.7(5)	15.0(5)	0.3(5)	-1.0(4)	-0.1(5)
C_3	18.7(5)	17.4(6)	18.9(6)	2.0(5)	1.4(5)	1.0(5)
C_4	24.8(6)	19.8(6)	22.5(7)	0.7(5)	7.3(5)	0.3(6)
C_5	34.9(8)	20.3(7)	17.4(6)	0.7(5)	5.4(5)	-4.3(6)
C_6	30.6(7)	20.4(6)	15.8(6)	2.4(5)	-2.0(5)	-3.5(6)
C_7	22.3(6)	14.0(5)	17.0(6)	1.1(5)	-3.3(5)	-0.7(5)
C_8	23.7(6)	19.3(6)	21.5(6)	1.5(5)	-6.8(5)	3.1(5)
C_9	18.5(6)	21.0(6)	25.1(7)	-0.7(5)	-4.1(5)	6.7(5)
C_{10}	17.4(5)	19.1(6)	18.7(6)	-1.5(5)	-1.8(5)	4.9(5)
C_{11}	18.5(6)	32.5(8)	23.6(7)	-6.2(6)	1.7(5)	9.3(6)
C_{12}	22.3(6)	38.3(9)	17.9(6)	-3.8(6)	3.5(5)	8.2(6)
C_{13}	19.5(6)	23.8(6)	12.9(5)	-0.5(5)	2.0(4)	2.7(5)
C_{14}	23.8(6)	26.7(7)	15.2(6)	0.6(5)	3.4(5)	0.1(6)
C_{14A}	20.7(6)	23.8(7)	14.4(6)	0.1(5)	2.5(4)	2.8(5)
C_{15}	30.5(7)	26.3(7)	16.5(6)	5.2(5)	5.8(5)	3.2(6)
C_{15A}	20.3(6)	32.6(8)	15.8(6)	0.4(6)	-0.4(5)	1.6(6)
C_{16}	27.0(7)	34.1(8)	14.9(6)	4.5(6)	2.5(5)	7.7(6)
C_{17}	33.9(9)	53.8(12)	29.6(9)	19.3(9)	-4.5(7)	8.3(9)
C_{18}	30.6(8)	36.5(9)	33.8(9)	3.7(8)	2.0(7)	-9.1(7)
C_{18A}	27.0(7)	26.0(8)	29.2(8)	4.0(6)	0.3(6)	-0.1(6)
B_1	17.8(6)	24.1(7)	15.8(6)	-0.9(6)	1.0(5)	3.3(6)

Table 5 Bond Lengths for ***BN*-PAH1**.

Atom	Atom	Length/Å	Atom	Atom	Length/Å
N_1	C_1	1.3797(16)	C_{10}	C_{11}	1.429(2)
N_1	B_1	1.4317(19)	C_{11}	C_{12}	1.359(2)
C_1	C_2	1.4333(17)	C_{12}	B_1	1.526(2)
C_1	C_{10}	1.4027(18)	C_{13}	C_{14}	1.409(2)
C_2	C_3	1.4182(19)	C_{13}	C_{14A}	1.411(2)
C_2	C_7	1.4253(17)	C_{13}	B_1	1.579(2)
C_3	C_4	1.374(2)	C_{14}	C_{15}	1.395(2)
C_4	C_5	1.407(2)	C_{14}	C_{18}	1.509(2)
C_5	C_6	1.374(2)	C_{14A}	C_{15A}	1.3939(19)
C_6	C_7	1.415(2)	C_{14A}	C_{18A}	1.511(2)

Atom	Atom	Length/Å	Atom	Atom	Length/Å
C_7	C_8	1.425(2)	C_{15}	C_{16}	1.386(2)
C_8	C_9	1.355(2)	C_{15A}	C_{16}	1.388(2)
C_9	C_{10}	1.4224(19)	C_{16}	C_{17}	1.509(2)

Table 6 Bond Angles for ***BN*-PAH1**.

Atom	Atom	Atom	Angle/˚	Atom	Atom	Atom	Angle/˚
C_1	N_1	B_1	125.65(11)	C_{12}	C_{11}	C_{10}	122.96(13)
N_1	C_1	C_2	121.44(11)	C_{11}	C_{12}	B_1	118.77(13)
N_1	C_1	C_{10}	118.03(12)	C_{14}	C_{13}	C_{14A}	118.20(13)
C_{10}	C_1	C_2	120.52(11)	C_{14}	C_{13}	B_1	121.26(13)
C_3	C_2	C_1	123.26(11)	C_{14A}	C_{13}	B_1	120.47(13)
C_3	C_2	C_7	118.29(12)	C_{13}	C_{14}	C_{18}	120.57(14)
C_7	C_2	C_1	118.45(11)	C_{15}	C_{14}	C_{13}	120.02(14)
C_4	C_3	C_2	121.24(13)	C_{15}	C_{14}	C_{18}	119.39(14)
C_3	C_4	C_5	120.29(13)	C_{13}	C_{14A}	C_{18A}	120.83(13)
C_6	C_5	C_4	119.98(13)	C_{15A}	C_{14A}	C_{13}	120.14(14)
C_5	C_6	C_7	121.07(13)	C_{15A}	C_{14A}	C_{18A}	118.99(13)
C_6	C_7	C_2	119.13(12)	C_{16}	C_{15}	C_{14}	121.65(14)
C_6	C_7	C_8	121.09(12)	C_{16}	C_{15A}	C_{14A}	121.48(14)
C_8	C_7	C_2	119.78(12)	C_{15}	C_{16}	C_{15A}	118.36(14)
C_9	C_8	C_7	120.42(12)	C_{15}	C_{16}	C_{17}	120.76(16)
C_8	C_9	C_{10}	121.77(13)	C_{15A}	C_{16}	C_{17}	120.88(16)
C_1	C_{10}	C_9	118.97(12)	N_1	B_1	C_{12}	114.31(13)
C_1	C_{10}	C_{11}	120.25(12)	N_1	B_1	C_{13}	117.05(12)
C_9	C_{10}	C_{11}	120.75(12)	C_{12}	B_1	C_{13}	128.64(13)

Table 7 Torsion Angles for ***BN*-PAH1**.

A	B	C	D	Angle/˚	A	B	C	D	Angle/˚
N_1	C_1	C_2	C_3	3.5(2)	C_{10}	C_1	C_2	C_7	2.6(2)
N_1	C_1	C_2	C_7	-176.22(12)	C_{10}	C_{11}	C_{12}	B_1	-0.7(3)
N_1	C_1	C_{10}	C_9	175.47(14)	C_{11}	C_{12}	B_1	N_1	-0.6(2)
N_1	C_1	C_{10}	C_{11}	-2.2(2)	C_{11}	C_{12}	B_1	C_{13}	178.67(17)
C_1	N_1	B_1	C_{12}	0.5(2)	C_{13}	C_{14}	C_{15}	C_{16}	0.7(2)
C_1	N_1	B_1	C_{13}	-178.85(13)	C_{13}	C_{14A}	C_{15A}	C_{16}	1.3(2)
C_1	C_2	C_3	C_4	-179.72(14)	C_{14}	C_{13}	C_{14A}	C_{15A}	-3.7(2)
C_1	C_2	C_7	C_6	-179.98(13)	C_{14}	C_{13}	C_{14A}	C_{18A}	174.09(13)
C_1	C_2	C_7	C_8	0.1(2)	C_{14}	C_{13}	B_1	N_1	111.33(16)
C_1	C_{10}	C_{11}	C_{12}	2.2(3)	C_{14}	C_{13}	B_1	C_{12}	-68.0(2)
C_2	C_1	C_{10}	C_9	-3.4(2)	C_{14}	C_{15}	C_{16}	C_{15A}	-3.1(2)
C_2	C_1	C_{10}	C_{11}	178.92(15)	C_{14}	C_{15}	C_{16}	C_{17}	177.36(15)
C_2	C_3	C_4	C_5	0.0(2)	C_{14A}	C_{13}	C_{14}	C_{15}	2.8(2)
C_2	C_7	C_8	C_9	-2.1(2)	C_{14A}	C_{13}	C_{14}	C_{18}	-178.83(15)
C_3	C_2	C_7	C_6	0.3(2)	C_{14A}	C_{13}	B_1	N_1	-65.63(19)
C_3	C_2	C_7	C_8	-179.63(13)	C_{14A}	C_{13}	B_1	C_{12}	115.07(19)
C_3	C_4	C_5	C_6	-0.3(2)	C_{14A}	C_{15A}	C_{16}	C_{15}	2.2(2)
C_4	C_5	C_6	C_7	0.6(2)	C_{14A}	C_{15A}	C_{16}	C_{17}	-178.34(15)
C_5	C_6	C_7	C_2	-0.6(2)	C_{18}	C_{14}	C_{15}	C_{16}	-177.74(15)
C_5	C_6	C_7	C_8	179.30(15)	C_{18A}	C_{14A}	C_{15A}	C_{16}	-176.57(14)
C_6	C_7	C_8	C_9	178.03(15)	B_1	N_1	C_1	C_2	179.73(13)
C_7	C_2	C_3	C_4	0.0(2)	B_1	N_1	C_1	C_{10}	0.9(2)
C_7	C_8	C_9	C_{10}	1.3(2)	B_1	C_{13}	C_{14}	C_{15}	-174.25(13)
C_8	C_9	C_{10}	C_1	1.4(2)	B_1	C_{13}	C_{14}	C_{18}	4.1(2)
C_8	C_9	C_{10}	C_{11}	179.10(15)	B_1	C_{13}	C_{14A}	C_{15A}	173.32(13)
C_9	C_{10}	C_{11}	C_{12}	-175.46(16)	B_1	C_{13}	C_{14A}	C_{18A}	-8.9(2)
C_{10}	C_1	C_2	C_3	-177.65(14)					

Table 8 Hydrogen Atom Coordinates (Å×10⁴) and Isotropic Displacement Parameters (Å²×10³) for ***BN*-PAH1**.

Atom	*x*	*y*	*z*	U(eq)
H_3	4340.5	4467.81	4593.8	22
H_4	3327.78	4431.42	5952.26	26
H_5	5186.71	3392.89	7180.62	29
H_6	8035.91	2368.53	7032.31	27
H_8	10484.33	1826.44	6121.99	27
H_9	11495.31	1744.1	4779.54	26
H_{11}	11068.18	2242.8	3198.3	30
H_{12}	9484.6	3391.47	1959.18	31
H_{15}	5208.05	8795.98	559.84	29
H_{15A}	1830.49	4533.87	761.95	28
H_{17A}	1031.85	6901.96	-290.46	60
H_{17B}	2492.05	8383.42	-512.47	60
H_{17C}	1317.78	8773.07	268.06	60
H_{18A}	8020.44	8887.25	1310.52	51
H_{18B}	8920.03	6937.52	1597.68	51
H_{18C}	8008.41	8163.69	2289.73	51
H_{18D}	2603.85	1911.47	1564.94	41
H_{18E}	3738.95	2342.06	2479.56	41
H_{18F}	4680.86	1441.51	1702	41
H_1	5540(30)	4590(30)	3480(12)	20(5)

7.2. 9-Hydro-8-mesityl-9,8-azaboranaphtho[1,2-*b*]thiophene (*BN*-PAH2)

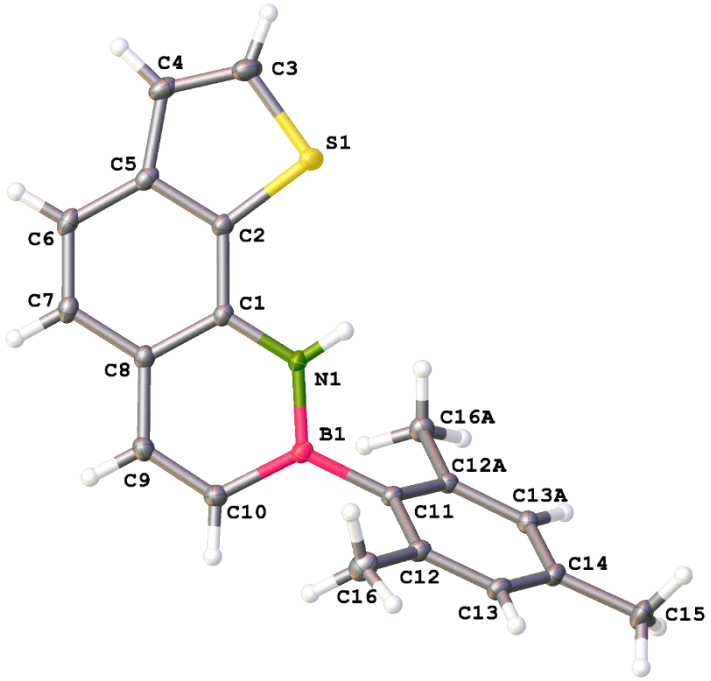

Single crystals of $C_{19}H_{18}BNS$ (***BN*-PAH2**) were grown by dissolving a small amount (ca. 5 mg) of the compound in DCM (ca. 200 µL) in a snap cap sample vial. Methanol (ca. 1 mL) was cautiously added on top of the solution to prevent mixing. Solvents were allowed to evaporate slowly at 25 °C by leaving the vial open for 7 d. CCDC Deposition Number: 1998252.

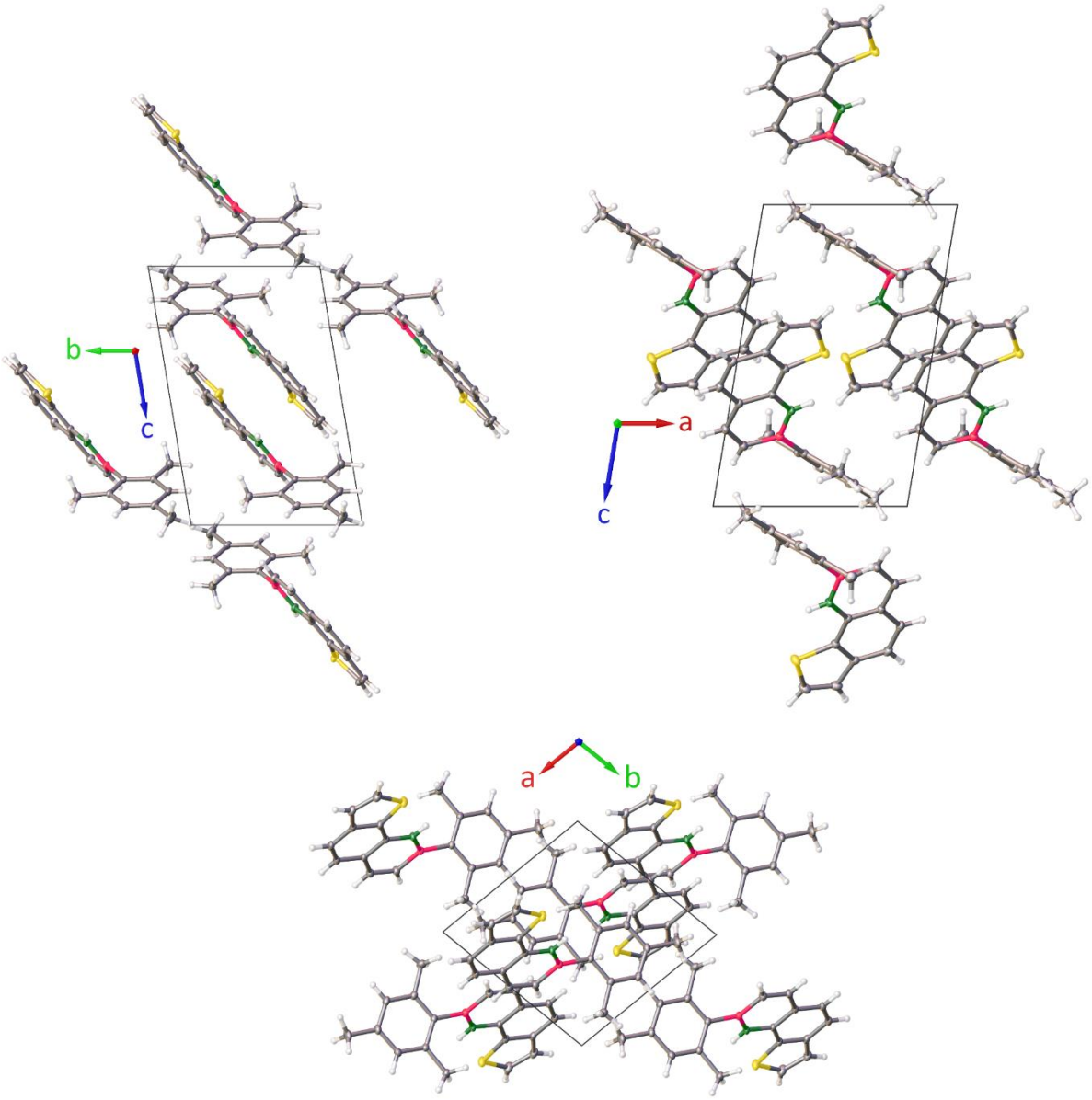

Fig. 39 Unit cell packing view of a ***BN*-PAH2** crystal along the *a, b* and *c*-axes.

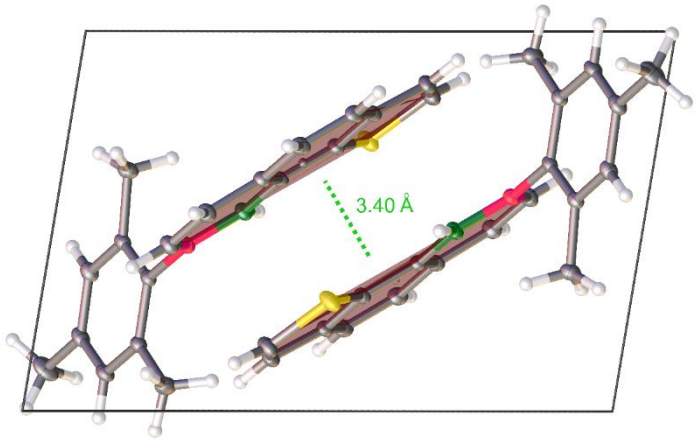

Fig. 40 Graphical representation of π-stacks and the regarding plane distance of ***BN*-PAH2**.

Table 9 Crystal data and structure refinement for ***BN*-PAH2**.

Empirical formula	$C_{19}H_{18}BNS$
Formula weight	303.21
Temperature/K	100.0
Crystal system	triclinic
Space group	P-1
a/Å	8.0030(3)
b/Å	8.2368(3)
c/Å	12.5344(5)
α/°	97.8090(10)
β/°	97.8300(10)
γ/°	100.0790(10)
Volume/Å^3	795.04(5)
Z	2
ρ_{calc}g/cm^3	1.267
μ/mm^{-1}	0.198
F(000)	320.0
Crystal size/mm^3	0.26 × 0.21 × 0.17
Radiation	MoKα (λ = 0.71073)
2Θ range for data collection/°	5.092 to 66.454
Index ranges	-12 ≤ h ≤ 12, -12 ≤ k ≤ 12, -19 ≤ l ≤ 19
Reflections collected	26776
Independent reflections	6092 [R_{int} = 0.0236, R_{sigma} = 0.0209]
Data/restraints/parameters	6092/0/206
Goodness-of-fit on F^2	1.041
Final R indexes [I>=2σ (I)]	R_1 = 0.0372, wR_2 = 0.1032
Final R indexes [all data]	R_1 = 0.0453, wR_2 = 0.1090
Largest diff. peak/hole / e Å^{-3}	0.52/-0.30

Table 10 Fractional Atomic Coordinates (×10^4) and Equivalent Isotropic Displacement Parameters (Å^2×10^3) for ***BN*-PAH2**. U_{eq} is defined as 1/3 of of the trace of the orthogonalized U_{ij} tensor.

Atom	*x*	*y*	*z*	U(eq)
S1	5577.6(3)	2891.8(3)	5098.4(2)	19.86(7)
N1	6803.7(10)	4748.4(9)	3184.0(6)	14.18(13)
C1	7915.7(11)	3899.3(10)	3717.1(7)	13.01(14)
C2	7480.8(11)	3035.1(10)	4566.8(7)	14.33(15)
C8	9544.1(11)	3894.0(10)	3412.2(7)	14.23(15)
C11	5744.1(11)	6503.6(10)	1759.9(7)	13.52(14)
C14	3180.8(12)	8070.1(12)	780.7(7)	17.59(16)
C13A	2888.4(11)	6343.3(11)	744.6(7)	16.22(15)
C9	10026.2(11)	4791.8(11)	2559.2(7)	16.89(16)
C12A	4135.1(11)	5551.8(10)	1220.9(7)	13.88(14)
C7	10683.9(11)	3024.0(11)	3964.7(8)	16.85(16)
C12	6053.6(11)	8250.4(11)	1779.7(7)	15.02(15)
C6	10249.0(12)	2181.2(11)	4790.0(7)	17.29(16)
C4	7887.6(13)	1402.2(12)	5940.6(8)	19.65(17)
C13	4778.8(12)	9005.9(11)	1294.5(7)	17.07(16)
C5	8617.0(12)	2173.8(11)	5104.7(7)	15.39(15)
C10	8955.1(12)	5632.7(11)	2018.0(7)	16.99(16)
C16A	3740.3(12)	3667.4(11)	1110.5(8)	17.92(16)
C3	6289.7(14)	1679.4(13)	6023.5(8)	22.86(19)
C16	7737.0(13)	9344.7(12)	2354.7(8)	21.51(18)
C15	1796.6(14)	8893.9(14)	278.7(10)	26.8(2)
B1	7166.1(12)	5638.2(12)	2314.8(8)	14.29(16)

Table 11 Anisotropic Displacement Parameters (Å^2×10^3) for ***BN*-PAH2**. The Anisotropic displacement factor exponent takes the form: $-2\pi^2[h^2a^{*2}U_{11}+2hka^*b^*U_{12}+\ldots]$.

Atom	U_{11}	U_{22}	U_{33}	U_{23}	U_{13}	U_{12}
S_1	21.53(11)	20.80(11)	23.67(12)	11.34(8)	10.40(8)	10.34(8)
N_1	13.7(3)	15.7(3)	16.2(3)	6.1(2)	4.0(2)	7.0(2)
C_1	13.9(3)	11.9(3)	14.0(3)	2.4(3)	1.6(3)	4.8(3)
C_2	16.7(4)	12.9(3)	15.2(3)	3.8(3)	3.7(3)	5.9(3)
C_8	13.8(3)	13.1(3)	16.4(3)	2.5(3)	2.2(3)	4.5(3)
C_{11}	15.8(3)	13.7(3)	13.1(3)	4.5(3)	3.8(3)	5.3(3)
C_{14}	18.3(4)	20.0(4)	18.9(4)	9.0(3)	5.4(3)	9.4(3)
C_{13A}	14.1(3)	19.1(4)	17.5(4)	6.4(3)	3.8(3)	5.3(3)
C_9	15.2(4)	17.9(4)	19.5(4)	4.5(3)	5.4(3)	5.5(3)
C_{12A}	15.1(3)	14.0(3)	14.7(3)	4.8(3)	5.0(3)	5.0(3)
C_7	14.2(3)	15.9(4)	20.7(4)	3.0(3)	0.8(3)	5.4(3)
C_{12}	18.0(4)	14.0(3)	14.2(3)	3.8(3)	3.4(3)	4.5(3)
C_6	17.5(4)	15.5(4)	19.0(4)	3.0(3)	-1.4(3)	6.9(3)
C_4	27.9(4)	16.9(4)	16.7(4)	6.5(3)	3.5(3)	8.4(3)
C_{13}	21.1(4)	15.1(4)	18.3(4)	6.9(3)	5.4(3)	7.4(3)
C_5	19.6(4)	12.7(3)	14.5(3)	2.7(3)	0.9(3)	6.1(3)
C_{10}	17.3(4)	18.3(4)	17.9(4)	6.4(3)	5.3(3)	5.7(3)
C_{16A}	18.4(4)	14.3(4)	21.9(4)	4.3(3)	4.2(3)	3.8(3)
C_3	31.2(5)	21.3(4)	21.8(4)	10.4(3)	10.5(4)	10.6(4)
C_{16}	23.3(4)	16.2(4)	22.7(4)	3.1(3)	-1.4(3)	1.9(3)
C_{15}	21.9(4)	29.1(5)	35.8(5)	17.2(4)	4.4(4)	13.0(4)
B_1	15.6(4)	13.8(4)	14.7(4)	3.7(3)	2.8(3)	4.9(3)

Table 12 Bond Lengths for ***BN*-PAH2**.

Atom	Atom	Length/Å	Atom	Atom	Length/Å
S_1	C_2	1.7358(9)	C_{14}	C_{13}	1.3929(13)
S_1	C_3	1.7322(10)	C_{14}	C_{15}	1.5076(13)
N_1	C_1	1.3822(10)	C_{13A}	C_{12A}	1.3957(11)
N_1	B_1	1.4273(12)	C_9	C_{10}	1.3608(12)
C_1	C_2	1.4079(12)	C_{12A}	C_{16A}	1.5121(12)
C_1	C_8	1.4078(12)	C_7	C_6	1.3718(13)
C_2	C_5	1.4048(11)	C_{12}	C_{13}	1.3978(12)
C_8	C_9	1.4375(12)	C_{12}	C_{16}	1.5102(13)
C_8	C_7	1.4201(12)	C_6	C_5	1.4141(13)
C_{11}	C_{12A}	1.4124(12)	C_4	C_5	1.4353(13)
C_{11}	C_{12}	1.4128(12)	C_4	C_3	1.3529(14)
C_{11}	B_1	1.5779(12)	C_{10}	B_1	1.5281(13)

Atom	Atom	Length/Å	Atom	Atom	Length/Å
C_{14}	C_{13A}	1.3939(13)			

Table 13 Bond Angles for ***BN*-PAH2**.

Atom	Atom	Atom	Angle/˚	Atom	Atom	Atom	Angle/˚
C_3	S_1	C_2	91.26(4)	C_{11}	C_{12A}	C_{16A}	121.42(7)
C_1	N_1	B_1	124.79(7)	C_{13A}	C_{12A}	C_{11}	120.04(8)
N_1	C_1	C_2	122.18(8)	C_{13A}	C_{12A}	C_{16A}	118.51(8)
N_1	C_1	C_8	119.54(8)	C_6	C_7	C_8	122.05(8)
C_8	C_1	C_2	118.28(7)	C_{11}	C_{12}	C_{16}	120.95(8)
C_1	C_2	S_1	126.71(6)	C_{13}	C_{12}	C_{11}	120.36(8)
C_5	C_2	S_1	111.40(6)	C_{13}	C_{12}	C_{16}	118.65(8)
C_5	C_2	C_1	121.88(8)	C_7	C_6	C_5	119.28(8)
C_1	C_8	C_9	119.21(7)	C_3	C_4	C_5	113.00(8)
C_1	C_8	C_7	119.32(8)	C_{14}	C_{13}	C_{12}	121.37(8)
C_7	C_8	C_9	121.46(8)	C_2	C_5	C_6	119.19(8)
C_{12A}	C_{11}	C_{12}	118.22(7)	C_2	C_5	C_4	111.48(8)
C_{12A}	C_{11}	B_1	120.93(7)	C_6	C_5	C_4	129.33(8)
C_{12}	C_{11}	B_1	120.84(8)	C_9	C_{10}	B_1	119.66(8)
C_{13A}	C_{14}	C_{15}	120.60(9)	C_4	C_3	S_1	112.86(7)
C_{13}	C_{14}	C_{13A}	118.19(8)	N_1	B_1	C_{11}	119.04(8)
C_{13}	C_{14}	C_{15}	121.21(9)	N_1	B_1	C_{10}	114.29(7)
C_{14}	C_{13A}	C_{12A}	121.79(8)	C_{10}	B_1	C_{11}	126.66(8)
C_{10}	C_9	C_8	122.48(8)				

Table 14 Torsion Angles for ***BN*-PAH2**.

A	B	C	D	Angle/˚	A	B	C	D	Angle/˚
S_1	C_2	C_5	C_6	-178.92(7)	C_{12A}	C_{11}	C_{12}	C_{13}	1.23(12)
S_1	C_2	C_5	C_4	0.41(10)	C_{12A}	C_{11}	C_{12}	C_{16}	179.17(8)
N_1	C_1	C_2	S_1	-0.84(13)	C_{12A}	C_{11}	B_1	N_1	-61.41(11)
N_1	C_1	C_2	C_5	179.96(8)	C_{12A}	C_{11}	B_1	C_{10}	118.32(10)
N_1	C_1	C_8	C_9	0.76(12)	C_7	C_8	C_9	C_{10}	179.94(8)
N_1	C_1	C_8	C_7	179.81(8)	C_7	C_6	C_5	C_2	-0.21(13)
C_1	N_1	B_1	C_{11}	178.14(8)	C_7	C_6	C_5	C_4	-179.41(9)
C_1	N_1	B_1	C_{10}	-1.62(13)	C_{12}	C_{11}	C_{12A}	C_{13A}	-1.26(12)
C_1	C_2	C_5	C_6	0.39(13)	C_{12}	C_{11}	C_{12A}	C_{16A}	176.63(8)
C_1	C_2	C_5	C_4	179.72(8)	C_{12}	C_{11}	B_1	N_1	119.23(9)
C_1	C_8	C_9	C_{10}	-1.04(14)	C_{12}	C_{11}	B_1	C_{10}	-61.04(12)
C_1	C_8	C_7	C_6	0.08(13)	C_{13}	C_{14}	C_{13A}	C_{12A}	1.05(13)
C_2	S_1	C_3	C_4	0.31(8)	C_5	C_4	C_3	S_1	-0.12(12)
C_2	C_1	C_8	C_9	-178.96(8)	C_3	S_1	C_2	C_1	-179.68(9)
C_2	C_1	C_8	C_7	0.09(12)	C_3	S_1	C_2	C_5	-0.41(7)
C_8	C_1	C_2	S_1	178.88(7)	C_3	C_4	C_5	C_2	-0.19(12)
C_8	C_1	C_2	C_5	-0.32(13)	C_3	C_4	C_5	C_6	179.06(9)
C_8	C_9	C_{10}	B_1	-0.04(14)	C_{16}	C_{12}	C_{13}	C_{14}	-178.05(8)
C_8	C_7	C_6	C_5	-0.02(14)	C_{15}	C_{14}	C_{13A}	C_{12A}	-178.76(9)
C_{11}	C_{12}	C_{13}	C_{14}	-0.07(13)	C_{15}	C_{14}	C_{13}	C_{12}	178.73(9)
C_{14}	C_{13A}	C_{12A}	C_{11}	0.12(13)	B_1	N_1	C_1	C_2	-179.65(8)
C_{14}	C_{13A}	C_{12A}	C_{16A}	-177.83(8)	B_1	N_1	C_1	C_8	0.64(13)
C_{13A}	C_{14}	C_{13}	C_{12}	-1.08(13)	B_1	C_{11}	C_{12A}	C_{13A}	179.36(8)
C_9	C_8	C_7	C_6	179.10(9)	B_1	C_{11}	C_{12A}	C_{16A}	-2.75(12)
C_9	C_{10}	B_1	N_1	1.29(13)	B_1	C_{11}	C_{12}	C_{13}	-179.39(8)
C_9	C_{10}	B_1	C_{11}	-178.45(9)	B_1	C_{11}	C_{12}	C_{16}	-1.45(13)

Table 15 Hydrogen Atom Coordinates (Å×10⁴) and Isotropic Displacement Parameters (Å²×10³) for ***BN*-PAH2**.

Atom	*x*	*y*	*z*	U(eq)
H_{13A}	1811.22	5687.32	386.1	19
H_9	11134.4	4798.4	2365.9	20
H_7	11781.84	3025.7	3756.31	20
H_6	11035.61	1608.75	5146.25	21
H_4	8466.78	763.25	6388.96	24
H_{13}	5007.14	10182.14	1315.6	20
H_{10}	9317.58	6213.37	1458.66	20
H_{16A}	4704.58	3216.55	866.81	27
H_{16B}	2694.4	3215.38	574.46	27
H_{16C}	3566.13	3348.83	1818.67	27
H_3	5628.24	1254.14	6534.99	27
H_{16D}	7916.72	9208.55	3124.06	32
H_{16E}	7704.55	10516.1	2304.55	32
H_{16F}	8681.94	9019.57	2008.76	32
H_{15A}	1109.83	8140.66	-364.19	40
H_{15B}	2328.62	9935.89	60.44	40
H_{15C}	1051.47	9140.56	813.39	40
H_1	5830(20)	4737(19)	3432(12)	30(4)

7.3. 1,13-Dihydro-2,12-dimesityl-1,13-diaza-2,12-diboradibenz[*a,j*]anthracene $CDCl_3$ adduct (***BN*-PAH4 · $CDCl_3$)**

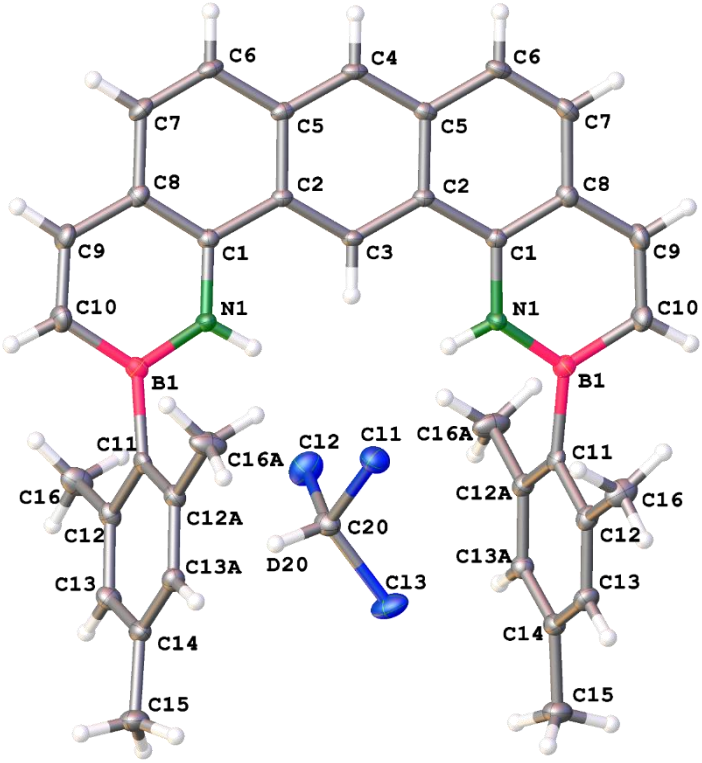

Single crystals of $C_{36}H_{34}B_2N_2 \cdot CDCl_3$ (***BN*-PAH4 · $CDCl_3$**) were grown by dissolving a small amount (ca. 10 mg) of the compound in $CDCl_3$ (ca. 450 µL) in an NMR tube. Solvents were allowed to evaporate slowly at 25 °C by leaving the capped vial for one month. CCDC Deposition Number: 1998254.

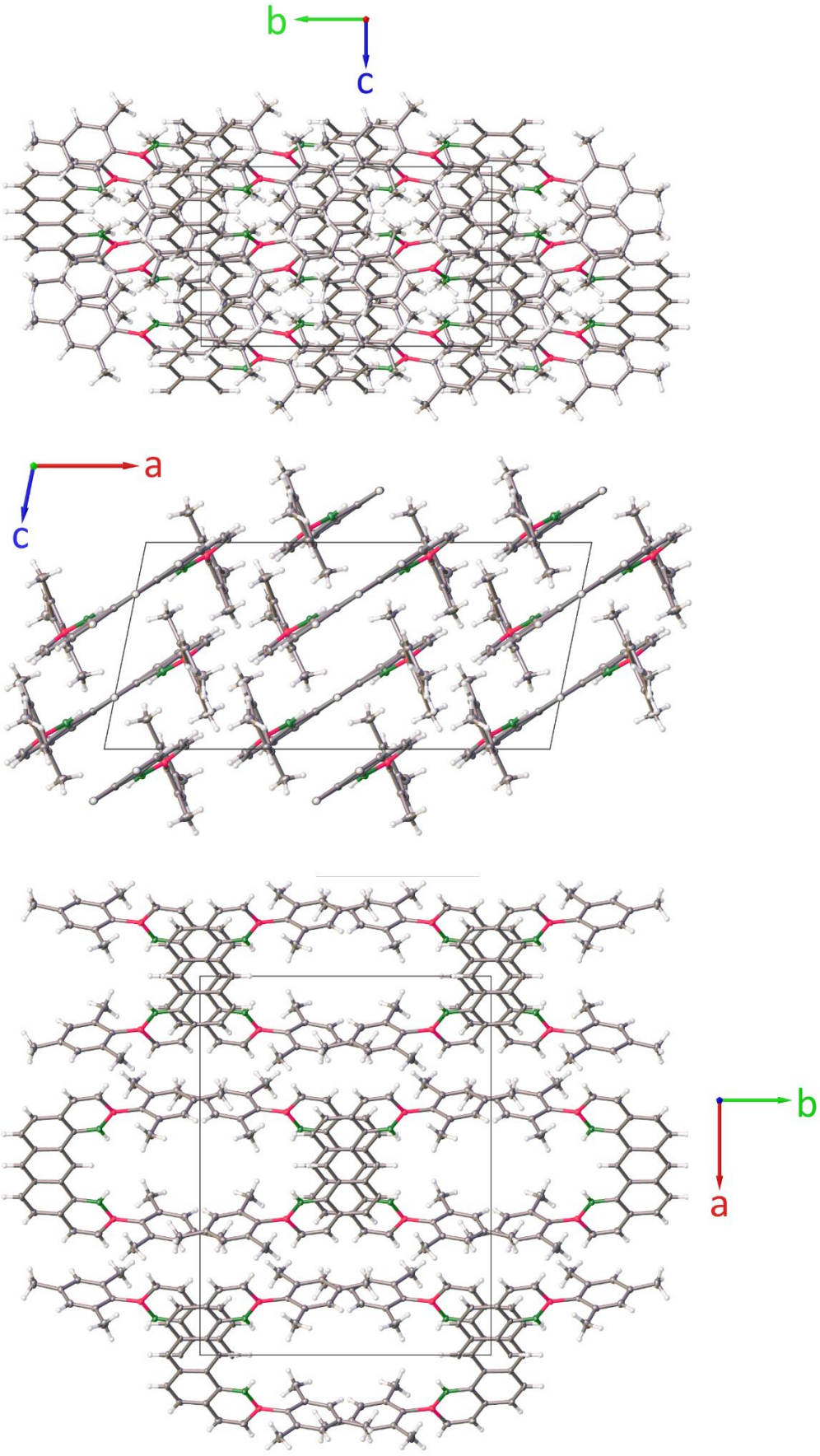

Fig. 41 Unit cell packing view of a ***BN*-PAH4 · $CDCl_3$** crystal along the *a, b* and *c*-axes. $CDCl_3$ molecules are omitted for clarity.

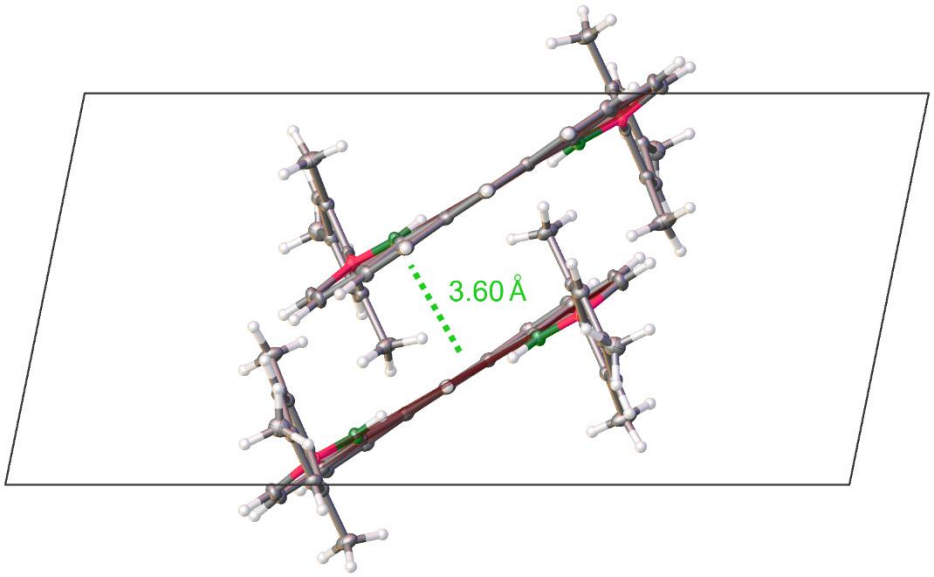

Fig. 42 Graphical representation of π-stacks and the regarding plane distance of ***BN*-PAH4 · CDCl$_3$**. $CDCl_3$ molecules are omitted for clarity.

Table 16 Crystal data and structure refinement for ***BN*-PAH4 · CDCl$_3$**.

Empirical formula	$C_{37}H_{34}B_2Cl_3DN_2$
Formula weight	636.64
Temperature/K	100.0
Crystal system	monoclinic
Space group	C2/c
a/Å	20.9278(6)
b/Å	15.7312(5)
c/Å	9.9126(3)
α/°	90
β/°	101.4570(10)
γ/°	90
Volume/Å^3	3198.39(17)
Z	4
ρ_{calc}g/cm^3	1.322
μ/mm^{-1}	0.317
F(000)	1328.0
Crystal size/mm^3	0.31 × 0.24 × 0.19
Radiation	MoKα (λ = 0.71073)
2Θ range for data collection/°	4.992 to 57
Index ranges	-28 ≤ h ≤ 28, -21 ≤ k ≤ 21, -13 ≤ l ≤ 13
Reflections collected	46636
Independent reflections	4056 [R_{int} = 0.0291, R_{sigma} = 0.0152]
Data/restraints/parameters	4056/0/225
Goodness-of-fit on F^2	1.029
Final R indexes [I>=2σ (I)]	R_1 = 0.0394, wR_2 = 0.1089
Final R indexes [all data]	R_1 = 0.0462, wR_2 = 0.1142
Largest diff. peak/hole / e Å^{-3}	0.41/-0.32

Table 17 Fractional Atomic Coordinates (×10^4) and Equivalent Isotropic Displacement Parameters (Å^2×10^3) for ***BN*-PAH4 · CDCl$_3$**. U_{eq} is defined as 1/3 of of the trace of the orthogonalized U_{IJ} tensor.

Atom	*x*	*y*	*z*	U(eq)
N_1	5964.5(5)	6538.8(6)	6251.0(10)	14.2(2)
C_1	5892.7(5)	5666.0(7)	6159.9(11)	13.0(2)
C_2	5431.4(5)	5231.5(7)	6827.8(11)	12.0(2)
C_3	5000	5660.2(10)	7500	12.5(3)
C_4	5000	3895.2(10)	7500	15.1(3)
C_5	5418.0(5)	4321.5(7)	6797.0(11)	13.6(2)
C_6	5833.1(6)	3871.8(7)	6054.5(12)	16.9(2)
C_7	6234.3(6)	4300.3(8)	5378.6(12)	17.5(2)
C_8	6279.5(5)	5209.3(7)	5420.4(12)	15.3(2)
C_9	6724.2(6)	5649.5(8)	4734.7(13)	19.1(2)
C_{10}	6807.5(6)	6506.6(8)	4808.2(13)	20.2(3)
C_{11}	6488.5(5)	8015.2(7)	5915.9(12)	14.1(2)
C_{12}	6233.1(6)	8601.8(8)	4875.3(12)	16.5(2)
C_{12A}	6860.7(6)	8330.9(8)	7150.7(12)	16.0(2)
C_{13}	6355.8(6)	9467.3(8)	5072.8(13)	18.9(2)
C_{13A}	6972.8(6)	9202.1(8)	7328.1(12)	16.3(2)
C_{14}	6728.8(6)	9779.7(7)	6294.5(13)	16.8(2)
C_{15}	6887.9(7)	10712.9(8)	6468.9(15)	24.6(3)
C_{16}	5817.0(7)	8291.1(9)	3545.8(14)	24.8(3)
C_{16A}	7169.4(8)	7737.4(9)	8287.6(14)	27.9(3)
B_1	6412.8(6)	7024.3(8)	5650.5(14)	15.4(3)
Cl_1	5507.1(6)	7953.9(8)	8821.8(15)	26.0(2)
Cl_2	4683.4(6)	8137.9(10)	6143.6(17)	31.9(3)
Cl_3	4847.0(3)	9541.2(4)	8068.8(8)	30.98(17)
C_{20}	5228.6(12)	8671.6(16)	7463(3)	19.8(5)
D_{20}	5610.09	8878.87	7087.33	24

Table 18 Anisotropic Displacement Parameters (Å²×10³) for ***BN*-PAH4 · CDCl₃**. The Anisotropic displacement factor exponent takes the form: $-2\pi^2[h^2a^{*2}U_{11}+2hka^*b^*U_{12}+\ldots]$.

Atom	U_{11}	U_{22}	U_{33}	U_{23}	U_{13}	U_{12}
N_1	14.8(4)	11.3(4)	17.7(5)	-1.3(4)	5.8(4)	-0.4(3)
C_1	12.8(5)	11.9(5)	13.7(5)	0.1(4)	1.6(4)	0.7(4)
C_2	12.6(5)	9.9(5)	12.9(5)	-0.2(4)	0.8(4)	0.2(4)
C_3	14.0(7)	8.5(6)	14.9(7)	0	2.7(6)	0
C_4	19.8(8)	8.5(7)	15.5(7)	0	0.0(6)	0
C_5	15.8(5)	11.0(5)	12.7(5)	-1.1(4)	-0.2(4)	1.7(4)
C_6	21.8(6)	11.1(5)	17.0(5)	-2.1(4)	1.8(4)	3.9(4)
C_7	18.1(5)	16.3(5)	18.0(6)	-3.8(4)	3.4(4)	5.1(4)
C_8	13.3(5)	16.1(6)	16.2(5)	-1.5(4)	2.6(4)	1.3(4)
C_9	15.9(5)	22.1(6)	21.0(6)	-3.4(5)	8.0(4)	1.3(4)
C_{10}	17.1(5)	22.5(6)	23.1(6)	-1.6(5)	9.0(5)	-3.0(5)
C_{11}	11.9(5)	15.6(5)	16.1(5)	1.1(4)	5.7(4)	-2.6(4)
C_{12}	14.1(5)	19.4(6)	15.7(5)	1.0(4)	2.6(4)	-2.5(4)
C_{12A}	15.7(5)	16.4(5)	16.1(5)	2.1(4)	3.9(4)	-0.5(4)
C_{13}	20.8(6)	17.5(6)	17.9(6)	4.2(4)	2.9(5)	1.0(4)
C_{13A}	16.2(5)	17.2(6)	15.5(5)	-1.3(4)	2.9(4)	-1.3(4)
C_{14}	16.9(5)	14.5(5)	20.1(6)	-0.1(4)	6.6(4)	0.1(4)
C_{15}	32.8(7)	14.6(6)	26.9(7)	-0.6(5)	7.0(5)	-0.1(5)
C_{16}	27.1(6)	24.8(6)	19.2(6)	1.3(5)	-3.7(5)	-5.8(5)
C_{16A}	38.2(8)	18.5(6)	21.6(6)	4.8(5)	-7.1(6)	-2.0(5)
B_1	14.0(6)	15.5(6)	16.4(6)	0.4(5)	2.5(5)	-2.1(4)
Cl_1	30.9(7)	21.6(5)	25.4(4)	4.3(3)	5.8(5)	1.4(4)
Cl_2	26.6(6)	35.8(7)	31.6(5)	-7.9(5)	1.7(5)	0.1(4)
Cl_3	25.8(3)	19.8(3)	46.7(4)	-6.7(3)	5.9(3)	6.0(2)
C_{20}	17.9(10)	17.5(11)	24.3(12)	2.2(9)	4.7(10)	0.8(8)

Table 19 Bond Lengths for ***BN*-PAH4 · CDCl₃**.

Atom	Atom	Length/Å	Atom	Atom	Length/Å
N_1	C_1	1.3822(14)	C_{11}	C_{12}	1.4080(16)
N_1	B_1	1.4281(16)	C_{11}	C_{12A}	1.4045(16)
C_1	C_2	1.4463(15)	C_{11}	B_1	1.5836(17)
C_1	C_8	1.3945(15)	C_{12}	C_{13}	1.3921(17)
C_2	C_3	1.3974(13)	C_{12}	C_{16}	1.5093(17)
C_2	C_5	1.4321(15)	C_{12A}	C_{13A}	1.3958(16)
C_4	C_5^1	1.3938(14)	C_{12A}	C_{16A}	1.5065(17)
C_4	C_5	1.3937(14)	C_{13}	C_{14}	1.3935(17)
C_5	C_6	1.4320(16)	C_{13A}	C_{14}	1.3886(17)
C_6	C_7	1.3533(18)	C_{14}	C_{15}	1.5077(17)
C_7	C_8	1.4332(16)	Cl_1	C_{20}	1.766(3)
C_8	C_9	1.4349(17)	Cl_2	C_{20}	1.767(3)
C_9	C_{10}	1.3596(18)	Cl_3	C_{20}	1.749(3)
C_{10}	B_1	1.5221(18)	C_{20}	D_{20}	1.0000

Table 20 Bond Angles for ***BN*-PAH4 · CDCl₃**.

Atom	Atom	Atom	Angle/°	Atom	Atom	Atom	Angle/°
C_1	N_1	B_1	125.16(10)	C_{12A}	C_{11}	B_1	120.84(10)
N_1	C_1	C_2	120.89(10)	C_{11}	C_{12}	C_{16}	119.78(11)
N_1	C_1	C_8	118.63(10)	C_{13}	C_{12}	C_{11}	120.36(11)
C_8	C_1	C_2	120.48(10)	C_{13}	C_{12}	C_{16}	119.85(11)
C_3	C_2	C_1	122.92(11)	C_{11}	C_{12A}	C_{16A}	120.93(11)
C_3	C_2	C_5	118.74(11)	C_{13A}	C_{12A}	C_{11}	120.48(11)
C_5	C_2	C_1	118.34(10)	C_{13A}	C_{12A}	C_{16A}	118.55(11)
C_2^1	C_3	C_2	122.29(14)	C_{12}	C_{13}	C_{14}	121.53(11)
C_5	C_4	C_5^1	122.49(15)	C_{14}	C_{13A}	C_{12A}	121.44(11)
C_2	C_5	C_6	119.56(10)	C_{13}	C_{14}	C_{15}	121.06(11)
C_4	C_5	C_2	118.81(11)	C_{13A}	C_{14}	C_{13}	118.09(11)
C_4	C_5	C_6	121.63(11)	C_{13A}	C_{14}	C_{15}	120.80(11)
C_7	C_6	C_5	120.52(11)	N_1	B_1	C_{10}	114.56(11)
C_6	C_7	C_8	121.77(11)	N_1	B_1	C_{11}	120.63(11)
C_1	C_8	C_7	119.16(11)	C_{10}	B_1	C_{11}	124.78(11)
C_1	C_8	C_9	119.95(11)	Cl_1	C_{20}	Cl_2	109.11(14)
C_7	C_8	C_9	120.88(11)	Cl_1	C_{20}	D_{20}	109.0
C_{10}	C_9	C_8	122.79(11)	Cl_2	C_{20}	D_{20}	109.0
C_9	C_{10}	B_1	118.83(11)	Cl_3	C_{20}	Cl_1	109.99(15)
C_{12}	C_{11}	B_1	120.84(11)	Cl_3	C_{20}	Cl_2	110.73(15)
C_{12A}	C_{11}	C_{12}	118.09(11)	Cl_3	C_{20}	D_{20}	109.0

Table 21 Torsion Angles for ***BN*-PAH4 · CDCl₃**.

A	B	C	D	Angle/°	A	B	C	D	Angle/°
N_1	C_1	C_2	C_3	5.24(16)	C_8	C_9	C_{10}	B_1	-0.09(19)
N_1	C_1	C_2	C_5	-174.73(10)	C_9	C_{10}	B_1	N_1	-2.29(18)
N_1	C_1	C_8	C_7	176.76(10)	C_9	C_{10}	B_1	C_{11}	175.74(12)
N_1	C_1	C_8	C_9	-2.12(16)	C_{11}	C_{12}	C_{13}	C_{14}	-0.27(19)
C_1	N_1	B_1	C_{10}	2.66(17)	C_{11}	C_{12A}	C_{13A}	C_{14}	-0.73(18)
C_1	N_1	B_1	C_{11}	-175.46(11)	C_{12}	C_{11}	C_{12A}	C_{13A}	-0.20(17)
C_1	C_2	C_3	C_2^1	-178.28(12)	C_{12}	C_{11}	C_{12A}	C_{16A}	-177.74(11)
C_1	C_2	C_5	C_4	176.60(8)	C_{12}	C_{11}	B_1	N_1	-106.47(13)
C_1	C_2	C_5	C_6	-3.16(16)	C_{12}	C_{11}	B_1	C_{10}	75.61(16)
C_1	C_8	C_9	C_{10}	2.42(19)	C_{12}	C_{13}	C_{14}	C_{13A}	-0.64(18)
C_2	C_1	C_8	C_7	-2.62(17)	C_{12}	C_{13}	C_{14}	C_{15}	176.76(12)
C_2	C_1	C_8	C_9	178.50(11)	C_{12A}	C_{11}	C_{12}	C_{13}	0.69(17)
C_2	C_5	C_6	C_7	-0.32(17)	C_{12A}	C_{11}	C_{12}	C_{16}	-178.53(11)
C_3	C_2	C_5	C_4	-3.37(14)	C_{12A}	C_{11}	B_1	N_1	79.17(15)
C_3	C_2	C_5	C_6	176.87(9)	C_{12A}	C_{11}	B_1	C_{10}	-98.75(15)
C_4	C_5	C_6	C_7	179.93(10)	C_{12A}	C_{13A}	C_{14}	C_{13}	1.13(18)
C_5	C_2	C_3	C_2^1	1.69(7)	C_{12A}	C_{13A}	C_{14}	C_{15}	-176.27(11)
C_5^1	C_4	C_5	C_2	1.70(7)	C_{16}	C_{12}	C_{13}	C_{14}	178.95(12)
C_5^1	C_4	C_5	C_6	-178.55(12)	C_{16A}	C_{12A}	C_{13A}	C_{14}	176.87(12)
C_5	C_6	C_7	C_8	2.47(18)	B_1	N_1	C_1	C_2	178.87(11)
C_6	C_7	C_8	C_1	-0.99(18)	B_1	N_1	C_1	C_8	-0.50(17)
C_6	C_7	C_8	C_9	177.87(11)	B_1	C_{11}	C_{12}	C_{13}	-173.83(11)

A	B	C	D	Angle/°	A	B	C	D	Angle/°
C_7	C_8	C_9	C_{10}	-176.44(12)	B_1	C_{11}	C_{12}	C_{16}	6.96(17)
C_8	C_1	C_2	C_3	-175.40(9)	B_1	C_{11}	C_{12A}	C_{13A}	174.31(11)
C_8	C_1	C_2	C_5	4.63(16)	B_1	C_{11}	C_{12A}	C_{16A}	-3.22(18)

Table 22 Hydrogen Atom Coordinates (Å×10^4) and Isotropic Displacement Parameters (Å^2×10^3) for ***BN*-PAH4 · $CDCl_3$**.

Atom	*x*	*y*	*z*	U(eq)
H_1	5710(8)	6809(11)	6751(18)	25(4)
H_3	4999.98	6264.05	7499.98	15
H_4	5000.01	3291.34	7500.03	18
H_6	5826.79	3268.08	6036.2	20
H_7	6492.84	3990.13	4862.56	21
H_9	6970.88	5328.46	4206.94	23
H_{10}	7106.83	6777.54	4342.11	24
H_{13}	6181.19	9853.89	4358.06	23
H_{13A}	7221.46	9404.45	8174.49	20
H_{15A}	6999.34	10851	7451.67	37
H_{15B}	6508.84	11048.85	6030.34	37
H_{15C}	7258.82	10845.55	6037.96	37
H_{16A}	6057.6	7861.44	3132.24	37
H_{16B}	5708.34	8769.84	2909.05	37
H_{16C}	5414.9	8040.18	3733.04	37
H_{16D}	6827.6	7437.39	8644.71	42
H_{16E}	7438.41	8065.05	9030.68	42
H_{16F}	7443.02	7323.82	7926.91	42

Table 23 Atomic Occupancy for ***BN*-PAH4 · $CDCl_3$**.

Atom	*Occupancy*	Atom	*Occupancy*	Atom	*Occupancy*
Cl_1	0.5	Cl_2	0.5	Cl_3	0.5
C_{20}	0.5	D_{20}	0.5		

7.4. 1,8-Dihydro-2,9-dimesityl-1,8-diaza-2,9-diboradibenz[*a,h*]anthracene (*BN*-PAH5)

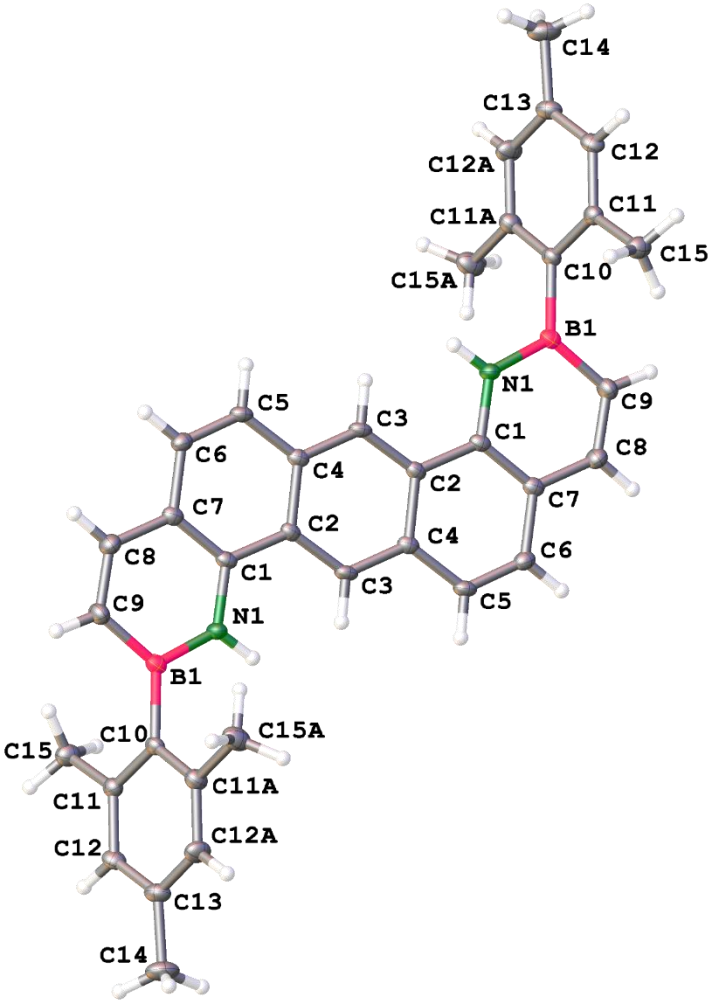

Single crystals of $C_{36}H_{34}B_2N_2$ (***BN*-PAH5**) were grown by dissolving a small amount (ca. 5 mg) of the compound in DCM (ca. 200 µL) in a snap cap sample vial. Methanol (ca. 1 mL) was cautiously added on top of the solution to prevent mixing. Solvents were allowed to evaporate slowly at 25 °C by leaving the vial open for 7 d. CCDC Deposition Number: 1998251.

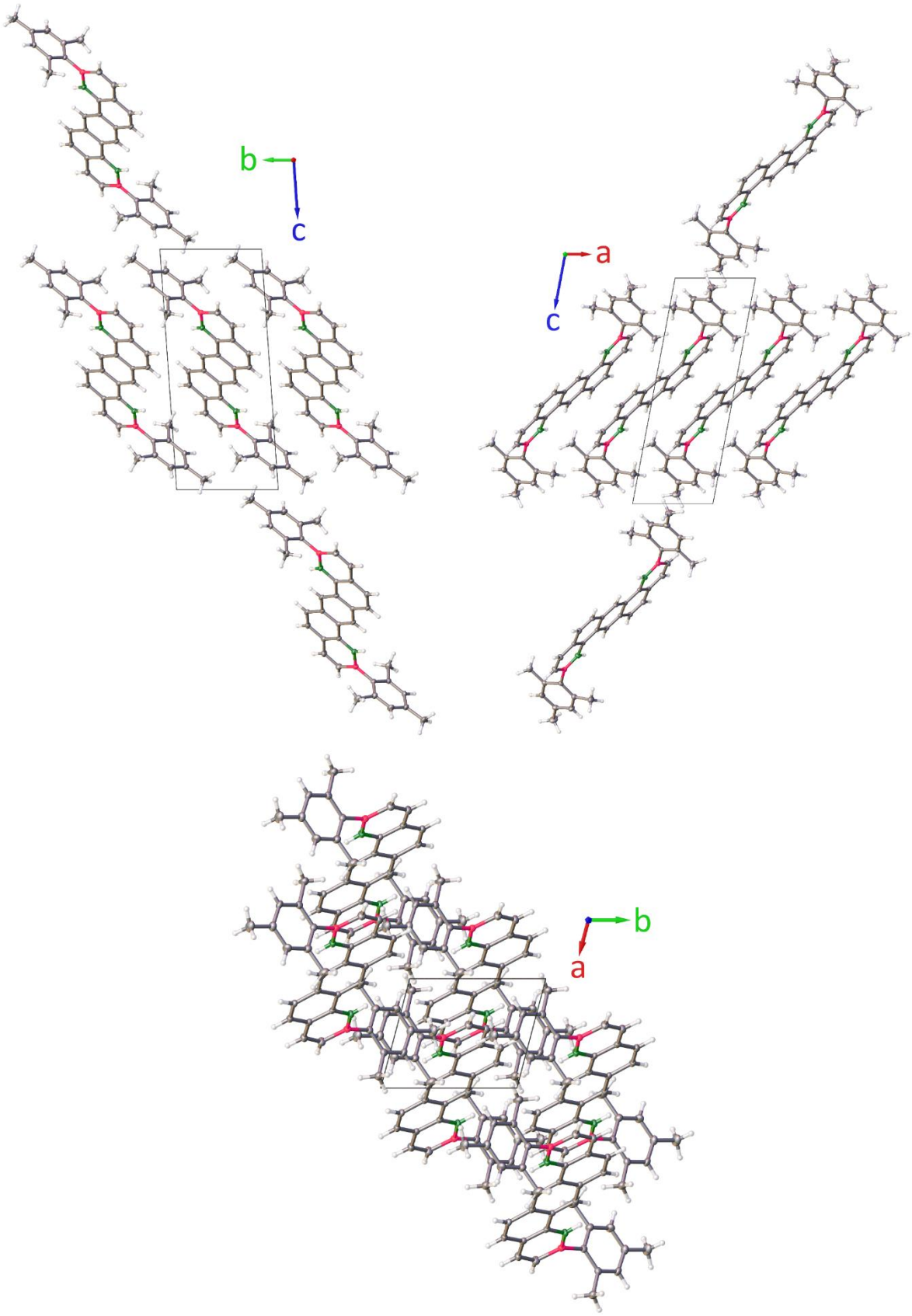

Fig. 43 Unit cell packing view of a ***BN*-PAH5** crystal along the *a, b* and *c*-axes.

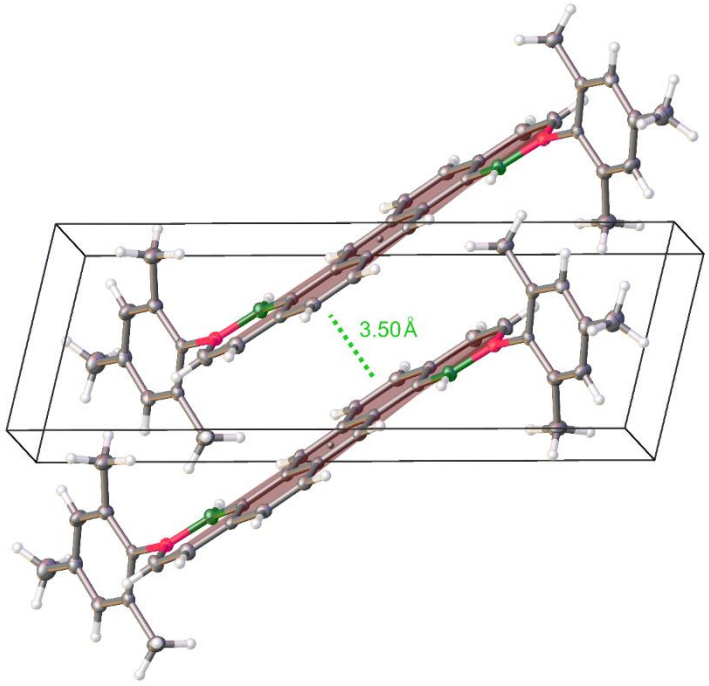

Fig. 44 Graphical representation of π-stacks and the regarding plane distance of ***BN*-PAH5**.

Table 24 Crystal data and structure refinement for ***BN*-PAH5**.

Empirical formula	$C_{36}H_{34}B_2N_2$
Formula weight	516.27
Temperature/K	100.0
Crystal system	triclinic
Space group	P-1
a/Å	6.0449(16)
b/Å	7.163(3)
c/Å	16.726(5)
α/°	91.335(15)
β/°	100.001(12)
γ/°	104.386(14)
Volume/Å^3	689.2(4)
Z	1
ρ_{calc}g/cm^3	1.244
μ/mm^{-1}	0.071
F(000)	274.0
Crystal size/mm^3	0.25 × 0.24 × 0.21
Radiation	MoKα (λ = 0.71073)
2Θ range for data collection/°	4.958 to 55.998
Index ranges	-7 ≤ h ≤ 7, -9 ≤ k ≤ 9, -22 ≤ l ≤ 22
Reflections collected	19599
Independent reflections	3325 [R_{int} = 0.0575, R_{sigma} = 0.0468]
Data/restraints/parameters	3325/0/188
Goodness-of-fit on F^2	1.029
Final R indexes [I>=2σ (I)]	R_1 = 0.0541, wR_2 = 0.1212
Final R indexes [all data]	R_1 = 0.0945, wR_2 = 0.1434
Largest diff. peak/hole / e Å^{-3}	0.26/-0.26

Table 25 Fractional Atomic Coordinates (×10^4) and Equivalent Isotropic Displacement Parameters (Å^2×10^3) for ***BN*-PAH5**. U_{eq} is defined as 1/3 of the trace of the orthogonalized U_{ij} tensor.

Atom	*x*	*y*	*z*	U(eq)
N_1	3242(3)	6357(2)	3265.6(8)	16.7(3)
C_1	2903(3)	4949(2)	3816.9(10)	15.2(4)
C_2	1445(3)	5018(2)	4409.7(10)	14.9(4)
C_3	319(3)	6479(2)	4478.0(10)	16.4(4)
C_4	-1115(3)	6503(2)	5045.8(10)	15.4(4)
C_5	2293(3)	1992(2)	4912.8(10)	17.0(4)
C_6	3657(3)	1982(2)	4355.9(10)	18.0(4)
C_7	3990(3)	3455(2)	3787.6(10)	16.1(4)
C_8	5400(3)	3389(3)	3189.6(11)	20.4(4)
C_9	5760(3)	4752(3)	2642.1(11)	21.0(4)
C_{10}	4695(3)	8051(2)	2028.3(10)	15.8(4)
C_{11}	6733(3)	9544(2)	2047.5(10)	17.0(4)
C_{11A}	2732(3)	8068(3)	1436.5(11)	20.5(4)
C_{12}	6757(3)	11002(2)	1508.6(10)	19.2(4)
C_{12A}	2796(3)	9586(3)	927.7(11)	23.8(4)
C_{13}	4781(3)	11080(3)	957.8(11)	22.0(4)
C_{14}	4771(4)	12739(3)	421.2(12)	31.6(5)
C_{15}	8904(3)	9627(3)	2668.8(11)	23.4(4)
C_{15A}	565(3)	6408(3)	1309.1(12)	28.3(5)
B_1	4600(3)	6402(3)	2644.3(12)	17.0(4)

Table 26 Anisotropic Displacement Parameters (Å²×10³) for ***BN*-PAH5**. The Anisotropic displacement factor exponent takes the form: $-2\pi^2[h^2a^{*2}U_{11}+2hka^*b^*U_{12}+...]$.

Atom	U_{11}	U_{22}	U_{33}	U_{23}	U_{13}	U_{12}
N_1	20.0(8)	14.9(7)	16.6(7)	4.7(6)	5.1(6)	5.6(6)
C_1	14.8(8)	14.6(8)	13.5(8)	2.6(6)	1.2(6)	-0.2(7)
C_2	13.1(8)	16.9(8)	12.6(8)	2.4(6)	1.3(6)	0.6(7)
C_3	17.7(9)	15.1(8)	14.2(8)	5.9(6)	0.9(7)	0.9(7)
C_4	15.0(8)	15.0(8)	13.4(8)	1.6(6)	0.3(6)	0.1(7)
C_5	18.5(9)	14.8(8)	15.9(8)	5.5(7)	1.4(7)	1.6(7)
C_6	17.5(9)	14.8(8)	21.0(9)	3.1(7)	1.6(7)	4.1(7)
C_7	15.0(8)	16.4(8)	14.5(8)	1.8(7)	0.7(7)	0.7(7)
C_8	22.6(10)	17.3(9)	23.3(9)	2.9(7)	5.8(7)	7.4(7)
C_9	23.6(10)	21.3(9)	21.0(9)	3.6(7)	10.0(7)	6.5(7)
C_{10}	18.7(9)	16.2(8)	14.1(8)	2.4(6)	6.2(7)	4.8(7)
C_{11}	19.2(9)	17.4(9)	15.7(8)	1.9(7)	5.2(7)	6.0(7)
C_{11A}	19.6(9)	20.9(9)	20.4(9)	4.0(7)	4.5(7)	3.0(7)
C_{12}	22.3(9)	13.6(8)	19.8(9)	1.6(7)	5.2(7)	0.2(7)
C_{12A}	21.4(10)	26.4(10)	20.9(9)	6.6(8)	-2.4(7)	5.1(8)
C_{13}	29.4(10)	18.7(9)	17.9(9)	4.9(7)	5.1(8)	5.6(8)
C_{14}	39.9(12)	25.0(11)	26.7(11)	11.6(8)	0.0(9)	5.8(9)
C_{15}	20.6(9)	22.7(9)	24.5(10)	4.4(7)	0.7(7)	3.5(7)
C_{15A}	22.4(10)	30.2(11)	27.2(10)	7.1(8)	1.8(8)	-1.2(8)
B_1	16.0(10)	18.1(10)	15.5(9)	2.4(7)	2.7(8)	1.7(8)

Table 27 Bond Lengths for ***BN*-PAH5**.

Atom	Atom	Length/Å	Atom	Atom	Length/Å
N_1	C_1	1.384(2)	C_9	B_1	1.517(3)
N_1	B_1	1.428(2)	C_{10}	C_{11}	1.412(2)
C_1	C_2	1.444(2)	C_{10}	C_{11A}	1.410(2)
C_1	C_7	1.392(2)	C_{10}	B_1	1.582(2)
C_2	C_3	1.395(2)	C_{11}	C_{12}	1.394(2)
C_2	C_4^1	1.435(2)	C_{11}	C_{15}	1.513(2)
C_3	C_4	1.395(2)	C_{11A}	C_{12A}	1.393(2)
C_4	C_5^1	1.438(2)	C_{11A}	C_{15A}	1.514(3)
C_5	C_6	1.348(2)	C_{12}	C_{13}	1.390(3)
C_6	C_7	1.436(2)	C_{12A}	C_{13}	1.388(3)
C_7	C_8	1.429(2)	C_{13}	C_{14}	1.506(2)
C_8	C_9	1.358(2)			

Table 28 Bond Angles for ***BN*-PAH5**.

Atom	Atom	Atom	Angle/°	Atom	Atom	Atom	Angle/°
C_1	N_1	B_1	125.40(15)	C_{11}	C_{10}	B_1	121.56(15)
N_1	C_1	C_2	120.86(15)	C_{11A}	C_{10}	C_{11}	117.72(15)
N_1	C_1	C_7	118.69(15)	C_{11A}	C_{10}	B_1	120.72(15)
C_7	C_1	C_2	120.45(15)	C_{10}	C_{11}	C_{15}	120.71(15)
C_3	C_2	C_1	123.53(15)	C_{12}	C_{11}	C_{10}	120.41(16)
C_3	C_2	C_4^1	118.02(15)	C_{12}	C_{11}	C_{15}	118.85(16)
C_4^1	C_2	C_1	118.44(15)	C_{10}	C_{11A}	C_{15A}	121.24(16)
C_4	C_3	C_2	122.71(15)	C_{12A}	C_{11A}	C_{10}	120.18(16)
C_2^1	C_4	C_5^1	119.45(15)	C_{12A}	C_{11A}	C_{15A}	118.51(16)
C_3	C_4	C_2^1	119.27(15)	C_{13}	C_{12}	C_{11}	121.77(16)
C_3	C_4	C_5^1	121.27(15)	C_{13}	C_{12A}	C_{11A}	122.15(17)
C_6	C_5	C_4^1	120.49(15)	C_{12}	C_{13}	C_{14}	121.48(17)
C_5	C_6	C_7	121.76(16)	C_{12A}	C_{13}	C_{12}	117.59(16)
C_1	C_7	C_6	119.38(15)	C_{12A}	C_{13}	C_{14}	120.92(17)
C_1	C_7	C_8	119.83(15)	N_1	B_1	C_9	113.84(16)
C_8	C_7	C_6	120.79(16)	N_1	B_1	C_{10}	119.17(16)
C_9	C_8	C_7	122.64(16)	C_9	B_1	C_{10}	126.96(16)
C_8	C_9	B_1	119.58(16)				

Table 29 Torsion Angles for ***BN*-PAH5**.

A	B	C	D	Angle/°	A	B	C	D	Angle/°
N_1	C_1	C_2	C_3	-0.8(2)	C_7	C_8	C_9	B_1	-1.2(3)
N_1	C_1	C_2	C_4	178.63(15)	C_8	C_9	B_1	N_1	1.6(2)
N_1	C_1	C_7	C_6	179.96(15)	C_8	C_9	B_1	C_{10}	-176.36(17)
N_1	C_1	C_7	C_8	-0.7(2)	C_{10}	C_{11}	C_{12}	C_{13}	2.3(3)
C_1	N_1	B_1	C_9	-1.7(2)	C_{10}	C_{11A}	C_{12A}	C_{13}	2.5(3)
C_1	N_1	B_1	C_{10}	176.45(15)	C_{11}	C_{10}	C_{11A}	C_{12A}	-3.9(3)
C_1	C_2	C_3	C_4	178.89(16)	C_{11}	C_{10}	C_{11A}	C_{15A}	173.01(16)
C_1	C_7	C_8	C_9	0.7(3)	C_{11}	C_{10}	B_1	N_1	110.02(19)
C_2	C_1	C_7	C_6	-0.3(2)	C_{11}	C_{10}	B_1	C_9	-72.1(2)
C_2	C_1	C_7	C_8	179.04(16)	C_{11}	C_{12}	C_{13}	C_{12A}	-3.7(3)
C_2	C_3	C_4	C_2	0.5(3)	C_{11}	C_{12}	C_{13}	C_{14}	175.35(17)
C_2	C_3	C_4	C_5	-178.53(16)	C_{11A}	C_{10}	C_{11}	C_{12}	1.6(2)
C_4	C_2	C_3	C_4	-0.5(3)	C_{11A}	C_{10}	C_{11}	C_{15}	179.65(16)
C_4	C_5	C_6	C_7	0.0(3)	C_{11A}	C_{10}	B_1	N_1	-70.3(2)
C_5	C_6	C_7	C_1	0.9(2)	C_{11A}	C_{10}	B_1	C_9	107.6(2)
C_5	C_6	C_7	C_8	-178.48(17)	C_{11A}	C_{12A}	C_{13}	C_{12}	1.3(3)
C_6	C_7	C_8	C_9	-179.92(17)	C_{11A}	C_{12A}	C_{13}	C_{14}	-177.76(18)
C_7	C_1	C_2	C_3	179.48(16)	C_{15}	C_{11}	C_{12}	C_{13}	-175.84(17)
C_7	C_1	C_2	C_4	-1.1(2)	C_{15A}	C_{11A}	C_{12A}	C_{13}	-174.45(18)
B_1	N_1	C_1	C_2	-178.45(16)	B_1	C_{10}	C_{11}	C_{15}	-0.6(2)
B_1	N_1	C_1	C_7	1.3(2)	B_1	C_{10}	C_{11A}	C_{12A}	176.37(17)
B_1	C_{10}	C_{11}	C_{12}	-178.70(16)	B_1	C_{10}	C_{11A}	C_{15A}	-6.7(3)

Table 30 Hydrogen Atom Coordinates (Å×10⁴) and Isotropic Displacement Parameters (Å²×10³) for ***BN*-PAH5**.

Atom	*x*	*y*	*z*	U(eq)
H_3	537.29	7498.46	4123.3	20
H_5	2108.8	998.57	5280.6	20
H_6	4418.96	974.7	4338.73	22
H_8	6112.68	2350.11	3174.33	25
H_9	6733.55	4673.37	2260.3	25
H_{12}	8162.04	11967.09	1517.9	23
H_{12A}	1435.33	9598.59	547.73	29

Atom	*x*	*y*	*z*	U(eq)
H_{14A}	4153.21	13697.11	675.5	47
H_{14B}	3791.48	12259.14	-110.22	47
H_{14C}	6360.53	13338.79	349.06	47
H_{15A}	8791.16	10242.45	3184.43	35
H_{15B}	10265.63	10378.41	2470.67	35
H_{15C}	9059.57	8312.89	2753.74	35
H_{15D}	495.06	5614.35	815.51	42
H_{15E}	-811.15	6918.59	1250.9	42
H_{15F}	609.12	5615.26	1778.59	42
H_{1}	2500(40)	7290(30)	3296(12)	24(5)

8. Hirshfeld Surface Analyses

Using the obtained single crystal data, we mapped the electrostatic potentials of the *BN*-PAHs on Hirshfeld surfaces, using the program Crystal Explorer 17.5.[17] Based on that, the respective two-dimensional fingerprint plots were generated,[18] displaying the quantified, individual close contacts of atoms of each element to the neighboring atoms. In the depicted images below, all interactions contributing less than 0.3% except the *BN* interactions were excluded. The fingerprint plots revealed a general non-participation of the *BN* units in intermolecular interactions. Consequently, the highest shares are contributed by interactions between the planar PAH scaffolds, which can be classified as dispersive C*H* ⋯ π-interactions and π-stacking. In ***BN*-PAH2**, the *NH* moieties of the azaborinine units displayed hydrogen bond interactions to the sulfur atoms in the thiophene units of neighboring molecules. As it can be seen from the unit cell packing view (Fig. 39 and 40), this explains why ***BN*-PAH2** forms parallel stacks and not a herringbone pattern like ***BN*-PAH1**. The Hirshfeld surfaces also clarify why ***BN*-PAH4** crystallized with a molecule of $CDCl_3$. Especially the two protons of the *NH* moieties that direct inside the molecule's cavity form interactions to the chlorine atoms of the $CDCl_3$. Furthermore, the aromatic planes of the mesityl groups are in close contact with the deuterium atom, exhibiting C*D* ⋯ π-interactions.

4-Hydro-3-mesityl-4,3-azaboraphenanthrene (*BN*-PAH1)

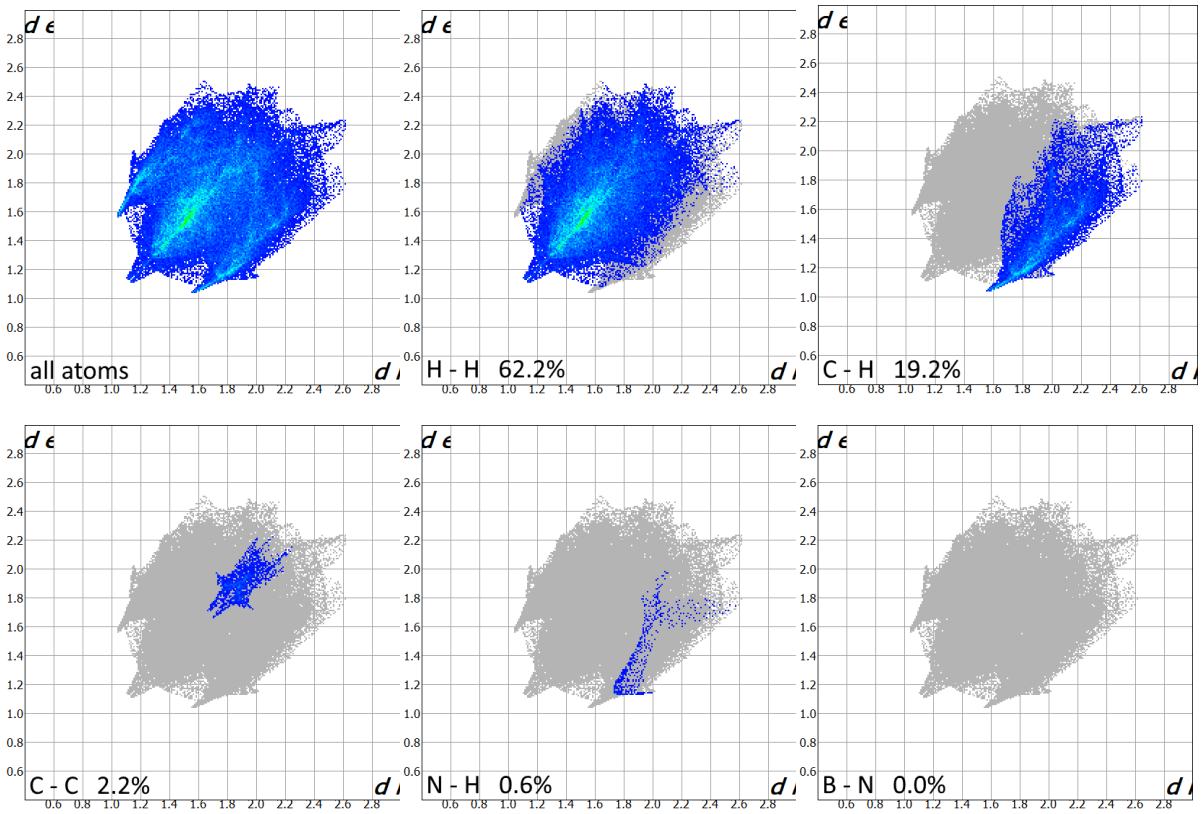

9-Hydro-8-mesityl-9,8-azaboranaphtho[1,2-*b*]thiophene (*BN*-PAH2)

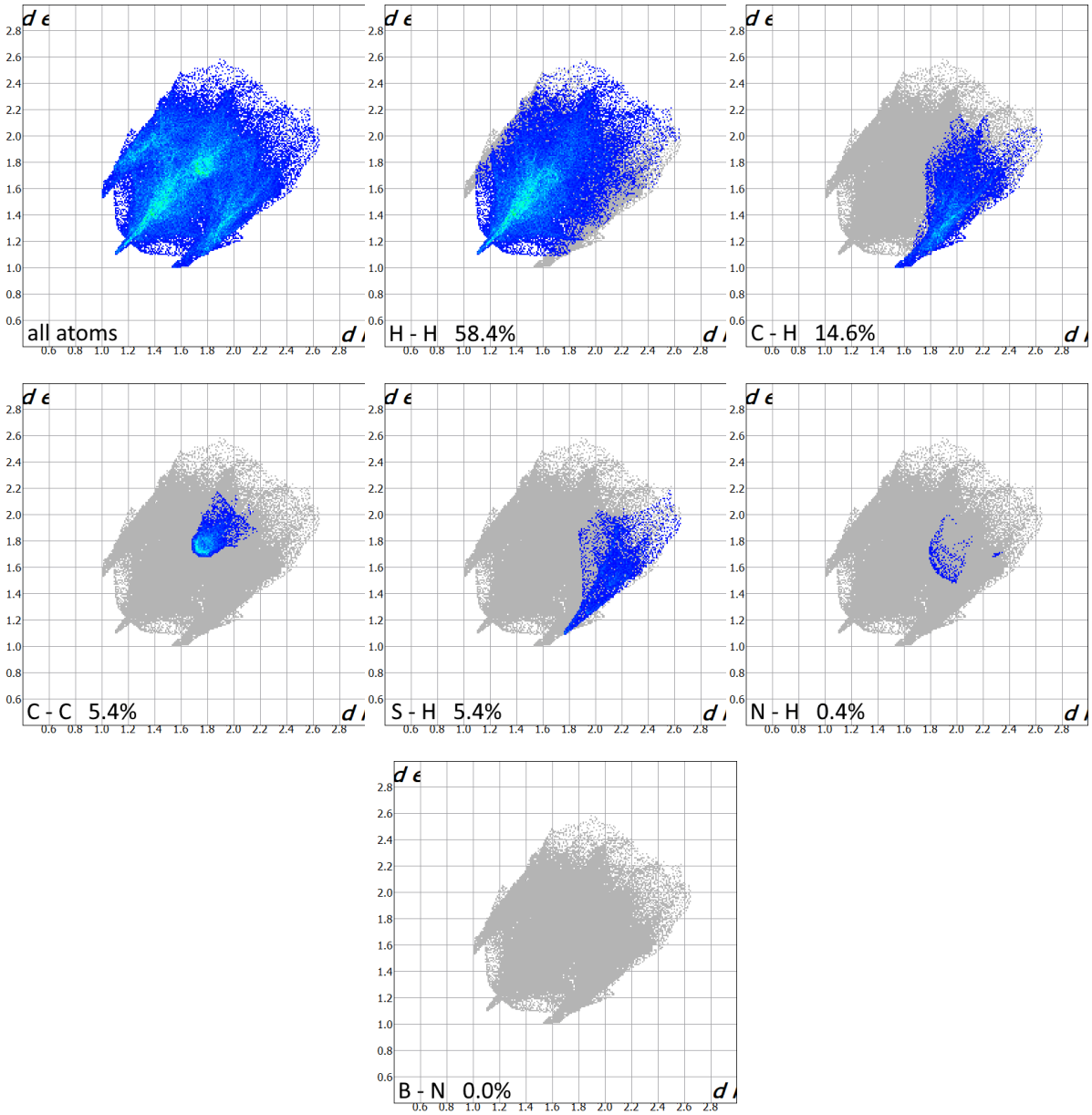

1,13-Dihydro-2,12-dimesityl-1,13-diaza-2,12-diboradibenz[*a,j*]anthracene $CDCl_3$ adduct (*BN*-PAH4 · $CDCl_3$)

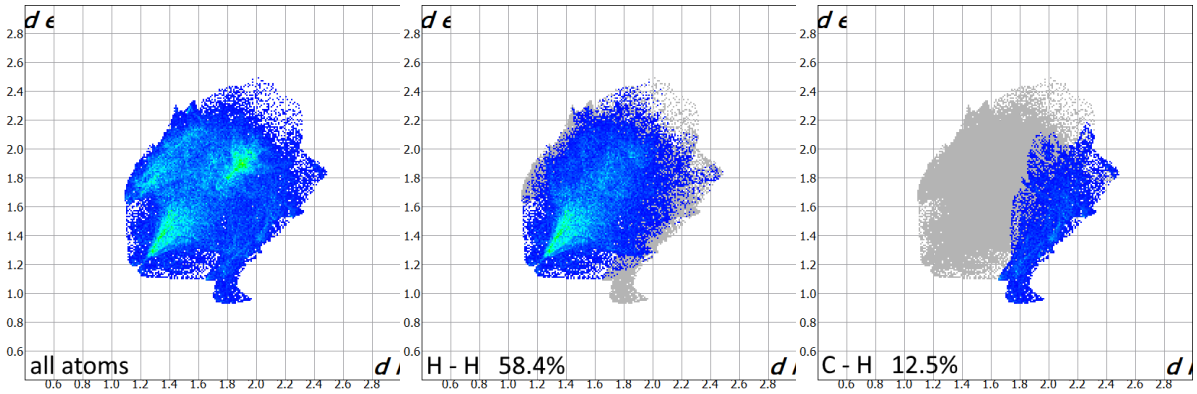

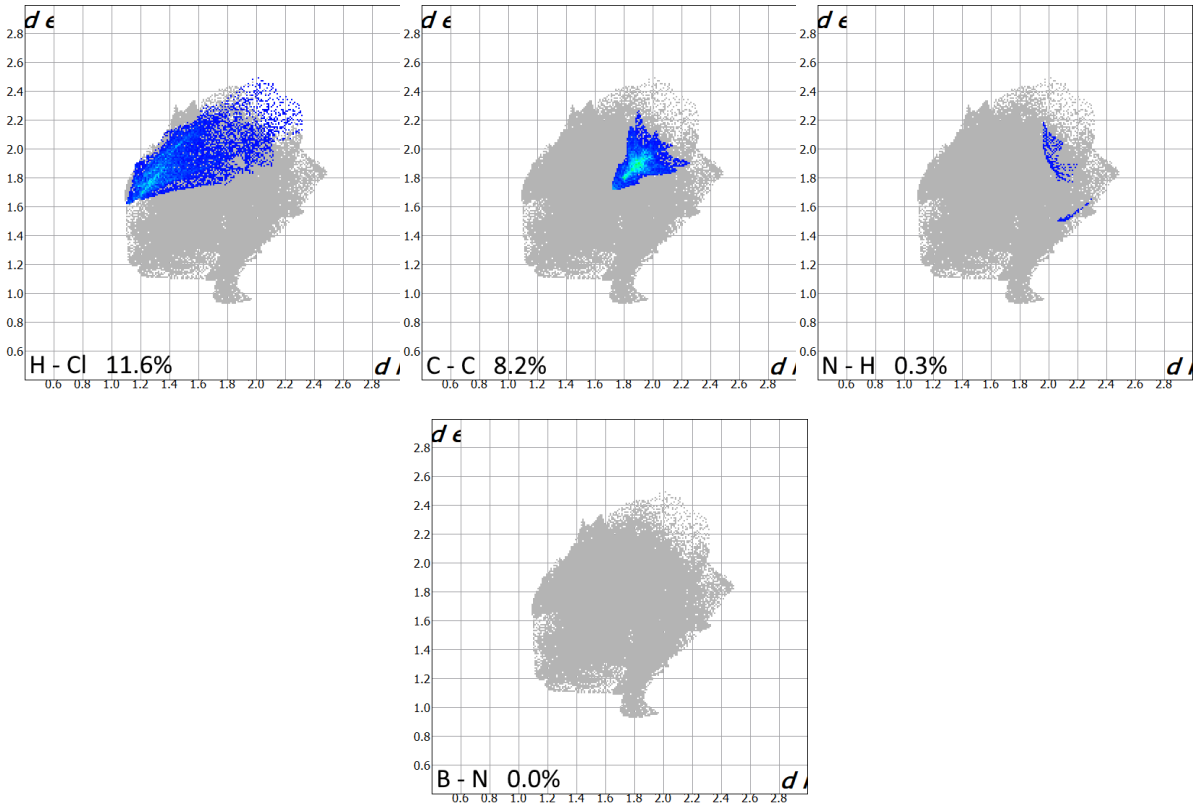

1,8-Dihydro-2,9-dimesityl-1,8-diaza-2,9-diboradibenz[*a,h*]anthracene (*BN*-PAH5)

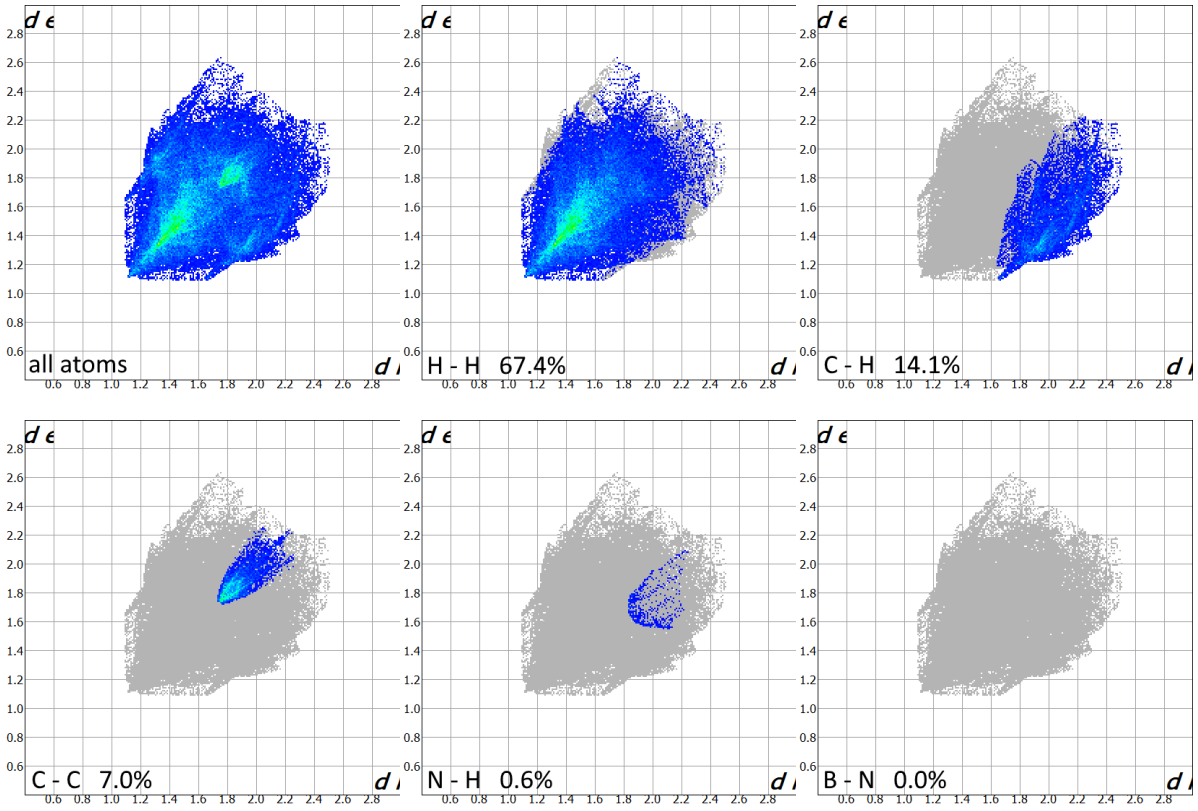

9. Calculations

9.1. Luminescence

The luminescence wavelengths of ***BN*-PAH1-6** were calculated with Orca 4.2.0.[19] The structures were pre-optimized using a universal force field method (UFF).[20] Ground state geometry optimizations were carried out with Density Functional Theory (DFT)[21,22] at the B3LYP[23-25] / cc-pVDZ[26] level of theory using the RIJCOSX[27,28] approximation. The absence of imaginary frequencies confirmed that the obtained geometries were indeed energetic minima. Geometry optimizations in the first electronically excited singlet state (S_1) were performed with time-dependent DFT (TD-DFT)[29] at the same level of theory as in the electronic ground state. Again, the absence of imaginary frequencies was assured, except for ***BN*-PAH6,** in which a low imaginary frequency of –13.6 cm^{-1} hinted towards numerical inaccuracy of the method in the S_1 state. Fluorescence wavelengths were determined at the minimum energy geometry of the S_1 state and are displayed in Fig. 45 – 50. In the case of ***BN*-PAH5**, an excited state dynamics (ESD)[30] calculation for the fluorescence spectra was additionally carried out (Fig. 51). The dipole moments obtained from the geometry optimizations of S_0 and S_1 and displayed in Table 31.

Table 31 Dipole moments of ***BN*-PAH1-6** in the ground singlet state (S_0) and the first electronically excited singlet state (S_1).

Compound	Dipole moment in S_0 [D]	Dipole moment in S_1 [D]
***BN*-PAH1**	1.51	2.24
***BN*-PAH2**	1.83	2.65
***BN*-PAH3**	2.77	3.68
***BN*-PAH4**	1.30	1.07
***BN*-PAH5**	0.02	0.09
***BN*-PAH6**	0.34	0.33

As it becomes evident, the dipole moments of small ***BN*-PAH1-3** are significantly higher than of larger ***BN*-PAH4-6**, which can be explained by a higher symmetry of the large PAHs (especially ***BN*-PAH5**). Moreover, the dipole moments of the small PAHs considerably increase upon excitation into S_1. On the other hand, the large PAHs in the excited state were not significantly more polar than in the electronic ground state, ***BN*-PAH4** was calculated to be even less polar in S_1 than in S_0.

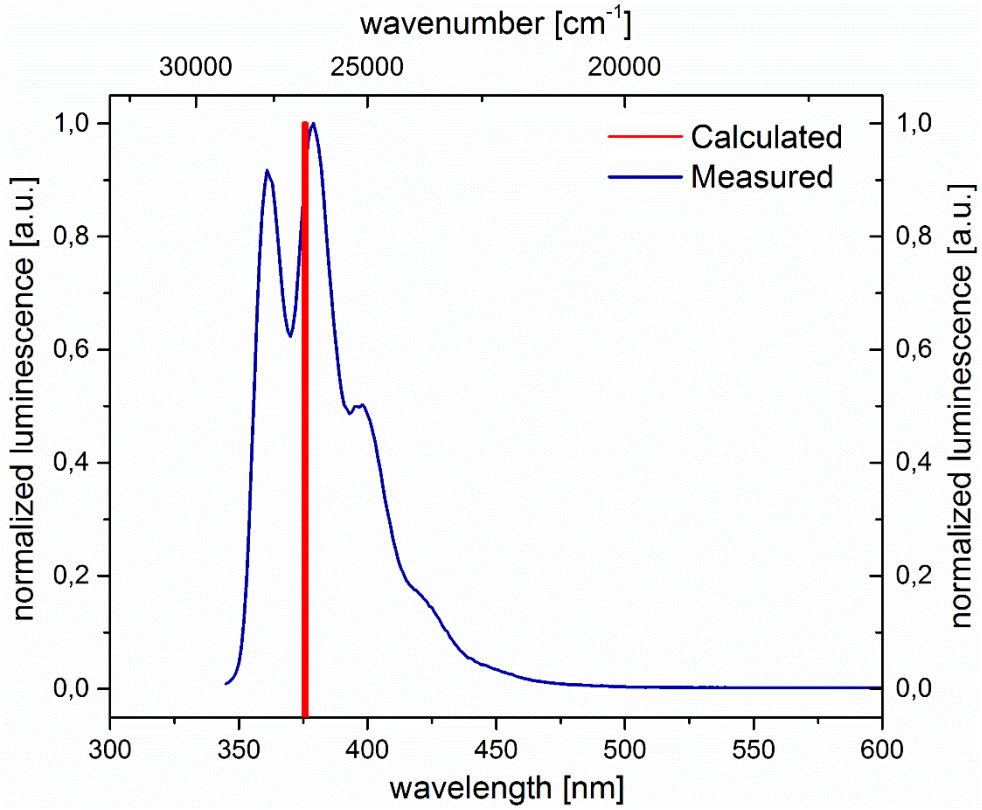

Fig. 45 Measured fluorescence spectrum (blue) and calculated fluorescence wavelength (red) of ***BN*-PAH1**. The calculated wavelength (λ = 375.7 nm) is 3.3 nm lower than the measured wavelength at the intensity maximum (λ_{max} = 379 nm).

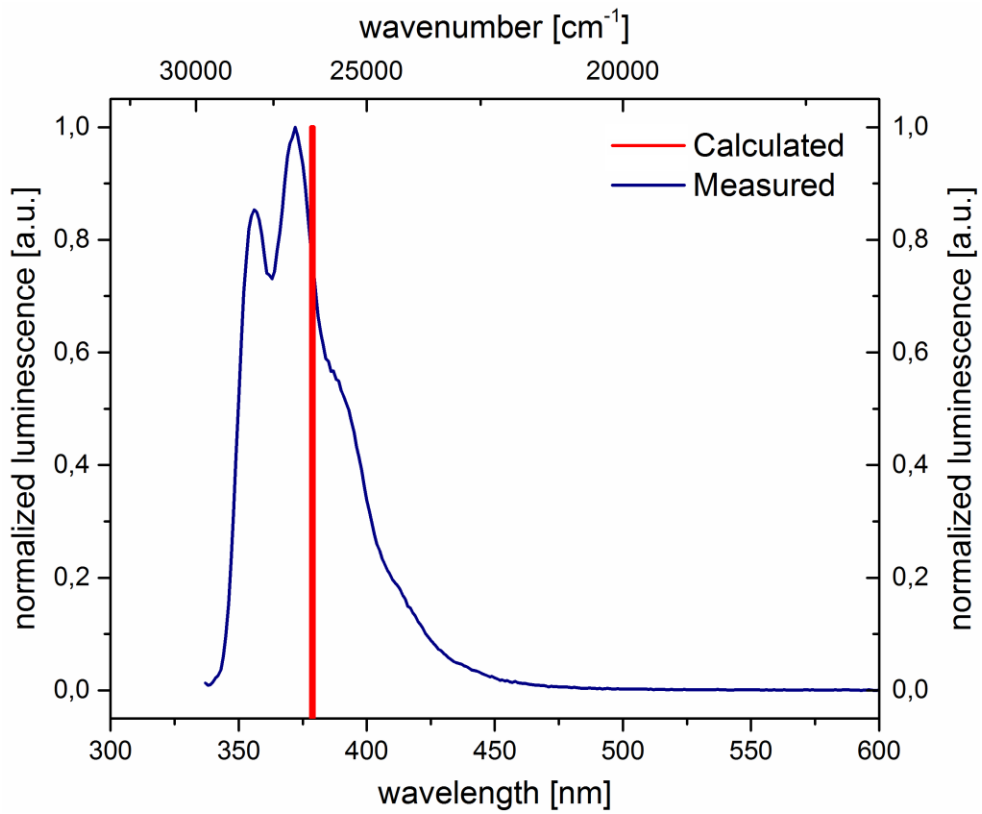

Fig. 46 Measured fluorescence spectrum (blue) and calculated fluorescence wavelength (red) of ***BN*-PAH2**. The calculated wavelength (λ = 378.8 nm) is 6.8 nm higher than the measured wavelength at the intensity maximum (λ_{max} = 372 nm).

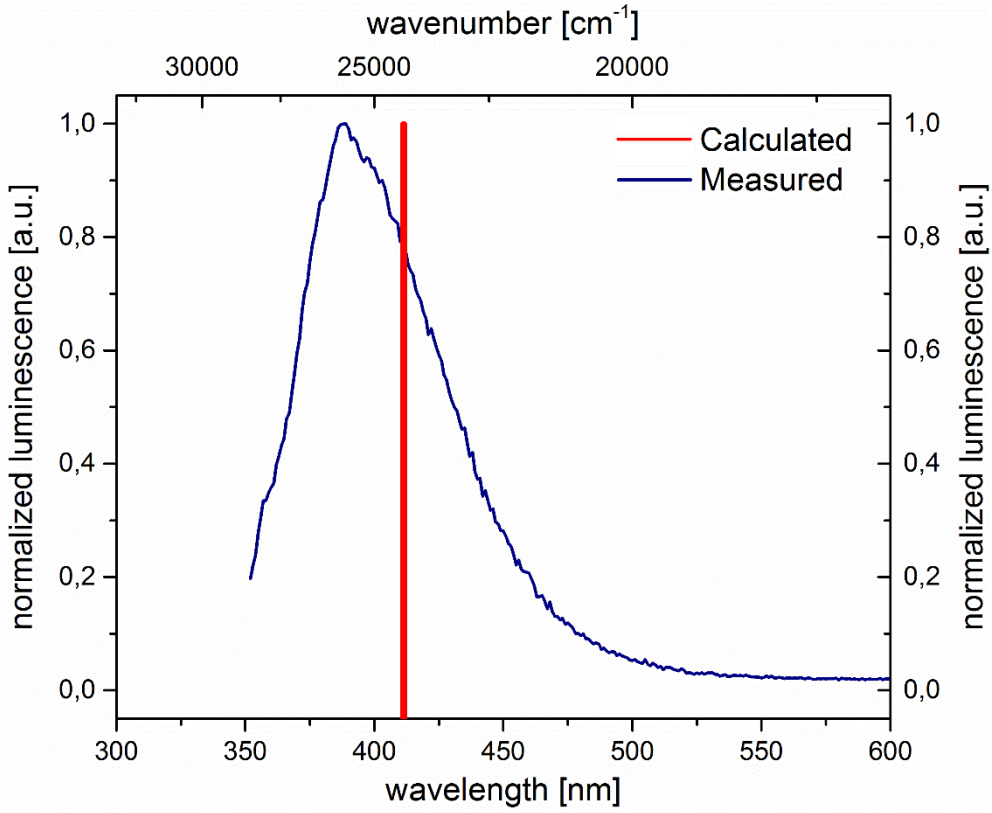

Fig. 47 Measured fluorescence spectrum (blue) and calculated fluorescence wavelength (red) of ***BN*-PAH3**. The calculated wavelength (λ = 411.4 nm) is 22.4 nm higher than the measured wavelength at the intensity maximum (λ_{max} = 389 nm).

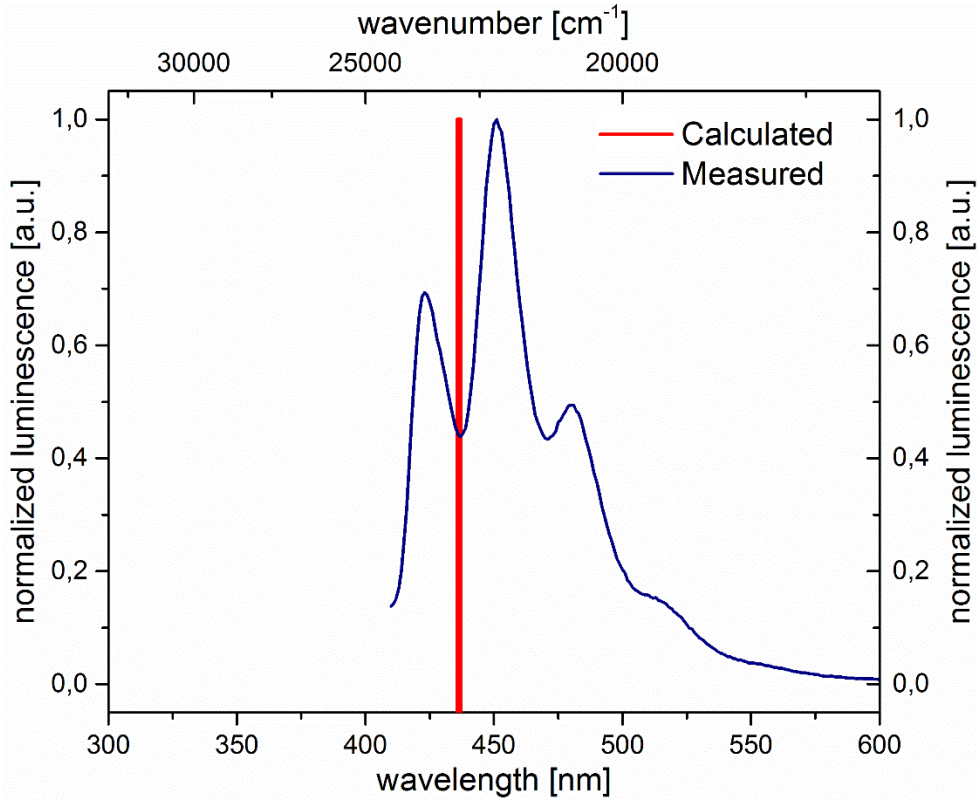

Fig. 48 Measured fluorescence spectrum (blue) and calculated fluorescence wavelength (red) of ***BN*-PAH4**. The calculated wavelength (λ = 436.4 nm) is 14.6 nm lower than the measured wavelength at the intensity maximum (λ_{max} = 451 nm).

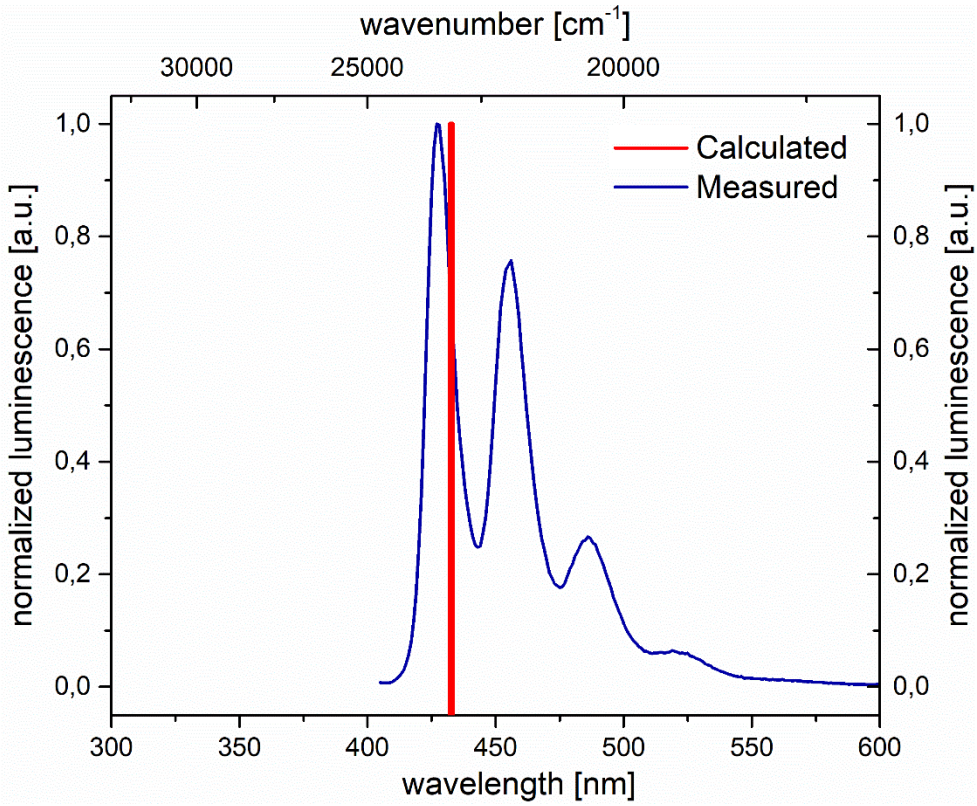

Fig. 49 Measured fluorescence spectrum (blue) and calculated fluorescence wavelength (red) of ***BN*-PAH5**. The calculated wavelength (λ = 432.7 nm) is 5.7 nm higher than the measured wavelength at the intensity maximum (λ_{max} = 427 nm).

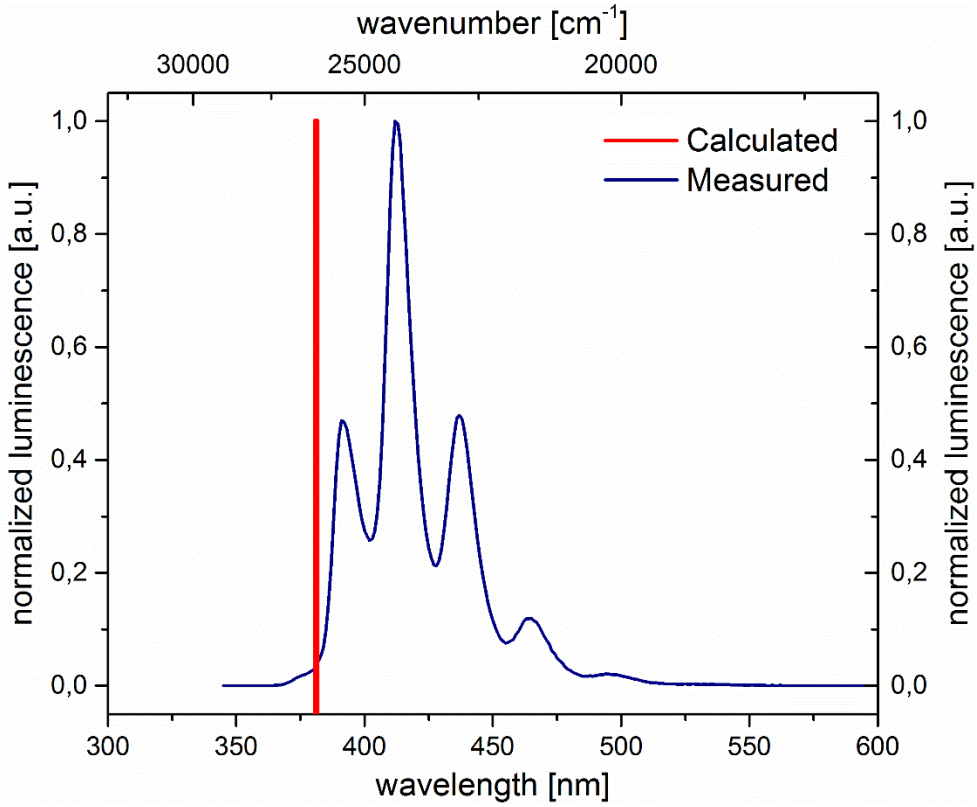

Fig. 50 Measured fluorescence spectrum (blue) and calculated fluorescence wavelength (red) of ***BN*-PAH6**. The calculated wavelength (λ = 381.1 nm) is 30.9 nm lower than the measured wavelength at the intensity maximum (λ_{max} = 412 nm).

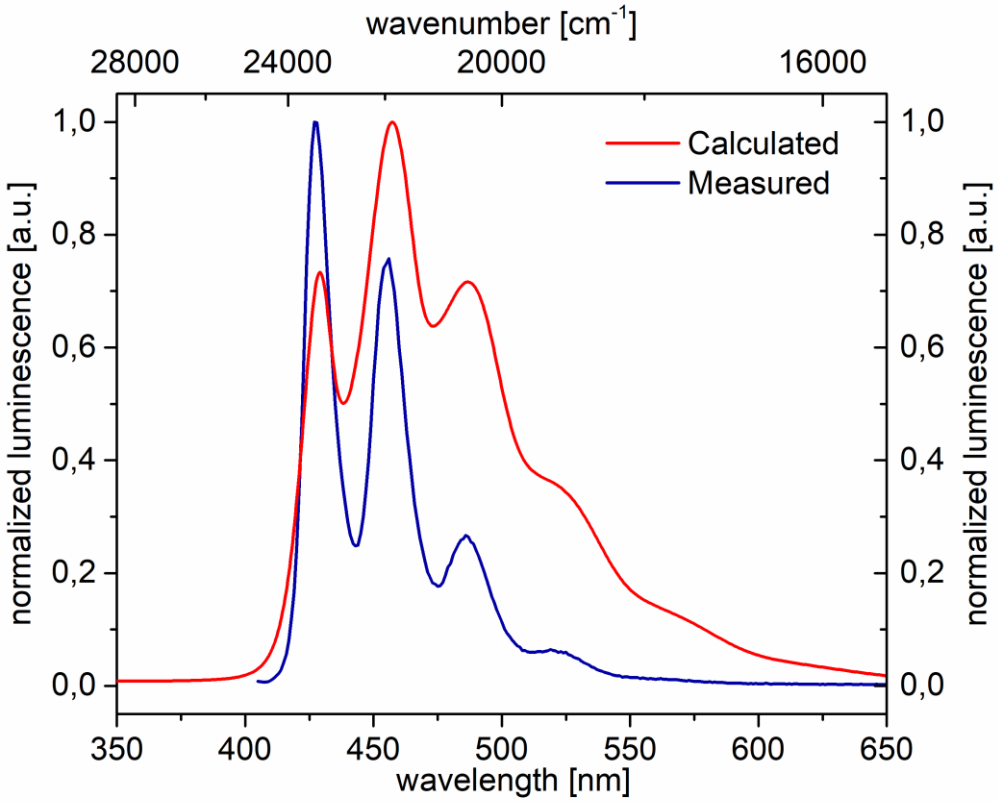

Fig. 51 Measured fluorescence spectrum (blue) and calculated fluorescence spectrum (red) of ***BN*-PAH5**. The calculated maxima (λ_{max} = 429 nm, 457 nm and 487 nm) correspond to the experimentally obtained intensity maxima (λ_{max} = 427 nm, 456 nm and 486 nm) despite a distinct broadening of the curve in the region above 500 nm.

9.2. Natural Transition Orbitals

To describe the nature of the S_1 state, out of which fluorescence takes place, we plotted the highest occupied (HONTOs) and the lowest unoccupied (LUNTOs) Natural Transition Orbitals, which were the main contributors to the S_1 states in all cases. The given percentages describe the share to which the displayed NTOs contribute to the transition (Fig. 52).

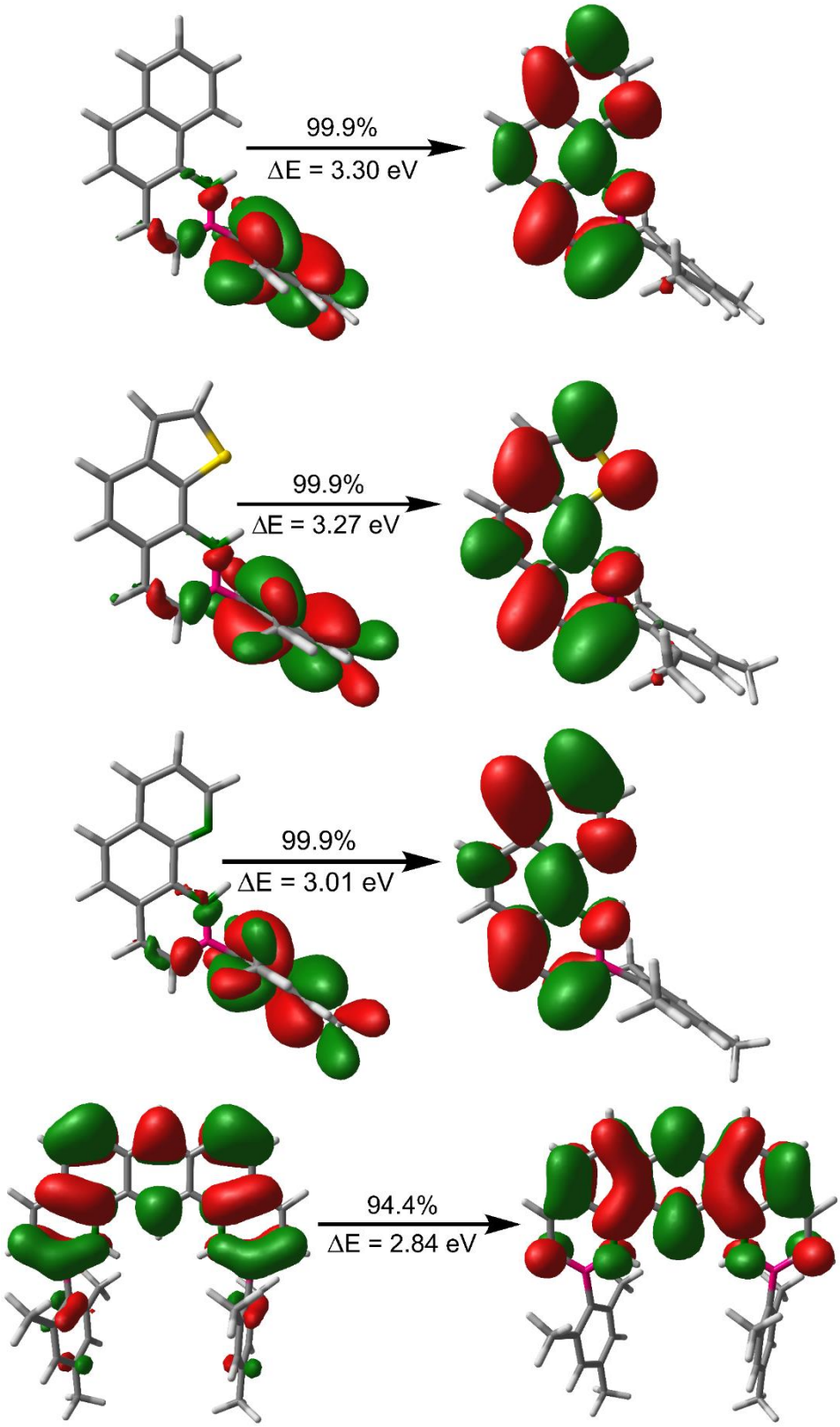

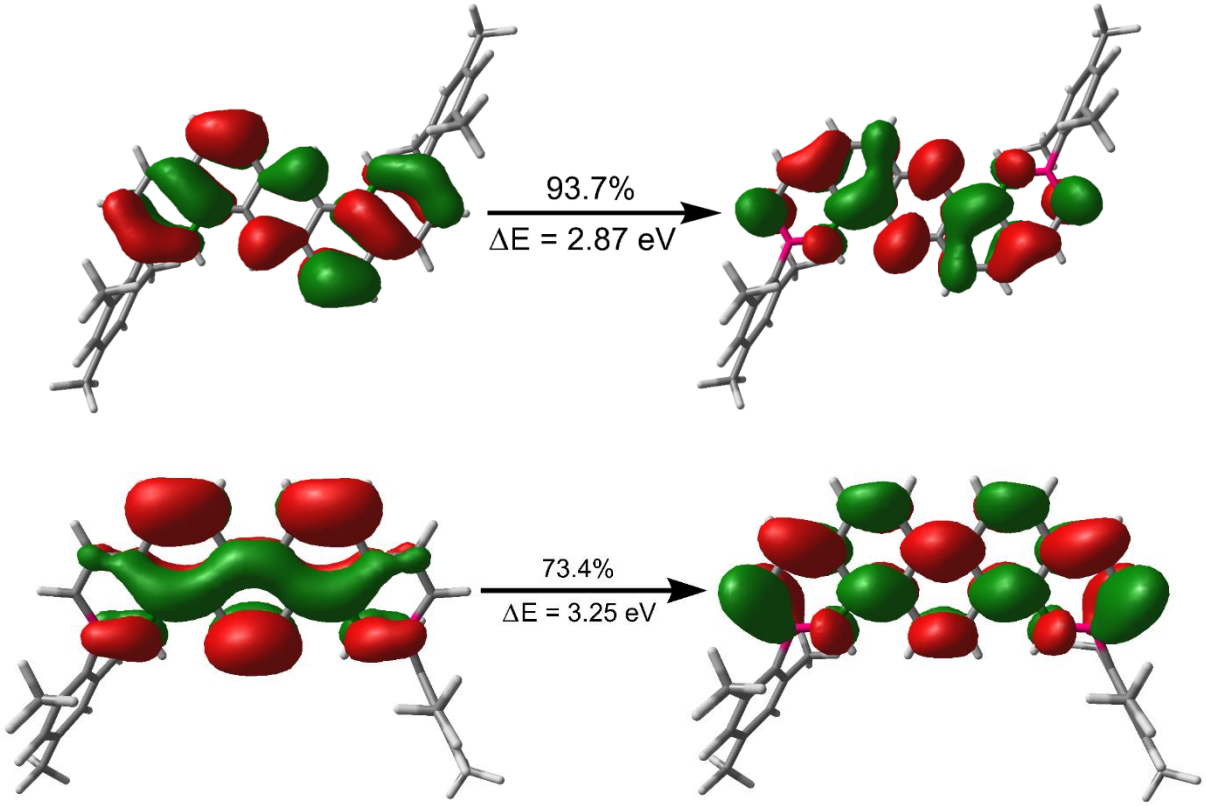

Fig. 52 NTO analysis of ***BN*-PAH1-6**.

The shapes of the NTOs for small ***BN*-PAH1-3** are very similar. Only minor fractions of the HONTOs are placed on the PAH scaffolds without involvement of the boron atoms, while most of the electron density is placed on the mesityl units. The mesityl units are not involved in the LUNTOs. This implies that, at the chosen level of theory, the occurring transition has a significant charge-transfer character, taking place between the mesityl-groups (donor) and the PAH scaffolds (acceptor). Despite the well-known problems of TD-DFT when treating charge-transfer states,[31] the focus in the present study is the reproduction of the fluorescence wavelengths, which the chosen level of theory achieves remarkably well (see Fig. 45 - 50).

In large ***BN*-PAH4-6**, the HONTO and the LUNTO spread over the whole PAH backbones, while the mesityl groups are not involved. This implies that the observed transitions are local π-π* transitions. In all cases except ***BN*-PAH6**, the HONTO → LUNTO transitions contribute to the S_1 state by more than 90%. In ***BN*-PAH6**, a significant contribution of the HONTO-1 → LUNTO+1 transition was found.

Detailed contributions to the S_1 states:

***BN*-PAH1:** 99.9% (HONTO → LUNTO).

***BN*-PAH2:** 99.9% (HONTO → LUNTO).

***BN*-PAH3:** 99.9% (HONTO → LUNTO).

***BN*-PAH4:** 94.4% (HONTO → LUNTO) + 3.1% (HONTO-1 → LUNTO+1) + 0.8% (HONTO-2 → LUNTO+2)

***BN*-PAH5:** 93.7% (HONTO → LUNTO) + 3.7% (HONTO-1 → LUNTO+1) + 0.7% (HONTO-2 → LUNTO+2)

***BN*-PAH6:** 73.4% (HONTO → LUNTO) + 25.5% (HONTO-1 → LUNTO+1) + 0.6% (HONTO-2 → LUNTO+2)

9.3. NICS Values

Calculations of the NICS(0)[32] (in plane nucleus-independent chemical shift) values were run with Q-Chem 5.2,[33] using the coordinates of optimized ground state structures as inputs. The isotropic shielding tensors were calculated at the MP2[34] / cc-pVDZ[26] level of theory.

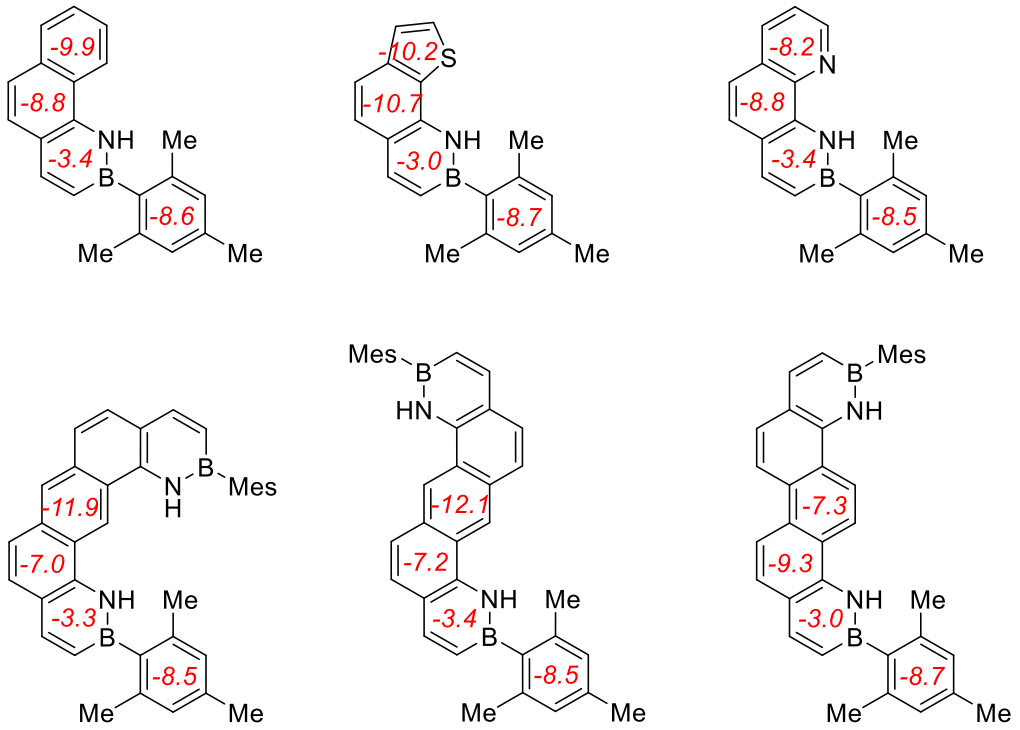

Fig. 53 NICS(0) values for ***BN*-PAH1-6**.

The results are in agreement with values for other PAHs with incorporated 1,2-azaborinine units, as the aromaticity of the azaborinine rings is on a medium level (–3.0 ppm to –3.4 ppm),[35] with the lowest values occurring when the neighboring ring is highly aromatic. Furthermore, all other (hetero)cycles display values between –7.0 ppm and –12.1 ppm, which indicates high aromaticity. While ***BN*-PAH4,5** contain an anthracene unit with significantly higher aromaticity of the central phenyl ring, ***BN*-PAH6** contains a central phenanthrene unit, where these findings are interchanged (Fig. 53).

9.4. Coordinates of the Optimized Structures

4-Hydro-3-mesityl-4,3-azaboraphenanthrene (*BN*-PAH1)

Table 32 Coordinates of the optimized structure in S_0.

Atom	x [Å]	y [Å]	z [Å]
C	-3.18856786319493	-1.80998740791657	-0.85180670142263
C	-2.06525843024307	-1.25047708017585	-0.20640051535855
N	-0.95693921087834	-2.04687331308883	-0.02005831979484
C	-3.16221041696596	-3.18916431305419	-1.26443219706196
B	-0.81497162376020	-3.41197280703501	-0.44255977122231
C	-2.07167171672952	-3.99844678022878	-1.08680818601623
H	-4.07143273372897	-3.56634521000396	-1.74917356895109
H	-2.13019585183502	-5.02946203885519	-1.44816563642767
H	-0.16440867524383	-1.59725324854696	0.42485524934593
C	-2.07824392660939	0.12836109439582	0.22453744873357
C	-3.23186491695977	0.92636242015452	-0.06705331326887
C	-3.24308637520961	2.29004074772239	0.32914952289615
C	-2.17330515332897	2.85130085459750	0.99885927917675
C	-1.04085734869362	2.06183336137329	1.30201926882070
C	-0.99693451190597	0.73364812171006	0.92052991830854
H	-4.12410434216567	2.89232113088936	0.09182046027684
H	-2.20322354094214	3.89926736116261	1.30563741838902
H	-0.19719187712169	2.50156269394663	1.83864285083311
H	-0.11117298035200	0.15034687703665	1.18267597215584
C	-4.34804205030423	0.33821454369392	-0.74152929778077
C	-4.32628765120046	-0.98120209246872	-1.10435369247090
H	-5.21709884108551	0.96282903526265	-0.96097637238676
H	-5.18533620970586	-1.42920064179721	-1.61075059169991
C	0.59945906646197	-4.09722670041134	-0.25889368676793
C	1.70020615787161	-3.65047930899834	-1.02816679981626
C	0.81201350030311	-5.14096315241973	0.67837471921241
C	2.96722443876918	-4.22337844595309	-0.84429908294673
C	2.09123894508120	-5.68530245724620	0.84343799334620
C	3.18878015966121	-5.23422116988611	0.09369714151016
H	3.80370155775257	-3.86060699563689	-1.45073565243046
H	2.23726247745899	-6.48284132092383	1.57946727074461
C	1.55681632940183	-2.54936072877964	-2.05965813732142
H	0.58621307556001	-2.58821073165485	-2.57735160067497
H	2.34569384046522	-2.62180220325717	-2.82468042173791
H	1.63856707871907	-1.54745119327863	-1.59999259446256
C	-0.33584342806810	-5.67734284230268	1.50834399120723
H	-0.87422042008788	-4.87218703538266	2.03633868132043
H	0.01751326727156	-6.39719018963374	2.26231411920713
H	-1.08170291036434	-6.19292896511952	0.87889697896516
C	4.56493874309407	-5.82378844140393	0.28918609470531
H	5.31158020106867	-5.31397883214741	-0.33761555283612
H	4.58657423459184	-6.89630262619983	0.02690409956606
H	4.89099993315297	-5.73802996813845	1.34006321413573

Table 33 Coordinates of the optimized structure in S_1.

Atom	x [Å]	y [Å]	z [Å]
C	-3.06856819024322	-1.80045096524192	-0.98346694528524
C	-2.01342958868293	-1.14522240822109	-0.26098861391418
N	-0.80846891558331	-1.86650544199090	-0.09454327418084
C	-2.90621811748126	-3.09238953771625	-1.50738692654355
B	-0.61730215150878	-3.19265625606847	-0.60339111403030
C	-1.71089392513508	-3.84795583327146	-1.35960677234796
H	-3.76206046292995	-3.51835715309844	-2.04465894838440
H	-1.67023493123902	-4.84831036266884	-1.79652671666698
H	-0.10870650742926	-1.38336042509748	0.45234342797272
C	-2.15860247409258	0.15727097665812	0.26762365260197
C	-3.41892409384464	0.85266428562728	0.09470031701096
C	-3.58714429496735	2.14166154315889	0.62356795472234
C	-2.56247039793576	2.79316064253360	1.32060498606464
C	-1.32932294615966	2.13130948676283	1.48633593081476
C	-1.12295366639835	0.85827588097473	0.98086216492690
H	-4.55105038427945	2.63890714335623	0.47615048311457
H	-2.71216283033996	3.79626349506929	1.72306516527025
H	-0.51562691156771	2.63107259714263	2.02056268120352
H	-0.14153593813564	0.40002130514667	1.12980486649611
C	-4.47088465302535	0.18434466738493	-0.62543966649433
C	-4.30146508879741	-1.06791503548104	-1.13683146975269
H	-5.42164865393438	0.70951044066480	-0.75720432879737
H	-5.11668151496525	-1.55321929676376	-1.68217509693907
C	0.78152654734530	-3.93493597260405	-0.31844337587621
C	1.90165887577729	-3.78882721030215	-1.21832830154953
C	0.91300159618256	-4.84395575615785	0.81916738281887
C	3.03220586893637	-4.55403700747287	-1.02250431985112
C	2.06647418353325	-5.59259548611832	0.98017778685718
C	3.13786632020555	-5.47977326717622	0.06753952202525
H	3.87799981400338	-4.46669841666787	-1.70955630641241
H	2.15786756168275	-6.28193870278294	1.82250924691400
C	1.80293079992764	-2.81852670597830	-2.36200679243981
H	0.96212104406492	-3.09054805207328	-3.01880554422194
H	2.73162480036477	-2.78678109312040	-2.94949466666102
H	1.57774271287854	-1.80731711977416	-1.99012448645485
C	-0.22375193581357	-4.95131571544663	1.78617263799188
H	-0.47714236748376	-3.95694597596794	2.18774430296312
H	0.00293495783896	-5.63394421571985	2.61617189279567
H	-1.13117933978601	-5.28749846943321	1.25955054659331
C	4.37452703837201	-6.30047443182931	0.21233783593495
H	5.26807537370532	-5.65233342261204	0.24584206025758
H	4.50355954476035	-6.94687094165331	-0.67526629211160
H	4.35635924218069	-6.93309878596960	1.10937311356488

9-Hydro-8-mesityl-9,8-azaboranaphtho[1,2-*b*]-thiophene (*BN*-PAH2)

Table 34 Coordinates of the optimized structure in S_0.

Atom	x [Å]	y [Å]	z [Å]
C	-3.23498812022992	-3.33076145045972	2.51386849563497
C	-4.30325198381267	-2.53160583781284	2.20886254609841
C	-4.19446132654076	-1.36662780850171	1.36609190910855
C	-2.92372930468792	-1.01960046084717	0.83546304677457
N	-1.82972647863753	-1.80874553421143	1.13118812060305
B	-1.85448130920810	-2.99902190897082	1.93413733120625
H	-3.40973022737452	-4.20146532789506	3.15347350167469
H	-5.30361840115277	-2.76032537150647	2.59698529024116
H	-0.95282989036745	-1.51667332110222	0.70883312381824
C	-3.97291335438289	0.89813292902682	-0.31745881239139
S	-1.38741388233611	0.75729185475870	-0.77026264104043
C	-3.64243757146875	1.99151338895320	-1.19673991848699
C	-2.31947853059609	2.04065843386260	-1.51766329063397
C	-5.32713390224292	-0.56530592743453	1.04359223365914
C	-5.23504338849232	0.53754095832975	0.22024486122891
H	-6.11738527322682	1.13220233047149	-0.02661632231275
H	-6.29189988985356	-0.85358605413817	1.46883588420614
C	-2.83845383964931	0.12209383049330	0.00476141904857
H	-4.37752272999078	2.70598094424053	-1.56963998934665
H	-1.80739392315156	2.76095121575190	-2.15339629218863
C	-0.51633493938677	-3.83141696690091	2.09373186137537
C	0.24332973639730	-3.78770929870794	3.29045686526965
C	-0.04597798500137	-4.63830905439255	1.02806446632528
C	1.43645873857052	-4.51314483275641	3.39299608791019
C	1.16098475077696	-5.34259368064938	1.16072117384493
C	1.92330708785477	-5.28788932318954	2.33214192278402
H	2.00707463023942	-4.46370567402810	4.32616174506103
H	1.51038560668973	-5.95581911589614	0.32427784949941
C	-0.20159471749972	-2.94570825603416	4.46705974573942
H	-1.27766901095381	-3.06520858188414	4.67293935541773
H	-0.02924119631816	-1.86948699954737	4.28261063850852
H	0.35022125948255	-3.21674244381689	5.37990574560997
C	-0.85548833752396	-4.80709837515903	-0.24330279652489
H	-1.17610403909740	-3.84554406995141	-0.67434110031833
H	-1.77790903559592	-5.38176607936320	-0.04728626433080
H	-0.28566126708653	-5.35017232503510	-1.01252850661525
C	3.23388529213306	-6.02837980898658	2.45874830727733
H	3.26562527651263	-6.64226287175103	3.37469810278971
H	4.08203487552061	-5.32344977438989	2.51437643177875
H	3.40911260168886	-6.69550935056832	1.60111287169613

Table 35 Coordinates of the optimized structure in S_1.

Atom	x [Å]	y [Å]	z [Å]
C	-3.17920106992876	-3.51705540829639	2.26820837315501
C	-4.29947160572948	-2.68711095122641	1.97254328366272
C	-4.20046593162305	-1.47798982234182	1.26223616044821
C	-2.91783641241598	-1.01476063569488	0.79177749058906
N	-1.78681233741983	-1.80582048822684	1.05961044606942
B	-1.86443067028638	-3.04896844567363	1.78214365881362
H	-3.35394096611625	-4.44252108257016	2.82230948566064
H	-5.30139053152615	-2.98457230584936	2.30330471533656
H	-0.91973944973603	-1.42570818191356	0.69928759321536
C	-3.98214348897043	0.99669961651413	-0.18836743152949
S	-1.36024193681091	0.93322501800663	-0.56658303062882
C	-3.64073711335462	2.17477567283081	-0.91442215268095
C	-2.30436537758726	2.29858343164574	-1.19615692339723
C	-5.34364686713560	-0.64734726429611	0.96786167179913
C	-5.24448071020729	0.53648749687860	0.27383380497025
H	-6.13952178461217	1.13246880545183	0.07342599501116
H	-6.31988298651790	-0.99109801109087	1.32045442518028
C	-2.83604388583565	0.18459261009071	0.09358426990636
H	-4.37824675640811	2.91879486809357	-1.22214969999261
H	-1.79103963196417	3.09715755911497	-1.72596305215408
C	-0.49888271308862	-3.86768942983012	2.00889983717987
C	0.31802100901522	-3.64057354426115	3.18005240976969
C	-0.07310389664470	-4.87783642898054	1.04266566390654
C	1.49262223263055	-4.34720567410643	3.33305411626650
C	1.11110150539617	-5.56726461516518	1.23720926551704
C	1.91824979811845	-5.32129458222912	2.37092746339724
H	2.12562233671966	-4.17305529493266	4.20655812902694
H	1.43338144067936	-6.31480110984306	0.50944339203050
C	-0.12722236837057	-2.62946755061835	4.19962981231759
H	-1.13356142875250	-2.88122506852240	4.56705387373283
H	-0.22006186508849	-1.63423776682121	3.73733960820987
H	0.57020432714907	-2.56858941557392	5.04688931598295
C	-0.93662231536363	-5.13727290534866	-0.15218664553757
H	-1.05914886435573	-4.21150546291380	-0.73819793146327
H	-1.95381463890523	-5.40916472471657	0.17053829625117
H	-0.52271239043175	-5.92467363230126	-0.79684780192540
C	3.20230568272395	-6.05038436991307	2.58352337580320
H	3.22883977047031	-6.50282805545151	3.59008206317821
H	4.04793421393718	-5.33842053859903	2.55173297692332
H	3.37303367834736	-6.83161247131880	1.83179869599814

10-Hydro-9-mesityl-10,9-azaborabenzo[*h*]quinoline (*BN*-PAH3)

Table 36 Coordinates of the optimized structure in S_0.

Atom	x [Å]	y [Å]	z [Å]
C	-4.23852247512224	-2.03040280615925	-1.16718093876828
C	-4.34328709558082	-0.66729852202609	-0.71594014718433
C	-3.23950812745478	-0.07933767981501	-0.06823568482428
N	-2.08716545626555	-0.79427952195370	0.12334464007408
B	-1.87515849547821	-2.14357336570216	-0.31220389406512
C	-3.09996262237362	-2.77195836015564	-0.99391181904301
C	-3.30635098509486	1.28623318015677	0.38699982377480
C	-4.50352404336256	2.03421374040826	0.17650334274110
N	-2.20420403078626	1.79952339263068	0.99551441165294
C	-4.51262061687188	3.37062355348947	0.64800718170991
C	-2.25537500362362	3.05184532184369	1.41839470416254
C	-3.39108914362622	3.88286228515578	1.27015301486602
C	-5.52426581732447	0.11718978968439	-0.91165226760424
C	-5.61097371878095	1.41816795571646	-0.48605443692181
H	-6.37227824882603	-0.34985804099948	-1.41942832464041
H	-6.51947135475253	2.00144793278843	-0.65299207708814
H	-5.40864397849604	3.98205273337873	0.51079082907714
H	-3.36752246964534	4.90674770843791	1.64777029474176
H	-1.35367981512729	3.43964842218100	1.90491145905318
H	-1.36957849493046	-0.25028334449584	0.60168555121102
H	-5.11856544132008	-2.45083236146829	-1.66932682968356
H	-3.09481751285025	-3.79514952055623	-1.38169964874619
C	-0.45797496181838	-2.81700120657362	-0.11740574739571
C	-0.30054985482612	-3.99801129306884	0.65548205087522
C	0.68876246087955	-2.26572618068674	-0.74056120612649
C	1.93689675017814	-2.88842708597170	-0.59269237790472
C	0.96307020328812	-4.58482503714010	0.79297793724004
C	2.09945760187838	-4.04495875974183	0.17318594922672
H	1.06274244397529	-5.49255968171763	1.39656515996461
H	2.80704496787894	-2.45466534305497	-1.09556430887819
C	0.61912307823387	-1.00171535577170	-1.57566189370856
H	-0.29745650890685	-0.94961142006533	-2.18259091472075
H	1.47851354868799	-0.93553920500704	-2.26117041862468
H	0.64017387055827	-0.09624633784463	-0.94302161039300
C	-1.48456950982998	-4.64237314244795	1.34887425151073
H	-2.08483923418215	-3.90776250647724	1.91078571907413
H	-1.15644151895012	-5.41911103833942	2.05627027249016
H	-2.16855641491639	-5.12293818882900	0.62766062646253
C	3.45629909466705	-4.68696280519636	0.33485860096668
H	3.43731034071878	-5.75277501870114	0.04852724192719
H	3.79818234160297	-4.63670811740805	1.38373358964478
H	4.21405024857670	-4.18752203849660	-0.28683010612578

Table 37 Coordinates of the optimized structure in S_1.

Atom	x [Å]	y [Å]	z [Å]
C	-3.92087512577760	-1.83149086498792	-1.62078608296496
C	-4.18968824474175	-0.60034687350459	-0.98628223098803
C	-3.20934633739608	-0.01231712572632	-0.12784130062511
N	-1.99206616290984	-0.67653625153313	0.07427353386704
B	-1.69439837185986	-1.91321602488230	-0.54587804368557
C	-2.71812997564104	-2.53430829292169	-1.45374403691875
C	-3.41340900484569	1.20983881723913	0.54139727193312
C	-4.65973395525756	1.90375451306562	0.36494684627173
N	-2.38926120258947	1.67776704848634	1.34901058681282
C	-4.83648304729948	3.11325762880651	1.04707080975252
C	-2.61660649777462	2.84343871951563	1.97301490578574
C	-3.78749451018461	3.59478691617351	1.87100661851200
C	-5.42122393244791	0.11904028827299	-1.14387835339953
C	-5.64756187556549	1.30746951869108	-0.50319952708248
H	-6.19083249611740	-0.30803053365540	-1.79413071591111
H	-6.59792000511604	1.83207369622316	-0.63963343736379
H	-5.77084492942096	3.66968401186073	0.93889807643451
H	-3.88183288115612	4.53721358767281	2.41301373815584
H	-1.79715872368479	3.20814172835049	2.60597747014766
H	-1.40364044602796	-0.13136018578356	0.70695020897985
H	-4.70889375083539	-2.23769814355170	-2.26796370219600
H	-2.59954669411882	-3.48893872576177	-1.97284523390834
C	-0.29461160931657	-2.63859406693787	-0.23267581167759
C	-0.17329441204952	-3.51538638474791	0.91111656895849
C	0.84220583831178	-2.50240729696373	-1.13656027903499
C	1.97476572558648	-3.27217609454038	-0.94051073578596
C	0.97314604327287	-4.26417573482931	1.07000816484979
C	2.06307227024825	-4.17490483551463	0.14562977186931
H	1.06560396082340	-4.94928962729980	1.91650889561128
H	2.81995351862799	-3.18751048656550	-1.62714913302474
C	0.74954875458329	-1.52876453425790	-2.27042505820479
H	-0.10528215975009	-1.78050400915115	-2.91819345306858
H	1.67185705991304	-1.50492034084065	-2.86718274396675
H	0.53953350553273	-0.51732813164715	-1.88648440709924
C	-1.31185469965220	-3.60909741698518	1.88681221551734
H	-1.55582318328951	-2.61431838564948	2.28912715157759
H	-1.07934848018775	-4.28739346763989	2.71925586233562
H	-2.22237401453001	-3.95866996320444	1.37536650430294
C	3.26105165044297	-5.03914055341673	0.34456374801829
H	2.98251808931061	-6.09814272818826	0.18331428171504
H	3.61896641955316	-4.97859846879613	1.38655229386471
H	4.08198789333765	-4.78875792487346	-0.33957923836690

1,13-Dihydro-2,12-dimesityl-1,13-diaza-2,12-diboradibenz[*a,j*]anthracene (*BN*-PAH4)

Table 38 Coordinates of the optimized structure in S_0.

Atom	x [Å]	y [Å]	z [Å]
C	-5.02336341373020	0.78103146636376	0.30830064591757
C	-4.94864069839598	2.14828177866896	0.22901786343885
C	-3.70628051729139	2.85671428963972	0.06832337128522
C	-2.50187745188784	2.13413666987552	-0.00385390412691
N	-2.55900690952773	0.76064121182574	0.02108781684829
B	-3.74177946804101	-0.04223875923816	0.17090968702556
H	-6.00827594252749	0.32716761049950	0.45633829060810
H	-5.85274951225105	2.76621210181291	0.29817914789630
H	-1.67623889181760	0.28363235440136	-0.12164714655218

Atom	x [Å]	y [Å]	z [Å]
C	-1.23072406124359	4.26692398238427	-0.15430380125774
C	-0.00026775465230	4.93944609092541	-0.20020476147267
C	1.23028289578730	4.26698981436569	-0.15587916467288
C	-3.66117102522695	4.29022897446517	-0.01476660741855
C	-2.48269460516511	4.96986545997807	-0.13559984239223
H	-2.47201109003581	6.06068296264767	-0.20314197570589
H	-4.60900627809160	4.83426242090614	0.01844433151950
C	-1.23120882946815	2.82813421302755	-0.08343279749275
H	-0.00032561479673	6.03282904152353	-0.24711294210622
C	-3.54730828700164	-1.61333209972632	0.11676631134416
C	-2.74035122597308	-2.28897231537626	1.06791606961122
C	-4.10292282169527	-2.36890431925641	-0.94827823573422
C	-2.47818494021528	-3.65965830565420	0.92279569628301
C	-3.81457931434252	-3.73474299543446	-1.06624578763764
C	-2.98646141500540	-4.39869487505938	-0.15202853267272
H	-1.85915673322055	-4.16394638383767	1.67244056925605
H	-4.24653736180827	-4.29465324550011	-1.90247248847050
C	-2.16307155432971	-1.56397709579340	2.27038636093893
H	-1.37368236004499	-0.84513172932865	1.99157822906954
H	-1.71736738866554	-2.27330309649044	2.98414870732957
H	-2.93368637429184	-0.98307524742448	2.80428824510495
C	-4.98888130944349	-1.71781968055552	-1.99074429290613
H	-4.41940933372736	-1.01794195288783	-2.62767041027668
H	-5.80072176047803	-1.13372726701379	-1.53075358580437
H	-5.44844452392801	-2.46971083765504	-2.65097064094682
C	-2.63949721028587	-5.85807088448030	-0.33746280520628
H	-2.27884328354166	-6.31410404961148	0.59788469471635
H	-1.84098755224572	-5.98175595049392	-1.09131190723655
H	-3.50525659209628	-6.44028026750240	-0.69332022539728
C	1.23093338974926	2.82821254727657	-0.08474524787497
C	-0.00009545589082	2.15754616698193	-0.04931086925821
H	0.00000787568679	1.07247505181282	0.07013100895270
C	2.48224137185244	4.96999668667544	-0.13895371961851
C	2.50171700393928	2.13431573748313	-0.00617123288400
C	3.66089960916231	4.29045823926213	-0.01936298307236
C	3.70616460088033	2.85698553195616	0.06435588020181
H	2.47141762055813	6.06079373454090	-0.20679785600463
H	4.60874418161848	4.83455123473360	0.01258461324943
N	2.55891307307413	0.76083910542722	0.01981149218041
C	4.94872334497029	2.14870914046676	0.22418650479311
C	5.02356523134588	0.78152616681951	0.30452178777866
B	3.74184857917167	-0.04187443594217	0.16924092793518
H	1.67598248783801	0.28367909903722	-0.12146092485299
C	3.54723791816274	-1.61302294513487	0.11764995346679
C	2.74065277653733	-2.28708924893209	1.07021050867655
C	4.10258587149426	-2.37033900401133	-0.94627394173827
C	2.47859193861258	-3.65805096000791	0.92755171842633
C	3.81451351599439	-3.73645582208049	-1.06168739585921
C	2.98677130053804	-4.39893212218812	-0.14605052983901
H	1.85980968434966	-4.16109195072106	1.67823633212443
H	4.24639261799489	-4.29778829275918	-1.89699718670398
C	4.98825870521860	-1.72092257490791	-1.99003178659153
H	4.41851246233885	-1.02241934998822	-2.62822300976993
H	5.44800370888898	-2.47389961191863	-2.64888653051169
H	5.79995462832604	-1.13569972292726	-1.53119926827077
C	2.16346611190415	-1.55995851474700	2.27142940664138
H	2.93409166635331	-0.97795304911350	2.80411645558022
H	1.71798337580883	-2.26802804351048	2.98657619234808
H	1.37393269023130	-0.84174385549730	1.99140017299336
C	2.64012414149772	-5.85873132382563	-0.32871649687712
H	1.84153090360078	-5.98401342935273	-1.08221511924091
H	2.27972122633179	-6.31310546822530	0.60753531972341
H	3.50597211012973	-6.44139547764356	-0.68361027443960
H	5.85287889274482	2.76672254772265	0.29197017057958
H	6.00864134968878	0.32780512824799	0.45193174505028

Table 39 Coordinates of the optimized structure in S_1.

Atom	x [Å]	y [Å]	z [Å]
C	-0.31017877336579	-0.80483721820665	-5.09315254639999
C	-0.29867587019531	-2.17302902532872	-4.99749287618729
C	-0.22062060353569	-2.86704092329076	-3.74574110440589
C	-0.15362227431259	-2.12556555327048	-2.50949638490962
N	-0.17889601444843	-0.75228374700198	-2.59547097075254
B	-0.25733147015702	0.02637936629399	-3.80696048490295
H	-0.38751473019860	-0.35430832043761	-6.08715957433281
H	-0.35445041211831	-2.80341001961613	-5.89336459855040
H	-0.10977744621194	-0.26029742606609	-1.71170709716328
C	-0.06748927356456	-4.23595970811418	-1.23554344374478
C	0.00011570890938	-4.91503673096754	0.00000674328141
C	0.06765666756503	-4.23596113751377	1.23555912621082
C	-0.20811308731744	-4.27628251303467	-3.68561243275078
C	-0.13472287776849	-4.94119081763051	-2.46910853126122
H	-0.12799293175077	-6.03421497319381	-2.44518450916956
H	-0.25942307264587	-4.84287557990951	-4.61836790095669
C	-0.07152590937561	-2.79671154810065	-1.24422301940073
H	0.00017490632411	-6.00862060050923	0.00000355273765
C	-0.30423711227981	1.60049292481144	-3.69824264453826
C	0.75377183349075	2.39388830965361	-4.20873764659854
C	-1.41510979482499	2.25813806408687	-3.10391246997161
C	0.68993329250871	3.79188189462287	-4.11754152372219
C	-1.44855486090957	3.65549267838259	-3.03767318358497
C	-0.40257065908591	4.44437425069267	-3.53726382649000
H	1.51966949226762	4.38743349007561	-4.51134323885317
H	-2.31962691533894	4.14529619191113	-2.58996793754528
C	1.97994536179866	1.75329871665044	-4.82420655795155
H	1.71511458666428	1.04486106331029	-5.62565612964688
H	2.65581353722420	2.51119843179835	-5.24850703896834
H	2.55285443982308	1.17762286076270	-4.07621581877857
C	-2.59414519437467	1.47170318845294	-2.56557279399881
H	-2.32181008982712	0.85215545553206	-1.69427739581900
H	-3.00028963072182	0.78039055201360	-3.32294729929345
H	-3.40762893896722	2.14211369094774	-2.25017127166853
C	-0.46523535018374	5.95007576007050	-3.44976066355172
H	0.43387560116779	6.41958011583664	-3.87672819509776
H	-0.55685240343958	6.28623151160856	-2.40274501941440
H	-1.34124326278936	6.34724114006442	-3.99121184430647
C	0.07153142706846	-2.79671866120123	1.24423851164315
C	-0.00012089145814	-2.11737854777877	0.00001840157392
H	-0.00057031466917	-1.02532457322923	0.00004525561506
C	0.13488929074859	-4.94118929198500	2.46913120916006
C	0.15367446053692	-2.12557698546044	2.50950750037548
C	0.20813314994109	-4.27628009430793	3.68564764198924
C	0.22058417243251	-2.86703802352928	3.74576707211332
H	0.12820851096541	-6.03421410855448	2.44520445994241
H	0.25939852412169	-4.84287223032469	4.61840525687812
N	0.17908726734650	-0.75232141297510	2.59545170688420
C	0.29859681019994	-2.17300192598616	4.99751162785971
C	0.30986854696236	-0.80480584754248	5.09315137050159
B	0.25735343222353	0.02637670412406	3.80691971661790
H	0.11030281233222	-0.26036656362471	1.71165995824332
C	0.30423091125845	1.60048164335758	3.69816218937643
C	1.41513518980663	2.25814368313344	3.10389708961427
C	-0.75397954015801	2.39388055644963	4.20864226712166
C	1.44859540119788	3.65549651518563	3.03771224503067
C	-0.68993535457221	3.79187353189645	4.11749872322166
C	0.40260615121321	4.44437344658525	3.53730045837685
H	2.31969625958515	4.14530823845895	2.59007289844619
H	-1.51968299751428	4.38742204960698	4.51128124781087
C	-1.98004796651490	1.75332015341414	4.82398796816272
H	-2.55292376402792	1.17770010516258	4.07593072105840
H	-2.65591292829484	2.51123757454405	5.24826415355578
H	-1.71531939103516	1.04484223521669	5.62543260823212
C	2.59423561201385	1.47175175537508	2.56563155471366
H	3.00028765089146	0.78036714648696	3.32298658671683
H	3.40775721411998	2.14219740885618	2.25040414364753
H	2.32202311134936	0.85229719616294	1.69421925225428
C	0.46531349625561	5.95007619629920	3.44988938052818
H	0.55699257095759	6.28628846961659	2.40289841361128
H	1.34130877759902	6.34718472423957	3.99140501604638
H	-0.43380319250459	6.41958096693821	3.87684242736981
H	0.35410897750832	-2.80336549614134	5.89341076609052
H	0.38690814407905	-0.35425035385605	6.08716875207456

1,8-Dihydro-2,9-dimesityl-1,8-diaza-2,9-diboradibenz[*a,h*]anthracene (*BN*-PAH5)

Table 40 Coordinates of the optimized structure in S_0.

Atom	x [Å]	y [Å]	z [Å]
C	0.38207786524544	-2.66199049057282	-2.67757110335130
C	0.35857771365328	-1.25686516707911	-2.60008964607584
N	0.30880704478952	-0.53360847761464	-3.77425572663534
C	0.37403042979641	-3.30715432947975	-3.96208664415015

Atom	x [Å]	y [Å]	z [Å]
C	0.32812726036327	-2.61110739661014	-5.14089541504847
B	0.26354402594534	-1.08315943731197	-5.10259545687780
H	0.28177597667611	0.47465063830270	-3.66495131920926
C	0.37355587089467	-0.59871510782054	-1.30533499291445
C	0.38406768432264	-1.41387083625408	-0.11480447667546
C	0.37850261213220	-0.79401595610544	1.14444309353483
C	0.37351946514164	0.59872146433467	1.30533925663738
C	0.38398694917849	1.41388031134232	0.11481109508265
C	0.37846145189153	0.79402479660576	-1.14443790875617
H	0.40117365003524	-4.40445695665648	-3.95354626177878
H	0.31602630456402	-3.17904772295032	-6.07660796749282
H	0.38566108969830	-1.45652909308202	2.01391325960010
H	0.38557707952094	1.45653842288703	-2.01390902146201
C	0.40096532940719	-2.84304600634481	-0.23695036395471
C	0.40553292397301	-3.43350392639935	-1.46614555592971
H	0.41223153470556	-3.44632667421480	0.67391220234525
H	0.42169263613180	-4.52358027882763	-1.55431406780004
C	0.35850497281316	1.25686940808123	2.60009110088936
C	0.40080990428826	2.84305664577155	0.23695652862508
C	0.38192373542677	2.66199609968825	2.67757385480519
C	0.40533595292740	3.43351539620177	1.46615183036246
C	0.37385237145111	3.30716065452100	3.96208874544141
N	0.30877653752638	0.53361145544582	3.77425539667540
B	0.26347845052471	1.08316005025893	5.10259347239316
C	0.32797715068586	2.61111036288870	5.14089727942794
H	0.28180907333353	-0.47464935770095	3.66495190944871
H	0.40090806173185	4.40446570132092	3.95355053967845
H	0.31582367768859	3.17904588911264	6.07661276640411
H	0.42143908027562	4.52359256405074	1.55431952171129
H	0.41205156218410	3.44633748411221	-0.67390682270407
C	0.08929593015056	-0.14405143172262	-6.36919465728842
C	-1.17762303299407	0.42033430366959	-6.66932674733192
C	1.15004332620127	0.07697424495644	-7.28093435783420
C	0.92816256614933	0.80509534318799	-8.46005261071776
C	-1.36824503930823	1.13069863584373	-7.86195254686152
C	-0.33155106881680	1.32075586135013	-8.78391143257314
H	1.76385994214015	0.97007415237312	-9.14824926873025
H	-2.35819672654839	1.54513985976013	-8.07925515005213
C	-2.34475904486682	0.27498574534675	-5.71450628821408
H	-2.18512730925925	0.85250968446542	-4.78742462486202
H	-2.50404467648107	-0.77225836965215	-5.40876554556938
H	-3.27658867506349	0.64410570703091	-6.16884318652975
C	2.53799064847281	-0.46483297068908	-7.00679234305659
H	2.83821891267213	-0.30864346501774	-5.95777174637756
H	3.28867302370005	0.02275357357743	-7.64674498369241
H	2.59452643683711	-1.55160666114570	-7.19684528103924
C	-0.58219994071570	2.02844916805385	-10.09594235694765
H	0.35311669839270	2.38496128384459	-10.55440113762914
H	-1.25400180344862	2.89331019792093	-9.97178857192168
H	-1.06648817240162	1.34852528447713	-10.82044486500371
C	0.08925430163901	0.14404353048822	6.36918966501668
C	-1.17768664213157	-0.42025509559737	6.66939367246217
C	1.15004407544260	-0.07707155828314	7.28085755817448
C	0.92818826956484	-0.80519925063487	8.45997711163836
C	-1.36828333097362	-1.13062315706778	7.86202043644427
C	-0.33154190069604	-1.32077410444178	8.78390759707387
H	-2.35825316252647	-1.54498763675573	8.07938587872813
H	1.76391834581976	-0.97025382385065	9.14811594556115
C	-0.58215646944659	-2.02848069858646	10.09593764323857
H	0.35317055620267	-2.38501470645389	10.55435766283594
H	-1.06640917078510	-1.34855984436946	10.82046675241859
H	-1.25397745353573	-2.89332873551450	9.97179546279149
C	2.53801233343097	0.46464029163957	7.00663225693159
H	2.59462954577962	1.55141094285482	7.19667544312912
H	2.83816967615935	0.30842556400631	5.95759473393581
H	3.28869907021463	-0.02299342370379	7.64654405759063
C	-2.34487916749119	-0.27477240615249	5.71466251090899
H	-2.18531834559561	-0.85218451586805	4.78749864714122
H	-2.50416013268827	0.77251355913043	5.40906046038150
H	-3.27668782211928	-0.64392520837165	6.16901510358356

Table 41 Coordinates of the optimized structure in S_1.

Atom	x [Å]	y [Å]	z [Å]
C	0.16013621574809	-2.77039666818434	-2.61777056505032
C	0.14528972811469	-1.32970287200092	-2.55464128641936
N	0.12076423472879	-0.64580291962273	-3.74918695056914
C	0.15921608107594	-3.44001716833994	-3.88350658307411
C	0.14063643955091	-2.76804270034972	-5.08162300346786
B	0.11279159517261	-1.23886197680341	-5.06674994131414
H	0.09862260594388	0.36587309233414	-3.67470177128267
C	0.15446141104477	-0.64548789962755	-1.29790451085183
C	0.16177464117567	-1.41958606069077	-0.08146148765454
C	0.16013064049784	-0.76909153232583	1.16809019369706
C	0.15464194096093	0.64472453095592	1.29741421592274
C	0.16202064233137	1.41881402082346	0.08096074554077
C	0.16020002148726	0.76832270463008	-1.16858381177645
H	0.17427376231246	-4.53665435820910	-3.84883377181723
H	0.14097364392675	-3.35137793251894	-6.00711832150684
H	0.16949311759331	-1.41147013019643	2.05195907139577
H	0.16962975577903	1.41070416102360	-2.05244875210714
C	0.17281762838808	-2.84049911072023	-0.17403404090843
C	0.17425377855773	-3.48760687119536	-1.40224328393815
H	0.18232047463664	-3.42741670337740	0.74789412963707
H	0.18555539532349	-4.58023520748170	-1.44080544846356
C	0.14568132771172	1.32896312444699	2.55413615838136
C	0.17330225279564	2.83972568335063	0.17349013217005
C	0.16082585622387	2.76966013215907	2.61722070140663
C	0.17495114833815	3.48685437651979	1.40168541170677
C	0.16021340800549	3.43933073119549	3.88292273929542
N	0.12110197738303	0.64511026876405	3.74871447734601
B	0.11346362861530	1.23824174201094	5.06626275426427
C	0.14169364131647	2.76740591981776	5.08106817986739
H	0.09878599552181	-0.36656548442244	3.67426818338201
H	0.17549055078396	4.53596321004001	3.84820233386408
H	0.14227502267812	3.35077425366727	6.00654172503544
H	0.18646620872023	4.57948078718792	1.44023324072277
H	0.18283422738779	3.42661837755600	-0.74845060758632
C	0.07044168099705	-0.27561675461980	-6.31888900110127
C	-1.16500148016325	0.15976532400650	-6.85095725253026
C	1.26857211795220	0.17462871491155	-6.92604447320085
C	1.21279685357283	1.03788827842255	-8.02670323160751
C	-1.18590460681704	1.02417389194440	-7.95554753989007
C	-0.00772509467253	1.47826886902597	-8.55663967588139
H	2.14796333991641	1.37843249829348	-8.48285052184042
H	-2.15032409290974	1.35336953853241	-8.35491602729175
C	-2.47097546081264	-0.30527836283945	-6.24109100155831
H	-2.56045313266755	0.00275420626891	-5.18522084758810
H	-2.55294551440823	-1.40550918656098	-6.25371424777072
H	-3.33619580184018	0.10593901979001	-6.78196569435735
C	2.61266769288172	-0.27685963914695	-6.39367945867660
H	2.75803878365801	0.02704226062337	-5.34280486000667
H	3.44080591251803	0.14741760839147	-6.98053631814535
H	2.70673459841615	-1.37599969577330	-6.41701299911979
C	-0.04105107447054	2.40408984977872	-9.74920570949325
H	0.35435018965852	1.90836853670615	-10.65310047711956
H	0.57942644149149	3.30026877339894	-9.58105714723732
H	-1.06488003267526	2.73869309287923	-9.97303596238285
C	0.07100606603489	0.27524888469181	6.31858989140136
C	-1.16444637064325	-0.16049017345990	6.85033622746806
C	1.26910162876852	-0.17411583278477	6.92648680277892
C	1.21327747676619	-1.03681648554150	8.02757602789623
C	-1.18540003584883	-1.02431982359694	7.95538171692512
C	-0.00726095071368	-1.47748911779342	8.55724768873912
H	-2.14982926284042	-1.35375486936130	8.35452507980171
H	2.14841669805536	-1.37667414513963	8.48428947587139
C	-0.04063958079561	-2.40272770750459	9.75026875858093
H	0.35604067876114	-1.90705067053749	10.65361630980978
H	-1.06465888946065	-2.73609795178643	9.97509806036662
H	0.57866162253442	-3.29969714698777	9.58198100539421
C	2.61320253999318	0.27769881951036	6.39441700451612
H	2.70686466423422	1.37688104429499	6.41744413326835
H	2.75901332785797	-0.02647545542019	5.34368548285832
H	3.44130665499005	-0.14610427492127	6.98166719117297
C	-2.47040064857965	0.30368378455194	6.23975992852006
H	-2.55928760442144	-0.00474494275745	5.18395887997600
H	-2.55292948126094	1.40387915723428	6.25197542955754
H	-3.33564185288878	-0.10777743714025	6.78041509604906

1,12-Dihydro-2,11-dimesityl-1,12-diaza-2,11-diborapicene (*BN*-PAH6)

Table 42 Coordinates of the optimized structure in S_0.

Atom	x [Å]	y [Å]	z [Å]
C	0.05996594090743	3.96341800119740	2.83921716052376
C	0.04916100344201	3.96833839897331	1.46863539768062
C	0.06791440148553	2.75365100720170	3.58438917451124
C	0.05975706730970	1.52467077316262	2.88565044720171
C	0.05596416021868	1.51348012271634	1.44192322793945
C	0.05057342701197	2.74958990821606	0.72773589470630
C	0.04910733810379	3.96832384961735	-1.46861914622764
C	0.05054417342142	2.74958000035102	-0.72770997932212
C	0.05984369616688	3.96339101323220	-2.83920105928765
C	0.06774262901026	2.75361772804405	-3.58436392730830
C	0.05589069378835	1.51346126469084	-1.44188329131191
C	0.05961477029565	1.52464497284977	-2.88561208652912
C	0.06106802871478	0.29825168893541	0.68461545018919
C	0.06102247581235	0.29824393297148	-0.68455693675440
N	0.05278946692248	0.35679188958275	-3.63108098063455
C	0.08125312343486	2.77549561236204	-5.02334618266087
B	0.05237331331512	0.27915682367982	-5.06658061701334
C	0.07910175322652	1.63505422986403	-5.77489575677510
C	0.08149197187544	2.77554005202941	5.02337125886370
C	0.07936783982064	1.63510598850975	5.77493233831707
B	0.05259106175882	0.27920385643163	5.06662896398977
N	0.05296110388153	0.35682578828417	3.63112954298665
H	0.07035005545988	-0.66804545240048	1.19307343958154
H	0.07027019276742	-0.66806055703729	-1.19300298509051
H	0.04058206207163	4.92476116108555	-0.95040021957882
H	0.06070616989012	4.90832275167970	-3.38896200508981
H	0.06084885008649	4.90835479689123	3.38896943962280
H	0.04059784472506	4.92477158232502	0.95040958251334
H	0.02804404302927	-0.50525219556321	3.09822554028061
H	0.02792333354591	-0.50528133577448	-3.09816864064207
C	-0.00198259351863	-1.11209903996711	-5.82322112033256
C	-1.23672583855376	-1.59035258280373	-6.33069708700992
C	1.17174127994544	-1.84978182336180	-6.10835879338511
C	-1.27930640343717	-2.77530009004018	-7.07520475512328
C	1.09369859245068	-3.03155970993063	-6.86224618380035
C	-0.12302230680061	-3.51654881032327	-7.35130811881616
H	-2.24140376394805	-3.12347850942769	-7.46522571797043
H	2.01385011159861	-3.58034365421561	-7.08737529701198
C	-0.00182147317013	-1.11205051866740	5.82326505647855
C	-1.23663868165881	-1.59036009383341	6.33050646748724
C	1.17187785072275	-1.84969884875787	6.10858439037982
C	-1.27931228914850	-2.77533925086203	7.07495638042295
C	1.09374248130217	-3.03150624948060	6.86241787115250
C	-0.12305186678953	-3.51656034232466	7.35123429677679
H	2.01387421312906	-3.58026475066385	7.08769078703050
H	-2.24146856053891	-3.12356996020590	7.46478511383121
C	-2.51817423613113	-0.81172221370773	6.11497621100390
H	-2.65269396503789	-0.51098336831259	5.06283124672840
H	-2.52482087997769	0.11884786610764	6.70834814547968
H	-3.39643278499004	-1.40197783320536	6.41794076115104
C	2.52765740116772	-1.37287063250883	5.62817123985982
H	2.67064811721986	-0.29617138640285	5.82006139777598
H	2.65368981869896	-1.52239290124625	4.54102494420330
H	3.34124025736655	-1.91512842039965	6.13250844748885
C	-0.20599498815448	-4.80123675809652	8.14211385871926
H	-0.84778155261281	-4.68620725534571	9.03106171479278
H	0.78534617320546	-5.13873863371742	8.48146807158874
H	-0.64455780674180	-5.61214158422189	7.53322193642053
C	2.52745336057775	-1.37302730758524	-5.62768568141699
H	2.65328645432510	-1.52258961120927	-4.54052195649785
H	2.67052411930156	-0.29632812862532	-5.81951616818440
H	3.34110259102693	-1.91530528419007	-6.13189431969539
C	-2.51827137912746	-0.81166638379869	-6.11539552882436
H	-2.52481202346476	0.11886651262393	-6.70882867861385
H	-2.65292922759032	-0.51085706825241	-5.06328899561543
H	-3.39650309616170	-1.40191872484307	-6.41844516309504
C	-0.20586022142217	-4.80118502226200	-8.14226391319146
H	0.78553385452076	-5.13870411896103	-8.48144627926742
H	-0.84747428467261	-4.68609414033090	-9.03132812631236
H	-0.64456493123214	-5.61210292770883	-7.53349160951931
H	0.09249304046321	3.76803946631550	5.49099925576258
H	0.09089284848448	1.72638648987698	6.86583258598626
H	0.09222138481637	3.76799179325712	-5.49098206707241
H	0.09056921305369	1.72632415750701	-6.86579766444618

Table 43 Coordinates of the optimized structure in S_1.

Atom	x [Å]	y [Å]	z [Å]
C	0.11977822992005	-3.99047862547092	-2.86385001752896
C	0.05511360240374	-4.00459333558817	-1.47874292600757
C	0.17048643002985	-2.78650511238052	-3.61246472311868
C	0.14891712492356	-1.55194081903694	-2.88501659262045
C	0.07493426131491	-1.54621330879873	-1.45313935256665
C	0.03285436857993	-2.80662100392687	-0.71910377597717
C	-0.05488918994701	-4.00489007855856	1.47857378606724
C	-0.03185057325114	-2.80677010825376	0.71920431544509
C	-0.11989690069130	-3.99109513630380	2.86369240507242
C	-0.17028544852686	-2.78728196036466	3.61257020513384
C	-0.07329887991659	-1.54651336052006	1.45352781853160
C	-0.14778481713662	-1.55254378961231	2.88539364140662
C	0.03707836162093	-0.35154374661044	-0.69624908818138
C	-0.03443071652860	-0.35169691680578	0.69696780953373
N	-0.19845980363925	-0.38443081097881	3.61874706468500
C	-0.24344961798883	-2.79393734345947	5.03777363573592
B	-0.27634475932158	-0.29386977208905	5.05898324420018
C	-0.30008661511823	-1.63495587539476	5.78428201704059
C	0.24283680637746	-2.79295642409324	-5.03772643998365
C	0.29939571692518	-1.63383233872491	-5.78396473287802
B	0.27683873394111	-0.29287161293200	-5.05830663598349
N	0.19978731337971	-0.38360350282087	-3.61813126513100
H	0.05962095236699	0.62139157601377	-1.19085818798495
H	-0.05615779535386	0.62112203142991	1.19184721172869
H	-0.01676474051819	-4.97052148484573	0.97655014595922
H	-0.13379814483292	-4.93847236763400	3.40873768710207
H	0.13298682850825	-4.93771590319280	-3.40915646472293
H	0.01655118188596	-4.97031927682338	-0.97693748787382
H	0.19626511570914	0.47643718496170	-3.08153970796423
H	-0.19479601253215	0.47575708209969	3.08238875492905
C	-0.31365927953915	1.12655784959706	5.75170856469557
C	-1.53072388806235	1.67206432688802	6.22306141042245
C	0.88425637567965	1.85175788842508	5.97303095656496
C	-1.53228528825029	2.89959354856438	6.90168879601060
C	0.84821939310340	3.07291063182838	6.65664613524996
C	-0.35285128805299	3.61443258879190	7.13508713938001
H	-2.48195492257674	3.30432150083635	7.26519846316535
H	1.78527367015047	3.61177283489143	6.83111832344167
C	0.31382308318094	1.12723056548926	-5.75175608111475
C	-0.88453766300819	1.85095825601205	-5.97540646347071
C	1.53090492070809	1.67331380223678	-6.22232298180504
C	-0.84890201299286	3.07129554891714	-6.66047197592209
C	1.53205323403901	2.89995729465009	-6.90257338076611
C	0.35219676951532	3.61331165358567	-7.13830336000265
H	2.48173392581796	3.30509787163365	-7.26560283410290
H	-1.78625945267292	3.60907363473127	-6.83663064377944
C	-2.21323408907091	1.30121394194360	-5.49802769383436
H	-2.26592183637456	1.25195004619369	-4.39665420932497
H	-2.37819911900877	0.27397661093324	-5.86455028290548
H	-3.05280008884436	1.92217340210358	-5.84463106890559
C	2.84149370715622	0.94899281327698	-5.99518170006021
H	2.80234801775411	-0.08693733676541	-6.37105838313462
H	3.08681361159371	0.88200306732596	-4.92095800432656
H	3.67610060089548	1.46100417362459	-6.49699213454829
C	0.36340124288271	4.92296841850496	-7.89036957473073
H	-0.27764344405177	4.87619833276075	-8.78711069707324
H	1.37890851179825	5.19270019121076	-8.21655604426545
H	-0.01989159280339	5.74877221658991	-7.26626972960033
C	2.21299835082280	1.30301611377846	5.49456355703640
H	2.26658307688087	1.25812938234632	4.39301543778077
H	2.37713995416817	0.27427862131003	5.85715519887085
H	3.05262379875352	1.92219130740046	5.84419345795574
C	-2.84092426528135	0.94631706650389	5.99822653558287
H	-2.80070891874855	-0.08893081193306	6.37584787238721
H	-3.08699506796280	0.87726520712568	4.92431122293010
H	-3.67555076604866	1.45856015145339	6.49977466291276
C	-0.36444951576325	4.92490279142094	7.88574336534421
H	-1.38047966245136	5.19620019466759	8.20899837671272
H	0.02158783909786	5.74955765489100	7.26185361518289
H	0.27413205989856	4.87822426434854	8.78427742408283
H	0.25118613711305	-3.77818483560420	-5.51956252166525
H	0.35155509129069	-1.71472717905394	-6.87357111486016
H	-0.25250882746510	-3.77924248290607	5.51944149752676
H	-0.35297259585417	-1.71629007981471	6.87382052291398

10. References

1. O. V. Dolomanov, L. J. Bourhis, R. J. Gildea, J. A. K. Howard and H. Puschmann, OLEX2: a complete structure solution, refinement and analysis program, *J. Appl. Cryst.*, 2009, **42**, 339-341.
2. G. M. Sheldrick, SHELXT - Integrated space-group and crystal-structure determination, *Acta Cryst. A*, 2015, **71**, 3-8.
3. G. M. Sheldrick, Crystal structure refinement with SHELXL, *Acta Cryst. A*, 2008, **64**, 112-122.
4. H. C. Brown and U. S. Racherla, Organoboranes. 44. A convenient, highly efficient synthesis of triorganylboranes via a modified organometallic route, *J. Org. Chem.*, 1986, **51**, 427-432.
5. H. Doi, T. Sakai, K.-i. Yamada and K. Tomioka, N-Allyl-N-tert-butyldimethylsilylamine for chiral ligand-controlled asymmetric conjugate addition to tert-butyl alkenoates, *Chem. Commun.*, 2004, **16**, 1850-1851.
6. H. Lee and S.-Y. Liu, Synthesis of 1,2-Azaborines and the Preparation of Their Protein Complexes with T4 Lysozyme Mutants, *J. Vis. Exp.*, 2017, **121**, e55154.
7. A. J. V. Marwitz, M. H. Matus, L. N. Zakharov, D. A. Dixon and S.-Y. Liu, A Hybrid Organic/Inorganic Benzene, *Angew. Chem. Int. Ed.*, 2009, **48**, 973-977.
8. H.-S. Lin and L. A. Paquette, A Convenient Method for Determining the Concentration of Grignard Reagents, *Synth. Commun.*, 1994, **24**, 2503-2506.
9. A. W. Baggett, M. Vasiliu, B. Li, D. A. Dixon and S.-Y. Liu, Late-Stage Functionalization of 1,2-Dihydro-1,2-azaborines via Regioselective Iridium-Catalyzed C–H Borylation: The Development of a New N,N-Bidentate Ligand Scaffold, *J. Am. Chem. Soc.*, 2015, **137**, 5536-5541.
10. G. R. Kiel, M. S. Ziegler and T. D. Tilley, Zirconacyclopentadiene-Annulated Polycyclic Aromatic Hydrocarbons, *Angew. Chem. Int. Ed.*, 2017, **56**, 4839-4844.
11. J. Marshall, B. C. Schroeder, H. Bronstein, I. Meager, S. Rossbauer, N. Yaacobi-Gross, E. Buchaca-Domingo, T. D. Anthopoulos, N. Stingelin, P. Beavis and M. Heeney, Benzocarborano[2,1-b:3,4-b′]dithiophene Containing Conjugated Polymers: Synthesis, Characterization, and Optoelectronic Properties, *Macromolecules*, 2014, **47**, 89-96.
12. M. B. Goldfinger, K. B. Crawford and T. M. Swager, Directed Electrophilic Cyclizations: Efficient Methodology for the Synthesis of Fused Polycyclic Aromatics, *J. Am. Chem. Soc.*, 1997, **119**, 4578-4593.
13. D. T. Y. Bong, E. W. L. Chan, R. Diercks, P. I. Dosa, M. M. Haley, A. J. Matzger, O. Š. Miljanić, K. P. C. Vollhardt, A. D. Bond, S. J. Teat and A. Stanger, Syntheses of Syn and Anti Doublebent [5]Phenylene, *Org. Lett.*, 2004, **6**, 2249-2252.
14. *Japan Pat.,* 2008147256, 2006.
15. D. J. Crouch, P. J. Skabara, J. E. Lohr, J. J. W. McDouall, M. Heeney, I. McCulloch, D. Sparrowe, M. Shkunov, S. J. Coles, P. N. Horton and M. B. Hursthouse, Thiophene and Selenophene Copolymers Incorporating Fluorinated Phenylene Units in the Main Chain: Synthesis, Characterization, and Application in Organic Field-Effect Transistors, *Chem. Mater.*, 2005, **17**, 6567-6578.
16. T. Dumslaff, PhD thesis, Johannes Gutenberg Universität Mainz, 2017.
17. M. A. Spackman and D. Jayatilaka, Hirshfeld surface analysis, *CrystEngComm*, 2009, **11**, 19-32.
18. M. A. Spackman and J. J. McKinnon, Fingerprinting intermolecular interactions in molecular crystals, *CrystEngComm*, 2002, **4**, 378-392.
19. F. Neese, The ORCA program system, *Wiley Interdiscip. Rev.: Comput. Mol. Sci.*, 2012, **2**, 73-78.
20. A. K. Rappe, C. J. Casewit, K. S. Colwell, W. A. Goddard and W. M. Skiff, UFF, a full periodic table force field for molecular mechanics and molecular dynamics simulations, *J. Am. Chem. Soc.*, 1992, **114**, 10024-10035.
21. P. Hohenberg and W. Kohn, Inhomogeneous Electron Gas, *Phys. Rev. B*, 1964, **136**, 864-871.
22. W. Kohn and L. J. Sham, Self-Consistent Equations Including Exchange and Correlation Effects, *Phys. Rev. A*, 1965, **140**, 1133-1138.
23. A. D. Becke, Density-functional exchange-energy approximation with correct asymptotic behavior, *Phys. Rev. A*, 1988, **38**, 3098-3100.
24. A. D. Becke, A new mixing of Hartree‐Fock and local density‐functional theories, *J. Chem. Phys.*, 1993, **98**, 1372-1377.
25. C. Lee, W. Yang and R. G. Parr, Development of the Colle-Salvetti correlation-energy formula into a functional of the electron density, *Phys. Rev. B*, 1988, **37**, 785-789.

26. T. H. Dunning Jr., Gaussian basis sets for use in correlated molecular calculations. I. The atoms boron through neon and hydrogen, *J. Chem. Phys.*, 1989, **90**, 1007-1023.

27. F. Weigend, A fully direct RI-HF algorithm: Implementation, optimised auxiliary basis sets, demonstration of accuracy and efficiency, *Phys. Chem. Chem. Phys.*, 2002, **4**, 4285-4291.

28. F. Neese, F. Wennmohs, A. Hansen and U. Becker, Efficient, approximate and parallel Hartree-Fock and hybrid DFT calculations. A 'chain-of-spheres' algorithm for the Hartree-Fock exchange, *Chem. Phys.*, 2009, **356**, 98.

29. R. Bauernschmitt and R. Ahlrichs, Treatment of electronic excitations within the adiabatic approximation of time dependent density functional theory, *Chem. Phys. Lett.*, 1996, **256**, 454-464.

30. B. d. Souza, F. Neese and R. Izsák, On the theoretical prediction of fluorescence rates from first principles using the path integral approach, *J. Chem. Phys.*, 2018, **148**, 034104.

31. A. Dreuw and M. Head-Gordon, Single-Reference ab Initio Methods for the Calculation of Excited States of Large Molecules, *Chem. Rev.*, 2005, **105**, 4009-4037.

32. P. v. R. Schleyer, C. Maerker, A. Dransfeld, H. Jiao and N. J. R. van Eikema Hommes, Nucleus-Independent Chemical Shifts: A Simple and Efficient Aromaticity Probe, *J. Am. Chem. Soc.*, 1996, **118**, 6317-6318.

33. Y. Shao, Z. Gan, E. Epifanovsky, A. T. B. Gilbert, M. Wormit, J. Kussmann, A. W. Lange, A. Behn, J. Deng, X. Feng, D. Ghosh, M. Goldey, P. R. Horn, L. D. Jacobson, I. Kaliman, R. Z. Khaliullin, T. Kuś, A. Landau, J. Liu, E. I. Proynov, Y. M. Rhee, R. M. Richard, M. A. Rohrdanz, R. P. Steele, E. J. Sundstrom, H. L. Woodcock, P. M. Zimmerman, D. Zuev, B. Albrecht, E. Alguire, B. Austin, G. J. O. Beran, Y. A. Bernard, E. Berquist, K. Brandhorst, K. B. Bravaya, S. T. Brown, D. Casanova, C.-M. Chang, Y. Chen, S. H. Chien, K. D. Closser, D. L. Crittenden, M. Diedenhofen, R. A. DiStasio, H. Do, A. D. Dutoi, R. G. Edgar, S. Fatehi, L. Fusti-Molnar, A. Ghysels, A. Golubeva-Zadorozhnaya, J. Gomes, M. W. D. Hanson-Heine, P. H. P. Harbach, A. W. Hauser, E. G. Hohenstein, Z. C. Holden, T.-C. Jagau, H. Ji, B. Kaduk, K. Khistyaev, J. Kim, J. Kim, R. A. King, P. Klunzinger, D. Kosenkov, T. Kowalczyk, C. M. Krauter, K. U. Lao, A. D. Laurent, K. V. Lawler, S. V. Levchenko, C. Y. Lin, F. Liu, E. Livshits, R. C. Lochan, A. Luenser, P. Manohar, S. F. Manzer, S.-P. Mao, N. Mardirossian, A. V. Marenich, S. A. Maurer, N. J. Mayhall, E. Neuscamman, C. M. Oana, R. Olivares-Amaya, D. P. O'Neill, J. A. Parkhill, T. M. Perrine, R. Peverati, A. Prociuk, D. R. Rehn, E. Rosta, N. J. Russ, S. M. Sharada, S. Sharma, D. W. Small, A. Sodt, T. Stein, D. Stück, Y.-C. Su, A. J. W. Thom, T. Tsuchimochi, V. Vanovschi, L. Vogt, O. Vydrov, T. Wang, M. A. Watson, J. Wenzel, A. White, C. F. Williams, J. Yang, S. Yeganeh, S. R. Yost, Z.-Q. You, I. Y. Zhang, X. Zhang, Y. Zhao, B. R. Brooks, G. K. L. Chan, D. M. Chipman, C. J. Cramer, W. A. Goddard, M. S. Gordon, W. J. Hehre, A. Klamt, H. F. Schaefer, M. W. Schmidt, C. D. Sherrill, D. G. Truhlar, A. Warshel, X. Xu, A. Aspuru-Guzik, R. Baer, A. T. Bell, N. A. Besley, J.-D. Chai, A. Dreuw, B. D. Dunietz, T. R. Furlani, S. R. Gwaltney, C.-P. Hsu, Y. Jung, J. Kong, D. S. Lambrecht, W. Liang, C. Ochsenfeld, V. A. Rassolov, L. V. Slipchenko, J. E. Subotnik, T. Van Voorhis, J. M. Herbert, A. I. Krylov, P. M. W. Gill and M. Head-Gordon, Advances in molecular quantum chemistry contained in the Q-Chem 4 program package, *Mol. Phys.*, 2015, **113**, 184-215.

34. C. Møller and M. S. Plesset, Note on an Approximation Treatment for Many-Electron Systems, *Phys. Rev.*, 1934, **46**, 618-622.

35. Y. Chen, W. Chen, Y. Qiao, X. Lu and G. Zhou, BN-Embedded Polycyclic Aromatic Hydrocarbon Oligomers: Synthesis, Aromaticity, and Reactivity, *Angew. Chem. Int. Ed.*, 2020, **59**, 7122-7130.

11. Author Contributions

Yannik Appiarius (Y.A.)	https://orcid.org/0000-0002-9849-6950
Tim Stauch (T.S.)	https://orcid.org/0000-0001-7599-3578
Enno Lork (E.L.)	https://orcid.org/0000-0002-0582-9913
Pascal Rusch (P.R.)	n.a.
Nadja C. Bigall (N.B.)	https://orcid.org/0000-0003-0171-1106
Anne Staubitz (A.S.)	https://orcid.org/0000-0002-9040-3297

Denoted above are the ORCID identification numbers of the authors.

The general idea and the concept were developed by Y.A. and A.S. All syntheses were planned and executed by Y.A., Unless state otherwise in this paragraph, all characterizations of the compounds were performed by Y.A. X-ray diffraction and the subsequent structure refinements were performed by E.L. P.R. and Y.A. performed the photoluminescence measurements and N.B. supervised the findings of the work. T.S. developed the calculation methodologies. Calculations were executed by Y.A. and T.S. All authors discussed the results and contributed to the final manuscript.